

# **Synthesis and Biological Evaluation of Trisindolyl-Cycloalkanes and Bis-Indolyl Naphthalene Small Molecules as Potent Antibacterial and Antifungal Agents**

Dissertation

Zur Erlangung des akademischen Grades

doctor rerum naturalium (Dr. rer. nat.)

Vorgelegt der

Naturwissenschaftlichen Fakultät I

Institut für Pharmazie

Fachbereich für Pharmazeutische Chemie

der Martin-Luther-Universität Halle-Wittenberg

von

Kaveh Yasrebi

Geboren am 09.14.1987 in Teheran/Iran (Islamische Republik)

Gutachter:

1. Prof. Dr. Andreas Hilgeroth (Martin-Luther-Universität Halle-Wittenberg, Germany)
2. Prof. Dr. Sibel Süzen (Ankara Üniversitesi, Turkey)
3. Prof. Dr. Michael Lalk (Ernst-Moritz-Arndt-Universität Greifswald, Germany)

Halle (Saale), den 21. Juli 2020

## Selbstständigkeitserklärung

Hiermit erkläre ich gemäß § 5 (2) b der Promotionsordnung der Naturwissenschaftlichen Fakultät I – Institut für Pharmazie der Martin-Luther-Universität Halle-Wittenberg, dass ich die vorliegende Arbeit selbstständig und ohne Benutzung anderer als der angegebenen Hilfsmittel und Quellen angefertigt habe. Alle Stellen, die wörtlich oder sinngemäß aus Veröffentlichungen entnommen sind, habe ich als solche kenntlich gemacht. Ich erkläre ferner, dass diese Arbeit in gleicher oder ähnlicher Form bisher keiner anderen Prüfbehörde zur Erlangung des Doktorgrades vorgelegt wurde.

Halle (Saale), den 21. Juli 2020

K. Yasrebi

Kaveh Yasrebi

## Acknowledgement

This study was carried out from June 2015 to July 2017 in the Research Group of Drug Development and Analysis led by Prof. Dr. Andreas Hilgeroth at the Institute of Pharmacy, Martin-Luther-Universität Halle-Wittenberg. I would like to thank all the people for their participation who supported my work in this way and helped me obtain good results.

First of all, I would like to express my gratitude to **Prof. Dr. Andreas Hilgeroth** for providing me with opportunity to carry out my Ph.D. studies, supervising adequately, and motivating me to work independently in order to develop myself and accomplish my project. I would also like to thank **Dr. Dieter Ströhl** at the Institute of Chemistry for measuring the 1D-<sup>1</sup>HNMR, 2D-<sup>1</sup>HNMR, and APT spectra and his useful consultations within NMR spectra interpretation, **Prof. Dr. Wolfgang Sippl**, **PD. Dr. habil. Matthias Schmidt** and **Dr. Tino Heimbürg** from the Research Group of Medicinal Chemistry for RP-HPLC results, **Mrs. Manuela Woigk** for Mass spectrometry data, **Mrs. Heike Rudolph** for IR measurements, **Mrs. Monika Lunow** and **Mr. Dirk Stolzenhain** for providing chemicals and glasswares at the Institute of Pharmacy. Many thanks to Pharmacy Diploma Student **Kerolos Ashraf** for synthesizing the compounds 23-40 as his diploma project and other colleagues **Fabian Lentz**, **Tim Fischer**, **Nico Schade**, **Cornelius Hempel**, **Tobias Mohs**, **Ansgar Opitz**, **Marius Seethaler**, and **Robin Gehrmann** for their supports and helps and providing appropriate atmosphere in the laboratory.

I would appreciate the chance to thank **Prof. Dr. Sibel Süzen** from Department of Pharmaceutical Chemistry, Ankara University, **Prof. Dr. Michael Lalk** from Institute of Biochemistry, Ernst-Moritz-Arndt-Universität Greifswald, **PD. Dr. Knut Ohlsen**, **Dr. Tobias Hertlein**, **Mr. Emmanuel Tola Adeniyi** from Institute of Molecular Infection Biology, Julius Maximilians Universität, Würzburg, and **PD. Dr. Frank Erdmann** from Institute of Pharmaceutical Biology and Pharmacology, Martin-Luther-Universität Halle-Wittenberg for carrying out the Bioassay part of this project.

At the end, I would like to sincerely thank my **mother** for her supports and encouragements within these four years.

## Table of Contents

1. Introduction.....	1
1.1 Chemistry of indole.....	1
1.1.1 The structure and reactivity of indole .....	1
1.1.2 Electrophilic substitution reactions by indoles .....	6
1.1.2.1 Michael addition of indoles .....	6
1.1.2.1.2 The factors affecting the Michael Addition of indoles to various $\alpha,\beta$ unsaturated compounds .....	9
1.1.2.2 Anti-Michael addition of indoles .....	10
1.1.2.3 Friedel-Crafts (F-C) reactions of indoles to epoxides.....	10
1.1.2.4 Electrophilic substitution reaction of indoles to carbonyl compounds such as aldehydes and ketones.....	12
1.1.2.4.1 The factors affecting the electrophilic substitution reactions of indoles to aldehydes and ketones.....	14
1.1.2.5 The electrophilic substitution reactions of indoles to isatins .....	15
1.2 Indoles in nature.....	16
1.2.1 Naturally occurring indole-containing compounds in marines and plants .....	16
1.2.2 Naturally occurring indole-containing compounds in microorganisms.....	19
1.3 Bacteria, cell growth mechanisms, and modes of action of some commercial antibacterial agents .....	20
1.3.1 Inhibition of cell metabolism (antimetabolites) .....	20
1.3.2 Inhibition of cell wall biosynthesis .....	20
1.3.3 Impairing the protein synthesis translation .....	23
1.3.4 Inhibition of nucleic acid transcription and replication .....	23
1.3.5 Fatty acid biosynthesis inhibition (FabI) .....	24
1.4 Drug resistance, the possible mechanisms, and examples .....	25
1.5 The infections and diseases caused by bacteria .....	27
1.5.1 Skin infection .....	27
1.5.2 Urinary tract infection .....	27
1.5.3 Otitis media.....	27



1.5.4 Brain infection .....	27
1.5.5 Respiratory infections .....	27
1.6 Structure-Activity Relationship (SAR).....	27
1.7 A review to bioactivities of synthetic indole-containing compounds and their SARs .....	28
1.7.1 Antibacterial and antifungal activities .....	28
1.7.1.1 The Structure-Activity Relationships (SARs) of the above indole-containing compounds .....	43
1.7.2 Anti-cancer activity.....	45
1.7.2.1 The Structure-Activity Relationship (SAR) of the above indolyl-derived compounds as Anti-cancer agent.....	46
1.7.3 Other biological activities of some indolyl-derived compounds .....	47
2. Results and Discussion .....	48
2.1 Synthesis part .....	48
2.1.1 The reactions of indoles with glutaric dialdehyde and malondialdehyde .....	48
2.1.2 The formation of (Z)-3,3',3'' tris products .....	55
2.1.2.1 The spectral data confirming the formation of (Z)-3,3',3'' tris products .....	59
2.1.2.2 The possible stereochemistry of chiral centres in hexahydrocyclohepta[b]indoles and tetrahydrocyclopenta[b]indoles.....	61
2.1.3 The electrophilic substitution reactions of indoles to <i>o</i> -phthal dialdehyde .....	64
2.1.3.1 The spectral data confirming the structures of 11- and 6-indolylbenzocarbazole compounds (compounds 23-37).....	72
2.1.4 The Acetylation reaction of indolylbenzo[b]carbazole.....	75
2.2 Bioassay part.....	77
3. Summary of work and conclusion .....	89
3.1 Summary of work.....	89
3.2 Conclusion .....	91
4. References.....	95
5. Experimental .....	107
5.1 Materials .....	107
5.1.1 Thin Layer Chromatography (TLC) .....	107
5.1.2 Column Chromatography.....	107
5.1.3 Ultra-Violet Lamp (UV Lamp).....	107
5.1.4 Melting Points.....	107
5.1.5 Reagents and solvents .....	107

5.2 Instruments.....	109
5.2.1 Electrospray Ionization Mass Spectrometry (ESI-MS) .....	109
5.2.2 Atmospheric Pressure Chemical Ionization Mass Spectrometry (APCI-MS) .....	109
5.2.3 Fourier Transform Infrared (FT-IR) .....	109
5.2.4 One Dimensional Proton Nuclear Magnetic Resonance (1D $^1\text{H}$ -NMR) .....	109
5.2.5 One Dimensional Carbon Nuclear Magnetic Resonance (1D $^{13}\text{C}$ -NMR) .....	110
5.2.5.1 Proton Coupled Carbon NMR .....	110
5.2.5.2 APT (Proton Decoupled Carbon NMR) .....	110
5.2.6 Two Dimensional Nuclear Magnetic Resonance (2D-NMR).....	110
5.2.7 Reversed-phase high performance liquid chromatography (RP-HPLC) .....	110
5.3 General Experimental Protocol to synthesize the compounds 1-22 .....	111
5.4 General Experimental Protocol to synthesize the compounds 23-37 and 40.....	112
5.5 Experimental Protocol to Acetylation of the compound 31 (compounds 38 and 39).....	112
5.6 The experimental protocols to the MIC values determination.....	158
5.6.1 The protocol to the bioassay of the compounds 1-22 .....	158
5.6.2 The protocols to the bioassay of the compounds 23-40.....	159
6. Appendix .....	161
6.1 NMR spectra .....	161
6.2 Curriculum Vitae .....	204
6.3 Publications.....	205

## List of Figures

Fig. 1 The structures of well-known aromatic heterocycles, PKI, Clopirac, and NADP <sup>+</sup> .....	2
Fig. 2 Examples of metal-catalysed reactions leading to indole formation .....	4
Fig. 3 Schematic mechanism of the Fischer indole synthesis and electrophilic substitution of indoles .....	5
Fig. 4 Michael addition of indoles to $\alpha,\beta$ -unsaturated compounds in the presence of Lewis acid and bis(oxazoline)-metal(II) complexes.....	8
Fig. 5 C-2 ( $\alpha$ ) Michael addition of indole .....	8
Fig. 6 Aza-Michael addition of indoles .....	9
Fig. 7 An example of Anti-Michael addition of indoles under basic conditions .....	10
Fig. 8 Carbonylation rearrangement in epoxides and the enantioselective reaction of indole with Styrene oxide .....	11
Fig. 9 The plausible mechanism of the synthesis of bis(indolyl)methanes .....	13
Fig. 10 Three component reaction of indoles in the presence of kojic acid .....	14
Fig. 11 The synthetic approaches to di(indolyl)-indolin-2-ones by <i>C. Praveen et al.</i> .....	15
Fig. 12 Some important indole-containing compounds in marines and plants.....	18
Fig. 13 some examples of indole-containing compounds in microorganisms .....	19
Fig. 14 The mechanism of FabI .....	24
Fig. 15 The structure of triclosan .....	28
Fig. 16 Synthesis of the 2,9-disubstituted 1,2,3,4-tetrahydropyrido[3,4-b]indoles by <i>M. A. Seefeld et al.</i> .....	29
Fig. 17 Synthesis of novel <i>N</i> -allyl and <i>N</i> -propargyl di(indolyl)indolin-2-ones by <i>C. Praveen et al.</i> .....	31
Fig. 18 melatonin analogous indole-3-aldehyde hydrazide/hydrazone derivatives synthesized by <i>Gurkok et al.</i> .....	32
Fig. 19 Synthesis of Isoxazolo[4,3-e]indoles by <i>Pordel et al.</i> .....	33
Fig. 20 The structure of the compounds synthesized by <i>B. V. Subba Reddy et al.</i> .....	34
Fig. 21 Scheme of a synthetic approach of substituted 1,2,3,4-tetrahydropyrazino[1,2-a]indoles by <i>R. K. Tiwari et al.</i> .....	37
Fig. 22 Some examples of oxazolones and oxazolidinones with biological activities and the scheme of the synthetic routes to indolyloxazolone derivatives by <i>E. R. Periera et al.</i> .....	40
Fig. 23 Synthetic approach to the mono- and bis-indolyloximes by <i>Prudhomme et al.</i> .....	43
Fig. 24 <i>Kumar et al.</i> 's synthetic route to the indolyl-1,2,4-triazoles .....	46

Fig. 25 Syntheses of hexahydrocyclohepta[b]indoles and tetrahydrocyclopenta[b]indoles....	49
Fig. 26 The plausible mechanism of our reactions to hexahydrocyclohepta[b]indoles and tetrahydrocyclopenta[b]indoles.....	50
Fig. 27 The observed possible product of our incomplete reaction .....	52
Fig. 28 The possible couplings and correlations between H <sub>a</sub> s, H <sub>b</sub> s, and H <sub>c</sub> s.....	53
Fig. 29 The plausible mechanism of formation of 1,1,4,4-tetra(1H-indol-3-yl)propane compounds .....	54
Fig. 30 The mechanism of the formation of (Z)-3,3',3'' tris products .....	55
Fig. 31 The possible dehydration processes in the reaction of glutaric dialdehyde with indoles .....	57
Fig. 32 The possible dehydration processes in the reactions of 2-bromo and 2-chloro-malondialdehydes with indoles.....	58
Fig. 33 The scheme of possible correlations of H <sub>2</sub> and H <sub>1</sub> and NOESY in compound 22 .....	60
Fig. 34 the possible couplings for H <sub>a</sub> and H <sub>b</sub> .....	61
Fig. 35 the possible coupling for H <sub>a</sub> , H <sub>b</sub> , and H <sub>c</sub> in tetrahydrocyclopenta[b]indole derivatives .....	63
Fig. 36 The reaction of indoles and <i>o</i> -phthaldialdehyde.....	65
Fig. 37 The possible mechanism of the formation of the first stereoisomer.....	66
Fig. 38 The possible mechanism of formation of the second stereoisomers .....	67
Fig. 39 Plausible mechanism to the first atropisomer.....	69
Fig. 40 The plausible mechanism to the formation of the second atropisomer .....	70
Fig. 41 Compound 28 .....	72
Fig. 42 The possible couplings of H <sub>a</sub> , H <sub>b</sub> , and H <sub>c</sub> in unsubstituted, 7-aza, and 5-NO <sub>2</sub> 11-indolylbenzocarbazole derivatives.....	73
Fig. 43 The position and the possible couplings of H <sub>a</sub> and H <sub>b</sub> in 6- and 11-indolylbenzocarbazole derivatives (compounds 32 and 31) .....	74
Fig. 44 The reaction of indole to thiophene-2,3-dicarbaldehyde.....	75
Fig. 45 The acetylation reaction.....	75
Fig. 46 The position of H, H <sub>1</sub> , and H <sub>2</sub> on unsubstituted indolylcarbazole, mono, and diacetylated derivatives.....	76

## List of Tables

Table. 1 MIC values ( $\mu\text{g/ml}$ ) of compounds 1, 6, 7, 8, 9, 10, 11 against Gram-positive bacteria.....	78
Table. 2 MIC values ( $\mu\text{g/ml}$ ) of compounds 1, 6, 7, 8, 9, 10, 11 against Gram-negative bacteria.....	79
Table. 3 MIC values ( $\mu\text{g/ml}$ ) of the compounds 1, 6, 7, 8, 9, 10, 11 against fungal species...	79
Table. 4 MIC values ( $\mu\text{g/ml}$ ) of the compounds 3 and 4 against Gram-positive bacteria.....	80
Table. 5 MIC values ( $\mu\text{g/ml}$ ) of the compounds 3 and 4 against Gram-negative bacteria and fungal species.....	81
Table. 6 MIC values ( $\mu\text{g/ml}$ ) of the compounds 12-22 against Gram-positive bacteria .....	83
Table. 7 MIC values ( $\mu\text{g/ml}$ ) of the compounds 12-22 against Gram-negative bacteria.....	84
Table. 8 MIC values ( $\mu\text{g/ml}$ ) of the compounds 12-22 against <i>C. albicans</i> .....	84
Table. 9 MIC values ( $\mu\text{g/ml}$ ) of the compounds 23-40 against Gram-positive bacteria .....	87
Table. 10 MIC values ( $\mu\text{g/ml}$ ) of our standards against Gram-positive bacteria.....	88
Table. 11 MIC values ( $\mu\text{g/ml}$ ) of our standards against Gram-negative bacteria and fungal species. ....	88

## List of Abbreviations

A	Absorbance
CH <sub>3</sub> CO <sub>2</sub> H	Acetic acid
HOAc	Acetic acid
(CH <sub>3</sub> O) <sub>2</sub> CO	Acetic anhydride
acac	Acetylacetone
ACP	Acyl carrier protein
OR	alkyloxy
AlPW <sub>12</sub> O <sub>40</sub>	Aluminiumdodecatungestophosphate
AlCl <sub>3</sub>	Aluminum chloride
Al(OTf) <sub>3</sub>	Aluminum triflate
A-site	Aminoacyl site
NH <sub>3</sub>	Ammonia
NH <sub>4</sub> OH	Ammonium hydroxide
Ar	Aryl
ARQ	Asterriquinone
atm	Atmosphere
APCI	Atmospheric pressure chemical ionization
ATR	Attenuated total reflectance
OBzl (OBn)	Benzyloxy
BIM	Bis(indolyl)methane
BOX	Bis(oxazoline)
Bi(OTf) <sub>3</sub>	Bismuth triflate
br	broad (FT-IR& NMR)
Br	Bromine
Bu	Butyl
<sup>13</sup> C-NMR	Carbon-13 nuclear magnetic resonance
CAN	Ceric ammonium nitrate
CeCl <sub>3</sub>	Cerium trichloride
δ	Chemical shift
Cl	Chlorine
CHCl <sub>3</sub>	Chloroform
<i>et al</i>	Colleagues
Cu	Copper
Cu(OTf) <sub>2</sub>	Copper diflate
Cu(OTf)	Copper flate
Cu(SbF <sub>6</sub> ) <sub>2</sub>	Copper hexafluoroantimonate
COSY	Correlation spectroscopy
DNA	Deoxyribonucleic acid
CH <sub>2</sub> Cl <sub>2</sub>	Dichloromethane
DCM	Dichloromethane

$C_4H_{10}O$	Diethylether
$(MeO)_2$	Dimethoxy (diMeO)
dap	Dimethyl amino pyrrole
DMF	Dimethyl formamide
DMSO	Dimethylsulfoxide
d	doublet (NMR)
dd	doublet of doublet (NMR)
dt	doublet of triplet
$Dy(OTf)_3$	Dysprosium triflate
EDG	Electron-donating group
EWG	Electron-withdrawing group
ESI	Electrospray ionization
ENR	Enoyl acyl carrier protein reductase
<i>E</i> -olefin	Entgegen (trans)
eq	Equivalent
<i>E</i>	Eritro
EtOH	Ethanol
Et	Ethyl
FabI	Fatty acid biosynthesis inhibition
F	Fluorine
HCOOH	Formic acid
FT-IR	Fourier transform infrared
gr	gram
GI	Growth inhibition
$GI_{50}$	Half of maximal of growth inhibition
HSV	Herpes simplex virus
Hz	Hertz
HMBC	Heteronuclear multiple bond correlation
HSQC	Heteronuclear single quantum correlation
HOMO	Highest occupied molecular orbital
HDAi	Histone deacetylase inhibitory
hr	Hour(s)
HIV	Human immunodeficiency virus
HCl	Hydrochloric acid
OH	Hydroxy
$NH_2OH$	Hydroxyl amine
$InBr_3$	Indium tribromide
$InCl_3$	Indium trichloride
IC	Inhibition concentration
ISC	Interstrand cross-link
$I_2$	Iodine
$Fe(ClO_4)_2$	Iron diperchlorate
$FeCl_3$	Iron trichloride
<i>i-pr</i>	Isopropyl
<i>i-pr</i> -OH	Isopropyl alcohol

Kbar	Kilobar
Ln(OTf) <sub>3</sub>	Lanthanum triflate
LCAO	Linear combination of atomic orbitals
Li	Lithium
LiAlH <sub>4</sub>	Lithium aluminum hydride
LiClO <sub>4</sub>	Lithium perchlorate
LPDE	Lithium perchlorate diethylether
Mg(OTf) <sub>2</sub>	Magnesium diflate
MS	Mass spectrometry
m/z	Mass/charge
m	medium (FT-IR)
MHz	Megahertz
m-RNA	Messenger ribonucleic acid
<i>m</i>	Meta
MRSA	Methicilin-resistant staphylococcus aureus
MSSA	Methicilin-suseptable staphylococcus aureus
OMe	Methoxy
CH <sub>3</sub>	Methyl
Me	Methyl
CH <sub>3</sub> I	Methyl iodide
MeCN	Methylcyanide (Acetonitrile)
CH <sub>2</sub>	Methylene
µg	Microgram
µg/disk	Microgram per disk
µg/ml	Microgram per mililitre
Mm	Micromolar
ml	Mililitre
mmol	Milimole
MIC	Minimal Inhibitory Concentration
min	minute
M	Molecularion
MHV	Mouse hepaptisis virus
MDRTB	Multidrug-resistant tuberculosis
m	multiplet (NMR)
TMGTf	<i>N,N,N,N</i> -tetramethylguanidinium triflate
TMGT	<i>N,N,N,N</i> -tetramethylguanidinium trifluoroacetate
NAM	<i>N</i> -acetyl muramic acid
NAG	<i>N</i> -acetylglucosamine
ng	Nanogram
ng/ml	Nanogram per mililitre
Ni(OTf) <sub>2</sub>	Nickel diflate
NAD	Nicotinamide adenine
NADP	Nicotinamide adenine dinucleotide phosphate
NO <sub>2</sub>	Nitro
NP-HPLC	Normal phase high performance liquid chromatography



n.a	not active
n.d	not determined
n.t	not tested
NMR	Nuclear magnetic Resonance
NOESY	Nuclear overhauser effect
1D-NMR	One dimensional nuclear magnetic resonance
<i>O</i>	Ortho
Pd	Palladium
PdNPs	Palladium (II) nanoparticles
Pd(OAc) <sub>2</sub>	Palladium acetate
Pd(OH) <sub>2</sub>	Palladium hydroxide
<i>p</i> -TsOH	<i>Para</i> toluene sulfonic acid
<i>p</i> -TSA	<i>Para</i> toluene sulfonic acid
PABA	<i>Para</i> -aminobenzoic acid
ppm	Part per million
PBP2a	Penicilin-binding protein
P-site	Peptidyl site
OPh	Phenoxy
Ph	Phenyl
POCl <sub>3</sub>	Phosphorus oxychloride
pg	Picogram
pg/ml	Picogram per mililitre
K	Potassium
KAl(SO <sub>4</sub> ) <sub>2</sub>	Potassium aluminum sulfate
KHSO <sub>4</sub>	Potassium bisulfate
KBr	Potassium bromide
K <sub>2</sub> CO <sub>3</sub>	Potassium carbonate
KOH	Potassium hydroxide
<i>t</i> BuOK	Potassium tertiary butanolate
PKC	Protein kinase C
PKI	Protein kinase inhibitor
APT	Proton decoupled carbon nuclear magnetic resonance
<sup>1</sup> H-NMR	Proton nuclear magnetic resonance
q	quartet (NMR)
R <sub>f</sub>	Retention factor
R <sub>t</sub>	Retention time
RP-HPLC	Reversed phase high performance liquid chromatography
Rh	Rhodium
RNA	Ribonucleic acid
rt	Room temperature
SmI <sub>3</sub>	Samarium triiodide
Ag(OTf)	Silver flate
s	Singlet (NMR)
Na	Sodium
NaBH <sub>4</sub>	Sodium borohydride

NaCN	Sodium cyanide
NaOEt	Sodium ethanolate
HCOONa	Sodium formate
NaH	Sodium hydride
NaSO <sub>3</sub>	Sodium sulfite
NaCl	Sodium chloride
NaOH	Sodium hydroxide
Na <sub>2</sub> SO <sub>4</sub>	Sodium sulfate
s	Strong (FT-IR)
H <sub>2</sub> SO <sub>4</sub>	Sulfuric acid
TaCl <sub>5</sub>	Tantalum pentachloride
BoC	<i>tert</i> - butyloxycarbonyl
tBu	Tertiary butyl
TBDMS	Tertiarybutyldimethylsilyl
TBME	Tertiarybutylmethylether
TBAHBr	Tetrabutylammonium hydrogen bromide
TBAHS	Tetrabutylammonium hydrogen sulfate
THF	Tetrahydrofuran
TMS	Tetramethylsilane
TLC	Thin layer chromatography
t-RNA	Transfer ribonucleic acid
NEt <sub>3</sub>	Triethyl amine
PO(OEt) <sub>2</sub>	Triethyl phosphite
P(OEt) <sub>3</sub>	triethyl phosphite
OTf	Triflate
TFA	Trifluoroacetic acid
TMSCl	Trimethylsilylchloride
TMSCN	Trimethylsilylcyanide
PPh <sub>3</sub>	Triphenyl phosphane
t	triplet (NMR)
2D-NMR	Two dimensional nuclear magnetic resonance
Tyr	Tyrosine
UV	Ultra violet
UDP	Uridine diphosphate
UTP	Uridine triphosphate
VRE	Vancomycin-resistant Enterocci
VRSA	Vancomycin-resistant staphylococcus aureus
v/v	volume/volume
w	weak (FT-IR)
Yb(OTf) <sub>3</sub>	Ytterbium triflate
YCl <sub>3</sub>	Yttrium trichloride
Zn	Zinc
ZnBr <sub>2</sub>	Zinc bromide
ZnCl <sub>2</sub>	Zinc dichloride
Zn(OTf) <sub>2</sub>	Zinc diflate

ZrCl <sub>4</sub>	Zirconium tetrachloride
Z-olefin	Zusammen (cis)
BINAP	(2,2'-bis (diphenylphosphino) -1,1'-binaphthyl)
(tBuO <sub>2</sub> C) <sub>2</sub> O	(2-Methylpropan-2-yl)oxycarbonyl tert-butyl carbonate
CDI	1,1'-Carbonyldiimidazole
[BMIM] BF <sub>4</sub>	1-butyl-3-methylimidazolium tetrafluoro borate
[BMIM] BF <sub>4</sub> -LiCl	1-butyl-3-methylimidazolium tetrafluoro borate doped with lithium chloride
EDC	1-Ethyl-3- (3-dimethylaminopropyl) carbodiimide
HOBt	1-hydroxybenzotriazole
Salen	2,2'-Ethylenebis(nitrilomethylidene)diphenol, N,N'-Ethylenebis(salicylimine)
DDQ	2,3-dichloro-5,6-dicyano-1,4-benzoquinone
DMAP	4-(dimethylaminopyridine)
IC <sub>50</sub>	50% inhibition concentration

## 1. Introduction

### 1.1 Chemistry of indole

#### 1.1.1 The structure and reactivity of indole

Aromatic heterocyclic nitrogen-containing compounds such as pyrrole, pyridine, pyridone, pyrimidine, thiazole, imidazole, and oxazole are very important in medicinal chemistry and biochemistry because they are part of the molecular scaffold of many biologically potent active agents and essential biological substances. For instance, clopirac as an anti-inflammatory agent contains a pyrrole ring, nicotinamide adenine dinucleotide phosphate (NADP<sup>+</sup>) which is a co-factor used in the formation of nucleic acids and lipids (anabolic reactions) contains both a pyridine and a pyrimidine ring, and a protein kinase inhibitor (PKI) 166 contains pyrimidine ring fused to a pyrrole (Fig. 1). The above aromatic heterocycles could also appear fused to a benzene ring. Among these benzene-fused heterocycles, indoles are the most important ones. Indole contains a pyrrole ring fused to a benzene<sup>1</sup>. Many main group and transition metals such as Lithium (Li), Zinc (Zn), Palladium (Pd), Copper (Cu), Rhodium (Rh) via aryl hydrazines, arylation of benzophenone hydrazones or *tert*-butylcarbazate, hydroamination of alkynes, hydroformylation of alkenes, heteroannulation and cyclization of 2-alkynylanilines, and Larock heteroannulation catalyse the synthetic approaches to indole<sup>2,3</sup>. Even though, iodine catalyses the synthesis of indole via azidocinnamates<sup>4,6</sup> (Fig. 2). In the Fischer indole synthesis, a phenylhydrazine reacts with a ketone through a multi-step metal catalysed pathway to produce indole (Fig. 3). Disconnection of C-C and C-N bonds of indoles leads to the corresponding ketones or phenylhydrazines. Indoles along with pyrroles highly tend to carry out aromatic electrophilic substitution reactions, whereas pyridine, pyridone, and pyrimidine are potent for aromatic nucleophilic substitutions<sup>1,5</sup>. C-3 ( $\beta$ ) position of indole is preferentially more appropriate for electrophilic substitution reactions because the highest occupied molecular orbital (HOMO) of indole shows higher electron density at C-3 ( $\beta$ ) than that at C-2 ( $\alpha$ ) based on linear combination of atomic orbitals (LCAO)<sup>7</sup> method (0.595 to 0.219)<sup>8</sup>.

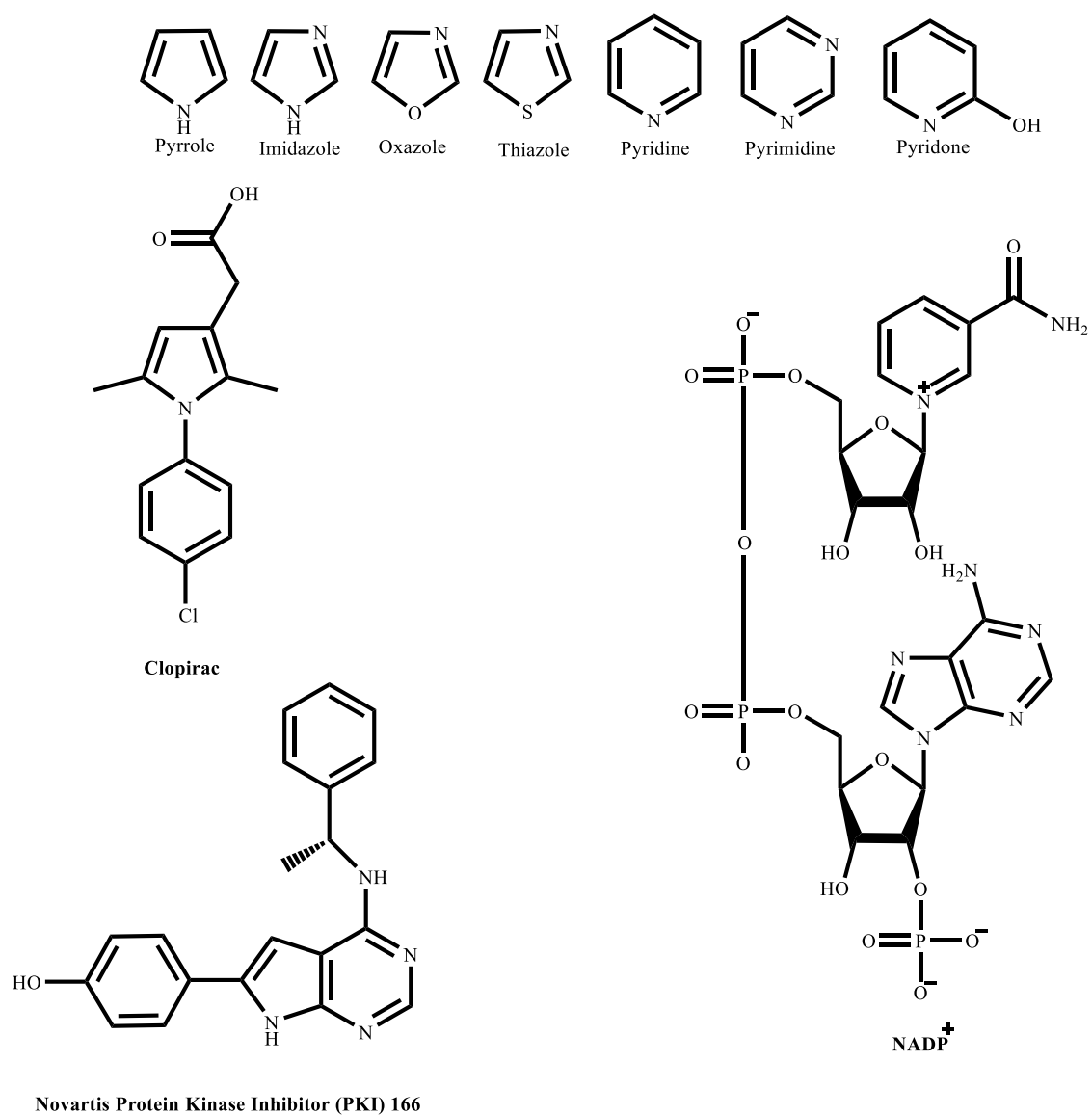
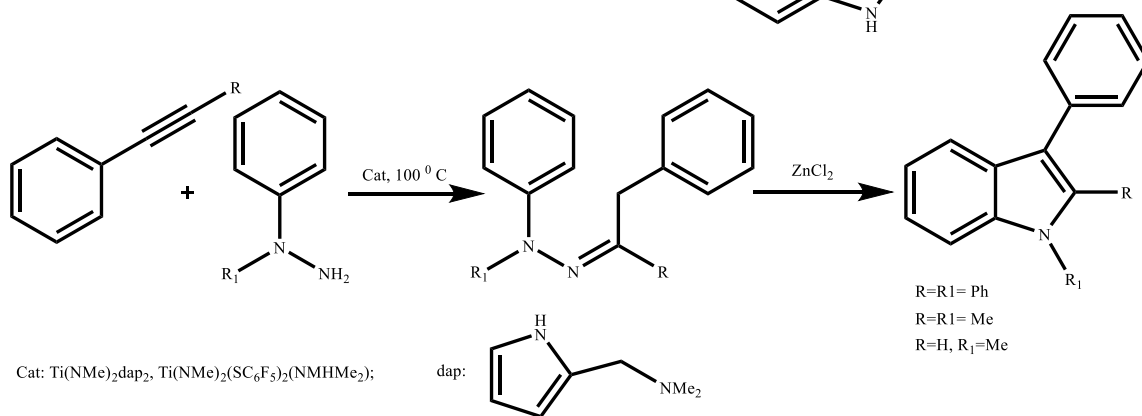
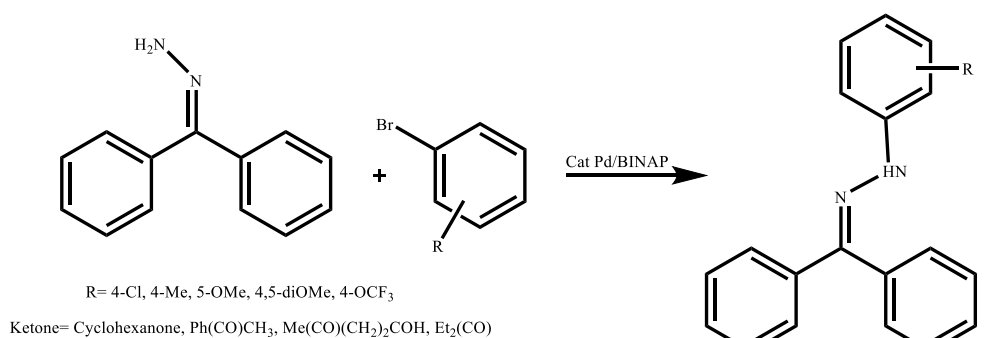
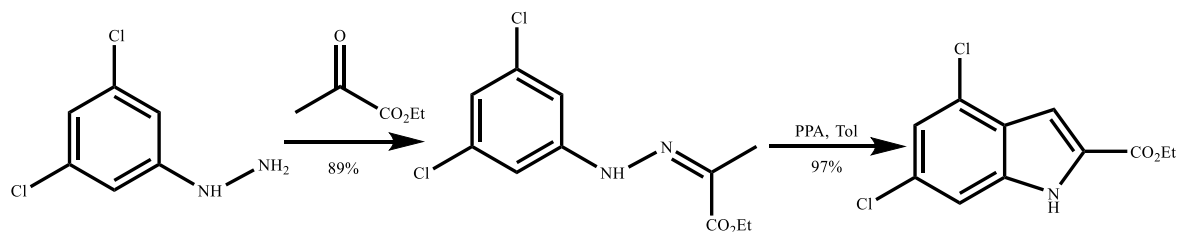
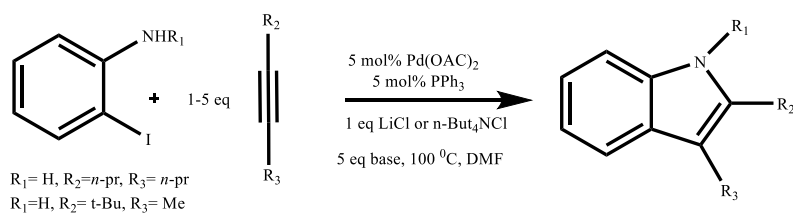


Fig. 1 The structures of well-known aromatic heterocycles, PKI, Clopirac, and NADP<sup>+</sup> <sup>1</sup>



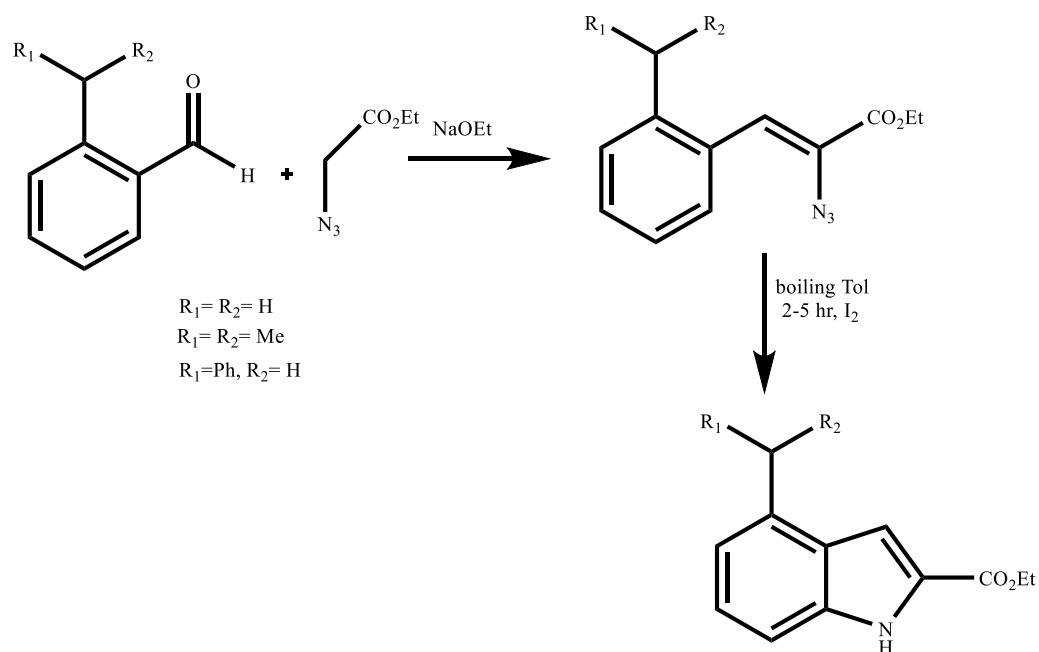
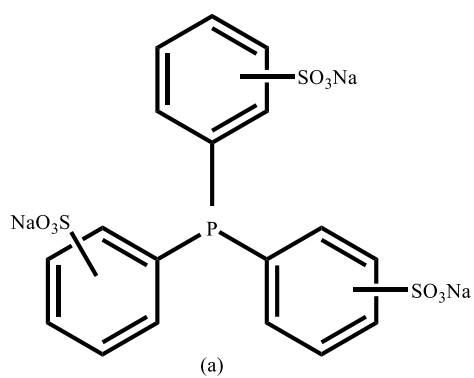
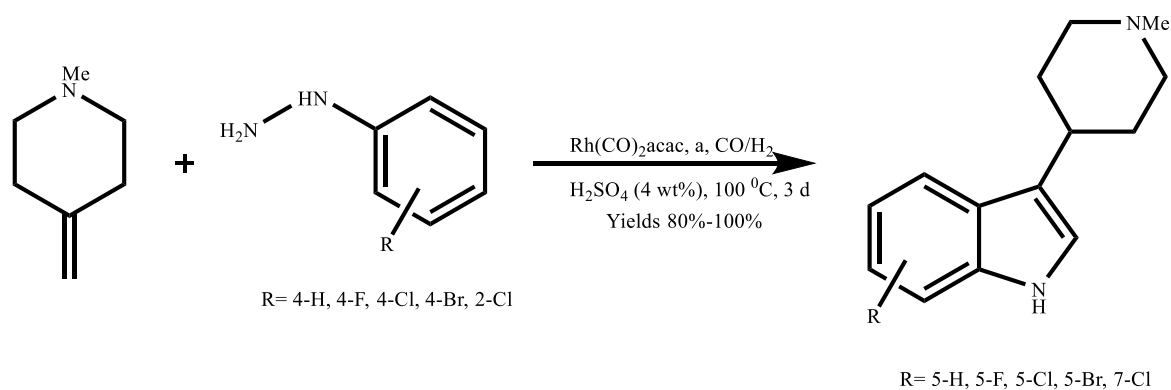


Fig. 2 Examples of metal-catalysed reactions leading to indole formation<sup>2,3,4,6</sup>

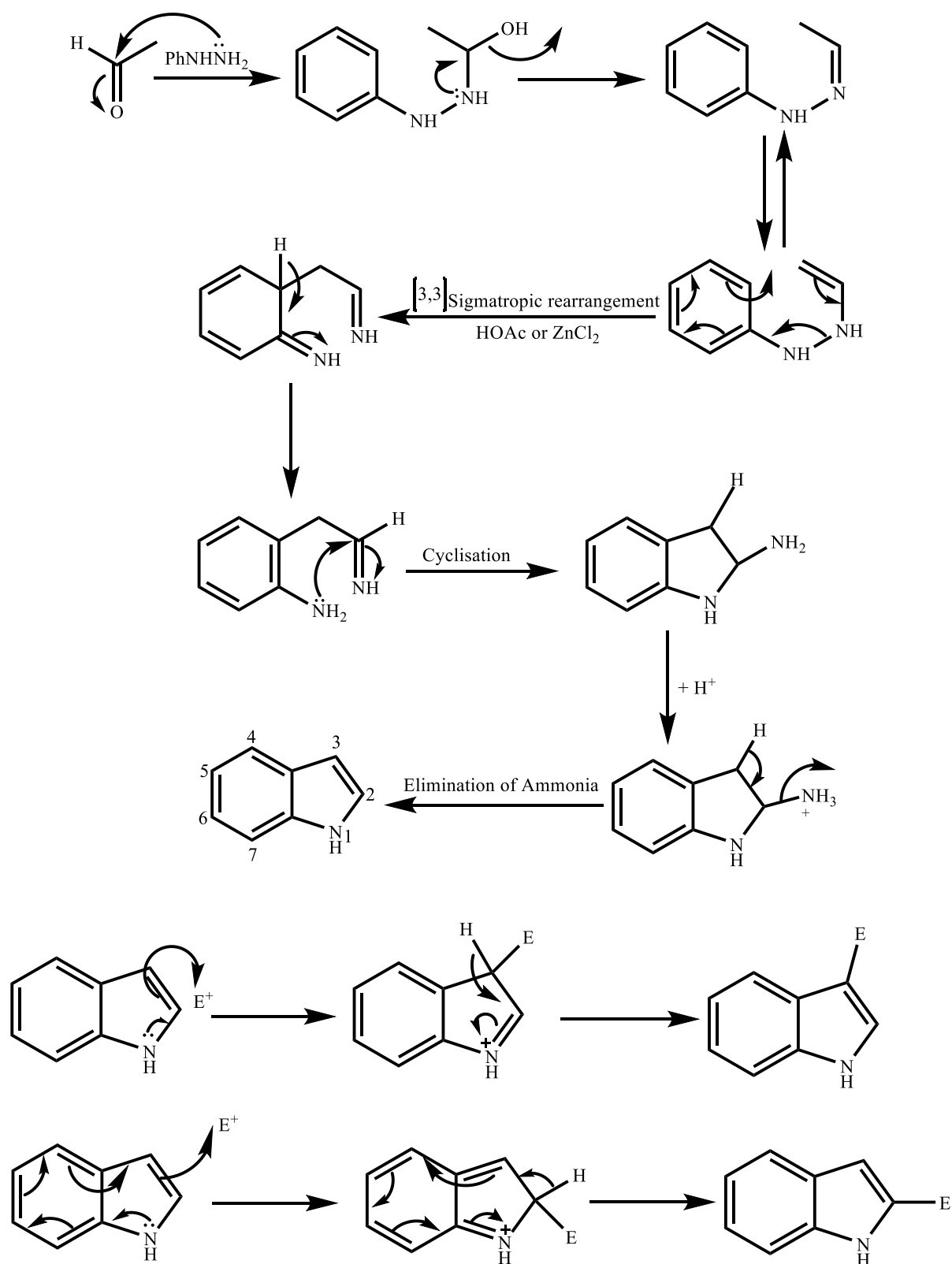


Fig. 3 Schematic mechanism of the Fischer indole synthesis and electrophilic substitution of indoles<sup>1,5</sup>

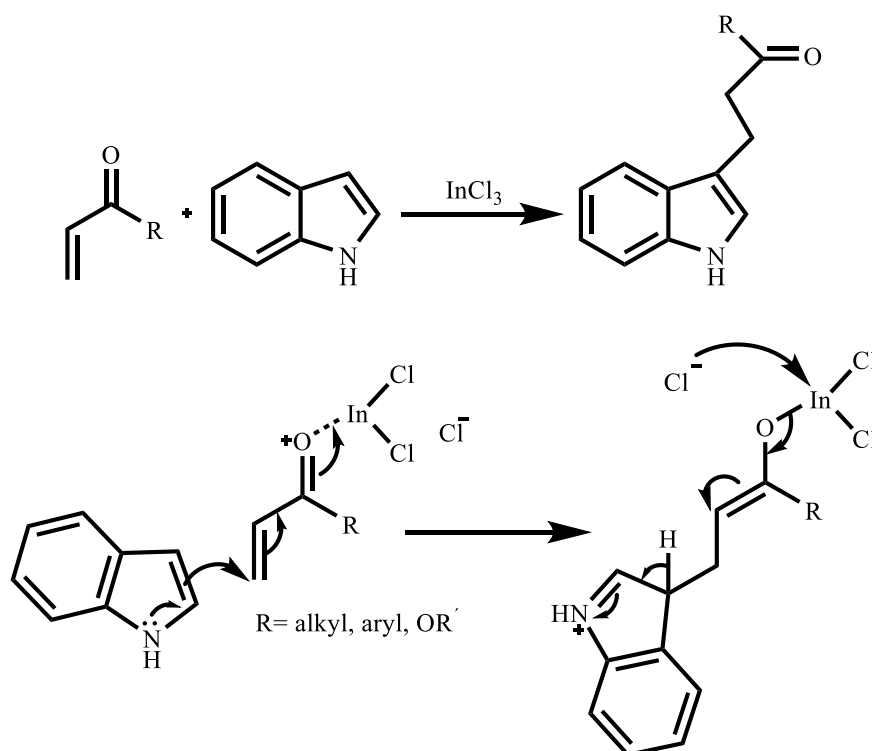


### 1.1.2 Electrophilic substitution reactions by indoles

#### 1.1.2.1 Michael addition of indoles

Indoles and 1-methyl-1*H* indoles carry out Michael addition (1,4-addition or conjugate addition) to electron deficient alkenes such as but-3-en-2-one, pent-3-en-2-one, cyclohex-2-en-1-one, 3-methylcyclohex-2-en-1-one, and 2-nitrovinylbenzene in the presence of lanthanide salts such as Yb(OTf)<sub>3</sub>·3H<sub>2</sub>O as Lewis acid at both high and ambient pressure in methylcyanide (MeCN)<sup>9</sup> and in Indium halides such as InCl<sub>3</sub> and InBr<sub>3</sub> under mild conditions (aqueous or non-aqueous media)<sup>10</sup> and CH<sub>2</sub>Cl<sub>2</sub><sup>11,14</sup> in high yields. Furthermore, InBr<sub>3</sub> catalyses the reaction of indoles with nitroalkenes in water under mild conditions<sup>12</sup>. InBr<sub>3</sub> can be recovered from the aqueous phase and reused with no loss of activity. InBr<sub>3</sub> (10 mol %) and trimethylsilyl cyanide (TMSCN) catalyse the sequential one-pot 1,4- and then 1,2-nucleophilic reaction of indoles with  $\alpha,\beta$ -unsaturated ketones<sup>13</sup>. Adding catalytic amount (10 mol %) of trimethylsilylchloride (TMSCl) to InBr<sub>3</sub> speeds up the Michael addition reactions of indoles in the syntheses of 1,3-bis(indol-3yl)butane-1-ones and leads to higher yields because it dramatically enhances the solubility of insoluble Indium-enone complex<sup>8</sup>. Beside Yb(OTf)<sub>3</sub>·3H<sub>2</sub>O and Indium salts, Bi(OTf)<sub>3</sub><sup>15</sup>, SmI<sub>3</sub><sup>16</sup>, AlPW<sub>12</sub>O<sub>40</sub><sup>17</sup> in MeCN, and ZrCl<sub>4</sub><sup>18</sup> in CH<sub>2</sub>Cl<sub>2</sub> catalyse the Michael addition of indoles with enones and lead to reactions with high yields. Catalytic amounts of hydrochloric acid (HCl) in ethanol (EtOH)<sup>19</sup> catalyse the reactions of indoles with 4-methylquinoline-2,5,8(1*H*)-trione and 1,4-dimethylquinoline-2,5,8(1*H*)-trione. Michael additions of indoles with unsaturated ketones (enones) in solvent-free<sup>20</sup> and anhydrous methanol (CH<sub>3</sub>OH) and ethanol (C<sub>2</sub>H<sub>5</sub>OH)<sup>21</sup> in catalytic amount of iodine (10 % mol) at room temperature and with nitroalkenes in chloroform (CHCl<sub>3</sub>) (0.5 ml) and diethylether (C<sub>2</sub>H<sub>5</sub>-O-C<sub>2</sub>H<sub>5</sub>) (0.5 ml) in iodine (30% mol)<sup>22</sup> have been reported. This method is inexpensive and non-toxic, and iodine is readily available. Ultrasound-accelerated Michael additions of indoles to ketones catalysed by ceric ammonium nitrate (CAN) (10% mol) in anhydrous methanol (3 hours, 86%)<sup>23</sup>, *p*-toluenesulfonic acid (*p*-TsOH) (10% mol) in anhydrous ethanol (1.5 hours, 94%)<sup>24</sup>, and potassium bisulfate (KHSO<sub>4</sub>) (100% mol) in anhydrous ethanol (3 hours, 95%)<sup>25</sup> at room temperature have also been reported. This reaction proceeds via single electron transfer or radical mechanisms. The advantages of this method are higher yields, shorter reaction times, and milder conditions. Chiral bis(oxazoline) (BOX)-metal (II) complexes of, for example, Cu(OTf)<sub>2</sub>, Cu(SbF<sub>6</sub>)<sub>2</sub>, Zn(OTf)<sub>2</sub> catalyse enantioselectively and highly yielded Michael additions of indoles to  $\alpha,\beta$ -unsaturated malonates in MeCN, Et<sub>2</sub>O, THF and CH<sub>2</sub>Cl<sub>2</sub> at -20, -25, and 0 °C<sup>26,28,29</sup> and to  $\alpha'$ -hydroxy

enones in  $\text{CH}_2\text{Cl}_2$ <sup>27</sup> at room temperature or 0 °C. The bis(oxazoline) (BOX) complexes of  $\text{Fe}(\text{ClO}_4)_2 \cdot x\text{H}_2\text{O}$ ,  $\text{CuOTf}$ ,  $\text{Mg}(\text{OTf})_2$ ,  $\text{AgOTf}$ ,  $\text{Pd}(\text{OAc})_2$ , and  $\text{Ni}(\text{OTf})_2$  catalyse asymmetric Friedel-Crafts alkylation of indoles to nitroalkenes<sup>30</sup> in toluene at 15 °C. Tridentate bis(oxazoline) (BOX) complexes of  $\text{Zn}(\text{OTf})_2$ <sup>31</sup> also catalyse the Friedel-Crafts alkylations of indoles to nitroalkenes in toluene at -20 °C.  $\text{Sc}(\text{OTf})_3$ <sup>32</sup> tridentate BOX complexes catalyse the alkylation of indoles to  $\alpha,\beta$ -unsaturated 2-Acyl imidazoles in methylcyanide at -40 °C. Chiral imidazolidinone HX salts of TFA, *p*-TsOH, 2- $\text{NO}_2\text{PhCO}_2\text{H}$  in  $\text{CH}_2\text{Cl}_2$  at -40 °C were utilized for fairly enantioselective Michael additions of indoles to  $\alpha$ - $\beta$  unsaturated aldehydes<sup>33</sup>. Aluminium Salen complexes were used as catalyst for enantioselective reactions between indoles and (*E*)-arylcrotyl ketones<sup>34,35</sup> in toluene and in the presence of 2,6-lutidine (10 mol %) at room temperature, -15 °C, and -20 °C and (*E*)-2-(2-nitrovinyl) furan and thiol in toluene and  $\text{CH}_2\text{Cl}_2$  in the presence of 2,6-lutidine (10 mol %) at room temperature<sup>36</sup>. The reduction of the nitro group to amino by lithium aluminum hydride ( $\text{LiAlH}_4$ ) is a key step to the synthesis of tryptamine lead compounds which possess various biological activities<sup>36</sup>. All these Michael additions occur at the C-3 ( $\beta$ ) position of indoles. Fig. 4 reveals a summary of the above conjugate additions.





increases (H, F, and OMe) the proportion of this product increases accordingly (56% to 80%). However, when the diethoxyphosphonate was replaced by ethyl formate the proportion of C-3 substituted product reached 100%. Hence, in acidic solutions, the nature of the conjugated molecule plays a significant role in the leading of this type of Michael addition of indoles. The electron-efficiency of the substituent comes after this factor. In basic solution (sodium hydride (NaH) in tetrahydrofuran (THF)), aza substituted product was only observed when the electron-efficiency of C-5 position increased (H, F, and OMe). However, when the diethoxyphosphonate was substituted with ethyl formate, 3'-substituted product was observed and as the electron-efficiency of the substituent on the 5'-position increased, the proportion of this product also increased. In the case of 5-nitroindole and ethyl formate, the aza substituted product was only observed. In fact, in basic solutions, the nature of the substituent on the 5'-position of indole plays a key role in the formation of products. The nature of the conjugated molecule comes after the first factor. Strong electron-withdrawing group (EWG) would lead to a sole aza-substituted product (Fig. 6)<sup>39</sup>.

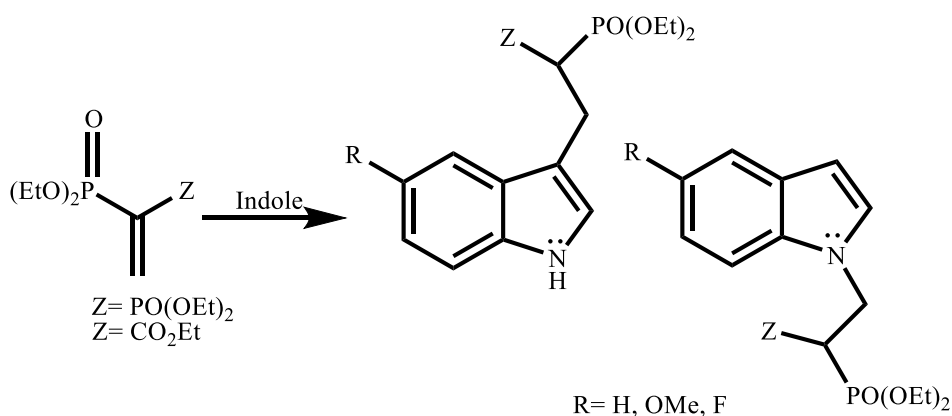


Fig. 6 Aza-Michael addition of indoles<sup>39</sup>

#### 1.1.2.1.2 The factors affecting the Michael Addition of indoles to various $\alpha,\beta$ -unsaturated compounds

The electron efficiency of substituents on indoles and Michael acceptors controls regioselectivity, yield and reaction time respectively. The amount and nature of the catalyst dominate yield and the proportion of enantiomeric excess (stereoselectivity) respectively (Indium and Ytterbium salts and chelating metal (II) and (III) complexes). In chiral chelating metal (II) and (III) complexes catalysed reactions, due to the regioselective binding of the

chelating agent and the other groups in case of branched enones and providing a steric hindrance for the nucleophile to attack, the formation of a specific enantiomer is favored. A catalytic amount of additives such as TMSCl to  $\text{InBr}_3$  enhances the yield (85% to 96%). The reaction conditions such as temperature and medium (polarity of the non-aqueous medium and acidity or basicity) lead to the change in the yield and proportion of enantiomeric excess and regioselectivity.

### 1.1.2.2 Anti-Michael addition of indoles

Conjugated acetylenes in the presence of triphenylphosphine as a basic catalyst undergo 1,3-addition ( $\alpha$ -addition) reaction by indoles via a vinylphosphine intermediate (olefin with the strong electron-withdrawing group) followed by a proton-shift and phosphine elimination step respectively. This reaction is an example of aza-addition of indoles (Fig. 7)<sup>8</sup>.

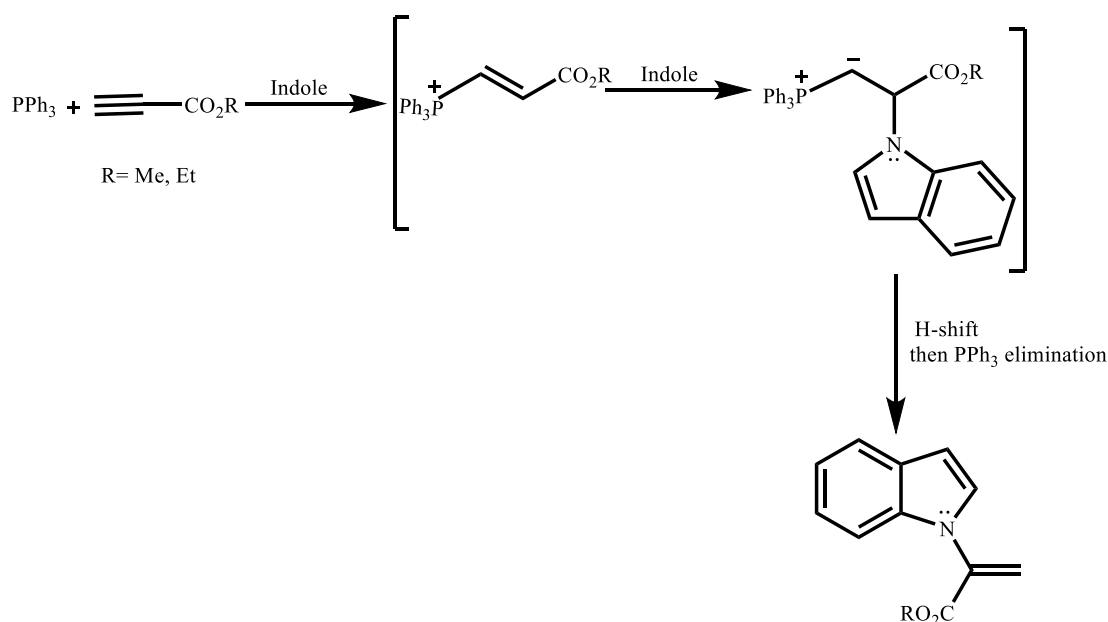


Fig. 7 An example of Anti-Michael addition of indoles under basic conditions<sup>8</sup>

### 1.1.2.3 Friedel-Crafts (F-C) reactions of indoles to epoxides

Previous studies on regioselectivity and stereoselectivity of Lewis acid catalysed reactions of epoxides confirmed the formation of two products due to the lack of regioselectivity in the ring opening step<sup>40</sup>. However, using  $\text{InCl}_3$  led to the enantioselective and regioselective

reactions in which only one product is a favor. In fact, aryl or alkyl epoxides in the presence of  $\text{InCl}_3$  in anhydrous THF at room temperature conducted carbonylation rearrangement<sup>41</sup> to form aryl and alkyl ketones or aldehydes. The ring-opening reactions of enantiomerically pure aromatic epoxides by indoles had been carried out at high pressure (10 Kbar)<sup>42</sup> at 42 °C in acetonitrile and on silica gel<sup>43</sup> at room temperature. *Bandini et al*<sup>44</sup> carried out studies on the reactions of indoles to styrene oxides in the presence of various Lewis acid catalysts such as  $\text{Cu}(\text{OTf})_2$ ,  $\text{Zn}(\text{OTf})_2$ ,  $\text{InCl}_3$ , and  $\text{InBr}_3$  in anhydrous  $\text{CH}_2\text{Cl}_2$ .  $\text{InBr}_3$  (5 and 1 mol %) showed the highest yields 64% and 70% respectively with the slight racemization (99% enantiomeric excess) because of the minor pathway via carbocation. In the other study undertaken by *Bandini et al*<sup>45</sup>  $[\text{Cr}(\text{salen})\text{Cl}]$  and  $[\text{Cr}(\text{salen})\text{SbF}_6]$  complexes (5 mol %) were used in TBME (*tert*-butyl methyl ether) and TBDMS (*tert*-butyldimethylsilyl) at room temperature to proceed the reaction of indole to a racemic mixture of styrene oxide. The results confirmed the formation of one stereoisomer with a fair enantiomeric excess of 56% due to kinetic resolution<sup>46</sup> (Fig. 8).

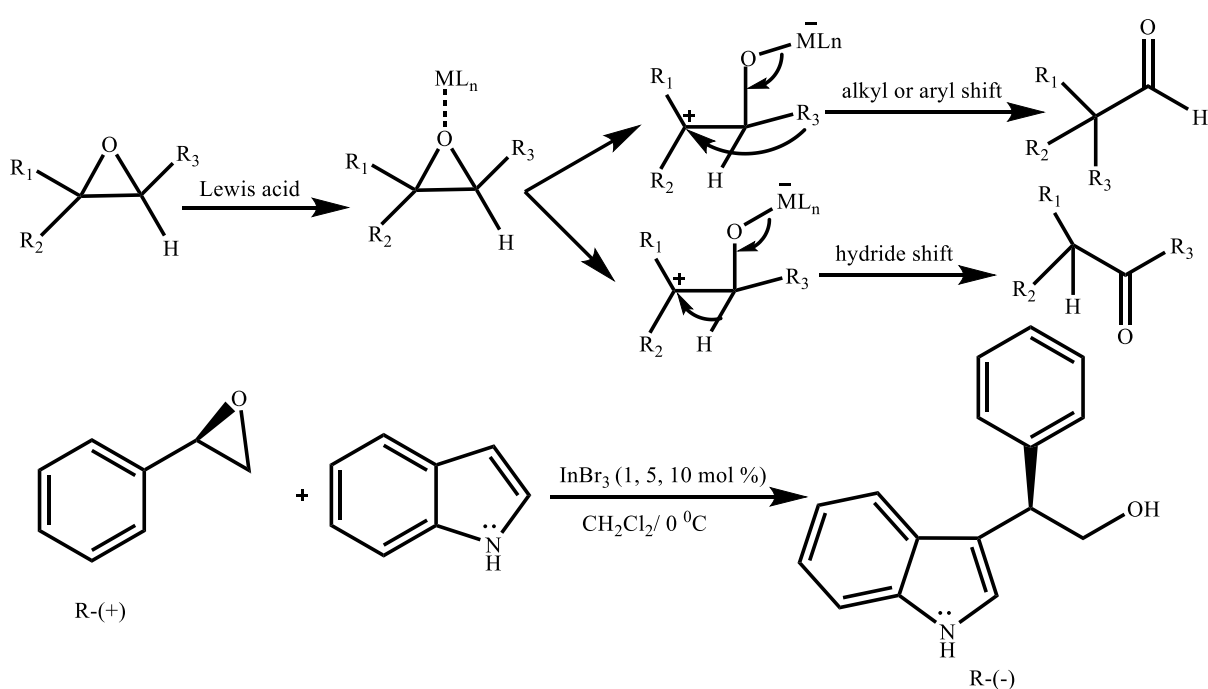


Fig. 8 Carbonylation rearrangement in epoxides and the enantioselective reaction of indole with Styrene oxide<sup>41,44</sup>

#### 1.1.2.4 Electrophilic substitution reaction of indoles to carbonyl compounds such as aldehydes and ketones

This type of reaction leads to the formation of an important class of biologically active compounds named bis(indolyl)methanes (BIMs). BIMs are well-known for their anti-bacterial<sup>58</sup>, anti-fungal<sup>59</sup>, histone deacetylase inhibitory (HDAi)<sup>60</sup>, and anti-cancer activities<sup>61</sup>. The formation of bis(indolyl)methanes in protic acids such as HCl<sup>47</sup> at room temperature, and Lewis acids, for example, Ln(OTf)<sub>3</sub><sup>48</sup> in aqueous ethanol, InCl<sub>3</sub><sup>49</sup> in MeCN, Dy(OTf)<sub>3</sub><sup>50</sup> in 1-butyl-3-methylimidazolium tetrafluoroborate ([BMIM]BF<sub>4</sub>), CeCl<sub>3</sub>, TaCl<sub>5</sub>, YCl<sub>3</sub>, and ZnCl<sub>2</sub><sup>51</sup> in CH<sub>3</sub>CN at room temperature, I<sub>2</sub><sup>52</sup> under free-solvent conditions, and protic solvents such as CH<sub>3</sub>OH and water<sup>53</sup> at room temperature has been reported. However, many Lewis acids are decomposed or deactivated by nitrogen-containing compounds within the trapping process; hence, more stoichiometric amounts of Lewis acids are required<sup>54</sup>. A. Kamal *et al*<sup>55</sup> designed the reactions between various electron-efficient and electron-deficient substituted aromatic and aliphatic aldehydes and indole catalysed by Al(OTf)<sub>3</sub> (0.5 mmol %) as Lewis acid in CH<sub>3</sub>CN at room temperature. The reactions resulted in the production of bis(indolyl)methanes in high yields (75-96%). Aromatic aldehydes with one slightly to moderately electron-rich substituent such as *i-pr* and Cl at *o* or *p*-position of the formyl group showed shorter reaction times (3,4, and 6 min) than aliphatic (methyl, ethyl, and butyl formaldehyde) and aromatic aldehydes with one strong electron-deficient and one or two electron-efficient substituent(s) such as NO<sub>2</sub>, OMe, and OH at *o*, *m*, and *p* positions. The aldehydes with lowest reaction times also showed relatively higher yields compared to the other aldehydes (90%-95%). Winstein S. *et al*<sup>57</sup> in 1959 had discovered that when lithium perchlorate/diethylether (LPDE) dissolves in the reaction medium, it noticeably enhances the polarity of the reaction medium. They had also found out that LPDE is even more polar than acetic acid (CH<sub>3</sub>CO<sub>2</sub>H). Heydari A. *et al*<sup>56</sup> used (5M) LPDE for the reactions of aldehydes, hydroxylamines, and trimethylsilyl cyanide to produce  $\alpha$ -cyanohydroxylamines at room temperature. J. S. Yadav *et al*<sup>51</sup> used (5 M) LPDE and LiClO<sub>4</sub> in MeCN as Lewis acid at room temperature in the reactions of indoles to aromatic and aliphatic aldehydes and heterocyclic ketones and 2-methyl-1-*H*-indole to *p*-methoxybenzaldehyde at room temperature. LPDE showed lower reaction times and higher yields (2-10 hours and 78%-95%) compared to those of LiClO<sub>4</sub>/MeCN (4-10 hours and 67%-92%). In LPDE, benzaldehyde with 2-methyl-1-*H*-indole and aryl aldehydes with strong one or two electron-rich substituent(s) such as OMe and OEt on phenyl ring with indole showed higher yields and

lower reaction times (2.0-4.0 hours and 90-95%) than aliphatic (pentanal) and heterocyclic aldehydes (cyclohexanecarbaldehyde) and heterocyclic ketones (cyclohexanone and cyclopentanone) with indoles (5.0-8.0 hours and 78%-89%). *m*-nitrobenzaldehyde with indole showed the lowest yield and highest reaction time than the other reactants (10 hours and 75%). 3,4-Dichlorobenzaldehyde with indole showed remarkable reaction time and yield (2.5 hours and 90%). In LiClO<sub>4</sub>/MeCN fairly similar results as LPDE with the exception of cyclopentanone which showed the lowest reaction time as *m*-Nitrobenzaldehyde were obtained. 10% lithium trifluoromethanesulfonate-lithium triflate (LiOTf) showed shorter reaction times (0.5-3 hours) than both LPDE and LiClO<sub>4</sub> in MeCN. The mechanism of the formation of bis(indolyl)methanes in the presence of a Lewis acid is shown in Fig 9.

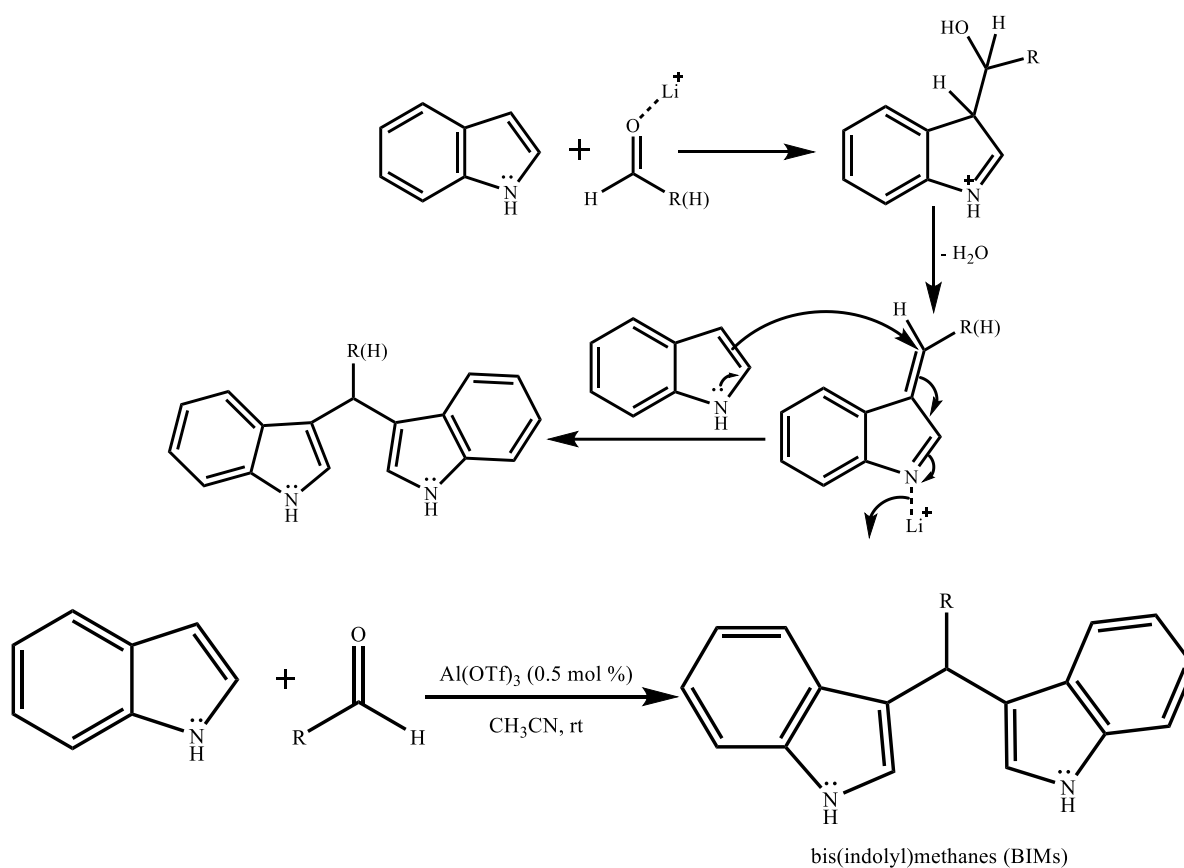


Fig. 9 The plausible mechanism of the synthesis of bis(indolyl)methanes<sup>55</sup>

*B. V. Subba Reddy et al*<sup>62</sup> designed a three-component reaction between Kojic acid, benzaldehydes, propionaldehyde, and indoles in the presence of InCl<sub>3</sub> at 120 °C (55-80 min and 75%-90%) (Fig. 10). One or two electron-rich substituent(s) such as OPh and OMe at *m*- or *p*-position of the benzaldehydes and electronegative halogens such as Br and Cl at the 5'-position of indoles led to the faster reactions with higher yields (55-70 min and 80%-90%)



than Cl and OPh at *p*- and 2'-position(s) of benzaldehydes and indoles respectively (75-85 min and 75%-85%). Propionaldehyde with 2-phenyl-1*H*-indole showed moderate reactivity (80 min and 80%) (Fig. 10).

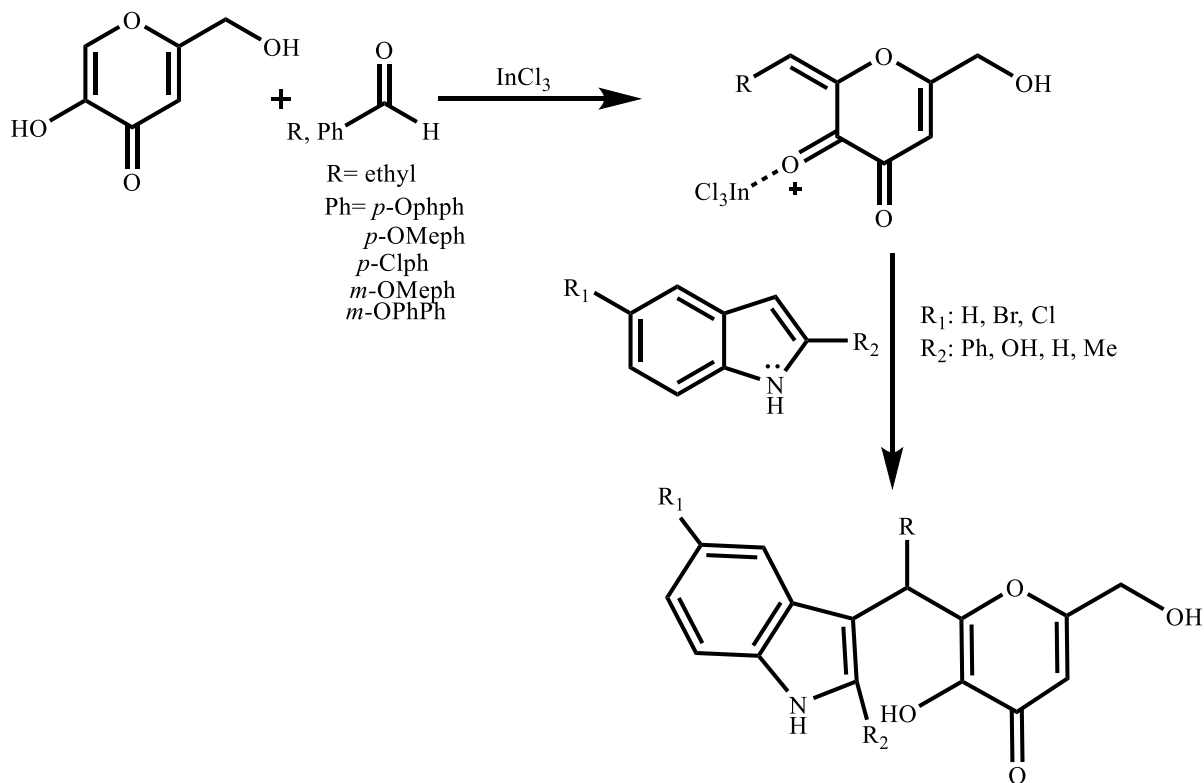


Fig. 10 Three component reaction of indoles in the presence of kojic acid<sup>62</sup>

#### 1.1.2.4.1 The factors affecting the electrophilic substitution reactions of indoles to aldehydes and ketones

In aromatic electrophilic substitution reactions of indoles with aldehydes, electron-efficacy of the substituents on the phenyl ring of benzaldehyde plays a significant role in the rate and the yield of the reactions. In fact, electron-rich substituents conduct the reactions more efficiently than electron-deficient substituents. Electronegative halogens such as Cl and Br could result in faster reactions with higher yields. In term of the reaction medium,  $\text{Al}(\text{OTf})_3/\text{MeCN}$  showed faster reactions than kojic acid and  $\text{InCl}_3$ ,  $\text{Li}(\text{OTf})$ , LPDE, and  $\text{LiClO}_4/\text{MeCN}$  respectively. However, all of the above reaction mediums showed high yields.

### 1.1.2.5 The electrophilic substitution reactions of indoles to isatins

Di(indolyl)indolin-2-ones are of great interest because of their various biological activities such as antiproliferation against human lung cancer and breast cancer A-549 and MDA-MB-231 cell lines<sup>63</sup>, antibacterial, and antifungal<sup>64</sup> activities. Di(indolyl)indolin-2-ones are the products of indoles and isatins via an electrophilic substitution reaction. These reactions are catalysed by transition metal salts, for example,  $\text{Cu}(\text{OTf})_2$ <sup>64</sup> and  $\text{FeCl}_3$  in  $\text{MeCN}$ <sup>66</sup>,  $\text{I}_2$  in  $\text{CH}_2\text{Cl}_2$ <sup>63</sup> and in *ipr*-OH<sup>70</sup>, palladium (II) nanoparticles (PdNPs)<sup>65</sup> in aqueous or non-aqueous media, ionic liquids<sup>67</sup> such as *N,N,N,N*-tetramethylguanidinium trifluoroacetate (TMGT), *N,N,N,N*-tetramethylguanidinium triflate (TMGT<sub>f</sub>), 1-butyl-3-methylimidazolium tetrafluoroborate ([BMIM]BF<sub>4</sub>), [BMIM]BF<sub>4</sub> doped with 60 mol % of LiCl ([BMIM]BF<sub>4</sub>-LiCl), CAN under Ultrasonic in EtOH<sup>68</sup>, silica sulfuric acid in  $\text{CH}_2\text{Cl}_2$ <sup>69</sup>, and potassium aluminum sulfate  $\text{KAl}(\text{SO}_4)_2 \cdot 12\text{H}_2\text{O}$  at room temperature<sup>71</sup>. In an investigation carried out by *C. Praveen et al*<sup>64</sup> that di(indolyl)-indolin-2-ones were obtained in the presence of  $\text{Cu}(\text{OTf})_2/\text{MeCN}$  (15-45 min and 85%-95%), the results are as follows: strong electron-rich substituents such as OMe at 5'-position of indole and strong to moderate electron-deficient groups such as  $\text{NO}_2$ , Cl, and Br at the 5'-position of isatins enhanced the rate and yield of the reactions respectively (15 min and 90%-95%). The reaction and the products are shown in Fig. 11.

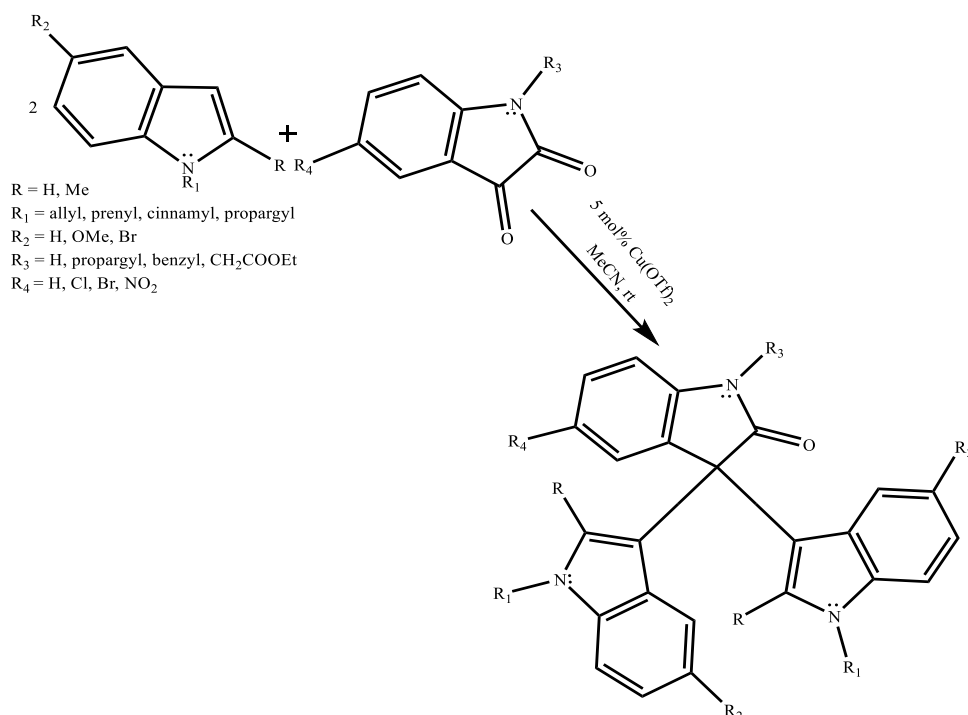


Fig. 11 The synthetic approaches to di(indolyl)-indolin-2-ones by *C. Praveen et al*<sup>64</sup>

## 1.2 Indoles in nature

Indolyl moiety is part of a wide variety of naturally occurring compounds extracted (isolated) from marine sponges and plants as well as microorganisms such as bacteria and fungi. Most of these naturally indole-containing compounds reveal a wide spectrum of biological activities as well as antibacterial, antifungal, antiviral, and anticancer activities. Here is an overview of some of these compounds including their bioactivities.

### 1.2.1 Naturally occurring indole-containing compounds in marines and plants

Bis-indolyl alkaloids, for example, Hamacantin A and Hamacantin B were isolated from deep-water marine sponge *Hamacantha* sp. by S. P. Gunasekera et al<sup>73</sup>. These two compounds showed antifungal activities against *Candida albicans* (*C. albicans*) and *Candida neoformans* (*C. neoformans*) with minimal inhibitory concentration (MIC) values of 1.6, 3.1 µg/ml and 6.2, 6.2 µg/ml respectively. Fascaplysin extracted from Fijian sponge *Fascaplysinopsis Bergquist* sp. by D. M. Roll et al<sup>76</sup> inhibited the growth of *Staphylococcus aureus* (*S. aureus*) and *Escherichia coli* (*E. coli*) with the zone of inhibitions of 15 mm and 8 mm at the concentrations of 0.1 and 5 µg/disk respectively. Fascaplysin was also active against *Saccharomyces cerevisiae* and *C. albicans* (zone of inhibitions of 20 mm and 11 mm at the concentrations of 0.1 and 1 µg/disk respectively) and murine leukemia cells L1210 with the IC<sub>50</sub> of 0.2 µg/ml. Grossularine-1 and grossularine-2 (examples of α-carbolines) were extracted from marine tunicate *Dendrodia grossularia* by C. Moquin et al<sup>80</sup>. Remarkable cytotoxicity against L1210 leukemia cells (6 and 4 µg/ml respectively), and solid human tumor cell lines of WiDr (colon) and MCF7 (breast) (up to 10 ng/ml) were observed. S. C. Bobzin et al<sup>83</sup> extracted Chelonin A, B, Bromochelonin B, and Chelonin C from marine sponge *Chelonaplysilla* sp. Chelonin A showed *in-vivo* anti-inflammatory activity (60% inhibition of PMA-induced inflammation of the mouse ear at a concentration of 50 pg/ear) and antibacterial activity against *Bacillus subtilis* (100 µg/ml). Meanwhile, Chelonin B and Bromochelonin B only showed antibacterial activities (100 µg/disk). N. Fusetani et al<sup>84</sup> isolated Orbiculamide A from marine sponge *Theonella* sp. Orbiculamide A showed cytotoxic activity against P388 murine leukemia cells (IC<sub>50</sub> value of 4.7 pg/mL). C. A. Bewley et al<sup>85</sup> extracted cyclic hexapeptides Microsclerodermins A and B from deep water sponge of the genus *Microscleroderma*. These compounds inhibited the growth of *C. albicans* (IC<sub>50</sub> ~ 2.5 µg/disk). Didemnimides A-D and E and isogranulatimide were extracted from Ascidian

*Didemnum granulatum* by R.G. S. Berlinck *et al*<sup>88</sup>. Keramamide A<sup>86</sup>, K, and L<sup>87</sup> are other cyclic peptides extracted from *Theonella* sp. Didemnimides A-D<sup>89</sup> were recognised to be the source of toxic secondary metabolites with potential cytotoxicity to defend against the attack of carnivorous fish. Isogranulatimide was likely to show cytotoxicity against cancerous (DNA-damaged) P-53 cell lines by plausible inhibition mechanism at the G2 checkpoint. Topsentin and some of its derivatives such as Bromotopsentin and 4,5-Dihydro-6'-deoxybromotopsentin were isolated from Caribbean deep-sea sponges of the family of *Halichondriidae* by S. Tsujii *et al*<sup>75</sup> and showed good *in-vitro* cytotoxicity against P388 murine leukemia cell line with the IC<sub>50</sub> Values of 2.0, 7.0, 4.0 µg/mL, respectively. Topsentin also showed 25%-50% and 50%-75% inhibitions at the concentration of 200 µg/disk and 20 µg/disk against herpes simplex virus (HSV-1) and mouse hepatitis virus (MHV) strain A-59, respectively. Bromotopsentin showed the 50%-75% inhibition against MHV at the concentration of 2 µg/disk. Nortopsentins A, B, and C showed antifungal activity against *C.albicans*. Topsentin A, B1, and B2 are defense chemicals in marine sponge *Topsentia genitrix* with weakly toxic effect for fish and dissociated cells of the freshwater marine sponge *Ephydatiafluviatilis*<sup>74</sup>. Martefragin A was extracted from sea alga *Martensia fragilis* Harvey. This compound showed strong inhibition activity in lipid peroxidation<sup>78</sup>. Convolutindole A which showed nematocidal activity was extracted from marine Bryozoan *Amathia convoluta*<sup>79</sup>. Caulerpin<sup>81,82</sup> has a structure similar to auxin and regulates the plant growth. This compound was extracted from green algal genus *Caulerpa* (a genus of seaweeds). Phytoalexins are antimicrobial and antioxidative agents which are induced by some plant species in response to pathogens attack. 3-Thiazole-2'-yl-indole (Camalexin) is a phytoalexin induced by crucifer *Camelina Sativa* and *A.thaliana* plant species in response to *Alternaria Brasicae* and *Pseudomonas syringae*, respectively.

Vinblastine, ajmalicine, tetrahydroalstonine, serpentine, reserpine, and akuammine<sup>72</sup>, 6-bromotryptamine, 2,2-bis(6'-bromo-3'-indolyl)ethylamine which are two derivatives of tryptamine, and 2,5-bis(6'-bromo-3'-indolyl)piperazine<sup>77</sup>, and manzamine A, B, and C<sup>90</sup> are other indole-containing compounds extracted from plants and marines.

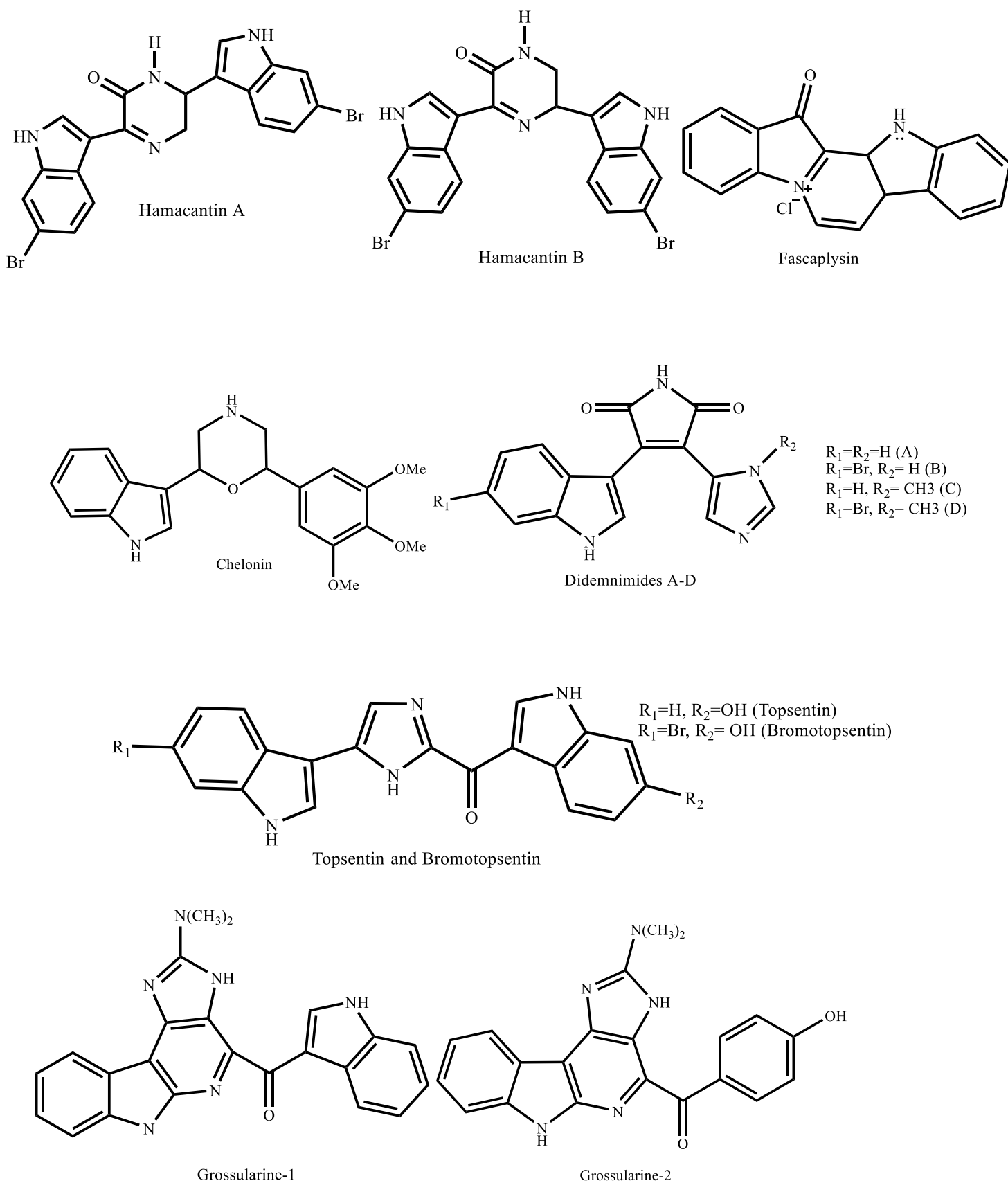


Fig. 12 Some important indole-containing compounds in marines and plants<sup>73,75,76,80,83,88,89</sup>

### 1.2.2 Naturally occurring indole-containing compounds in microorganisms

2-Methyl-5-(3-indolyl)oxazole pimprinine was isolated from *Streptomyces pimprina*. Pimprinethine was isolated from *Streptomyces cinnamoneus*. Pimprinaphine (2,5-disubstituted (3-indolyl)oxazole) was isolated from *Streptoverticillium olivoreticuli*. Other derivatives such as 2-ethyl, 2-n-propyl, and 2-n-butyl were also extracted and isolated from *Streptomyces cinnamoneus* and *Streptoverticillium waksmanii* respectively<sup>91</sup>. 2-Isobutyl-5-(3-indolyl)oxazole (Labradorin 1) and 2-n-pentyl-5-(3-indolyl)oxazole (Labradorin 2) were extracted from *Pseudomonas syringae* pv. *Coronafaciens*<sup>92</sup>. Labradorin 1 revealed half of maximal of growth inhibitions (GI<sub>50</sub>) of 6.2, 3.9, 5.1, 9.8, 3.5, and 4.0 µg/ml against BXP-3 (pancreas-a), MCF-7 (breast), SF-268 (CNS), NCI-H460 (lung-NSC), KM20L2 (colon), and DU-145 (prostate) cell lines respectively, while Labradorin 2 had GI<sub>50</sub> values of 9.6, 27.4, 58.8, 9.6, 9.7, and 11.4 µg/ml against above human cancer cell lines. Asterriquinone and its derivatives (ARQ) (bis-indolyl derivatives) as metabolites of biosynthesis of indolepyruvic acid<sup>94</sup> were isolated from mycelium of *Aspergillus terreus* IFO 6123<sup>93</sup>. Kaji A et al<sup>97,98</sup> examined the anti-cancer activity of Asterriquinone A and its derivatives. These compounds showed antitumor activity against mouse leukemia P388 cells with the IC<sub>50</sub> values of 0.07-1.50 µM via formation of DNA interstrand cross-link (ISC), intercalation in genomic DNA, arresting G1, and finally apoptotic cell death. These compounds also showed antidiabetic activity as insulin receptor tyrosine kinase activating agent (insulin mimetic)<sup>95</sup>. Aspergillamide A and the corresponding *E*-olefin, aspergillamide B were extracted from the mycelium of a cultured marine fungus genus *Aspergillus*. Aspergillamide A was active toward the human colon carcinoma cell line HCT-116 with IC<sub>50</sub> value of 16 µg/ml<sup>96</sup>.

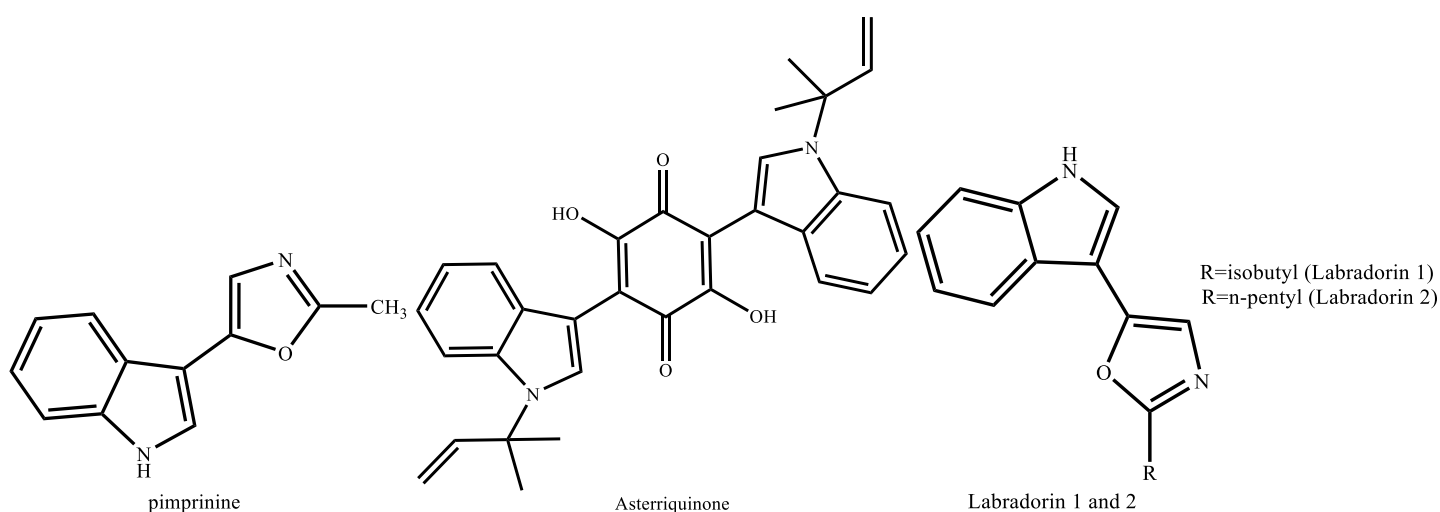


Fig. 13 some examples of indole-containing compounds in microorganisms<sup>91,92,93</sup>

### **1.3 Bacteria, cell growth mechanisms, and modes of action of some commercial antibacterial agents**

Bacteria are the brilliant members of the prokaryotic (unicellular) organisms. In contrast to eukaryotic cells (animal cells), prokaryotes do not possess mitochondria (cellular energy supplying organelle) and a membrane-bound nucleus. However, they possess cytoplasm nucleoid (DNA and RNA), ribosomes, cell wall, and cell membrane. Nucleoid and ribosomes are in the cytoplasm surrounded by a cell membrane. The cell wall surrounds the cell membrane. Eukaryotic cells do not have a cell wall. The modes of action of anti-bacterial agents toward bacterial cell growth and multiplying are as follows:

**1.3.1 Inhibition of cell metabolism (antimetabolites)** The good example of anti-bacterial agents acting via this mechanism is a group of sulfonamides. These agents mimic the *p*-aminobenzoic acid (PABA); one of the normal substrates for the dihydropteroate synthetase, and inhibit the biosynthesis of tetrahydrofolate which is a co-enzyme factor providing one-carbon units for the synthesis of pyrimidine nucleic acid bases for the DNA synthesis via a competitive route to dihydropteroate synthetase. Other sulfonamide analogs are sulfathiazole, sulfadiazine, sulfadoxine, sulfamethoxazole, and sulfones. Most of the sulfonamides are bacteriostatic (they only prevent the bacteria from growing and multiplying and do not reveal mortal effect). Trimethoprim which has a diaminopyrimidine structure is against dihydrofolate reductase that catalyses the conversion of dihydrofolate to tetrahydrofolate in the further step from sulfonamides. Cotrimoxazole contains both trimethoprim and sulfamethoxazole. Hence, the safe levels of both anti-bacterial agents can cause a good clinical effect as one single drug in much higher levels with subsequent side effect can cause (sequential blocking).

**1.3.2 Inhibition of cell wall biosynthesis** The cell wall of bacteria is made up of peptidoglycans. The chains of peptidoglycans are cross-linked. A peptidoglycan chain contains the chain of D- and L-amino acids connected via peptide bonds and parallel sugar backbones that have two sugar types: *N*-acetylmuramic acid (NAM) and *N*-acetylglucosamine (NAG). The peptide chain connects to NAM. Different bacterial species in terms of Gram-stain possess different cell wall thicknesses (Gram-positive bacteria contain 50-100 peptidoglycan layers or 20-40 nm and Gram-negative bacteria have two layers or 2-7 nm). Biosynthesis of peptidoglycans and the bacterial cell wall is a chain-synthetic route involving 30 enzymes. The cell wall is porous and the water molecules can enter the cell, but

the porous prevents the cell wall from swelling and bursting. In the first step, uridine triphosphate (UTP) is bound to NAG to form UDP-NAG structure. In the second step, UDP-NAG converts to UDP-NAM by enolpyruvate transferase. Fosfomycin acts as an inhibitor for this enzyme. In the third step, L-alanine-D-glutamic acid-L-lysine tripeptide is linked to NAM (UDP-NAM-tripeptide). In mammals only the L-amino acids are available; however, bacteria are capable of converting L-amino acids to D-amino acids (racemae) and linking them by the enzymes L-alanine racemize and D-alanine-D-alanine ligase, respectively. D-cycloserine mimics the structure of D-alanine and inhibits the two enzymes. After the D-alanine-D-alanine dipeptide is built, it connects to the L-lysine to form UDP-NAM-pentapeptide (UDP-NAM-L-alanine-D-glutamic acid-L-lysine-D-alanine-D-alanine). Bactoprenol (C55 carrier lipid) is a protein which connects to NAM and acts as an anchor to hold the NAM-pentapeptide moiety. Peptidoglycan synthase incorporation with translocase enzyme transports NAM-pentapeptide moiety to the outer surface of the cell membrane, flips out the NAM-pentapeptide, and connects one NAG to NAM. In Gram-positive bacteria such as *S. aureus* pentaglycine moiety is also added to L-lysine in this step. Transglycosidase enzyme binds this new moiety to the rest of the peptidoglycan chain and bactoprenol is released. Bactoprenol available on the outer surface of the cell membrane contains phosphate group. Phosphotase enzyme dephosphorylates this form of bactoprenol and converts it to the active form. Bacitracin inhibits the phosphotase enzyme. Vancomycin molecule has a heptapeptide backbone containing five aromatic rings. This heptapeptide chain can bind to the L-lysine-D-alanine-D-alanine terminal site via hydrogen-bonding and block this site. It then dimerizes to provide the opposite and the adjacent peptidoglycan chains with a big blocking surface that prevents transglycosidase and transpeptidase from approaching. Glycopeptide dimers are likely to change the physical properties of the cell membrane because glycopeptides enhance the activity of aminoglycosides by increasing their absorption through the cell membrane. Glycopeptides likely disrupt RNA synthesis. Vancomycin was firstly used against penicillin-resistant *Staphylococcus aureus* but was then replaced by methicillin. It is now again used against MRSA. Size of vancomycin limits its effectiveness against Gram-positive and Gram-negative bacteria because it is unable to cross through the outer cell membrane of Gram-negative bacteria but it does work against Gram-positive bacteria because the cell wall biosynthesis is carried out on the outer surface of the inner cell membrane. In 1989 and 1996, the resistance to vancomycin by Enterococci (VRE) and *S. aureus* (MRSA) was reported chronologically. Teicoplanin A<sub>2-5</sub>, telavancin, and eremomycin are the other members of the glycopeptides family. The final step of bacterial cell wall



biosynthesis is the cross-linking of peptide chains; that means that the peptide chains are linked together via the displacement of D-alanine from one chain by glycine in another one in *S. aureus* and by L-lysine in Gram-negative bacteria such as *E. coli*. This step is catalysed by the transpeptidase enzyme. Transpeptidase binds to the outer surface of a cell membrane and the serine residue of it ( $\alpha$ -amino acid with the  $\beta$ -hydroxyl group) acts as a nucleophile and attacks the carbonyl group in the D-alanine-D-alanine dipeptide in the terminal site of a peptidoglycan chain and kicks out the terminal D-alanine. In the next step, the amino group of adjacent glycine or L-lysine attacks the D-alanine and makes cross-link by kicking out the O-serine group.  $\beta$ -Lactam drugs which possess cyclic amide structure such as penicillin mimic the D-alanine-D-alanine dipeptide and are attacked on the amido group by transpeptidase accordingly. As a result of this attack, the lactam opens and CO(O-serine) and amino groups are formed. The adjacent glycine or lysine group will no longer have an active site to attack, no cross-linking will occur, and the bacteria will no longer be able to grow and multiply. Due to the resistance of some bacterial species to penicillin, for example, *Pseudomonas aeruginosa* and *S. aureus*, methicillin was introduced as a replacement for penicillin. Methicillin has a structure similar to penicillin but it contains a fairly electron-withdrawing bulky group on the side chain of the  $\beta$ -lactam which reduces the nucleophilic attack by  $\beta$ -lactamase enzyme and hydrolysis. The fairly hydrophobic bulky groups on the side chain of lactam lead to a better activity against Gram-positive bacteria but less activity against Gram-negative bacterial strains. Hydrophilic groups might lead to more or less activity against Gram-positive but more activity against Gram-negative bacteria because the Gram-negative bacteria have the outer cell-membrane made up of lipopolysaccharide. This membrane has porins. Small-sized hydrophilic negative charged drugs can pass through the porins to reach the inner cell membrane. The space between the outer cell membrane and the cell wall is known as periplasmic space. Aminopenicillins such as ampicillin (Penbritin) and amoxicillin (Amoxil), carboxypenicillins such as carbenicillin, carfecillin and indanyl carbenicillin (prodrugs for carbenicillin), and ureidopenicillins are broad-spectrum  $\beta$ -lactam drugs (effective against both Gram-positive and Gram-negative bacteria) because of their bulky hydrophilic amino, carboxyl, and urea groups on the side chain of  $\beta$ -lactam. Cephalosporins are the second major group of  $\beta$ -lactam drugs. The first, second, third, fourth, and fifth generations of cephalosporins including cephalosporin C, cephamycins, ceftazidime and its analogs such as ceftriaxone, cefepime and cefpirome, and ceftaroline fosamil inhibit the bacterial cell wall biosynthesis via the same mechanism as penicillins. Carbapenems including imipenem, meropenem, and ertapenem are the other  $\beta$ -lactams inhibiting the

bacterial cell wall synthesis in a similar way to penicillins and cephalosporins. Carbapenems have the broadest spectrum activity of all the  $\beta$ -lactam antibiotics.

**1.3.3 Impairing the protein synthesis translation:** The function of the ribosome is to provide a place on which translation (protein biosynthesis) is carried out. Ribosome contains two subunits, the small subunit which contains 30S particles and binds to messenger RNA, and a large subunit that contains 50S particles and binds to small subunit-mRNA to provide a binding surface for aminoacyl-transfer RNA (tRNA). tRNA has two binding sites: peptidyl (P-site) and aminoacyl (A-site) sites. Aminoglycosides such as streptomycin and gentamycin C1a bind to the small subunit of the ribosome and prevent the movement of the ribosome along mRNA. As a result, the shortened proteins are released. Tetracyclines such as tetracycline, chlortetracycline (aureomycin), and doxycycline also bind to the small subunit of the ribosome and prevent the aminoacyl tRNA from binding. Chloramphenicol binds to the large subunit of the ribosome and apparently inhibits the movement of ribosomes along mRNA and the peptidyl transferase reaction by which the peptide chain is prolonged. Chloramphenicol binds to the same region as macrolides as well as erythromycin. Clarithromycin, azithromycin, and telithromycin are the other members of this group. Lincosamides, for example, lincomycin and clindamycin are identical to macrolides in terms of their mode of action. Quinupristin and dalfopristin are the extracts of pristinamycin which bind to the two different regions of the ribosome's large subunit. Apparently, the binding of dalfopristin increases the affinity of the ribosome for quinupristin (synergic effect). Quinupristin inhibits peptide chain elongation, while dalfopristin interferes with the transfer of the peptide chain from one tRNA to the next. Oxazolidinones bind to the large subunit of the ribosome and prevent it from combining with the small subunit to form ribosome. Linezolid and radezolid are examples of oxazolidinone drugs.

**1.3.4 Inhibition of nucleic acid transcription and replication** Quinolones and fluoroquinolones such as nalidixic acid, enoxacin, and ciprofloxacin inhibit the DNA transcription and replication by stabilizing the complexes between DNA and topoisomerases. In Gram-positive bacteria, the stabilized complexes are between DNA and topoisomerase IV enzyme while in Gram-negative bacteria the main target for fluoroquinolones is the complex between DNA and a topoisomerase II enzyme called DNA gyrase. It has the same role as

topoisomerase IV in reverse and is required when the DNA double helix is being supercoiled after replication and transcription. Ofloxacin, levofloxacin, moxifloxacin, and besifloxacin are the fourth and fifth generations of fluoroquinolones in response to the resistance of *S. aureus* species to fluoroquinolones. Aminoacridines such as proflavine act via direct interaction with DNA (intercalation). Rifamycins, as well as rifampicin, inhibit the start of RNA synthesis by binding non-covalently to DNA-dependent RNA polymerase. Rifaximin is another semisynthetic analog of rifamycins. Nitroimidazoles (metronidazole) and nitrofurantoin undergo reduction within bacterial cells to form radical species that are toxic for DNA. Fidaxomicin; a narrow-spectrum drug, inhibits transcription in *Clostridium difficile* (*C. difficile*) species by inhibiting RNA polymerase<sup>99</sup>.

**1.3.5 Fatty acid biosynthesis inhibition (FabI):** Cell growth of some strains of *E. coli* and *S. aureus* processes via fatty acid biosynthesis. Each step of this synthesis is catalysed by an individual enzyme. In the final step, *trans*-2-enoyl ACP should be reduced to acyl ACP. This reaction is catalysed by an enzyme known as enoyl-acyl carrier protein reductase (ENR) (FabI). 4-Hydroxybenzyl-*N*-substituted-(4-hydroxyphenyl)(1,3,4,5-tetrahydro-2H-pyrido[4,3-*b*]indol-2-yl)methanone uses two different sites when it binds to FabI-NAD<sup>+</sup> complex in *S. aureus* and *E. coli*. Co-crystallization results showed that the benzamide moiety of this compound is surrounded by lipophilic residues in which Tyr 146 appears to participate in an orthogonal  $\Pi$ -stacking interaction with the aromatic ring. The 4-hydroxy substituent on the ring is closely flanked by Met 206 and Phe 203 which may account for the observed steric effects. The carbonyl oxygen of this compound is apparently involved in a hydrogen bonding interaction to the 20-ribose hydroxyl of NAD<sup>+</sup> and to the hydroxyl group of Tyr 156. This particular active-site interaction is analogous to that reported for triclosan in which a phenol hydroxyl acts with similar capacity. Triclosan has multiple cellular targets and its mode of action is not exclusively FabI<sup>100-103</sup>.

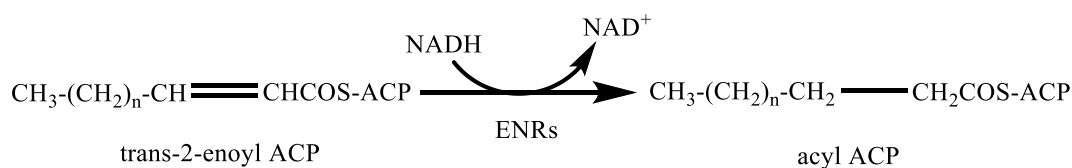


Fig. 14 The mechanism of FabI<sup>103</sup>

The other possible mechanisms are plasma membrane disrupting caused by valinomycin, gramicidin A, polymixin B, and daptomycin. Isoniazid, ethambutol, and pyrazinamides inhibit the mycobacterial cell wall synthesis by inhibiting the synthesis of mycolic acid (an essential precursor for mycobacterial cell wall) and by inhibiting arabinosyl transferase enzyme (a necessary enzyme for mycobacterial cell wall biosynthesis)<sup>99</sup>.

#### **1.4 Drug resistance, the possible mechanisms, and examples**

Mutations in the DNA and genes of organisms may cause drug resistance. In drug resistance, the safe doses (levels) of a drug are no longer effective against pathogenic organisms. Hence, higher doses should be introduced to overcome this problem. Nevertheless, in patients with acute infectious diseases or immune deficiency as well as HIV suffering and organ transplant patients, higher doses of antibiotics can risk their lives. As a result, many investigations and attempts have been made to introduce new bioactive agents. The possible reasons for drug resistance and some examples are given below:

In sulfonamide drugs because of the competitive mechanism of these drugs and reversibility, some Staphylococci, Pneumococci, and Gonococci can acquire resistance by synthesizing more PABA. Mutations leading to dihydropteroate synthetase modification reduce the tendency of the enzyme to bind sulfonamide molecules or by decreased cell membrane permeability for sulfonamides. Some strains of *E. coli* have revealed resistance to trimethoprim. In the case of  $\beta$ -lactam drugs such as penicillin,  $\beta$ -lactamase enzyme-mutant of transpeptidase is released. This enzyme has a serine residue-similar to transpeptidase and can attack the drug molecules and open the ring to form an ester.  $\beta$ -Lactamase can convert the ester to the carboxylic acid by hydrolysis. Both Gram-positive and Gram-negative bacteria release  $\beta$ -lactamase enzyme; hence, both types showed resistance against penicillin and other agents with lactam moiety. Moreover, the Gram-negative bacteria showed more resistance because of releasing more enzymes and trapping in the periplasmic space. The mutations leading to high levels of transpeptidase or the formation of penicillin-binding protein 2a (PBP2a) may result in resistance. Although this protein has a lower tendency to penicillin than transpeptidase, it could result in resistance. Some Enterococci and Pneumococci strains showed resistance to penicillin because of PBP2a. 95% of *S. aureus* strains detected in hospitals became resistant to methicillin (MRSA) and the other  $\beta$ -lactamase-resistant penicillins as a result of mutations in the transpeptidase enzyme. Both penicillins and

cephalosporins show poor activity against MRSA with PBP2a. Vancomycin-resistant *Staphylococcus aureus* (VRSA) and Vancomycin-resistant Enterococci (VRE) are the results of a possible modification in cell wall precursors by which the terminal-D-alanine in a peptide chain is replaced by D-lactic acid. D-lactic acid leads to four hydrogen bonds instead of five (inadequate hydrogen-bonding) between the vancomycin molecule and the terminal site. As a result, the terminal site will no longer be blocked and transglycopeptidase and transpeptidase enzymes can work. Some Gram-negative bacteria have proteins in their outer cell membrane which pump back penicillin out of the periplasmic space. It reduces the concentration and effectiveness of the drug by efflux drug effect.

As we implied, the mutations in the nucleoid of bacteria lead to drug resistance. These mutations can be caused by various acts. For instance, incomplete treatment of patients leads to resistance. Streptomycin-resistant *E. coli* and multi-drug resistant tuberculosis (MDRTB) are examples of this type of drug resistance. Another factor is to introduce the common antibiotics to human and animals to combat infections or to obtain other purposes such as increasing the weight in animals. Penicillin V and G are examples of this type of drug resistance. The other possible factor is that the considerable amount of antibiotics is excreted and it provides an opportunity for the bacteria in the environment to acquire resistance. The solution is to add the protecting group to the drug. For example, adding nitrobenzylcarbamate to cephalosporin. The hydrazine group of nitrobenzylcarbamate reacts with cephalosporin when it is exposed to the light and deactivates the antibiotic drug. Administering two antibiotics simultaneously may lead to better effects. Minocycline with loperamide showed better activity than minocycline alone. This effect was also explained in the previous sections. The other attempts to deal with drug resistance are: introducing new kinase inhibitors, new aminoacyl transfer RNA, isoleucyl tRNA, and tyrosine tRNA synthetases inhibitors. Mupirocin and tavaborole were introduced as aminoacyl transfer RNA and leucine tRNA synthetases inhibitors respectively. Mupirocin also showed anti-MRSA activity. The genetic information responsible for drug resistance is transferred via two major mechanisms: transduction and conjugation. In transduction, plasmids (a separate part of DNA of bacteria) which can be transmitted from one bacterium to another one are involved. They transmit new genetic information from resistant cells to susceptible ones to distribute resistance in a bacterial population (genetic information for  $\beta$ -lactamase is transmitted by plasmids). In conjugation, two bacterial cells build a connecting bridge by which the genetic information is transmitted<sup>99</sup>.

## 1.5 The infections and diseases caused by bacteria

Pathogenic Gram-positive and Gram-negative bacterial strains can cause various infections. Some of these infections and bacterial species responsible for are listed below<sup>104</sup>:

**1.5.1 Skin infections: Impetigo;** *S. aureus* and  $\beta$ -Hemolytic *streptococci*, **Cellulitis;** *Streptococcus Pyrogenes*, *Pseudomonas Aeruginosa*, *Enterobacter*, *E. coli*, *Cryptococcus neoformans*, and *Haemophilus Influenza*, **Folliculitis;** *S. aureus*, **Ecthyma;** *Pseudomonas Aeruginosa*, *S. aureus*, *Proteus*, and *E. coli*.

**1.5.2 Urinary tract infection:** *E. coli*, *Klebsiella spp*, *Proteus*, *S. aureus*, and *Enterococcus*.

**1.5.3 Otitis media:** *Streptococcus pneumonia*, nontypable *Haemophilus influenza*, *Moraxella catarrhalis*, and *S. aureus*.

**1.5.4 Brain infection: meningitis;** *Neisseria meningitides*, *S. aureus*, *Streptococcus pneumonia*, *Haemophilus influenza type B*, and *Mycobacterium Tuberculosis*, **brain abscess;** aerobic and anaerobic streptococci (60-70% of the cases) with *Streptococcus milleri* gp (*Streptococcus anginosus*, *Streptococcus constellatus*, and *Streptococcus intermedius*).

**1.5.5 Respiratory infections: Pneumonia;** *Streptococcus pneumoniae*, streptococci type B and A, *Mycoplasma pneumonia*, *Chlamydia pneumonia*, and *Chlamydia trachomatis*.

## 1.6 Structure-Activity Relationship (SAR)

The analogs of a pharmacologically active lead compound often show biological activities. However, these activities could be similar to that of a lead compound or different. Structure-Activity Relationship (SAR) sets the stage for developing new bioactive compounds by analyzing (interpreting) the changes in the structure of analogs of a lead compound. These changes include introducing of new substituents to an occupied or unoccupied position. Generally, pharmacokinetic, pharmacodynamic, and chemical properties of a drug rely on the solubility of drug molecules in water or lipids (the presence of hydrophilic or hydrophobic groups), the size and the shape of drug molecules (some large molecules cannot pass through the cell membrane to approach the receptor or target cell, some drugs inhibit enzymes or bind receptors via ionic bonds, Van-der-Walls interactions,  $\pi$ - $\pi$  stackings, s-bridging, and hydrogen-bonding, and some large functional groups provide steric hindrance by which the

function of the drug molecule varies from the lead compound), and electron-efficiency effects (the presence of electron-rich or electron-deficient substituents). These changes can lead to positive or negative biological effects<sup>105</sup>.

## 1.7 A review to bioactivities of synthetic indole-containing compounds and their SARs

### 1.7.1 Antibacterial and antifungal activities

Bis(indolyl)methanes synthesized by A. Kamal *et al*<sup>55</sup> showed moderate growth inhibition activities against *Bacillus subtilis* (MTCC 441), *Staphylococcus aureus* (MTCC 96), *Escherichia coli* (MTCC 443), *Pseudomonas aeruginosa* (MTCC 1688), *Pseudomonas oleovorans* (MTCC 617), and *Klebsiella pneumonia* (MTCC 618) with the zone of inhibitions of (9-18 mm) compared to streptomycin (19-29 mm). These compounds also revealed antifungal activities (9-18 mm) compared to (22 and 23 mm) against *C. albicans*, *R. oryzae*, and *A. niger*.

M. A. Seefeld *et al*<sup>103</sup> resulted that 4-hydroxybenzyl-*N*-substituted-(4-hydroxyphenyl)(1,3,4,5-tetrahydro-2H-pyrido[4,3-*b*]indol-2-yl)methanone and 4-hydroxybenzyl-*N*-substituted-(4-phenyl)(1,3,4,5-tetrahydro-2H-pyrido[4,3-*b*]indol-2-yl)methanone showed highest antibacterial activities against *S. aureus* and *E. coli* FabI respectively (IC<sub>50</sub> was 0.11 and 2.7  $\mu$ M respectively). Triclosan was used as a positive standard (IC<sub>50</sub> of triclosan was 1.1 and 0.43  $\mu$ M against *S. aureus* FabI and *E. coli* FabI respectively).

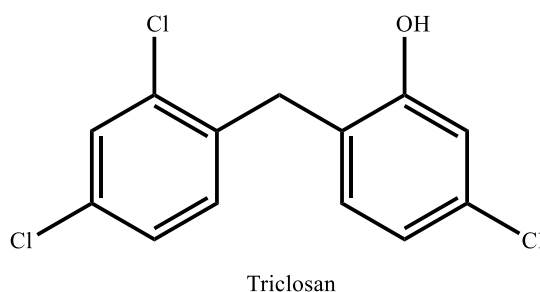


Fig. 15 The structure of triclosan

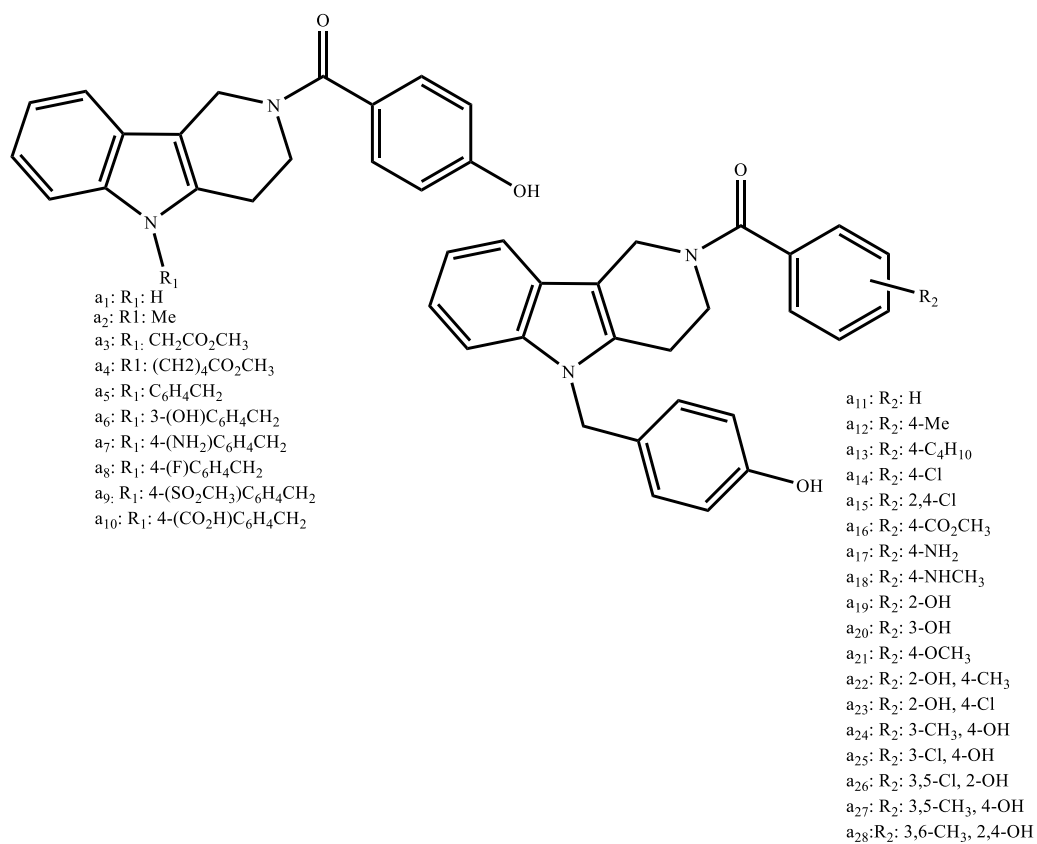
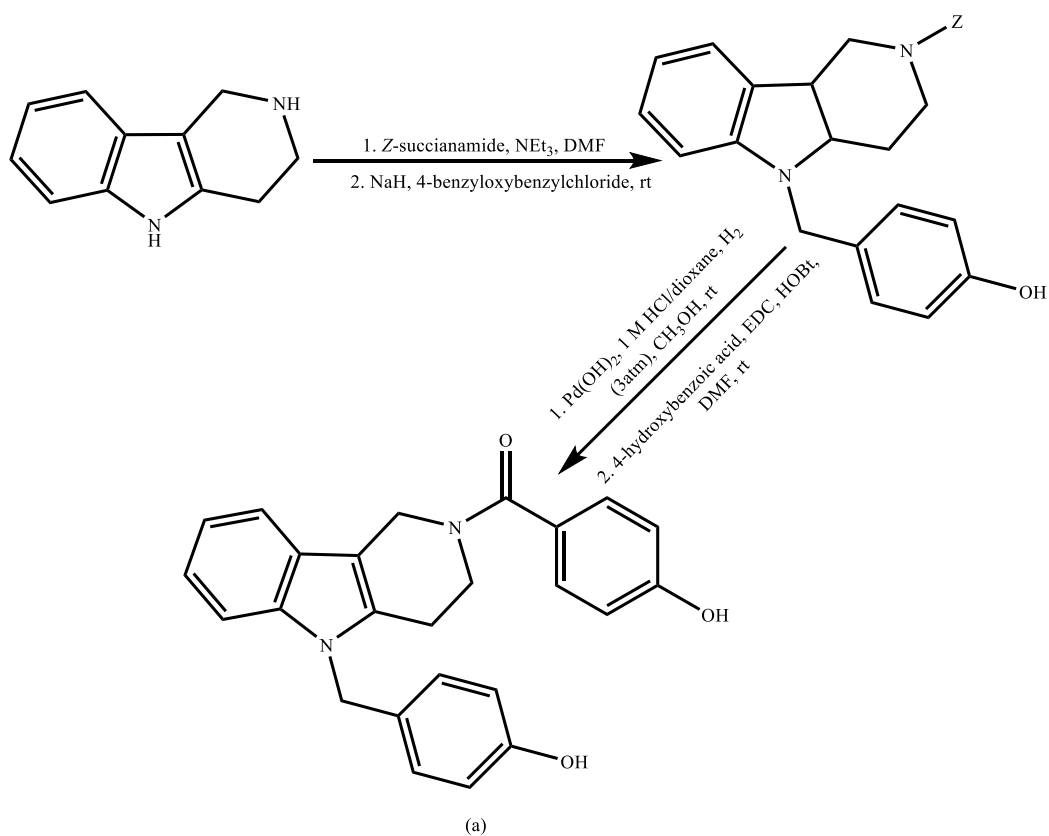
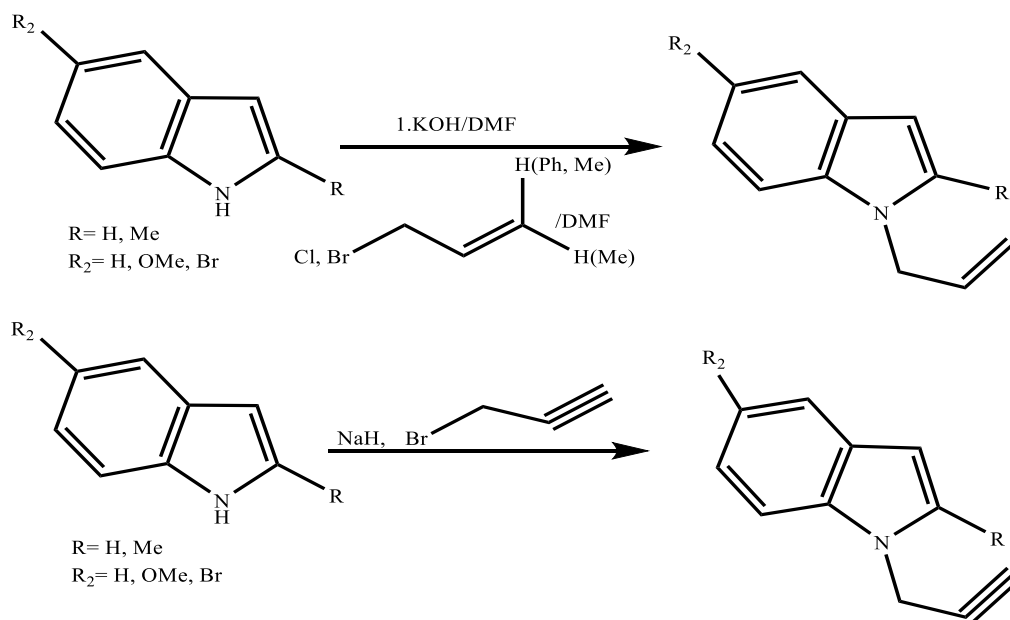


Fig. 16 Synthesis of the 2,9-disubstituted 1,2,3,4-tetrahydropyrido[3,4-b]indoles by M. A.

Seefeld et al<sup>103</sup>



In an experiment carried out by C. Praveen *et al*<sup>64</sup> among different synthesized di(indolyl)indolin-2-ones, 1'-phenyl-1,1''-di(prop-2-yn-1-yl)-[3,3':3',3''-terindolin]-2'-one showed highest antibacterial activities against Gram-positive *Staphylococcus aureus* (MSSA 22) and Gram-negative *Escherichia coli* (K 12) strains with the zones of the inhibition of 15 and 17 mm respectively. 2,2''-Dimethyl-1,1''-di(prop-2-yn-1-yl)-[3,3':3',3''-terindolin]-2'-one and 5,5''-dibromo-1,1''-bis(3-methylbut-2-en-1-yl)-1'-(prop-2-yn-1-yl)-[3,3':3',3''-terindolin]-2'-one showed size of zone of inhibition of 15 mm against both bacterial strains. *Amikacin* was the standard (zone of inhibitions of 17 and 18 mm against *S. aureus* and *E. coli* respectively). They also evaluated the antifungal activities of new *N*-allyl and *N*-propargyl di(indolyl)indolin-2-ones against *Candida albicans* (ATCC 10231). The compounds from 2-Me-1-propargyl indole and isatin, 1-allyl indole and 5-NO<sub>2</sub> isatin showed the highest activities (15 mm). The growth inhibition size of *Ketoconazole* as standard was 16 mm.



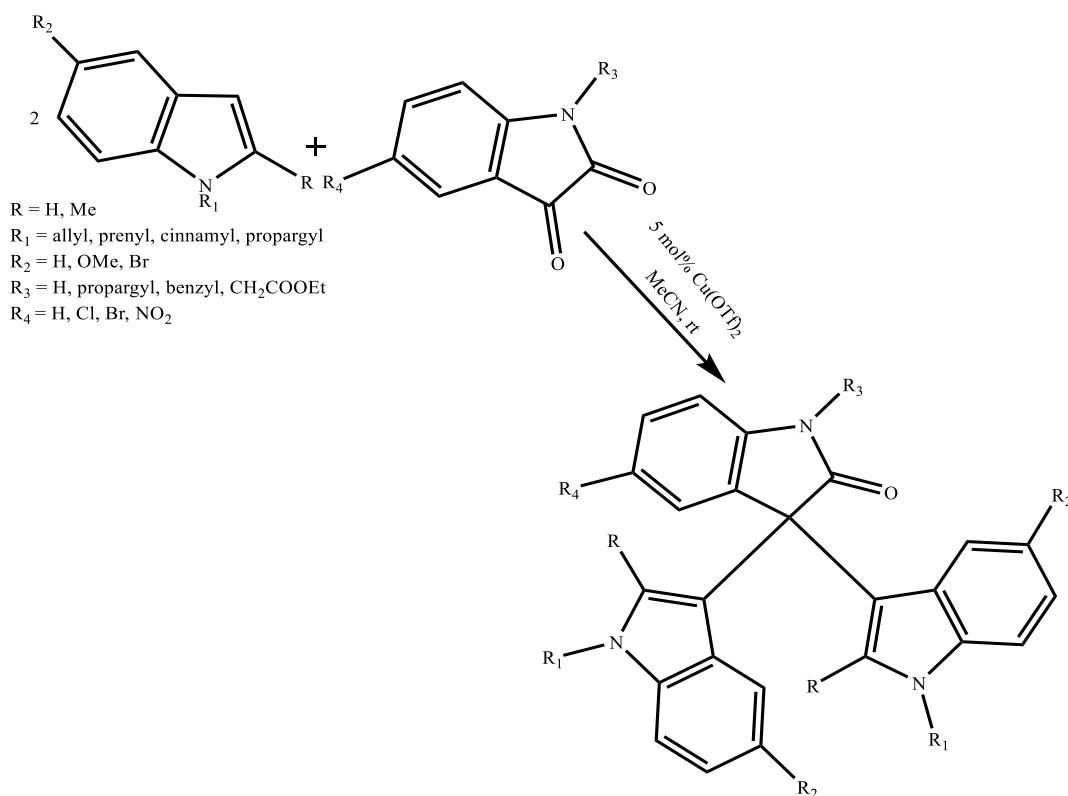


Fig. 17 Synthesis of novel *N*-allyl and *N*-propargyl di(indolyl)indolin-2-ones by C. Praveen *et al*<sup>64</sup>

Gurkok *et al* tested melatonin<sup>106</sup> analogous indole-3-aldehyde hydrazide/hydrazone derivatives against *Staphylococcus aureus*, *Escherichia coli*, and *Bacillus subtilis*. The MIC values were between 6.25-100  $\mu\text{g/ml}$ . Against *Staphylococcus aureus*, none of the compounds showed higher activity than ampicillin, sultamicillin, and ciprofloxacin. Fluconazole was inactive. Against *E. coli*, ampicillin, sultamicillin, and fluconazole were inactive but ciprofloxacin was highly active (MIC value of 0.09  $\mu\text{g/ml}$ ). Against *Bacillus subtilis*, they showed higher activity than fluconazole which was inactive. Every compound revealed higher activities than sultamicillin, ampicillin, fluconazole against *E. coli* and higher than fluconazole against *Bacillus subtilis*. The examined melatonin analogous indole-3-aldehyde hydrazide/hydrazone derivatives against *Candida albicans* showed significant activities with MIC value of 3.125-100  $\mu\text{g/ml}$ . The MIC of fluconazole was 0.78  $\mu\text{g/ml}$ . Against MRSA standard every compound was significantly active (MIC was between 6.25 and 100  $\mu\text{g/ml}$ ) compared to sultamicillin, fluconazole, and ciprofloxacin since these were inactive and the majority of the compounds was more active (MIC was 6.25  $\mu\text{g/ml}$ ) than ampicillin (MIC was about 12.5  $\mu\text{g/ml}$ ). Against MRSA isolate every compound showed

significant activities (MIC values were between 6.25 and 100  $\mu\text{g/ml}$ ) compared to sultamicillin, fluconazole, ciprofloxacin, and ampicillin as these references were inactive.

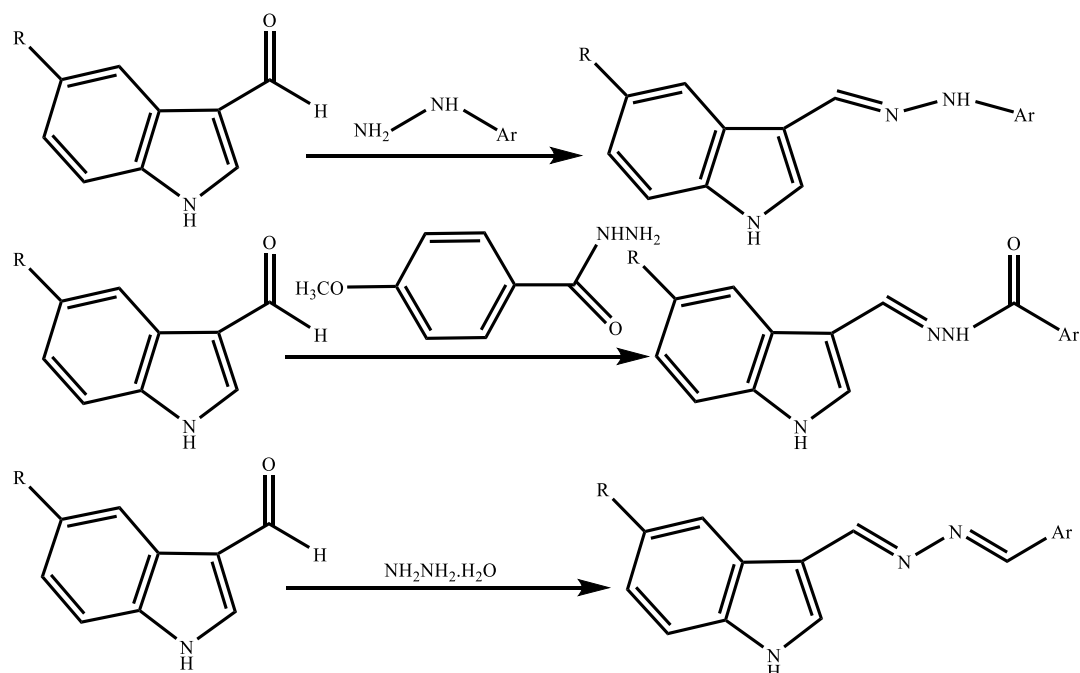


Fig. 18 melatonin analogous indole-3-aldehyde hydrazone/hydrazone derivatives synthesized by Gurkok *et al*<sup>106</sup>

Pordel *et al*<sup>107</sup> synthesized a novel class of isoxazolo[4,3-e]indoles that responded positively to methicillin-susceptible *S. aureus* (MSSA—ATCC 1112). Every compound showed better inhibition activities (MIC values of 4.3-15.3  $\mu\text{g/ml}$ ) than erythromycin with the MIC value of 32  $\mu\text{g/ml}$ . However, they showed lower activities compared to cephalexin (MIC value of 4.6  $\mu\text{g/ml}$ ) except *1-Bu*-indolyl and *4-methyl-5-phenyl* isoxazole substituted compounds which showed highest biological activities amongst the tested compounds (MIC value of 4.3  $\mu\text{g/ml}$ ). *1-Isobutyl* indole and *4-methyl-5-phenyl* isoxazole substituted substances showed highest inhibition activities after the above compound (MIC value of 5.0  $\mu\text{g/ml}$ ). These compounds against *Staphylococcus aureus* pathogenic strain [methicillin resistant *S. aureus* (MRSA)] showed higher activities (MIC of 4.3-22  $\mu\text{g/ml}$ ) than those of erythromycin and cephalexin (MIC values of 32.0 and 72.0 respectively). *1-Bu*-indolyl-*4-methyl-5-phenyl* isoxazole substituted compound showed the highest activity amongst every compound tested (MIC value of 4.3  $\mu\text{g/ml}$ ). *1-isobutyl-4-methyl-5-phenyl* isoxazole substituted substance showed highest inhibition activity after the above compound (MIC value of 5.0  $\mu\text{g/ml}$ ).

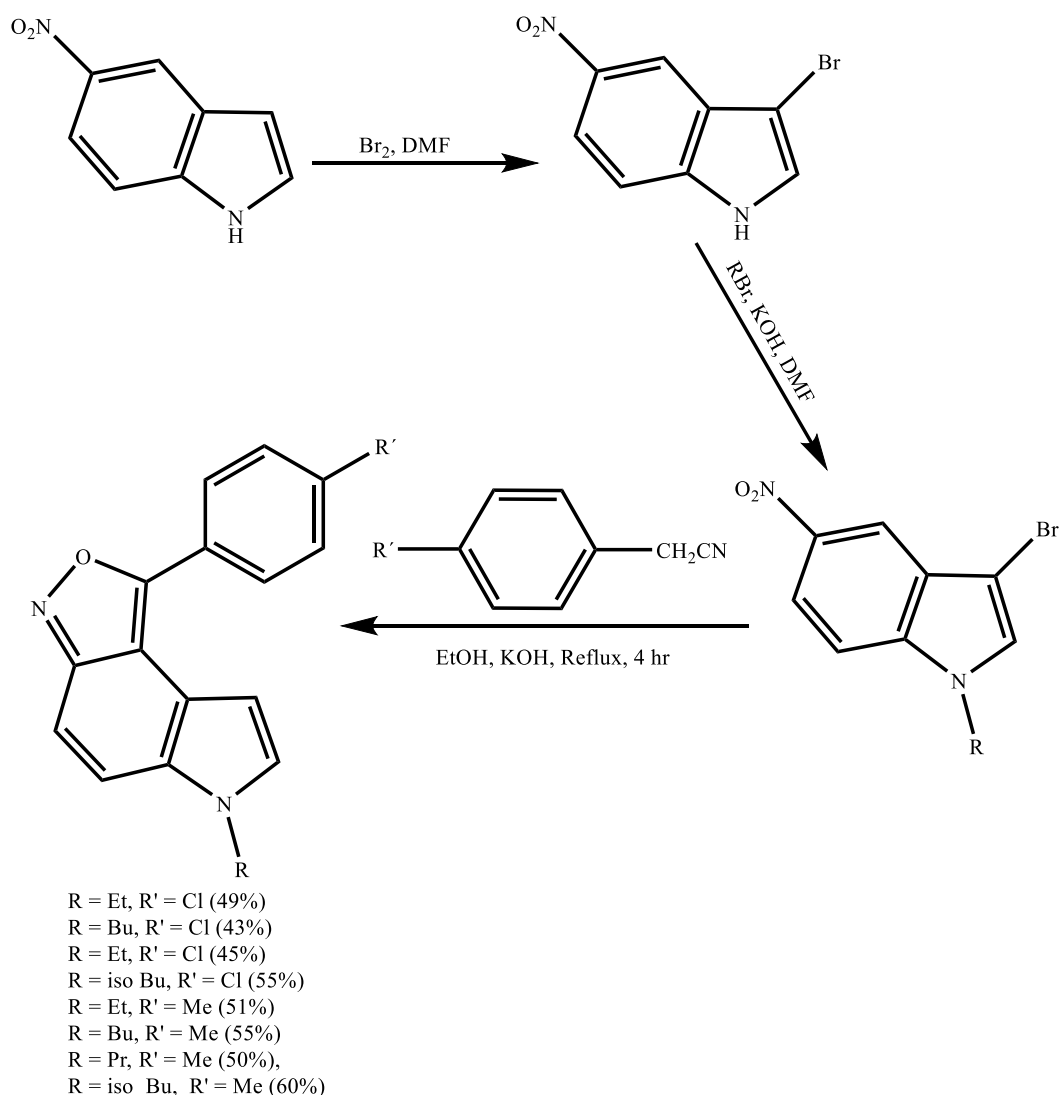


Fig. 19 Synthesis of Isoxazolo[4,3-e]indoles by Pordel *et al*<sup>107</sup>

B. V. Subba Reddy *et al*<sup>62</sup> tested their 2,5-disubstituted-1*H*-indol-3-yl-2-monosubstituted methane-3-hydroxy-6-(hydroxymethyl)-4*H*-pyran-4-one compounds against *Bacillus subtilis* (MTCC 441), *Staphylococcus aureus* (MTCC 96), *Staphylococcus epidermidis* (MTCC 2639), *Escherichia coli* (MTCC 443), *Pseudomonas aeruginosa* (MTCC 741), and *Klebsiella pneumonia* (MTC 618). The compounds showed MIC values of 4.68-150 µg/ml. 2-((5-chloro-1*H*-indol-3-yl)(4-methoxyphenyl)methyl)-3-hydroxy-6-(hydroxymethyl)-4*H*-pyran-4-one showed significant activities against *S. aureus*, *E. coli*, and *Pseudomonas aeruginosa* (*P. aeruginosa*) with the MIC values of 2.34 (more active than streptomycin with MIC value of 6.25 µg/ml), 4.68 (more active than both streptomycin and penicillin with MIC values of 6.25 and 12.5 µg/ml respectively), and 4.68 (more active than penicillin with MIC of 12.5 µg/ml) respectively. 3-Hydroxy-6-(hydroxymethyl)-2-(1-(2-phenyl-1*H*-indol-3-yl)propyl)-4*H*-pyran-

4-one showed good activities against *S. aureus* and *E. coli* with MIC value of 9.37 µg/ml being more active than penicillin. 3-Hydroxy-6-(hydroxymethyl)-2-((2-hydroxyphenyl)(2-phenyl-1H-indol-3-yl)methyl)-4H-pyran-4-one showed a significant MIC of 4.68 µg/ml against *S. aureus* being more active than streptomycin. 2,5-Disubstituted-indol-3-yl-2-methane-monosubstituted-3-hydroxy-6-(hydroxymethyl)-4H-pyran-4-one were examined against *Candida albicans* (MTCC 227), *Candida rugosa* (NCIM 3462), *Saccharomyces cerevisiae* (MTCC 36), *Rhizopus oryzae* (MTCC 262), and *Aspergillus niger* (MTCC 282) at concentrations of 100 and 150 µg/ml. The sizes of the zone of inhibition obtained were between 0-21 mm. 2-((5-Chloro-1H-indol-3-yl)(4-methoxyphenyl)methyl)-3-hydroxy-6-(hydroxymethyl)-4H-pyran-4-one showed sizes of inhibition of 20 and 21 mm at the concentration of 150 µg/ml against *Aspergillus niger* and *Saccharomyces cerevisiae* respectively. 3-Hydroxy-6-(hydroxymethyl)-2-((3-phenoxyphenyl)(1H-indol-3-yl)methyl)-4H-pyran-4-one revealed sizes of inhibition of 19, 19, and 18 mm at 150 µg/ml against *Candida albicans*, *Saccharomyces cerevisiae*, and *Candida rugosa* respectively. 2-((5-Bromo-1H-indol-3-yl)(4-methoxyphenyl)methyl)-3-hydroxy-6-(hydroxymethyl)-4H-pyran-4-one showed sizes of inhibition of 18 and 19 mm at 150 µg/ml against *Candida albicans* and *Candida rugosa* respectively. Amphotericin as standard showed sizes of inhibition of 25, 22, 23.5, and 22 mm against *Aspergillus niger*, *Candida rugosa*, *Candida albicans*, and *Saccharomyces cerevisiae* respectively.

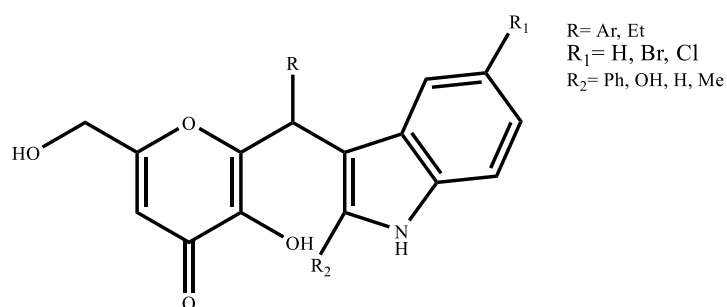
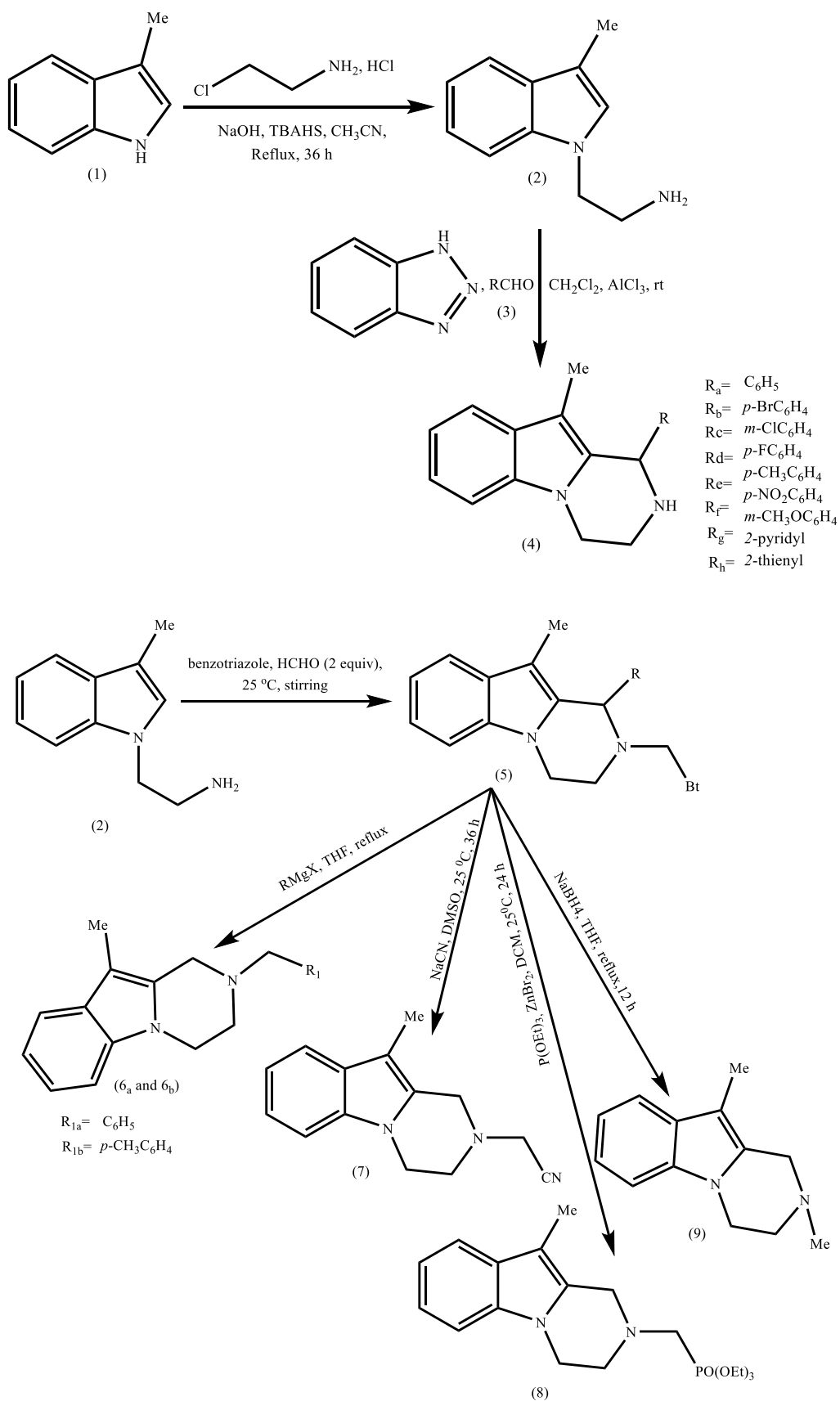


Fig. 20 The structure of the compounds synthesized by B. V. Subba Reddy *et al*<sup>62</sup>

One report showed the activity of *n*-propyl pyrazinoate towards pyrazinamide resistant *Mycobacterium tuberculosis*<sup>108</sup>. R. K. Tiwari *et al*<sup>109</sup> synthesized and tested substituted 1,2,3,4-tetrahydropyrazino[1,2-*a*]indoles against *Staphylococcus aureus* (MTCCB 737), *Streptomyces thermonitrificans* (MTCCB 1824), *Salmonella typhi* (MTCCB 733), *Pseudomonas aeruginosa* (MTCCB 741), *Escherichia coli* (MTCCB 1652). The compounds showed MIC values of 3.75-60 µg/disk and were mostly active against every bacterial strain

tested except *E. coli*. 10-Methyl-1-phenyl-1,2,3,4-tetrahydropyrazino[1,2-a]indole, 1-(3-Chlorophenyl)-10-methyl-1,2,3,4-tetrahydropyrazino[1,2-a]indole, and 10-Methyl-1-(pyridin-2-yl)-1,2,3,4-tetrahydropyrazino[1,2-a]indole showed MIC of 3.75 µg/disk against *Pseudomonas aeruginosa*, *Streptomyces thermonitrificans*, and *Staphylococcus aureus* respectively. 1-(4-Fluorophenyl)-10-methyl-1,2,3,4-tetrahydropyrazino[1,2-a]indole revealed MIC of 7.5 µg/disk against *Streptomyces thermonitrificans*. 10-Methyl-1-(p-tolyl)-1,2,3,4-tetrahydropyrazino[1,2-a]indole, 10-Methyl-1-(4-nitrophenyl)-1,2,3,4-tetrahydropyrazino[1,2-a]indole, and 1-(4-Fluorophenyl)-10-methyl-1,2,3,4-tetrahydropyrazino[1,2-a]indole compounds showed substantial activities with MIC values of 7.5-60 µg/disk. They were active against every bacterial strain tested. 1,3-Dimethylpyrazino[1,2-a]indole and 3-Methyl-1-phenylpyrazino[1,2-a]indole were also active against all the bacterial strains although they showed lower bacterial activities compared to those of the above three discussed compounds with the MIC value of 60 µg/disk. Gentamycin and doxycycline HCl were used as standards (MIC ranges of 0.5-1 and 1.0-2.0 µg/disk). In the cytotoxic analysis using hemolytic assay the percent lysis of the three compounds which showed substantial activities and gentamycin was plotted against the logarithm of the concentration of these compounds. Based on the cytotoxicity results of the above compounds with remarkable MIC values, they concluded that these compounds were less harmful to normal bacteria and target cells than gentamycin due to the less percent lysis at high concentrations than that of gentamycin. As a result, these four compounds could be introduced as new safe materials for developing new effective drugs. Some triazino[5,6-b]indoles have been reported to have antifungal properties<sup>111</sup>.



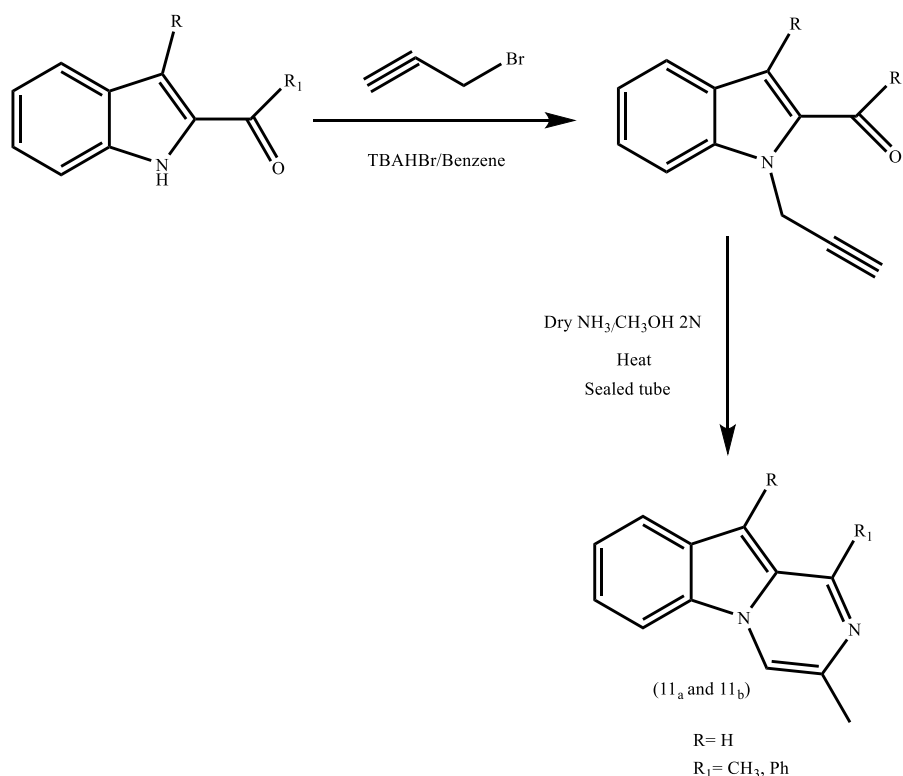
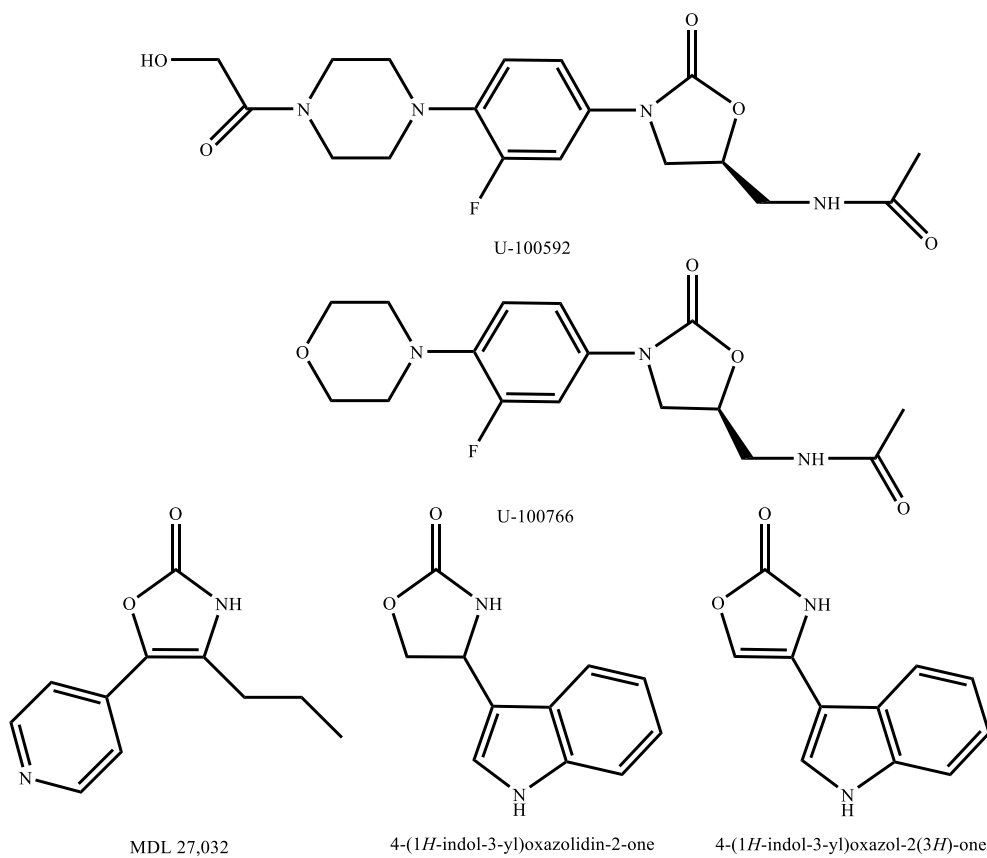


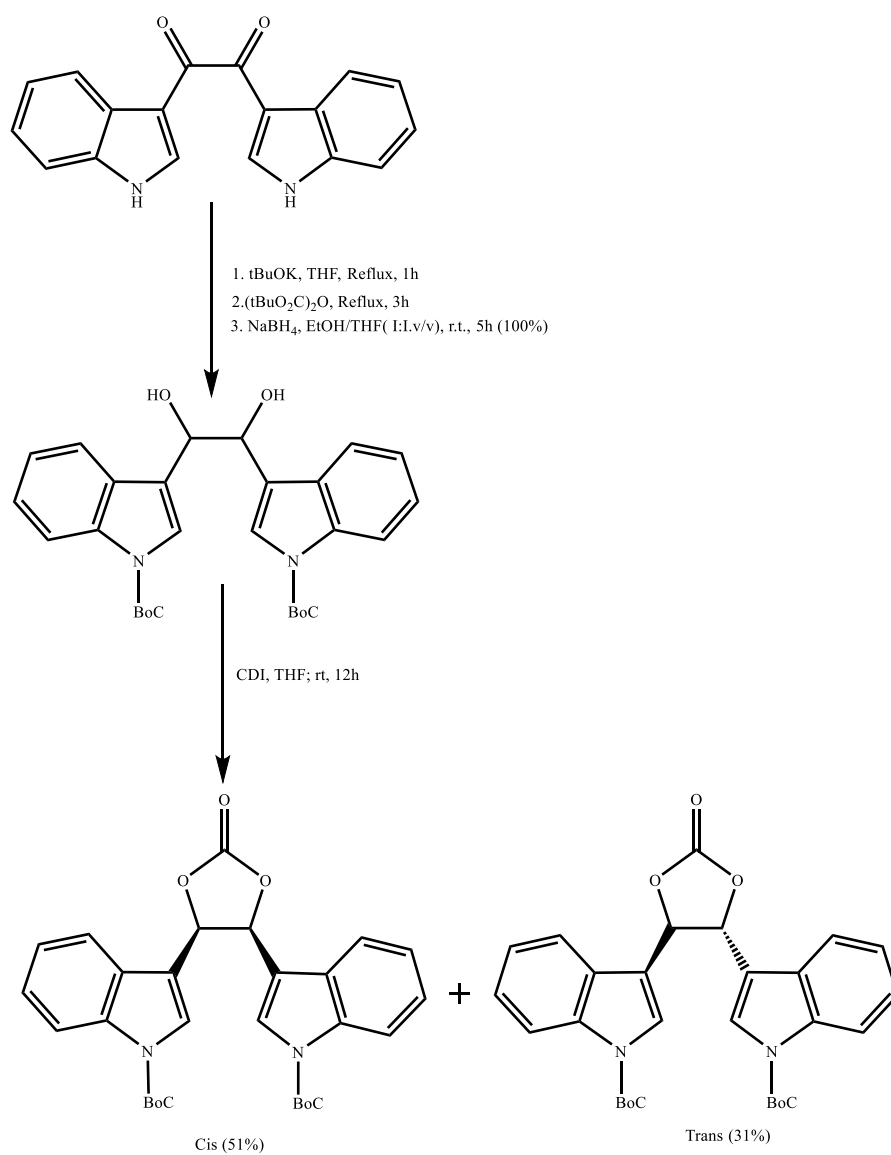
Fig. 21 Scheme of a synthetic approach of substituted 1,2,3,4-tetrahydropyrazino[1,2-a]indoles by R. K. Tiwari *et al*<sup>109</sup>

*E. R. Periera et al*<sup>111</sup> tested their synthesized indole-substituted oxazolidinones, oxazolones, pyrrolidinone, imidazolidinones and imidazolines against *Streptomyces chartreusis*, *Streptomyces griseus*, *Bacillus cereus*, *Pseudomonas aeruginosa*, *Proteus mirabilis*, and *Escherichia coli*. 4,5-Di(1H-indol-3-yl)imidazolidin-2-one derivative showed highest activities. It was strongly active with sizes of inhibition of 12-15 mm against *Streptomyces chartreusis* and *Streptomyces griseus* concerning both growth and sporulation inhibitions. 4-(1H-indol-3-yl)oxazol-2(3H)-one showed strong activities (sizes of inhibition of 12-15 mm) against *Streptomyces chartreusis* concerning both growth and sporulation inhibitions and *Streptomyces griseus* concerning only sporulation inhibition. 4-(1H,1'H-[2,2'-biindol]-3-yl)oxazolidin-2-one showed strong sporulation growth against *Streptomyces griseus* (size of zone of inhibition of 12-15 mm). 4-(1H-indol-3-yl)oxazolidin-2-one showed significant and strong activities against *Escherichia coli* with sizes of growth inhibition of greater than 15 mm and 12-15 mm at the concentrations of 300 and 150 µg/ml respectively. *E. R. Periera et al*<sup>111</sup> later investigated the antibacterial activities of 3-N-substituted-4,5-bis(3-indolyl)oxazol-2-ones against *Bacillus cereus*, *Corynebacterium equi*, *Enterococcus faecalis*, *Streptomyces chartreusis*, and *Escherichia coli*. (S)-2-(4,5-Di(1H-indol-3-yl)-2-oxooxazol-3(2H)-



yl)propanoic acid showed the highest sporulation inhibition activity against *Streptomyces chartreusis* with the size of inhibition of 18 mm (Fig. 22).





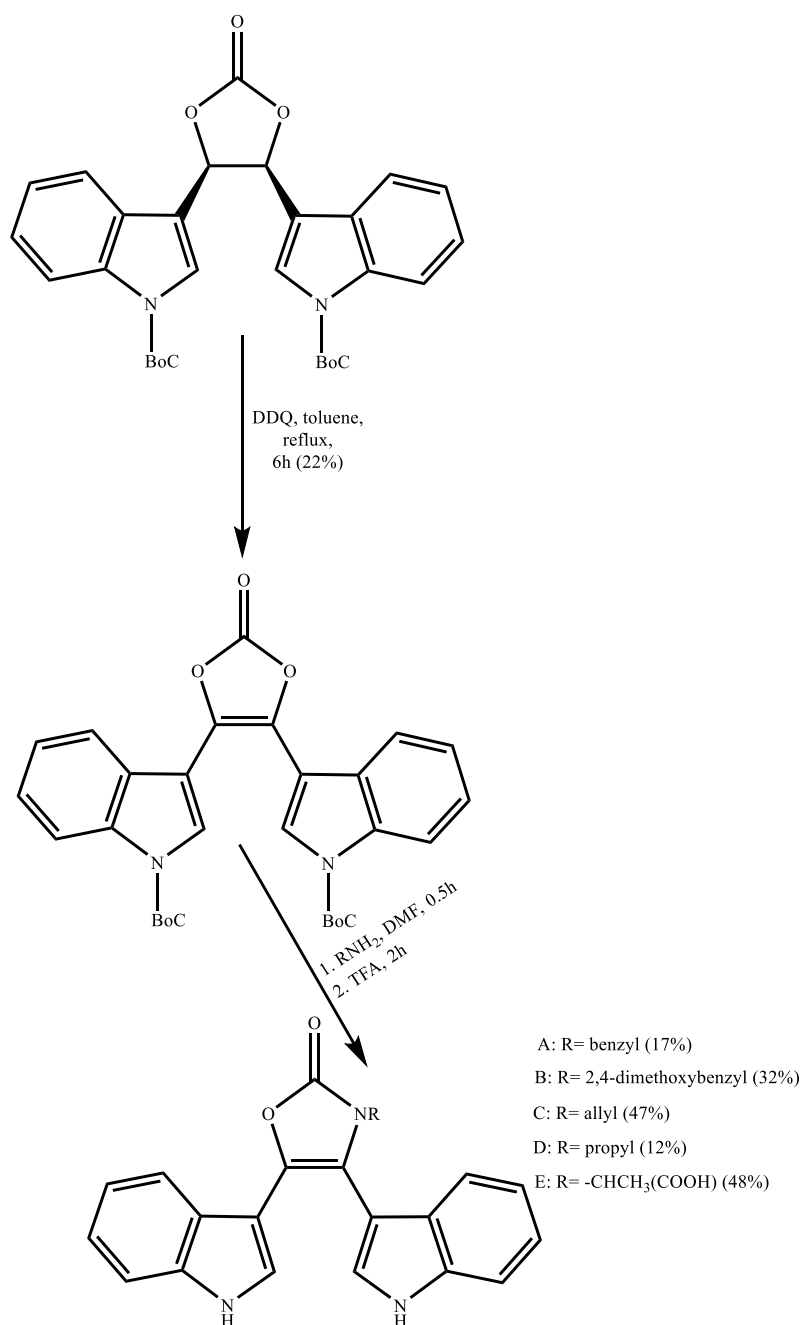
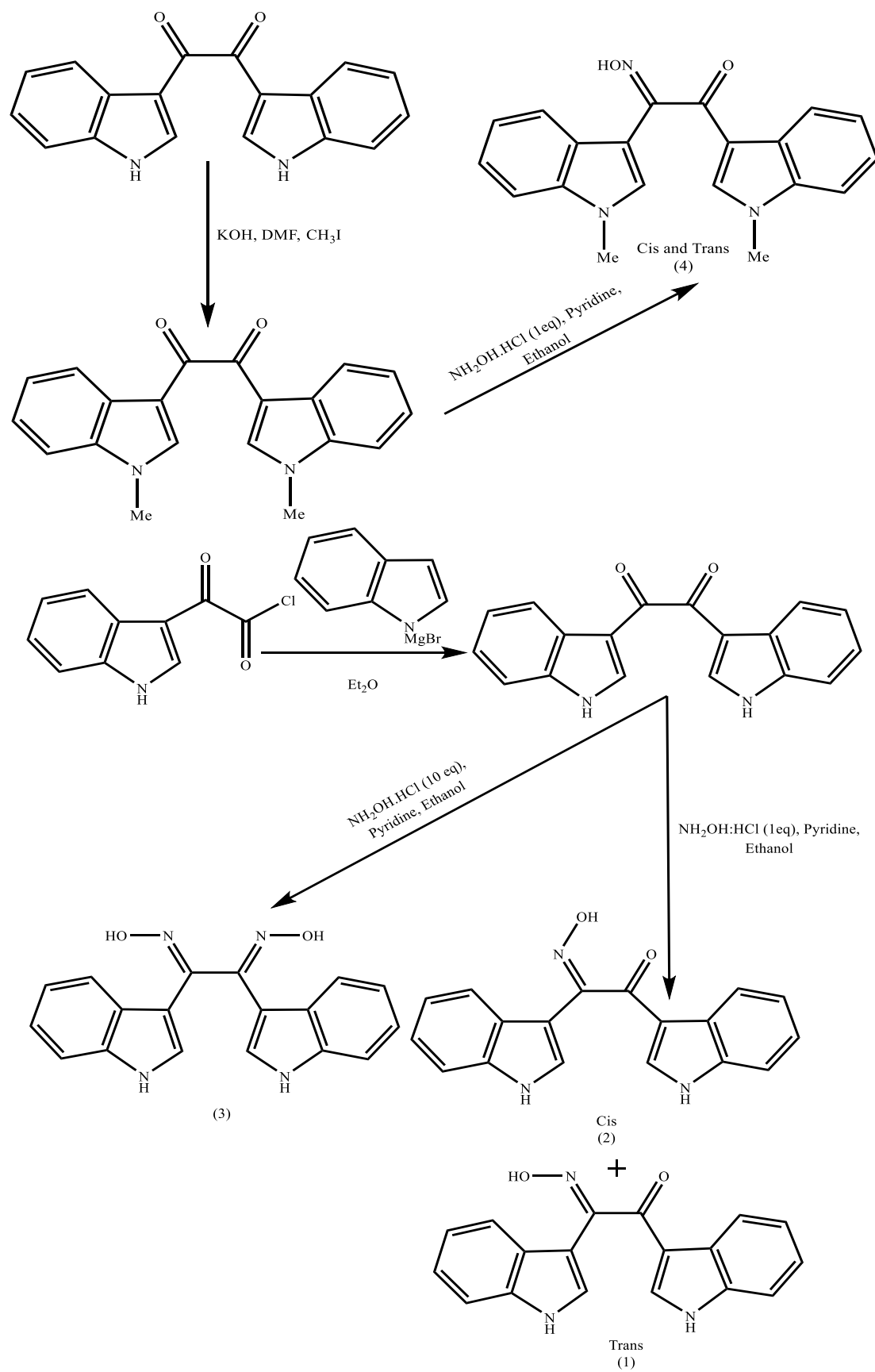


Fig. 22 Some examples of oxazolones and oxazolidinones with biological activities and the scheme of the synthetic routes to indolyloxazolone derivatives by *E. R. Periera et al*<sup>111,112</sup>

*Prudhomme et al*<sup>113</sup> tested the growth inhibition of their mono- and bis-indolyloxime derivatives whose structures were similar to protein kinase C (PKC) inhibitors bisindolylmaleimides against *E. coli* ATCC 11303, *B. cereus* ATCC 14579, *S. chartreusis* NRRL 11407 non-pathogenic strains. (Z)-2-(Hydroxyimino)-1,2-di(1H-indol-3-yl)ethan-1-one was the most active compound compared to the other compounds since it showed good (10-12 mm) and strong (13-15 mm) growth and sporulation inhibitory activities against *B.*

*cereus* ATCC 14579 and *S. chartreusis* NRRL 11407 respectively. (E)-2-(Hydroxyimino)-1,2-di(1H-indol-3-yl)ethan-1-one showed moderate (8-9 mm) and significant (13-15 mm) growth and sporulation inhibitory activities against *B. cereus* ATCC 14579 and *S. chartreusis* NRRL 11407 respectively. Methyl (E)-2-(hydroxyimino)-2-(1H-indol-3-yl)acetate and methyl (Z)-2-(hydroxyimino)-2-(1H-indol-3-yl)acetate showed good growth inhibitory activities against *S. chartreusis* NRRL 11407. In the second investigation, they assessed the antibacterial activities of their synthesized compounds against *Staphylococcus aureus* SG511, SG 285, Exp54146, *Streptococcus pyogenes* A561 and 77A, *Enterococcus faecium* M78L, *Serratia* RG 2532, *Proteus mirabilis* A235, *Proteus vulgaris* A232, *Escherichia coli* UC1894, 078, TEM, 1507E, DC0, and DC2, *Salmonella typhimurium* MZ11, and *Klebsiella pneumonia* 52145 pathogenic strains. Only (E)-2-(hydroxyimino)-1,2-di(1H-indol-3-yl)ethan-1-one and (Z)-2-(hydroxyimino)-1,2-di(1H-indol-3-yl)ethan-1-one were active against *S. aureus* SG511, *S. aureus* 285, *S. aureus* Exp54146, *S. pyogenes* A561, *S. pyogenes* 77A, *E. faecium* M78L, *E. coli* TEM, *E. coli* 1507E, *E. coli* DC0, and *E. coli* DC2. Both compounds showed similar anti-bacterial activities against *S. aureus* SG511 and *S. aureus* 285 with the MIC values of 20 and 40 µg/ml respectively. Mono and bisindolyloxime compounds whose structures were similar to protein kinase C (PKC) inhibitors bisindolylmaleimides do not take PKC inhibition pathway as the IC<sub>50</sub> values were 100 mg/ml and enzyme inhibition was most likely to be the mode of action.



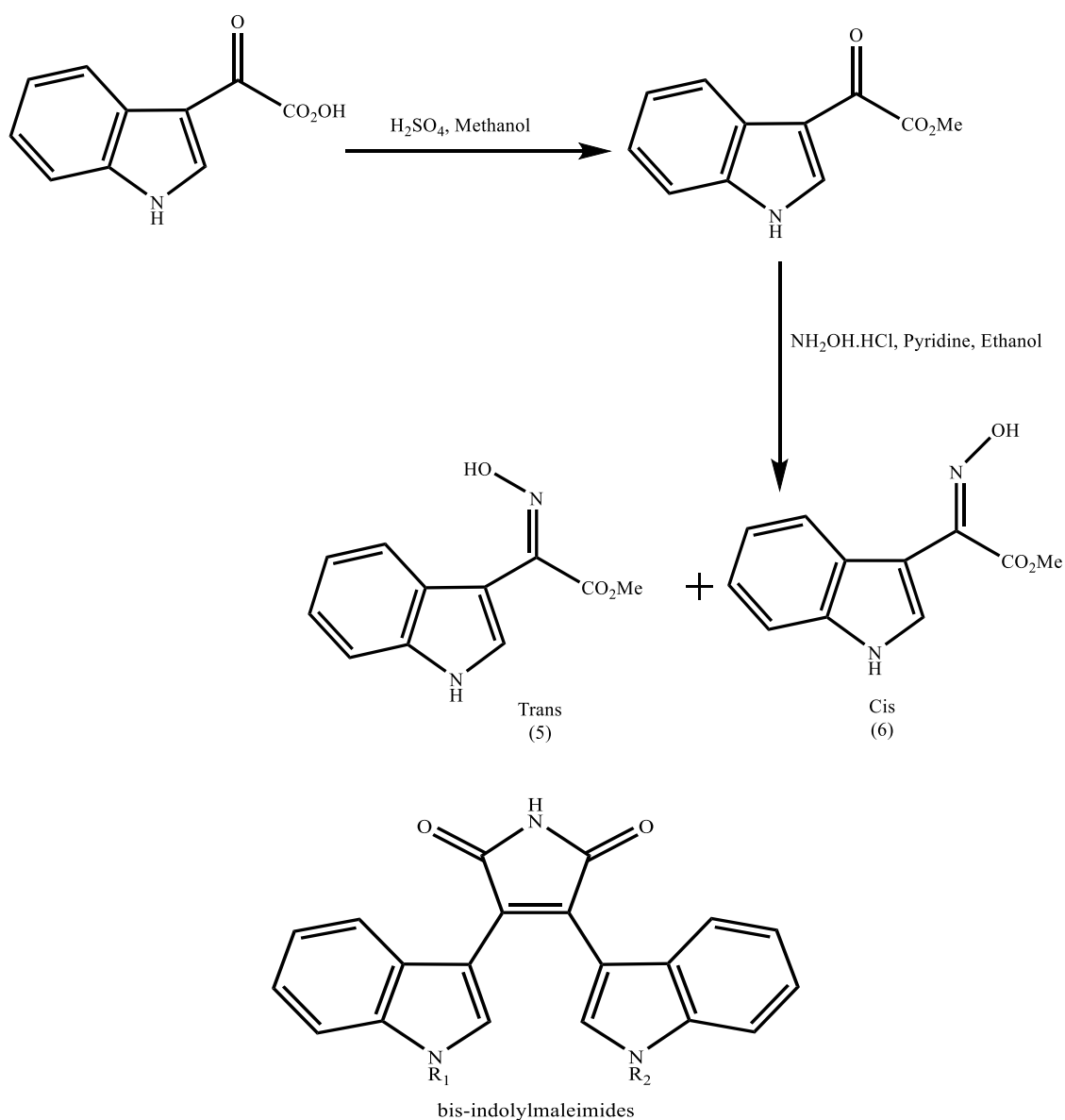


Fig. 23 Synthetic approach to the mono- and bis-indolylloximes by *Prudhomme et al*<sup>113</sup>

#### 1.7.1.1 The Structure-Activity Relationships (SARs) of the above indole-containing compounds

In bis(indolyl)methanes, weak electron-donating groups (EDGs) such as methyl and ethyl could raise the antibacterial activities against both Gram-positive and Gram-negative bacterial strains and antifungal activities against *C. albicans*, *Rhizopus oryzae* (*R. oryzae*), and *Aspergillus niger* (*A. niger*). After alkyl, strong electron-withdrawing groups (EWGs) such as  $\text{NO}_2$  could have the same effect but not as strong as methyl and ethyl groups [A. Kamal *et al*]<sup>55</sup>. The presence of hydroxybenzyl-*N*-substitution and hydroxyl group

specifically plays a significant role in the antibacterial activities of phenyl(1,3,4,5-tetrahydro-2H-pyrido[4,3-b]indol-2-yl)methanone derivatives against *S.aureus* and *E.coli* FabIs because hydroxyl group could enhance the solubility of these compounds in membrane cross passing [M. A. Seefeld *et al*]<sup>103</sup>. Electron-withdrawing groups at the 5-position of isatin and electron-donating groups (EDGs) at the 5-position of indolyl moieties in *N*-allyl and *N*-propargyl di(indolyl)indolin-2-ones molecular scaffolds led to the lower antibacterial activities. The lower, the electronegativity of halogen substituted isatin moiety was, the higher, was the activity. Electron-withdrawing (EWG) and electron-donating (ED) groups at the 1-position of indole and isatin moieties respectively enhanced the antibacterial activity remarkably (1-propargyl indole and 1-phenyl isatin). EDG at 2-position of indole moiety resulted in higher activity. Totally, the replacement of *1-H* on isatin moiety with EDGs or EWGs led to the higher antibacterial activity although the role of EWGs was more significant. EWGs and EDGs at 5-position of isatin and indolyl moieties led to the higher antifungal activities. Likewise, the lower, the electronegativity of halogen substituted isatin moiety was, the higher was, the activity. EWGs and EDGs at 1-position of indole and isatin moieties respectively enhanced the antifungal activities with 1-propargyl indole and 1-phenyl isatin. On the other hand, EDG at 2-position of indole moiety resulted in higher activity. However, the effect of EWGs and EDGs at 5-position of isatin and 2-position of indole moieties respectively on antifungal activities were more significant compared than those on antibacterial activities [C. Praveen *et al*]<sup>64</sup>.

In Gurkuk *et al*<sup>106</sup> investigations, the introduction of halogens such as fluorine, chlorine, and bromine on both indolyl and hydrazine sites enhanced the antibacterial activities.

In *N*-substituted-4-substituted-5-phenyl isoxazoloindoles, the addition of one carbon atom to the linear alkyl chain at 1-position of indole (ethyl to propyl and propyl to butyl) led to the enhanced inhibition effect against both MRSA and MSSA. The substitution of linear alkyl by branched one (Bu to iso-Bu) led to the reduced antibacterial effects against both MRSA and MSSA strains. The substitution of EWG of chlorine by EDG of methyl at 4-position of 5-phenyl substituted isoxazole led to the enhanced inhibition effect against both MRSA and MSSA [Pordel *et al*]<sup>107</sup>.

In the compounds containing mono-indolyl aryl and alkyl substituted methane and kojic acid moieties, electronegative atoms such as chlorine and bromine at 5-position of indolyl moiety are likely to enhance the anti-bacterial activities. Aryl methane compounds with *meta* EDGs

such as OH, phenoxy, and OMe show higher anti-bacterial and anti-fungal activities than *para* substituted ones and the stronger, the EDG, the more effective, the compound [B. V Subba Reddy *et al*]<sup>62</sup>.

Among the 1,2,3,4-tetrahydropyrazino [1,2-*a*]indoles, the compounds with free NH group on pyrazino ring and substitution on 1- position showed higher antibacterial activities compared to those with no free NH group against all bacterial strains used. Among 10-methyl-1-phenyl-1,2,3,4-tetrahydropyrazino[1,2-*a*]indole substituted compounds, electronegative heteroatoms or EWGs on the *para* position of the phenyl moiety led to a better response to all bacterial strains than those whose scaffolds which have *meta*-substituted phenyl moieties, the stronger, the EWD or electronegative heteroatom has been, the more active was, the compound. Regarding the compounds with no free NH group on the pyrazino ring, derivatives in order of activities are *N*-methyl, acetonitrile, *p*-methylbenzyloxy, benzyloxy, benzotriazolyl, and diethoxyphosphinate substituted compounds [R. K. Tiwari *et al*]<sup>109</sup>.

Based on E.R. Periera *et al*<sup>111</sup> investigations, the compounds with bis indolyl moiety showed higher activities than mono-indolyl oxazolones and oxazolidinones.

In Prudhomme *et al*<sup>113</sup> study on anti-bacterial activities of mono and bisindolyloxime compounds whose structures were similar to protein kinase C (PKC) inhibitors bisindolylmaleimides, the noticeable outcome was the effect of *H-1* in indolyl ring on antibacterial activity. They also found out that by introducing other groups such as hydroxyl on the indolyl moiety, the membrane crossing would be easier and the antibacterial activity would remarkably increase.

### 1.7.2 Anti-cancer activity

Kumar *et al*<sup>114</sup> reported the anti-cancer activities of indolyl-1,2,4-triazole derivatives against a panel of human cancer cell lines [prostate (PC3, DU145, and LnCaP, breast (MCF7 and MDA-MB-231), pancreatic (PaCa2)]. 3-(3',4',5'-trimethoxyphenyl)-5-(*N*-methyl-3'-indolyl)-1,2,4-triazole and 3-(4'-piperidiny)-5-(*N*-methyl-3'-indolyl)-1,2,4-triazole showed highest activities against every cell line tested. The first bioactive compound revealed IC<sub>50</sub> values of 6.9, 10.2, 2.3, 1.4, 4.7, and 0.8  $\mu$ M on LnCaP, DU145, PC3, MCF7, MDA-MB-231, and PaCa2 respectively. The second compound showed IC<sub>50</sub> values of 6.9, 6.0, 3.2, 1.6, 2.6, and 3.2  $\mu$ M in the same order as above.



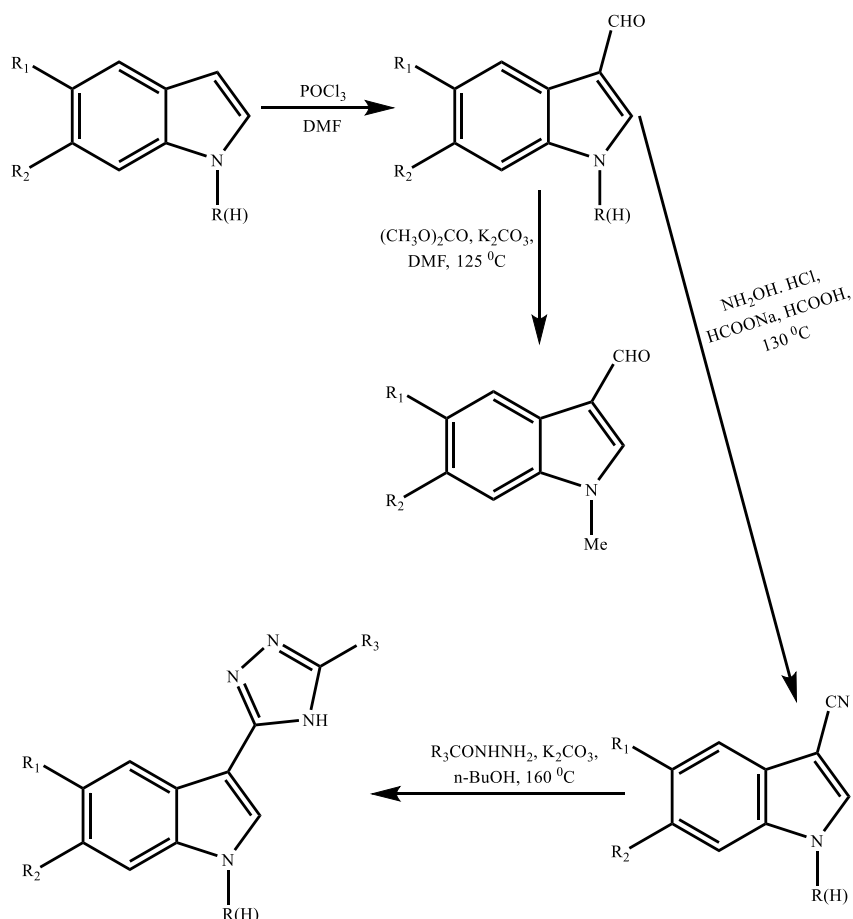


Fig. 24 *Kumar et al*'s synthetic route to the indolyl-1,2,4-triazoles<sup>114</sup>

### 1.7.2.1 The Structure-Activity Relationship (SAR) of the above indolyl-derived compounds as Anti-cancer agent

Among the indolyl-1,2,4-triazoles synthesized by *Kumar et al*<sup>114</sup> the groups such as phenyl and piperidinyl at 5-position of triazole moiety, OH, OBn, and  $OCH_3$  at 3,4, and 5-positions of phenyl ring, slightly electron-donating groups such as methyl at *N*-position of indole, and presence of halogens as well as fluorine and chlorine on phenyl ring play a significant role in biological activities of their synthesized compounds.

### **1.7.3 Other biological activities of some indolyl-derived compounds**

Other biological activities of indolyl-derived compounds are histamine receptor blocking activity<sup>115</sup>, reverse transcriptase inhibition<sup>116</sup>, anti-convulsant (anti-seizure, antiepileptic) agent and platelet aggregation inhibition<sup>91</sup>.

## 2. Results and Discussion

Indoles have usually been of great interest to medicinal chemists because of the wide variety of biomolecules including receptors<sup>117</sup>, Hormones, neurotransmitters, enzymes and antibacterial, antifungal, anticancer, and antiviral agents have an indolyl moiety. Since the 1980s until today many investigations and studies have been undertaken to introduce new synthetic or naturally occurring indole-containing compounds as bioactive agents. However, the applications of indolyl-derived compounds as drugs are more widespread and have attracted much more attention rather other applications. The main reason is a request for the new drugs because of the appearance of new pathogenic species and specifically new resistance to current drugs. As we discussed in the introduction section, many mono- and bis-indoyl alkaloids showed potential bioactivities against pathogenic bacterial strains. In our work, we focus on the novel-class of synthetic indolyl-derived compounds. We designed and proposed a novel synthetic approach for condensation reactions of indoles with various aromatic and aliphatic dialdehydes. We planned to utilize glacial acetic acid as a mild protic acid and non-aqueous solvent to catalyse the reactions. Previously, acetic acid<sup>39,118</sup> and other protic acids and solvents such as HCl<sup>47</sup> and aqueous CH<sub>3</sub>OH<sup>53</sup> had been used in reactions of indoles with electrophiles. After synthesizing the compounds and elucidating the structures, the potential biological activities of the synthesized compounds (antibacterial and antifungal activities) were evaluated.

### 2.1 Synthesis part

#### 2.1.1 The reactions of indoles with glutaric dialdehyde and malondialdehyde

In the first and second parts of our study, we focus on the electrophilic substitution reactions of unsubstituted and substituted indoles with glutaric dialdehyde and substituted malondialdehydes.

2%-70% Acidic (pH of 3-4) aqueous solutions of glutaric dialdehyde are commercially available. In organic chemistry laboratories, glutaric dialdehyde is obtained after the vacuum distillation of aqueous solution whose boiling point is approximately at 187 °C. Generally, aqueous solution of glutaric dialdehyde consists of roughly thirteen different species in equilibrium depending on the factors such as temperature, pH, and concentration. Free glutaric dialdehyde, hemiacetal of its hydrate, and oligomers of previous species are the

abundant (dominant) species. At temperatures higher than room temperature, the relative abundance of free glutaric dialdehyde is also higher<sup>119</sup>. The main application of glutaric dialdehyde is to cross-link proteins particularly enzymes in order to immobilize them. Moreover, glutaric dialdehyde is applicable to histochemistry, microscopy, cytochemistry, chemical sterilization, and biomedical and pharmaceutical sciences. Aldehydes usually react with amino acid side-chains such as lysine, tyrosine, and tryptophan at the pH range of 2-11 because of the nucleophilic feature of this functional group. This reaction is reversible at the above pH range; nevertheless, between pH 7.0 and 9.0 a little reversibility is observed. In cross-linking, glutaric dialdehyde reacts with lysine residues ( $\epsilon$ -amino group) of proteins in the unprotonated form at low pHs<sup>120</sup>.

Malondialdehyde is commercially available in a form of 1,1,3,3-tetramethoxypropane. The form of malondialdehyde required for the reactions was obtained via acid hydrolysis of 1,1,3,3-tetramethoxypropane<sup>121</sup>. Malondialdehyde is used as a marker for oxidative stress<sup>122</sup>.

The electrophilic substitution reaction of indoles to aldehydes and ketones in the presence of Lewis acids processes via the formation of azafulvenium intermediate<sup>51,55</sup> to harvest bis(indolyl)methanes (BIMs). It is expected that the reaction of indoles with dialdehydes such as glutaric dialdehyde and malondialdehyde processes via the same mechanism<sup>123</sup>. In the first and second parts of our investigation, we expected to obtain hexahydrocyclohepta[b]indole and tetrahydrocyclopenta[b]indole derivatives. Fig. 25 shows the synthetic route to these products.

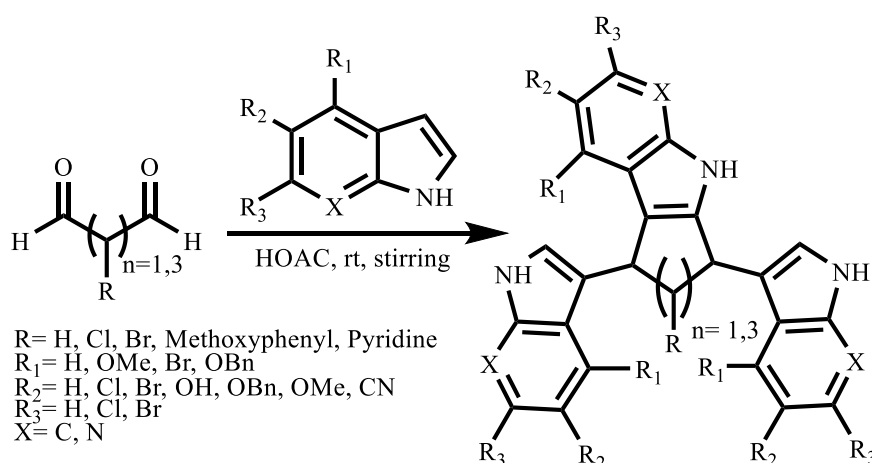


Fig. 25 Syntheses of hexahydrocyclohepta[b]indoles and tetrahydrocyclopenta[b]indoles

The plausible mechanism of the above reaction is shown below:

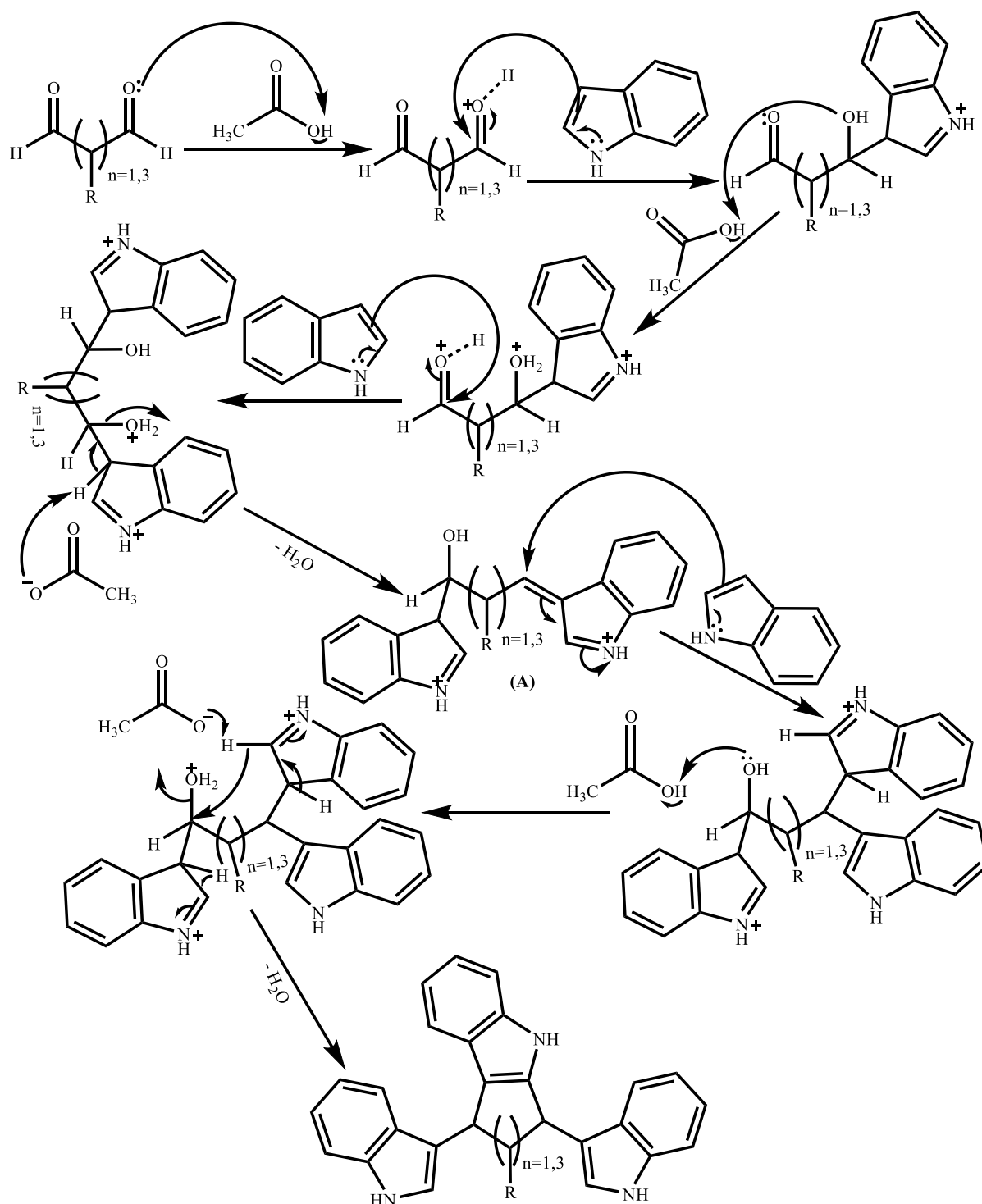


Fig. 26 The plausible mechanism of our reactions to hexahydrocyclohepta[b]indoles and tetrahydrocyclopenta[b]indoles<sup>123</sup>

According to the mechanism, the electrophile malondialdehyde or glutaric dialdehyde is initially protonated in the presence of acetic acid as protic solvent. As we discussed in the introduction section, the electron density at C-3 ( $\beta$ ) position of indole is the highest; therefore, indole most likely attacks the electron-withdrawing site of  $\text{C}=\text{OH}^+$  via the C-3 nucleophile. The hydroxyl (OH) group formed as a result of first indole molecule addition is protonated followed by the protonation of the adjacent carbonyl functional group on dialdehyde and the addition of the second indole molecule respectively. The conjugate base of acetic acid (acetate ion) ( $\text{CH}_3\text{COO}^-$ ) attacks the  $\text{H}_\beta$  on indole to proceed the dehydration step (water elimination step) which leads to the formation of azafulvenium intermediate (**A**). In the next step, the third indole molecule attacks the less-hindered site of alkene functional group and the first indole molecule added is aromatised. The second hydroxyl group formed by attacking the second indole molecule is protonated and the attack of conjugate base of acetic acid to  $\text{H}_\alpha$  leads to a long-distance dehydration; the  $\text{H}_\alpha$  of one indole molecule and  $\text{OH}_2^+$  ion on another indole molecule are involved, in this case, the dehydration is favoured because of the closure of 5 and 7-membered rings. However, the formation of a 5-membered ring (tetrahydrocyclopentaindole) product is more favoured because of the higher stability of cyclopentene compared to cycloheptene<sup>1,46</sup>.

In our proposed mechanism, only one synthetic route is shown. The difference between the mechanisms is related to the attack site of the second indole molecule; in our mechanism, the second indole molecule attacks the second protonated carbonyl group; however, this indole molecule is also likely to attack the less-hindered site of olefin group after the formation of azafulvenium intermediate; that is, two indole molecules could be located on the one side of the intermediate which is in agreement with the proposed mechanism to the formation of bis(indolyl)alkaloids<sup>51</sup>. The evidence proving this plausible mechanism is the formation of 3,3'-(5-oxopentane-1,1-diyl)bis(1H-indole-5-carbonitrile) as the result of the observed incomplete reaction of indole-5-carbonitrile to glutaric dialdehyde (Fig. 27). The  $^1\text{H}$ -NMR spectrum of this compound showed one singlet broad peak with the peak integration of 2 at 10.62 ppm (NHs) and one triplet sharp peak with the integration of 1 at 9.72 ppm (aldehydic proton). The aromatic region (8-7 ppm) also showed 4 different peaks with the integration of 2 for each peak confirming two symmetrical indolyl moieties in the structure. Another peak at 2.55 ppm with the coupling pattern of a triplet of doublet and peak integration of 2 proves the two protons on the other side of the aldehydic group. Lower  $^3\text{J}$  value (coupling constant) of aldehydic proton is probably because of the electron-withdrawing group (EWG) of  $\text{C}=\text{O}$

(1.59 compared to 7.28 Hz). The peak of 366.53 Dalton in the ESI-Mass spectrum of the compound confirmed this structure. For further spectral data, please refer to the Experimental and Appendix sections.

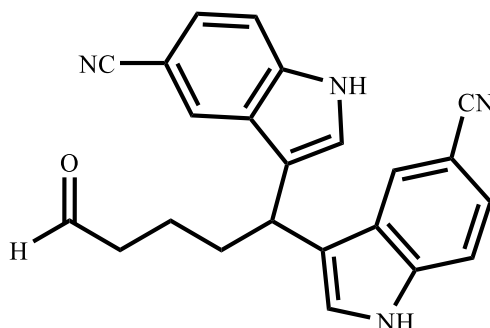


Fig. 27 The observed possible product of our incomplete reaction

During our investigations, we also successfully isolated tetraindolyl compounds beside our trisindolyl products (hexahydrocyclohepta[b]indoles and tetrahydrocyclopenta[b]indoles) (Fig. 28). The formation of these tetraindolyl products had been expected because of the excess amount of indoles in our experiments. The formation of 1,1,4,4-tetra(1H-indol-3-yl)propane products (tetraindolyl compounds) was proved by the mechanism of the reaction<sup>123</sup> and the structures of these products were elucidated by <sup>1</sup>H-NMR (Experimental Section). Fig. 29 shows the mechanism to the formation of these products.

As can be clearly seen, the formation mechanism of these compounds contains the same steps as those of trisindolyl products with the exception of the final ring closure step. In case of the tetraindolyl product formation, the fourth indole molecule attacks the less-hindered site of the olefin group on the iminium intermediate molecule to aromatise the indole molecule and form the tetraindolyl product respectively (Fig. 29).

The <sup>1</sup>H-NMR spectrum of 3,3',3'',3'''-(pentane-1,1,5,5-tetrayl)tetrakis(1H-indol-5-ol), showed one broad signal with the peak integration of 4 at 9.56 ppm. This peak was assigned to four pyrrolic protons in indole moieties of the structure. In the range of 7.15-6.62 ppm, four signals at 7.14, 6.98, 6.96, and 6.62 ppm with the peak integration of four for each peak were observed. These peaks stood for four different aromatic protons at the indole moiety because the molecule is symmetrical and each aromatic proton of one indole molecule is chemically equivalent to those of other indole molecules. A triplet signal with the coupling constant (J) of 7.43 Hz and the integration of two at 4.27 ppm was observed (H<sub>as</sub>). Furthermore, two

multiple peaks in the ranges of 2.39-2.35 ppm and 1.22-1.19 ppm with the peak integrations of four and two were observed for  $H_b$ s and  $H_c$ s (Fig. 28).

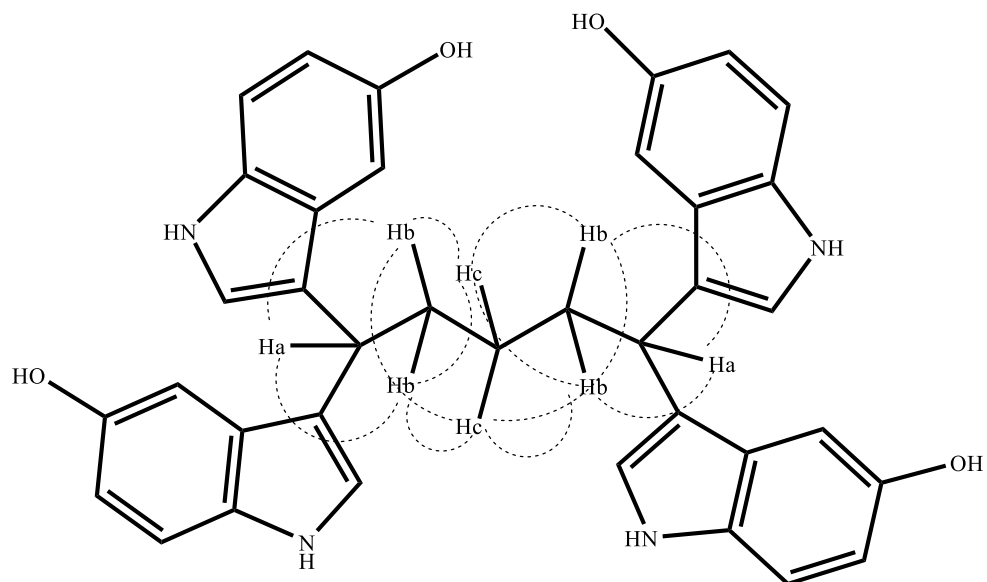


Fig. 28 The possible couplings and correlations between  $H_a$ s,  $H_b$ s, and  $H_c$ s



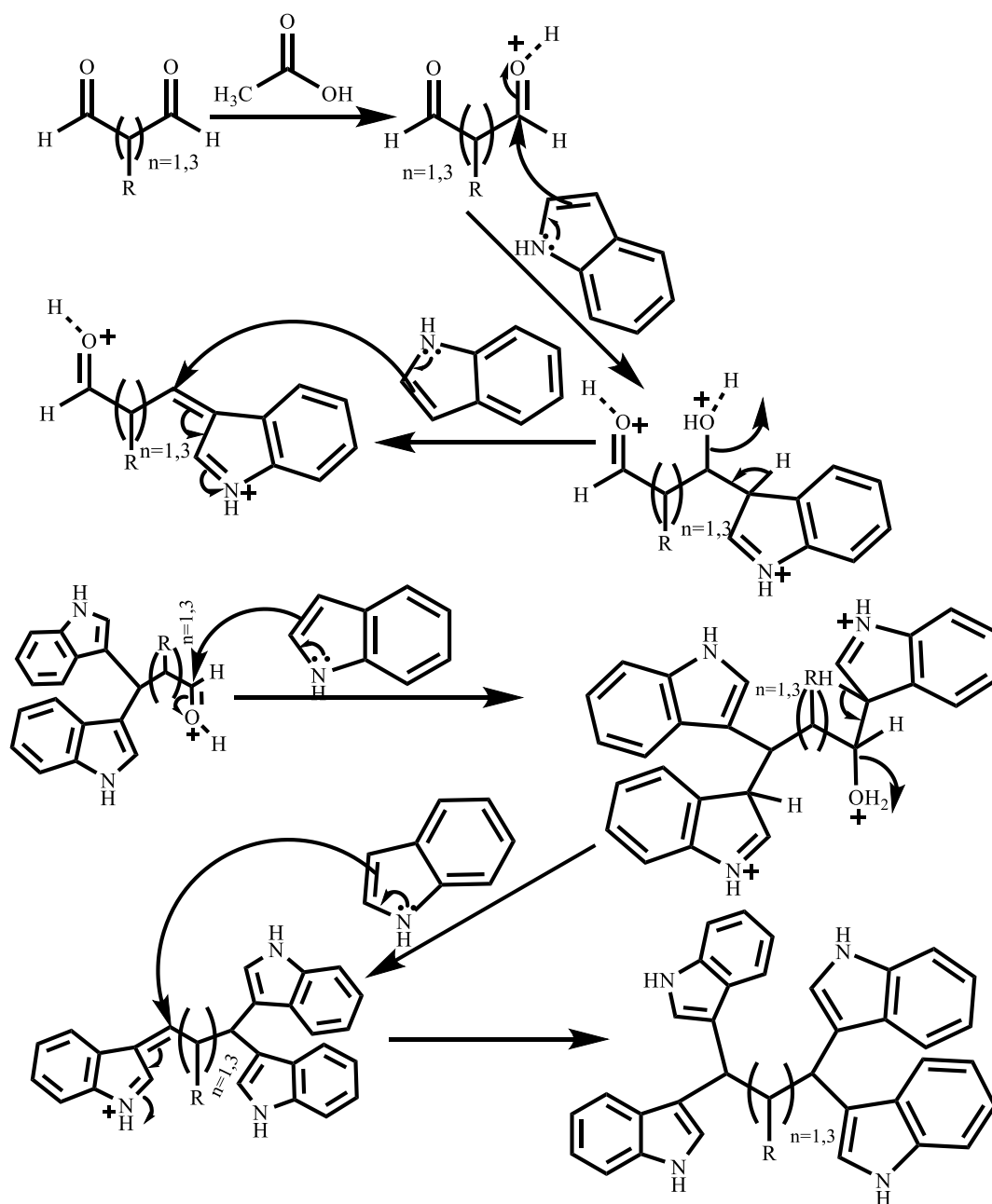


Fig. 29 The plausible mechanism of formation of 1,1,4,4-tetra(1H-indol-3-yl)propane compounds<sup>123</sup>

### 2.1.2 The formation of (Z)-3,3',3'' tris products

In the reactions of glutaric dialdehyde with substituted and unsubstituted indoles, the two predicted products- hexahydrocyclohepta[b]indoles and 3,3',3''-(pentane-1,1,5,5-tetrayl)tetrakis indoles with the exception of 5-carbonitrile indole were obtained and their structures were elucidated by  $^1\text{H}$ -NMR (Experimental Section). However, in some reactions of substituted malondialdehydes with indoles, (Z)-3,3',3'' tris products were obtained beside the tetrahydrocyclopenta[b]indoles. Fig. 30 shows the possible mechanism to the formation of these products.

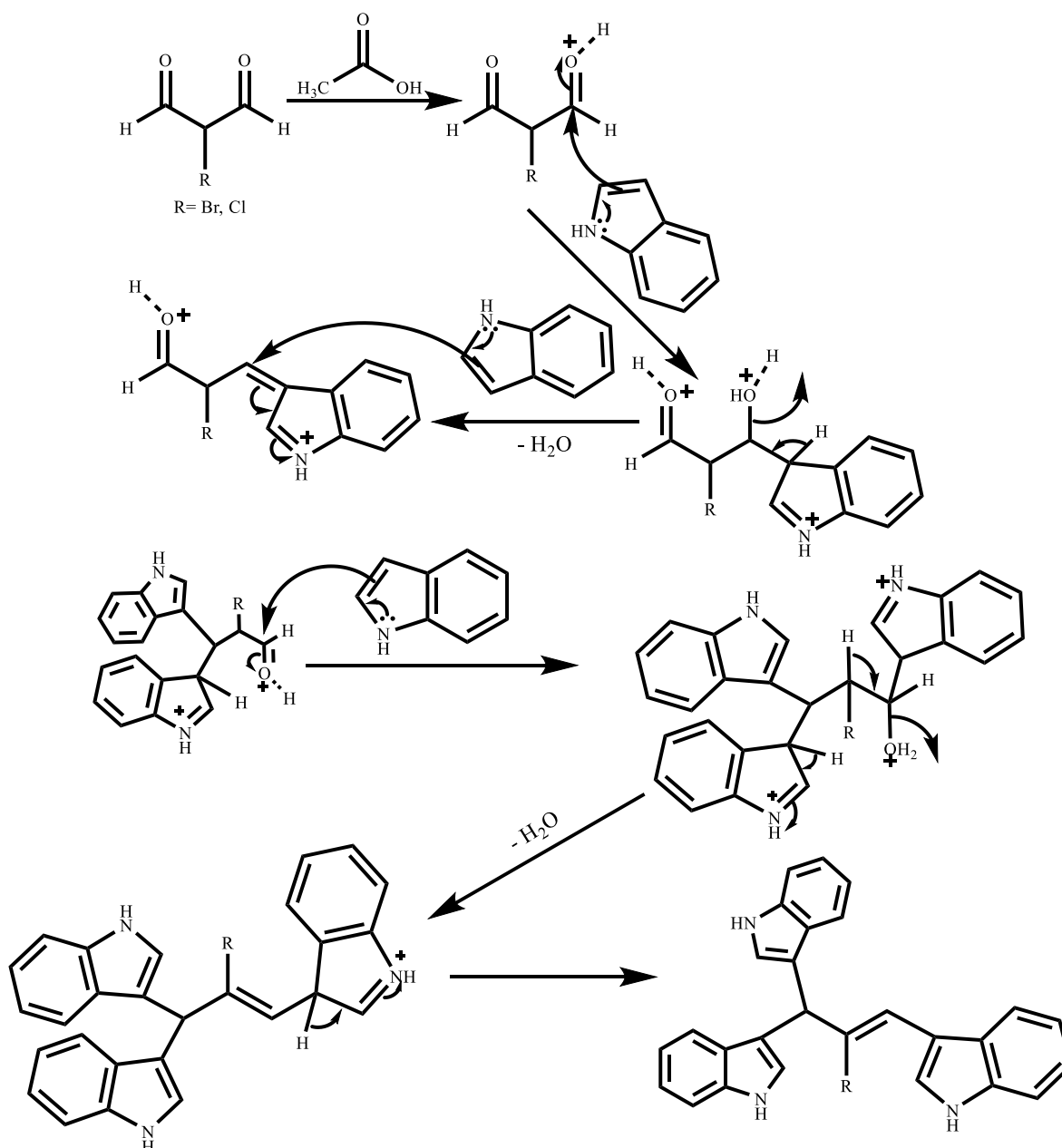


Fig. 30 The mechanism of the formation of (Z)-3,3',3'' tris products

The steps of the above mechanism are as follows:

- 1- Malondialdehyde molecule is protonated in the presence of glacial acetic acid.
- 2- The first indole molecule attacks the protonated carbonyl group followed by water elimination and formation of an azafulvenium intermediate respectively.
- 3- The second nucleophile attacks the double bond and the first indole molecule is aromatised.
- 4- The attack of the third indole molecule to the another protonated carbonyl group leads to the dehydration and the formation of a substituted alkene group accordingly.  
Aromatisation occurs after the attack of acetate ion to  $H_\beta$  near the iminium intermediate.

The water elimination (dehydration) of alcohols involves E1 mechanism. In E1 mechanism, a carbocation is formed in the first step as a result of the leaving a group. In the next step, the base attacks the adjacent group possessing the *trans* or *anti* stereochemistry to the leaving group to remove it and to form a more substituted alkene. Since a carbocation is formed in the first step, the carbocation rearrangement is likely to happen via the H or R shift to form a more stable carbocation. It is expected that tertiary alcohols are the most reactive alcohols in E1 mechanism and the reactivity decreases going to the secondary and primary alcohols. In the dehydration process, the leaving group is  $OH_2^+$ . In E2 mechanism, the attack of the base to the adjacent proton and leaving a group occurs in one step. Generally, the factors which affect the elimination mechanism are the nature of the leaving group, the nature of the base, the electronic and steric effects of substituents in the reactant molecule, and the solvent effects. The secondary alcohols can process the dehydration via E1 or E2<sup>46</sup>. The possible dehydration processes in the reactions of indoles with glutaric dialdehyde and substituted malondialdehydes are shown in Figures 31 and 32.

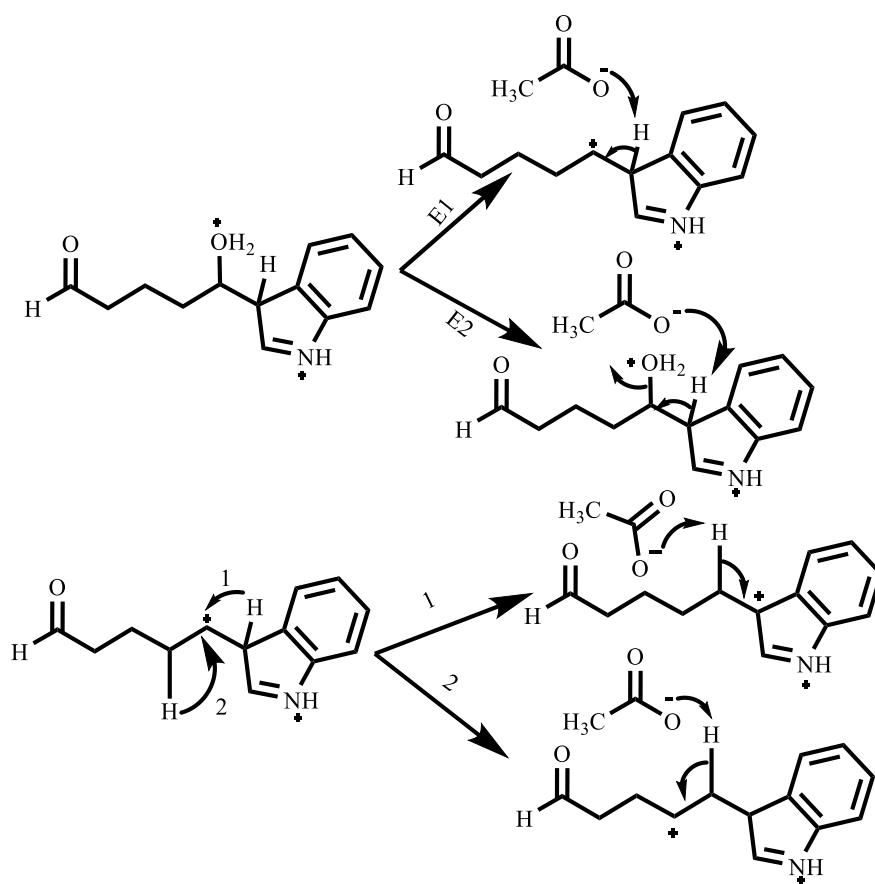


Fig. 31 The possible dehydration processes in the reaction of glutaric dialdehyde with indoles

Based on the above scheme, in E1 dehydration, a secondary carbocation is initially formed as a result of leaving H<sub>2</sub>O. In the next step, two proton shifts are likely to occur. The proton shift 1 leads to a tertiary carbocation followed by the attack of the base and the formation of azafulvenium intermediate respectively. The second proton shift leads to a secondary carbocation which is not likely to be as favoured as a tertiary carbocation because the tertiary carbocation is more stable than the secondary carbocation and the formation of a major product is likely to happen via the formation of a tertiary carbocation. Furthermore, based on the plausible mechanism for the reactions of indoles with aldehydes which leads to the formation of azafulvenium intermediate, the first proton shift is more likely to happen. If our molecule undergoes the E2 dehydration, the favourable product will be the same as E1. To conclude, in both E1 and E2 dehydrations the favourable plausible product will be the same and the formation of trisindolyl and tetraindolyl products takes place under both dehydration processes. However, molecules can process via E1, E2 or both of them depending on the other factors mentioned above.

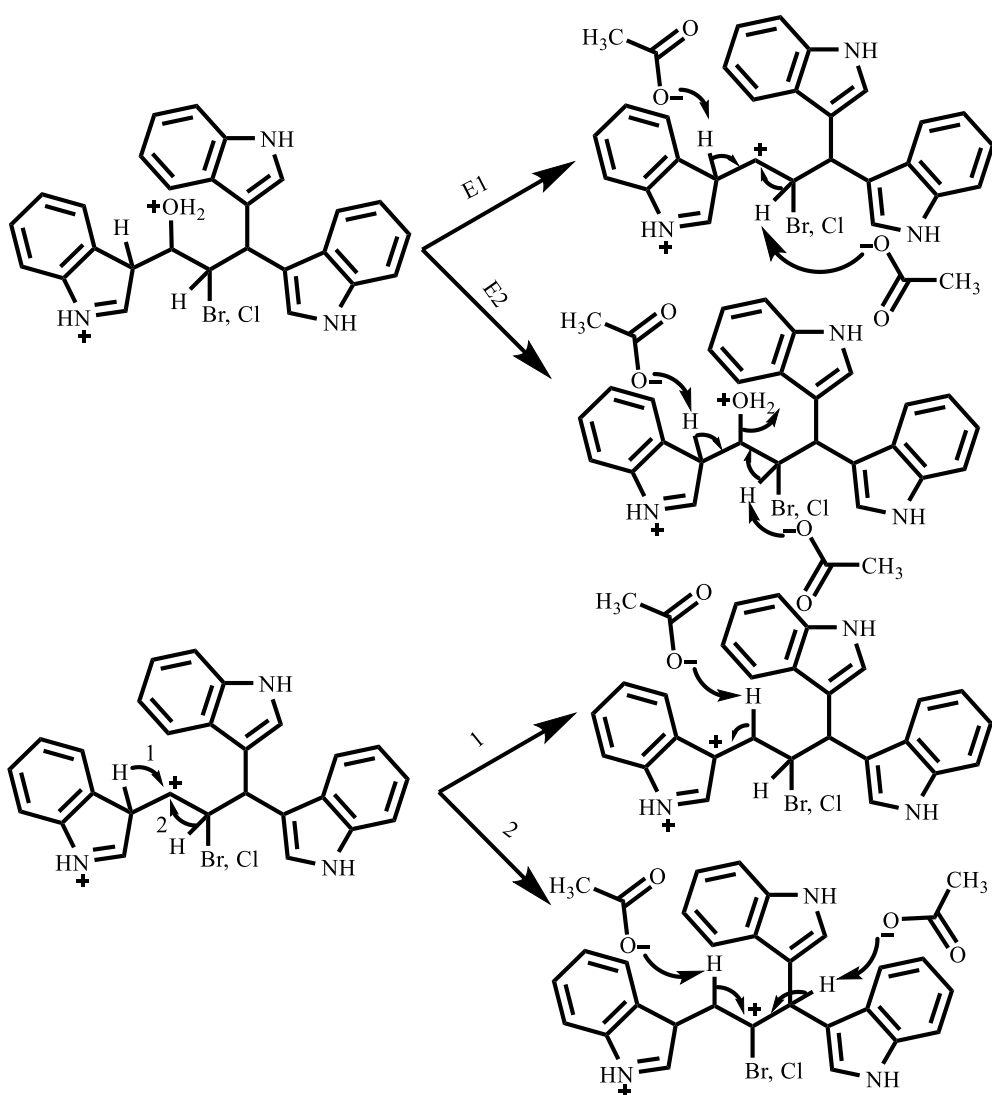


Fig. 32 The possible dehydration processes in the reactions of 2-bromo and 2-chloro-malondialdehydes with indoles

In the reactions of 2-bromo or 2-chloro malondialdehydes with indoles, E1 dehydration leads to a secondary carbocation followed by two possible proton shifts. The first possible proton shift results in the formation of a tertiary carbocation and azafulvenium intermediate, attack of fourth indole molecule or long-distance ring closure, and a tetraindolyl or trisindolyl product respectively. The second proton shift leads to another tertiary carbocation with two possible attacks for acetate ion which result in (Z)-3,3',3'' tris products (left side) and another product (right side). The attack of the acetate ion from the right side does not seem to be favorable because of the steric hindrance of two fairly bulky indole molecules. However, the attack of acetate ion from the left side seems to be favorable because of the sterically less-hindered site of the attack. The dehydration process via E2 also leads to three products: the

tetraindolyl or trisindolyl product as a result of azafulvenium intermediate and the attack of fourth indole molecule or long-distance ring closure respectively (left side) and the (Z)-3,3',3'' tris product as the result of the attack of acetate ion to less-hindered site and the formation of favourable alkene (substituted alkene) (right side). In Z-conformation the steric hindrance and electronic repulsion effects because of bulky and electron-rich indole molecules seem to be less than those in E-conformation; therefore, the Z-conformation is likely to be more favorable than E-conformation.

#### **2.1.2.1 The spectral data confirming the formation of (Z)-3,3',3'' tris products**

The  $^1\text{H}$ -NMR spectra of the products which are most likely to possess the above structure showed one peak with the integration of 1 at the range of 5.88 to 6.05 ppm depending on the electron property and the position of substituents on both indoles and malondialdehydes. The splitting pattern of this peak varies from quartet with the J value between 0.80 and 1.10 Hz for  $^4\text{J}$  to singlet. This peak is assigned Proton 2 in the structure. Meanwhile, for the proton 1, peaks with the chemical shifts between 7.16 and 7.40 ppm and variable splitting patterns of singlet, doublet, and doublet of doublet were assigned. In the case of doublet of doublet splitting, J value of approximately 0.9 Hz was observed which was in accordance with that of proton 2 (Experimental Section and Fig. 33).

2D-NMR spectrum (NOESY) of the compound below (number 22) showed a correlation between proton with the chemical shift of 5.88 ppm and protons with the chemical shifts of 7.26, 7.46, and 7.55 ppm attributed to  $\text{H}_1$ ,  $\text{H}_{3\text{s}}$ , and  $\text{H}_{4\text{s}}$  respectively (Fig. 33). The APT spectrum of this compound showed one CH peak in aliphatic (up-field) region-46.437 ppm. The HSQC spectrum also showed a correlation between this carbon and the proton at 5.88 ppm (Appendix section).

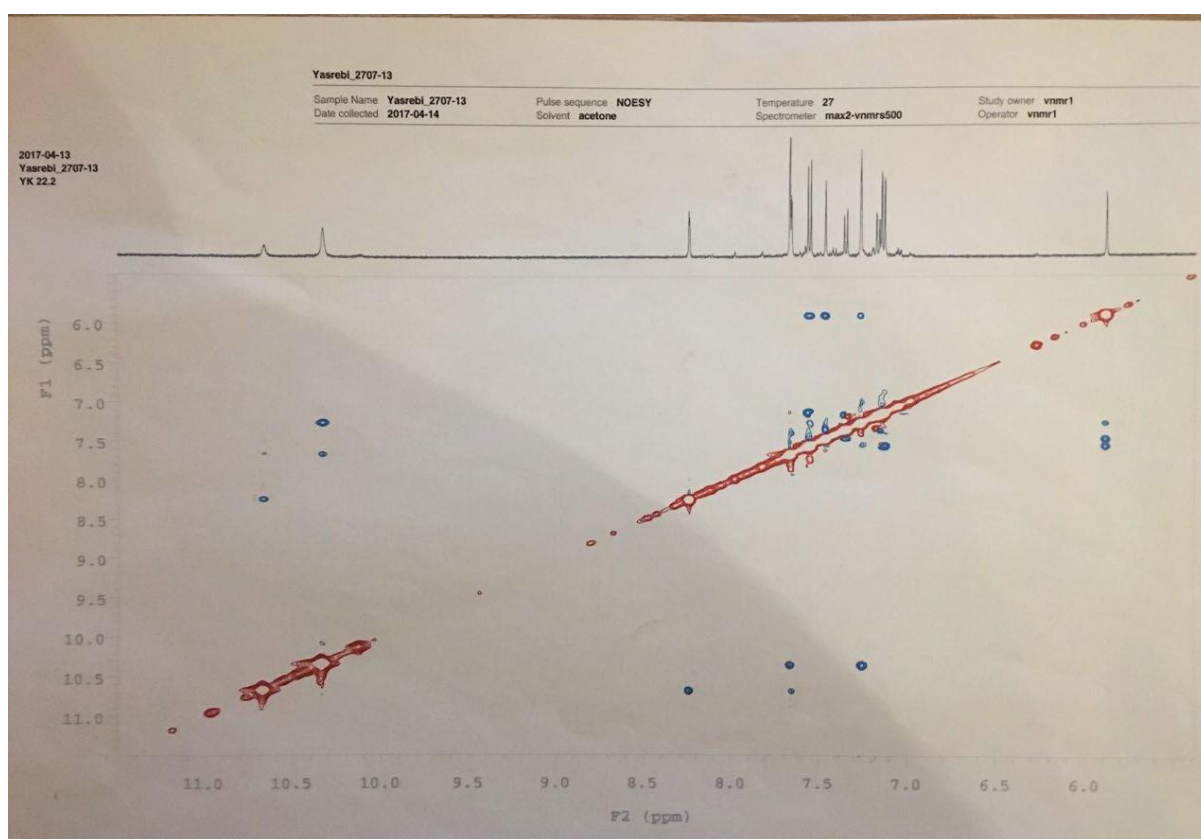
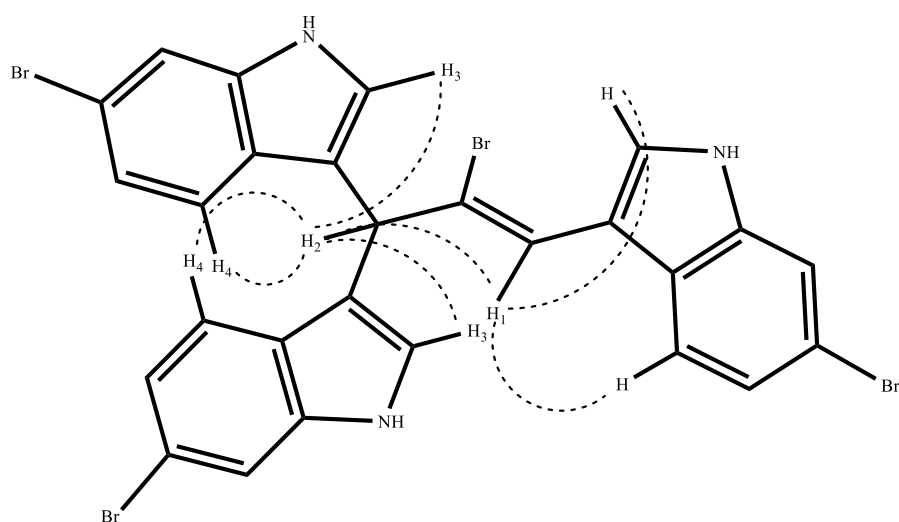


Fig. 33 The scheme of possible correlations of H<sub>2</sub> and H<sub>1</sub> and NOESY in compound 22

### 2.1.2.2 The possible stereochemistry of chiral centres in hexahydrocyclohepta[b]indoles and tetrahydrocyclopenta[b]indoles

The assignment of  $^1\text{H}$ -NMR spectra of asymmetrical (chiral) hexahydrocyclohepta[b]indole products (no possible symmetry operation such as plane ( $\delta_n$ ) and axis ( $C_n$ ) of symmetry<sup>124</sup>) revealed signals at the chemical shifts between 3.98 and 5.64 ppm with the multiplicities of triplet and triplet of doublet with regard to  $H_a$ . These spectra also showed other signals at slightly higher chemical shifts of 3.98 to 6.08 ppm most possibly because of the inductive effect of the electronegative nitrogen atom with the same multiplicities of  $H_a$ . These peaks are assigned to  $H_b$ . Due to the molecule which is asymmetrical,  $H_a$  and  $H_b$  are chemically different; therefore, two different signals corresponding these two protons are observed in  $^1\text{H}$ -NMR spectra of these compounds. The possible correlation and splitting of  $H_a$  and  $H_b$  by neighbouring protons are revealed in Figure 34. The coupling constants for  $H_a$  and  $H_b$  were mostly between 8-6 Hz ( $^3J$ ) (vicinal coupling) (arrows) and approximately 1.00 Hz ( $^4J$ ) (long-range coupling) (dots) in triplet and triplet of doublet coupling patterns respectively (Experimental Section for the compounds 1, 6, 7, 8, 9, 10, 11).

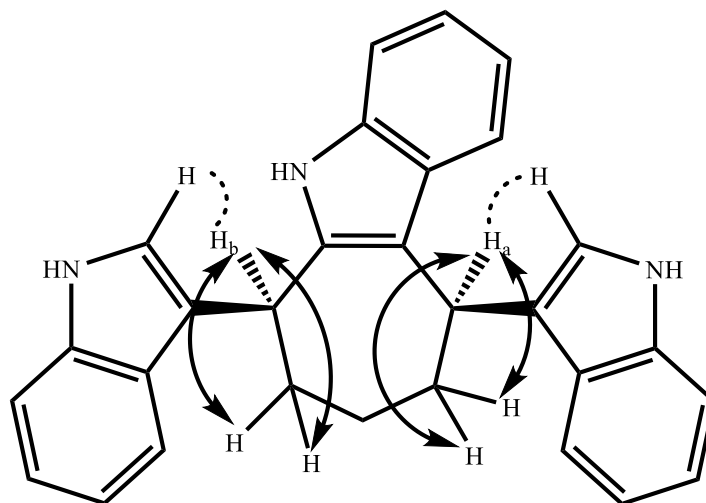


Fig. 34 the possible couplings for  $H_a$  and  $H_b$

The possible configurations of these two chiral centres are (*S/R*- two indole molecules are pointing out of the plane) or (*R/S*- two indole molecules are pointing in the plane) and the stereochemistry of *cis* or orientation of *syn*. This is probably because of the ring-size of cycloheptane which reduces the steric hindrance and allows the two indole molecules to take the same orientation.



In terms of the  $^1\text{H}$ -NMR spectra of tetrahydrocyclopenta[b]indole products (compounds 3, 4, 12, 13, 15, 16, 17, 18, 19, and 21) three aliphatic proton signals were observed: two different signals at the chemical shift range of 3.60-5.75 ppm with the multiplicities of doublet, doublet of doublet, and doublet of doublet of doublet corresponding to  $\text{H}_a$  and  $\text{H}_b$  and one signal at the range of 4.12-5.47 ppm with the multiplicities of triplet and doublet of doublet corresponding to  $\text{H}_c$ . Similar to the hexahydrocyclohepta[b]indole products, the difference of the chemical shift of  $\text{H}_a$  and  $\text{H}_b$  arose from the inductive effect of electron-withdrawing group of NH. The signal of  $\text{H}_c$  mostly appeared at up-field region than those of  $\text{H}_a$  and  $\text{H}_b$  with the exception of (pyridin-4-yl)-1,2,3,4-tetrahydrocyclopenta[b]indole and 5-bromo-1H-indol-3-yl)-2-chloro-1,2,3,4-tetrahydrocyclopenta[b]indole products in which the strong electron-withdrawing groups of pyridine and chlorine led to the down-field signals. Figure 35 shows the possible coupling and correlation of  $\text{H}_a$ ,  $\text{H}_b$ , and  $\text{H}_c$ . The coupling constants for  $\text{H}_c$  were in the range of 8-7 Hz ( $^3\text{J}$ ) because this proton couples to  $\text{H}_a$  and  $\text{H}_b$ .  $\text{H}_a$  and  $\text{H}_b$  which are not chemically equivalent; that is, these two protons are not interchangeable through symmetry operations such as plane ( $\sigma_n$ ) and axis ( $\text{C}_n$ ) of symmetry<sup>124</sup>. This is because of the asymmetrical molecular scaffolds of our products. However, the coupling pattern of triplet was mostly observed for  $\text{H}_c$  due to accidental degeneracy of peak total, partial coincidence or peak overlapping<sup>124</sup>. In case of doublet of doublet multiplicity, the J values were fairly similar. For  $\text{H}_a$  and  $\text{H}_b$ , there is coupling to  $\text{CH}_c$  ( $^3\text{J}$ ) with the coupling constant of 8-7 Hz, and two different long range couplings ( $^4\text{J}$  and  $^5\text{J}$ ) with the J values of 2-1 and 1-0 Hz approximately (Experimental Section).

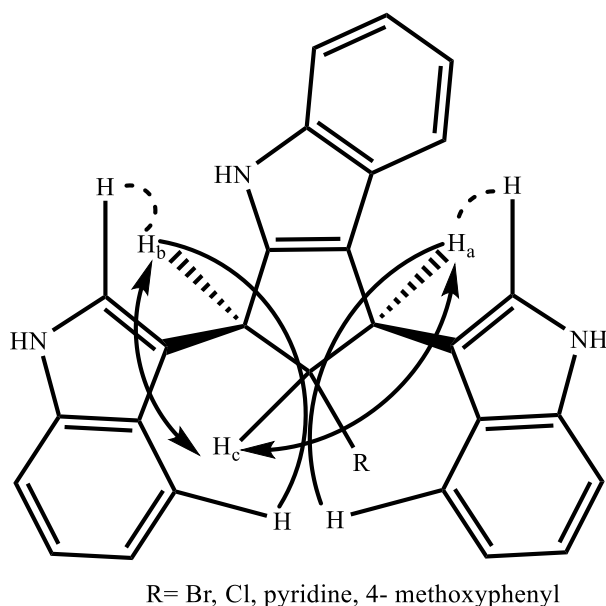


Fig. 35 the possible coupling for  $H_a$ ,  $H_b$ , and  $H_c$  in tetrahydrocyclopenta[b]indole derivatives

In tetrahydrocyclopenta[b]indole products, three chiral centres corresponding to  $CH_a$ ,  $CH_b$ , and  $CH_c$  are observed. As we discussed above, the favourable configurations and the stereochemistry or orientation of  $CH_b$  and  $CH_a$  on cyclohepta-indole products were considered (*S/R*) or (*R/S*) and *cis* or *syn* respectively because of the ring size of cycloheptane. In the case of cyclopenta-indole products, the smaller ring size should favour the configurations of *R/R* when the indole attached to  $CH_b$  is pointing in the plane and the indole attached to  $CH_a$  is pointing out and *S/S* when the indoles attached to  $CH_b$  and  $CH_a$  are pointing out and in of the plane respectively and the stereochemistry of *trans* or *anti* in order to reduce the steric hindrance caused by two indole molecules and to form the more stable structure of the molecular scaffold. However, the  $^1\text{H-NMR}$  data showed two different signals for two chemically different  $H_b$  and  $H_a$  with the similar  $^3J$  values (coupling constants of 8-7 Hz). The similar situation had been observed for  $H_b$  and  $H_a$  on cyclohepta-indole derivatives. Based on this observation, the possible stereochemistry was likely to be *cis* and the orientation of  $H_b$  and  $H_a$  was possibly *syn*. The configurations of  $CH_b$  and  $CH_a$  were likely to be *R/S* or *S/R* when the both indoles attached to  $CH_b$  and  $CH_a$  are pointing out or in of the plane respectively (Experimental Section).

The chemistry of cyclopentane shows that this molecule is a regular pentagon in two dimensions but in three dimensions it mostly appears in conformations of envelope because it distorts very slightly into the envelope. Because of the freedom of rotation cyclopentane converts to other conformations such as twist. The energy differences between the envelope

and twist conformations are very low and many conformations of envelope and twist with different dihedral angle relationships exist in an individual structure<sup>125</sup>; therefore, variable vicinal coupling constants are observed in cyclopentane. In envelope conformations is  $^3J_{\text{cis}} > ^3J_{\text{trans}}$  and in twist conformations is  $^3J_{\text{trans}} > ^3J_{\text{cis}}$ . In some cyclopentanes, the *cis* protons will have the dihedral angle of  $0^\circ$  and *trans* protons have the angle of approximately  $120^\circ$ . Hence, the coupling constant of *cis* protons is greater than that of *trans* (10-8 Hz to 9-2 Hz). However, there are many cases in which  $^3J_{\text{trans}} > ^3J_{\text{cis}}$  or the J values of *cis* and *trans* protons are identical. In rigid cyclopentanes (bicyclo structures) the endo-endo or exo-exo protons (*syn* orientation) reveal higher coupling constants than endo-exo (*anti* orientation). As a result, the determination of the stereochemistry of vicinal protons in 5-membered rings by evaluating the coupling constants is not reliable<sup>126</sup>.

The above finding confirmed that the configuration of  $\text{CH}_c$  and the orientation of  $\text{H}_c$  to  $\text{H}_a$  and  $\text{H}_b$  could not be determined by considering the coupling constants. However, the similar J values resulted from the couplings of  $\text{H}_c$  to  $\text{H}_a$  and  $\text{H}_b$  revealed that the stereochemistry for  $\text{H}_a$  and  $\text{H}_b$  is likely to be *cis* for different stereoisomers (diastereomers) of cyclopentaindole compounds.

### 2.1.3 The electrophilic substitution reactions of indoles to *o*-phthaldialdehyde

*O*-phthaldialdehyde or benzene-1,2-dicarbaldehyde can be obtained by the hydrolysis of  $\alpha, \alpha, \alpha', \alpha'$ -tetrachloro-ortho-xylene but this compound is now commercially available. In the 1980s, *o*-phthaldialdehyde was used for amino acid analysis and determination of peptides by HPLC<sup>127,128</sup>.

In the third part of our study, we focus on the reactions of substituted and unsubstituted indoles with *o*-phthaldialdehyde. The reactions led to the formation of indolobenzo[b]carbazole derivatives (Fig. 36)

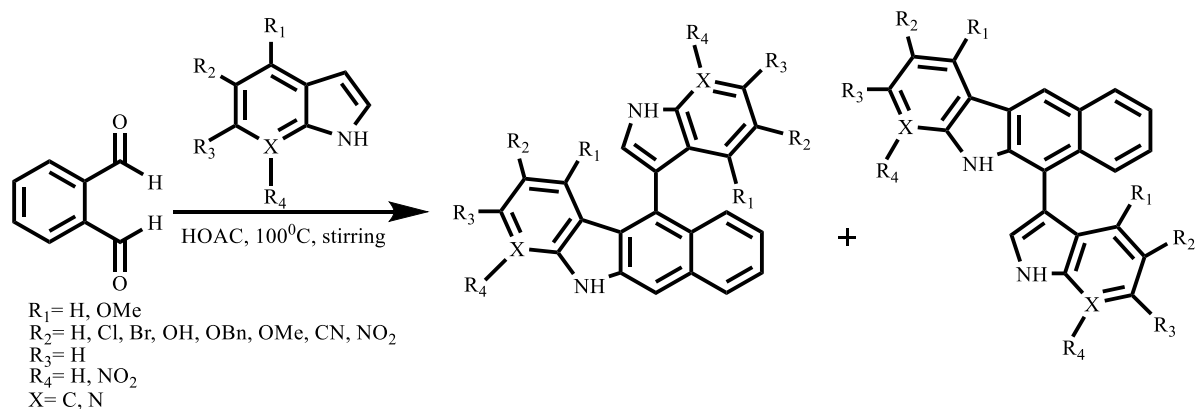


Fig. 36 The reaction of indoles and *o*-phthalaldehyde

The synthesis of indolylbenzocarbazoles attracted remarkable attention in 1990s because of the similar structure to ellipticine<sup>129</sup> which inhibits DNA replication by inhibiting the topoisomerases. The mechanism is likely to be a DNA intercalation<sup>130</sup>. This compound was firstly isolated in the year 1959 from the leaves of *Ochrosia elliptica* Labill<sup>131</sup>. In the same year, this compound was firstly synthesized from the reaction of indole to 3-acetylpyridine in the presence of  $\text{ZnCl}_2$ <sup>132</sup>. Bergman J. et al<sup>133</sup> and Rao M. et al<sup>134</sup> carried out the studies on the synthesis of indolylbenzocarbazoles in 1988 and 1995 chronologically. In 1994, Boogard A. et al<sup>135</sup> synthesized acetylated ellipticine which showed very low cytostatic activity. Many attempts have been made to synthesize new indolylbenzocarbazoles by using  $\text{FeCl}_3/\text{ClCH}_2\text{CH}_2\text{Cl}$  at room temperature<sup>136</sup>, *N*-Carbamoyl  $\text{N} \rightarrow \text{C}$  translocation<sup>137</sup>, intramolecular dehydro Diels-Alder Reactions<sup>138</sup>, and indium-catalyzed annulation of 2-aryl- and 2-heteroarylindoles with propargyl ethers<sup>139</sup>. The main reason is possibly the applications of indolylbenzocarbazole containing molecules-ellipticine analogues such as stauorsporine as a protein kinase C Inhibitor<sup>140</sup>, carbazomycin B as an inhibitor for 5-lipoxygenase, anti-fungal and weak anti-bacterial agent<sup>141</sup>, carbazomadurin A as a neuronal cell-protecting agent<sup>142</sup>, carvedilol as a drug used for the treatment of hypertension and angina<sup>143</sup>, carazolol as a high-affinity  $\beta$ -adrenoceptor antagonist<sup>144</sup>, and clausenamine A as an anti-cancer agent against various human cancer cell lines<sup>145</sup> in medicine.

In 1999, Black D. et al<sup>129</sup> offered two novel stereoselective electrophilic substitution reactions of indoles to *o*-phthalaldehyde. In the first reaction, phosphoryl chloride in anhydrous  $\text{CHCl}_3$  (62-67%) and in the second one, *p*-TsOH in anhydrous MeOH (79%) catalysed the reactions to indolylbenzo[b]carbazoles. The possible mechanisms of these two reactions are shown in the Figures 37 and 38.

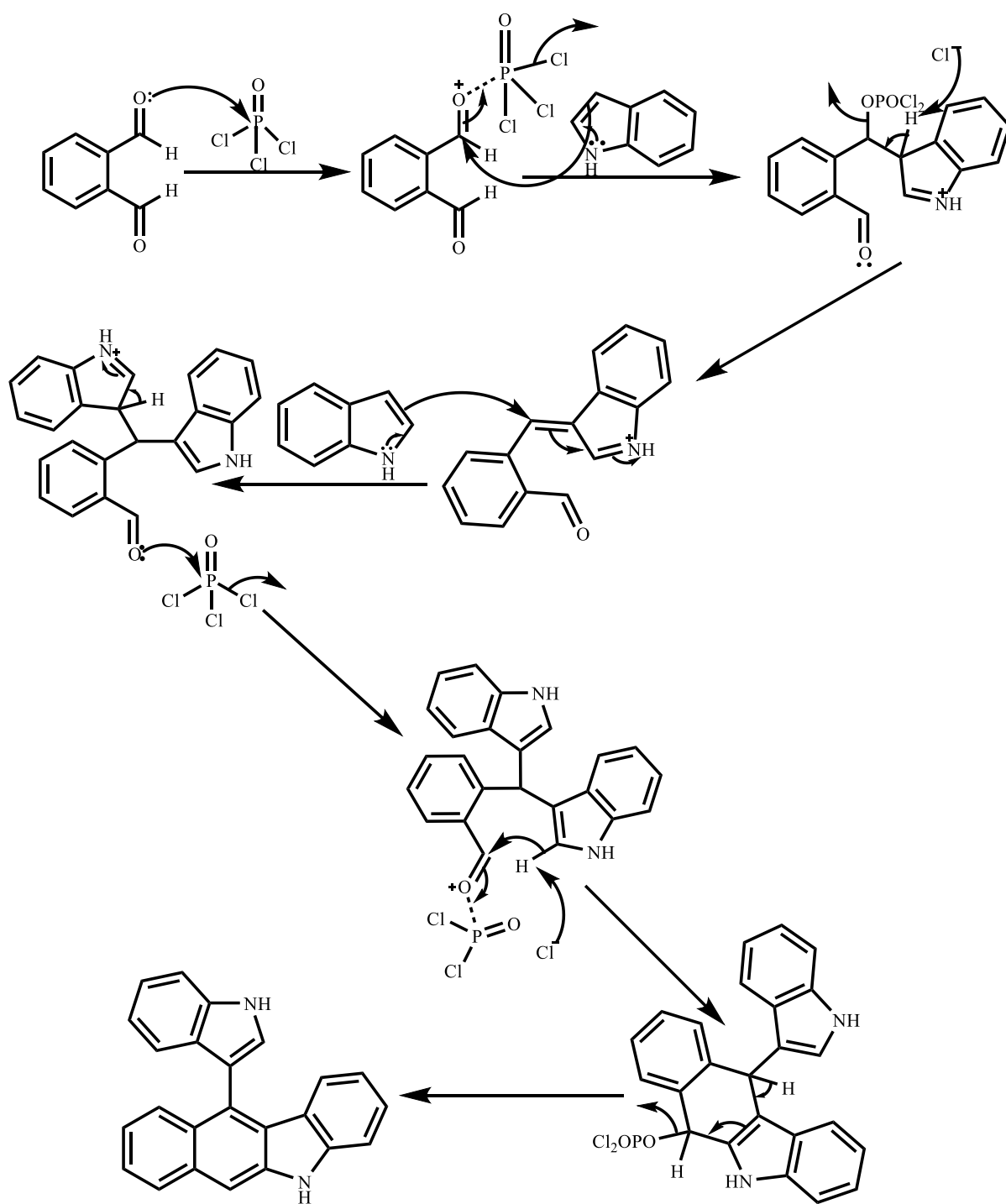


Fig. 37 The possible mechanism of the formation of the first stereoisomer<sup>129</sup>

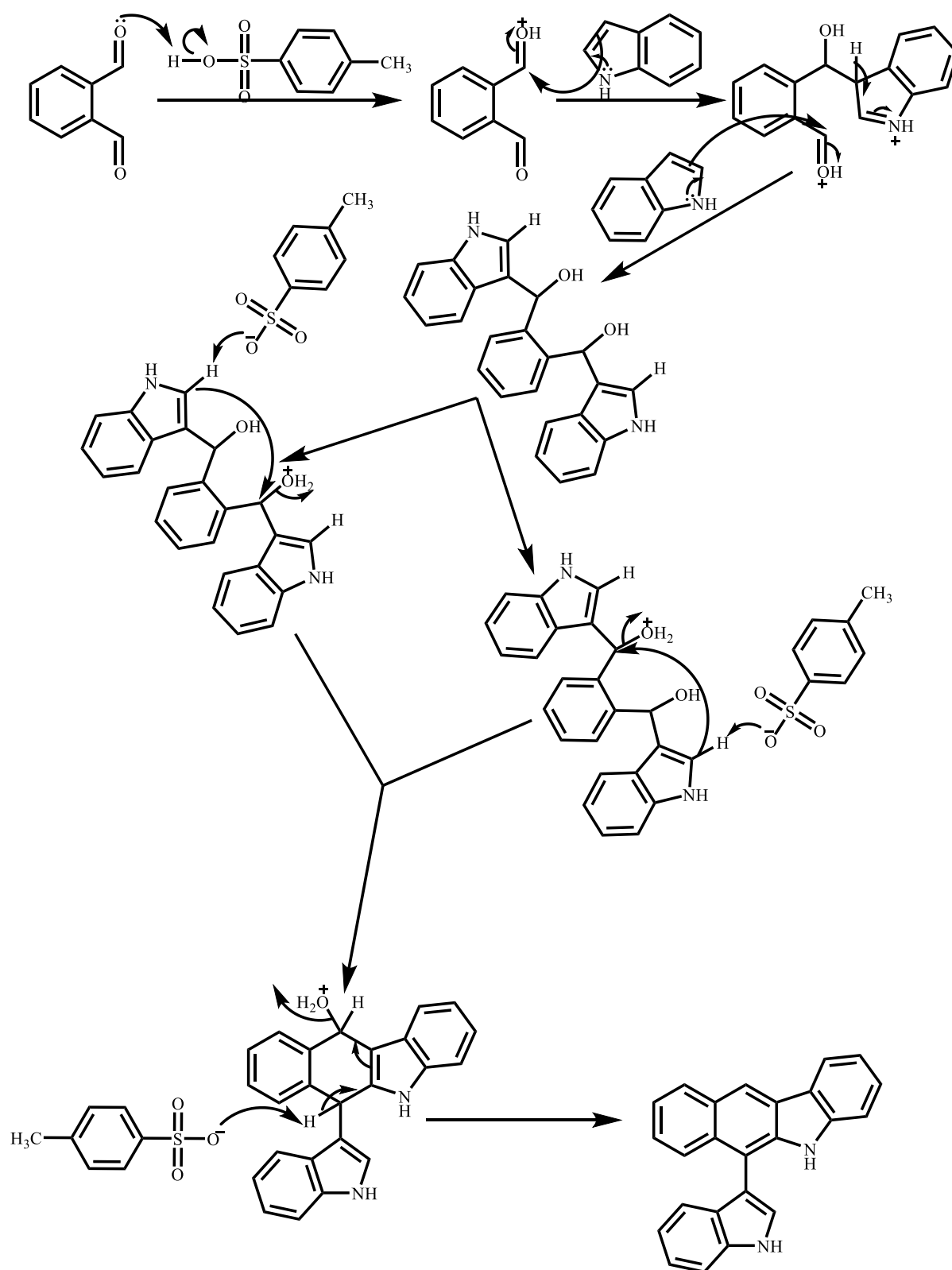


Fig. 38 The possible mechanism of formation of the second stereoisomers<sup>129</sup>

In 2014, Zou. J. F *et al*<sup>146</sup> carried out the same reaction using *p*-TsOH in various solvents such as MeOH, CH<sub>3</sub>CN, and THF at room temperature (87:13 was the ratio of the second

stereoisomer to the first stereoisomer for TsOH/MeOH). Their observations confirmed the formation of the two stereoisomers in various ratios. They continued investigating this reaction by using I<sub>2</sub> in CH<sub>3</sub>CN, Lewis acids such as FeCl<sub>2</sub>, FeCl<sub>3</sub>, Al(OTf)<sub>3</sub>, and Bi(OTf)<sub>3</sub> in MeOH, THF, and CH<sub>3</sub>CN. Finally, they found out that in FeCl<sub>2</sub>/MeOH, TsOH/DCM, and TsOH/CH<sub>3</sub>CN the ratios of the first stereoisomer to the second stereoisomer were 9:91, 82:18, and 50:50 respectively.

In our investigation, we used glacial acetic acid as a mild acid catalyst for the electrophilic substitution reactions of our substituted and unsubstituted indoles to *o*-phthaldialdehyde. We obtained both two atropisomers 1 and 2 in various ratios. The structures of both atropisomers were elucidated by <sup>1</sup>H-NMR. The formation of the first stereoisomer is considered to be the result of the formation of azafulvenium intermediate followed by attacking the second indole molecule to the same site as first indole molecule, cyclisation, dehydration, and aromatization. However, for the second stereoisomer, two aldehyde groups undergo attacks by two indole molecules followed by dehydration and cyclisation, second dehydration, and finally aromatization. The possible mechanisms of our reactions led to the first and second atropisomers are shown in Figures 39 and 40.

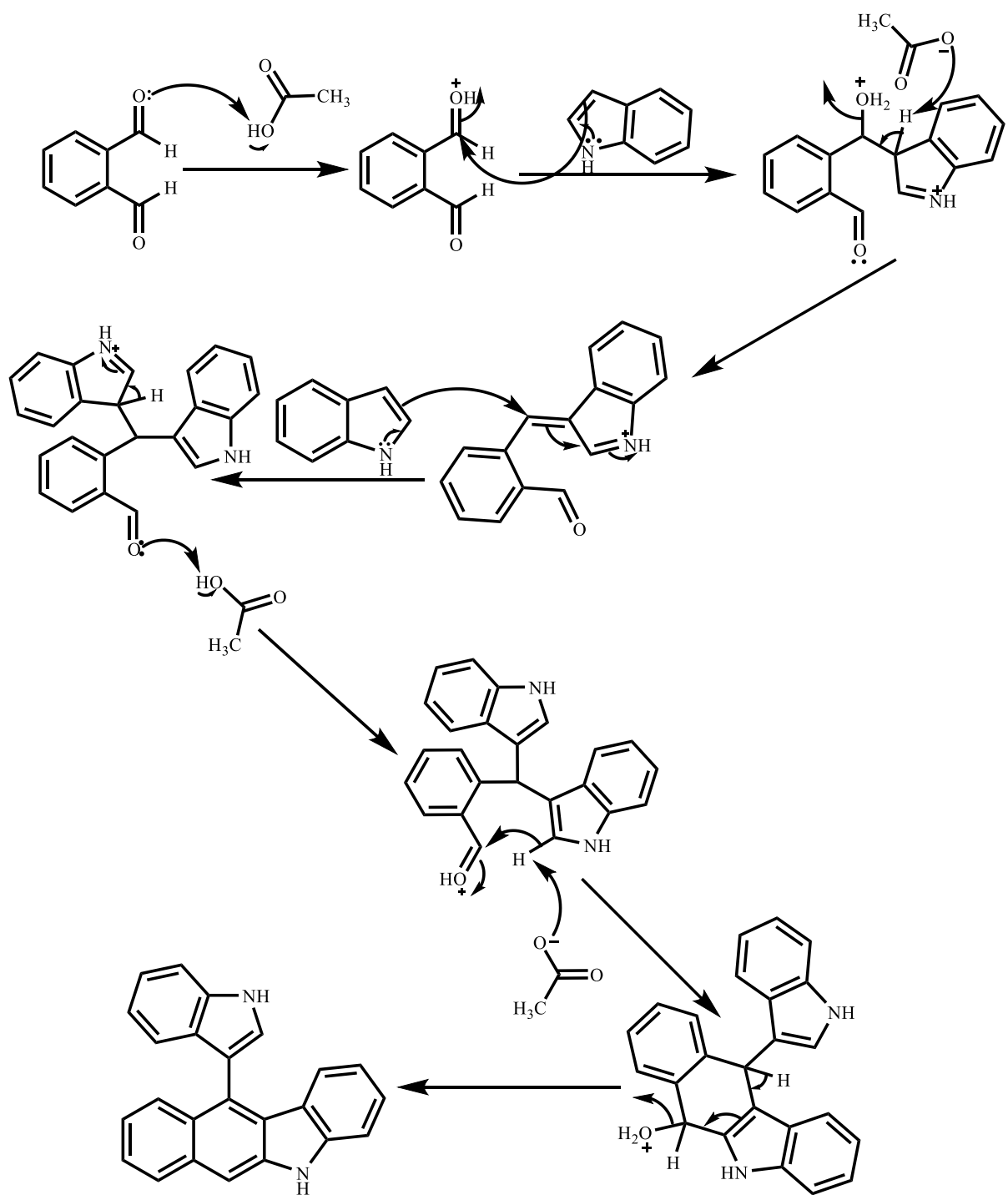


Fig. 39 Plausible mechanism to the first atropisomer<sup>146</sup>



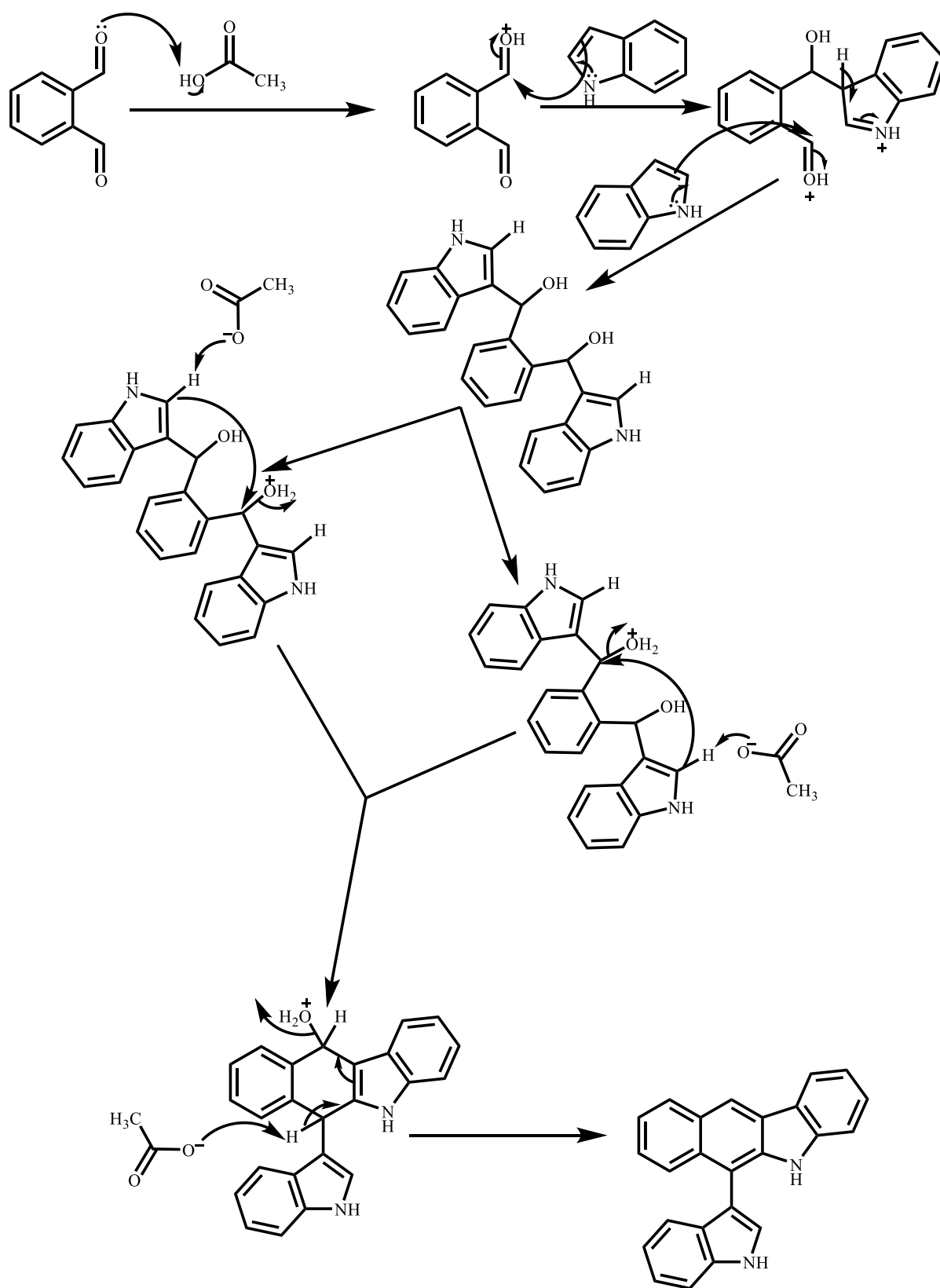


Fig. 40 The plausible mechanism to the formation of the second atropisomer<sup>146</sup>

In the first mechanism, one carbonyl group on *o*-phthaldialdehyde is initially protonated in the presence of our protic acid. In the next step, the first indole molecule attacks this electrophile site via the electron-rich C-3 ( $\beta$ ) position leading to the addition of first indole molecule to our electrophile. The strong leaving group of  $\text{OH}_2^+$  is formed by the protonation of hydroxyl group in the presence of acetic acid. The conjugate base (acetate ion) carries out the dehydration (water elimination) process and leads the reaction to the formation of azafulvenium intermediate. The second indole molecule attacks the less hindered site of double bond to add to the forming molecule followed by re-aromatization. The second carbonyl group on *o*-phthaldialdehyde is protonated. In this step, the acetate ion attacks the  $\text{H}_\alpha$  on either of indole molecules. The main reason for this process is the formation of the stable and favourable 6-membered ring. In the last step,  $\text{H}_2\text{O}$  leaves the intermediate followed by re-aromatization to form the 11-indolylbenzocarbazole products (Fig. 39).

In the second plausible mechanism, after the protonation of carbonyl group and the addition of first indole molecule, the second indole molecule attacks the second protonated carbonyl group and leads the reaction to the formation of a diol intermediate. At this step, there are two possible routes toward ring-closure and dehydration. Both routes lead to the same product because of the same possibility and the symmetry of the dicarbinol intermediate. The 6-indolylbenzocarbazole product is formed after ring-closure, dehydration, and aromatization respectively (Fig. 40).

The compound 5-(1H-pyrrolo[2,3-b]pyridin-3-yl)-10,11-dihydro-5H-benzo[f]pyrido[2,3-b]indol-10-ol (compound 28) resulted from the reaction between *o*-phthaldialdehyde and 7-azaindole and was isolated successfully during our investigations (Fig. 41). The  $^1\text{H}$ -NMR of this compound showed one broad signal at 5.95 ppm corresponding to OH function and 13 protons in the chemical shift range of 8.34-6.42 ppm. The APCI-Mass spectrum of this compound showed the  $m/z$  of 351.1 Dalton ( $[\text{M}^+ - \text{H}]^+$ ). The FT-IR (ATR) spectrum of this compound revealed one strong vibrational band at  $1687\text{ cm}^{-1}$  corresponding to  $\text{C}=\text{N}$  (Experimental Section). This compound was the evidence proving our plausible mechanism to the 11-indolylbenzocarbazole products.

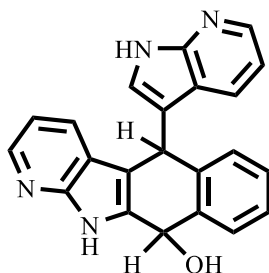


Fig. 41 Compound 28

In the reactions of *o*-phthaldialdehyde with 5-bromo, 5-cyano, 5-nitro, 7-aza, and 7-nitro substituted indoles, we obtained the 11-indolylbenzocarbazole derivative. In the similar reactions between *o*-phthaldialdehyde and 5-chloro substituted and unsubstituted indoles, both 11- and 6-indolylbenzocarbazoles were obtained; however, the major products (the products with the higher percentage yields) were the 11-indolylbenzocarbazoles. On the other hand, in the reactions of *o*-phthaldialdehyde with 5-methoxy, 5-benzyloxy, 5-hydroxy, and 4-methoxy substituted indoles, we obtained the 6-indolylbenzocarbazole product derivative. The above finding indicated that the strong to medium electron-withdrawing groups (EWGs) such as bromine, chlorine, cyano, nitro, and aza conducted the reactions via the first mechanism (via the formation of azafulvenium intermediate); however, the electron-rich (electron-donating) (EDGs) substituents such as hydroxy, methoxy, and benzyloxy directed the reaction via the second mechanism (the formation of dicarbinol intermediate). This finding clearly revealed the importance of the electron property of substituents on the mechanism of this type of reaction.

#### 2.1.3.1 The spectral data confirming the structures of 11- and 6-indolylbenzocarbazole compounds (compounds 23-37)

The  $^1\text{H}$ -NMR spectra of 11-indolylbenzocarbazole derivatives showed the proton signals with the total peak integration of 12 (for unsubstituted derivative the total peak integration was 14) in the down-field region (aromatic protons region) in the range of 8.56-6.72 ppm. The signal with the highest chemical shift in this range corresponds to  $\text{H}_a$  with the exceptions of 7-aza and 5- $\text{NO}_2$  derivatives in which the signals with the highest chemical shift corresponded to  $\text{H}_b$  and  $\text{H}_c$  respectively. The splitting patterns of  $\text{H}_a$  were doublet of doublet of triplet, doublet of doublet, and doublet of doublet of doublet. The coupling constants ( $J$  values) of  $\text{H}_a$  as a result of the coupling to the neighbouring protons were in the ranges of 8-7, 2-1, and 1-0 Hz

arising from vicinal couplings ( $^3J$ ),  $^4J$ , and long-range coupling of  $^5J$  respectively. In the case of 7-aza derivative, the vicinal coupling constants for  $H_b$  were approximately 5 Hz. This is because of the strong electron-withdrawal effect of aza<sup>124</sup> which led to the higher chemical shifts (8.33 and 8.30 ppm) but lower  $J$  value than that of  $H_a$  (the signal of  $H_a$  appeared at 8.08 ppm). In 5-NO<sub>2</sub> derivative the strong electron-withdrawal effect of nitro also led the signal of the  $H_c$  to the higher chemical shift (8.56 ppm) than that of  $H_a$  (8.26 ppm). The electron property of substituents only affects the vicinal coupling constants; so that, the  $^4J$  and  $^5J$  values remain unchanged in the case of a strong neighbouring EWG<sup>124</sup>. The noticeable chemical shift of the  $H_a$  is probably because of the electron effect of indole moiety at 11-position. The position of  $H_a$ ,  $H_b$ , and  $H_c$  and the possible couplings are shown in Fig. 42.

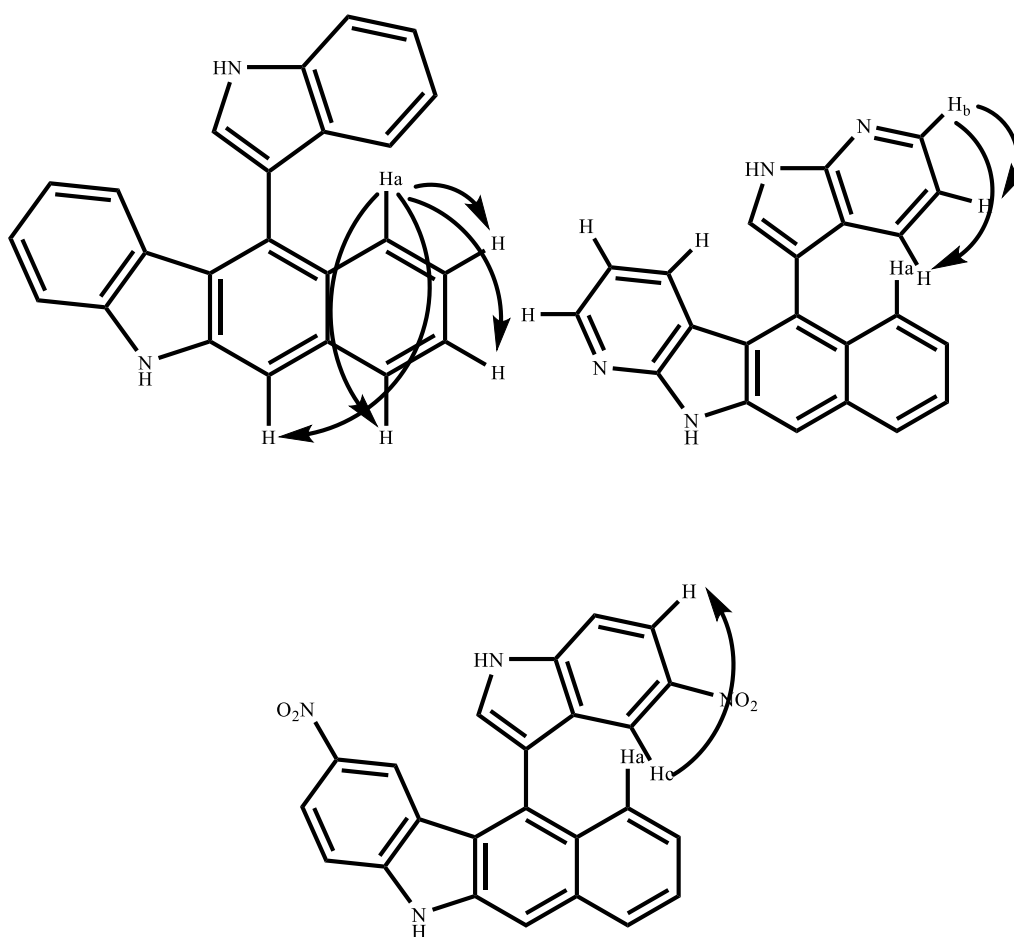


Fig. 42 The possible couplings of  $H_a$ ,  $H_b$ , and  $H_c$  in unsubstituted, 7-aza, and 5-NO<sub>2</sub> 11-indolylbenzocarbazole derivatives

The  $^1\text{H}$ -NMR spectra of 6-indolylbenzocarbazole derivatives showed the proton signals with the total peak integration of 12 (for unsubstituted derivative the total peak integration was 14) in the down-field region (aromatic protons region) in the range of 8.79-6.60 ppm. The signal with the highest chemical shift in this range corresponds to  $\text{H}_a$  (Fig. 43) with the exceptions of 5-OMe and 5-OH derivatives in which the signals with the highest chemical shift corresponded to other protons. The splitting patterns for  $\text{H}_a$  and  $\text{H}_b$  (Fig. 43) were singlet and triplet. The coupling constants ( $J$  values) of  $\text{H}_a$  and  $\text{H}_b$  as a result of the coupling to the neighbouring protons were 0.55 and 0.63 Hz (the coupling constants of  $^4J$  and long-range  $^5J$ ). The chemical shift of  $\text{H}_a$  compared to  $\text{H}_b$  in 11-indolylbenzocarbazoles showed low-field shift because of the electron property of neighbouring NH. A comparison between the chemical shifts of  $\text{H}_a$  and  $\text{H}_b$  in the two stereoisomers of unsubstituted indolylbenzocarbazole and 5-chloro substituted indolylbenzocarbazole showed that the signal of this proton appeared at low-field shift in 6-indolylcarbazole derivatives than  $\text{H}_b$  in 11-indolylbenzocarbazoles (8.79 (singlet) ppm to 7.95 (triplet) ppm in 5-chloro derivative and 8.72 (singlet) ppm to 7.94 (triplet) ppm in unsubstituted derivative). Figure 43 shows the position of  $\text{H}_a$  and  $\text{H}_b$  and the possible couplings to neighbouring protons in the two stereoisomers (Experimental Section for the compounds 29-32).

The both 11- and 6-indolylbenzocarbazole derivatives showed two broad singlet signals in the range of 12.50-9.55 ppm corresponding to two NH functions.

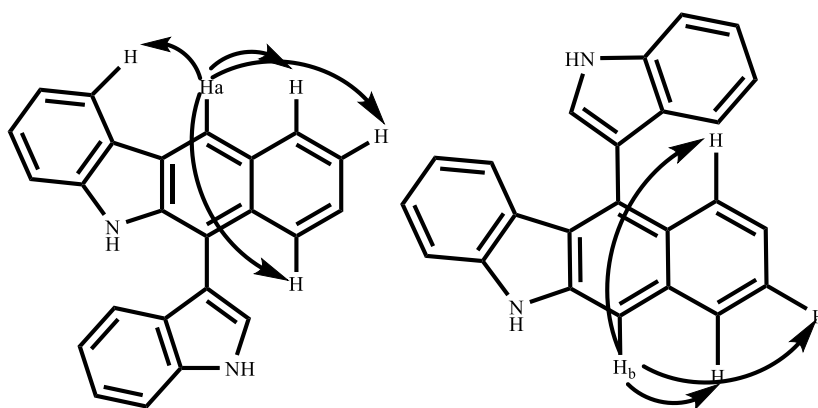


Fig. 43 The position and the possible couplings of  $\text{H}_a$  and  $\text{H}_b$  in 6- and 11-indolylbenzocarbazole derivatives (compounds 32 and 31)

In the similar reaction, thiophene-2,3-dicarbaldehyde was used rather *o*-phthalaldialdehyde to form indolylthieno[b]carbazole (compound 40). The spectral data confirmed the formation of these two stereoisomers. The reaction is shown below (Fig. 44).

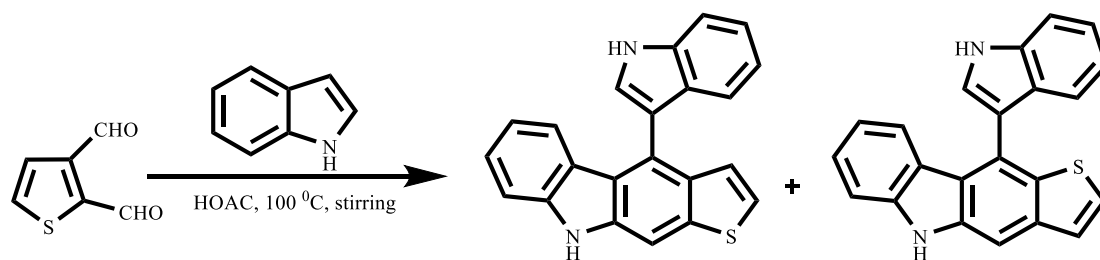


Fig. 44 The reaction of indole to thiophene-2,3-dicarbaldehyde

The  $^1\text{H}$ -NMR spectrum of 10-(1H-indol-3-yl)-5H-thieno[3,2-b]carbazole (compound 40) (right stereoisomer) showed two signals at the chemical shifts of 7.33 and 7.21 ppm with the multiplicities of doublet (J value of 5.63 Hz) and doublet of doublet (J values of 5.74 and 1.03 Hz) respectively. The lower coupling constant than that of ordinary coupling constant for aromatic protons (8-7 Hz) was because of the high electronegativity effect of sulfur atom and the higher chemical shift of one signal compared to the other one also revealed the inductive effect of sulfur heteroatom<sup>124</sup>. Furthermore, one singlet signal at the chemical shift of 8.03 ppm corresponded to the 5-position proton was observed (Experimental Section for compound 40).

The  $^1\text{H}$ -NMR spectrum of 4-(1H-indol-3-yl)-9H-thieno[2,3-b]carbazole (left stereoisomer), showed two signals at the higher chemical shifts than those for 10-thienoindole (7.57 and 7.51 ppm) probably because of the electron effect of the indole moiety. One singlet signal at the chemical shift of 7.96 corresponding to the 9-position proton was observed. For each stereoisomer, two singlet broad signals at the chemical shifts of approximately 10.70 and 10.35 ppm corresponding to two NH functions were observed.

#### 2.1.4 The Acetylation reaction of indolylbenzo[b]carbazole

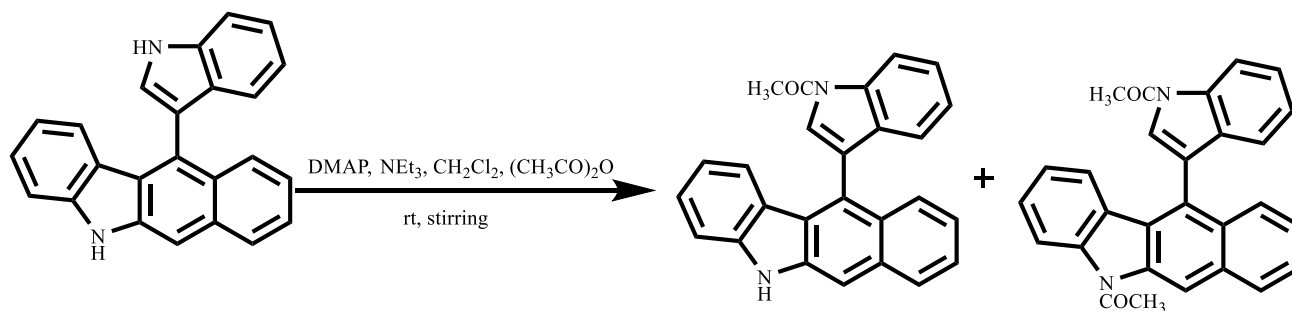


Fig. 45 The acetylation reaction of indolylbenzo[b]carbazole

In the last step of our synthetic part, we acetylated the 11-indolylbenzocarbazole stereoisomer of the unsubstituted indolylbenzocarbazole (compound 31). The reaction led to the formation of mono- and di-acetylated derivatives (compounds 38 and 39). The structures of both products were elucidated by  $^1\text{H}$ -NMR.

The  $^1\text{H}$ -NMR spectrum of monoacetylated derivative (compound 38), showed one singlet signal at the chemical shift of 8.05 ppm corresponding to  $\text{H}_1$  (Fig. 46). There was also one signal with highest chemical shift of 8.66 ppm and the multiplicity of doublet of triplet (coupling constants in accordance with vicinal and long-range ( $^5\text{J}$ ) couplings). The other characteristic signals were one singlet broad peak at 10.41 ppm and one singlet signal at 2.83 ppm corresponding to NH and acetyl functions respectively.

The  $^1\text{H}$ -NMR spectrum of diacetylated derivative revealed one singlet peak at 8.99 ppm corresponding to  $\text{H}_2$  (Fig. 46), no signal at the common region of NH function and two singlet signals at 2.82 and 3.05 ppm corresponding to two acetyl functions.

11-indolylbenzocarbazole derivative of unsubstituted indolylbenzocarbazole showed one singlet signal at 7.94 ppm corresponding to H (Fig. 46). This signal is identical to  $\text{H}_1$  and  $\text{H}_2$  in mono and diacetylated products. As a result, in diacetylated derivative a dramatic low-field shift was observed; however, in monoacetylated derivative no significant shift was observed. Based on the above finding, the structure of monoacetylated derivative was proposed. Figure 46 shows the position of H,  $\text{H}_1$ , and  $\text{H}_2$  on three above derivatives.

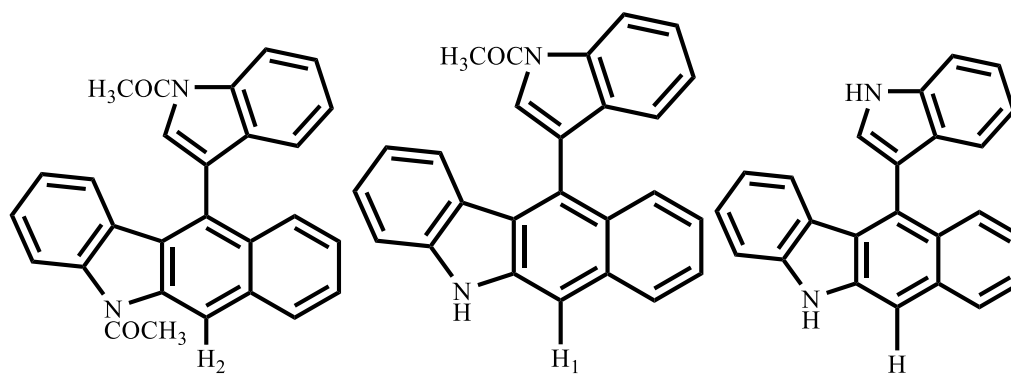
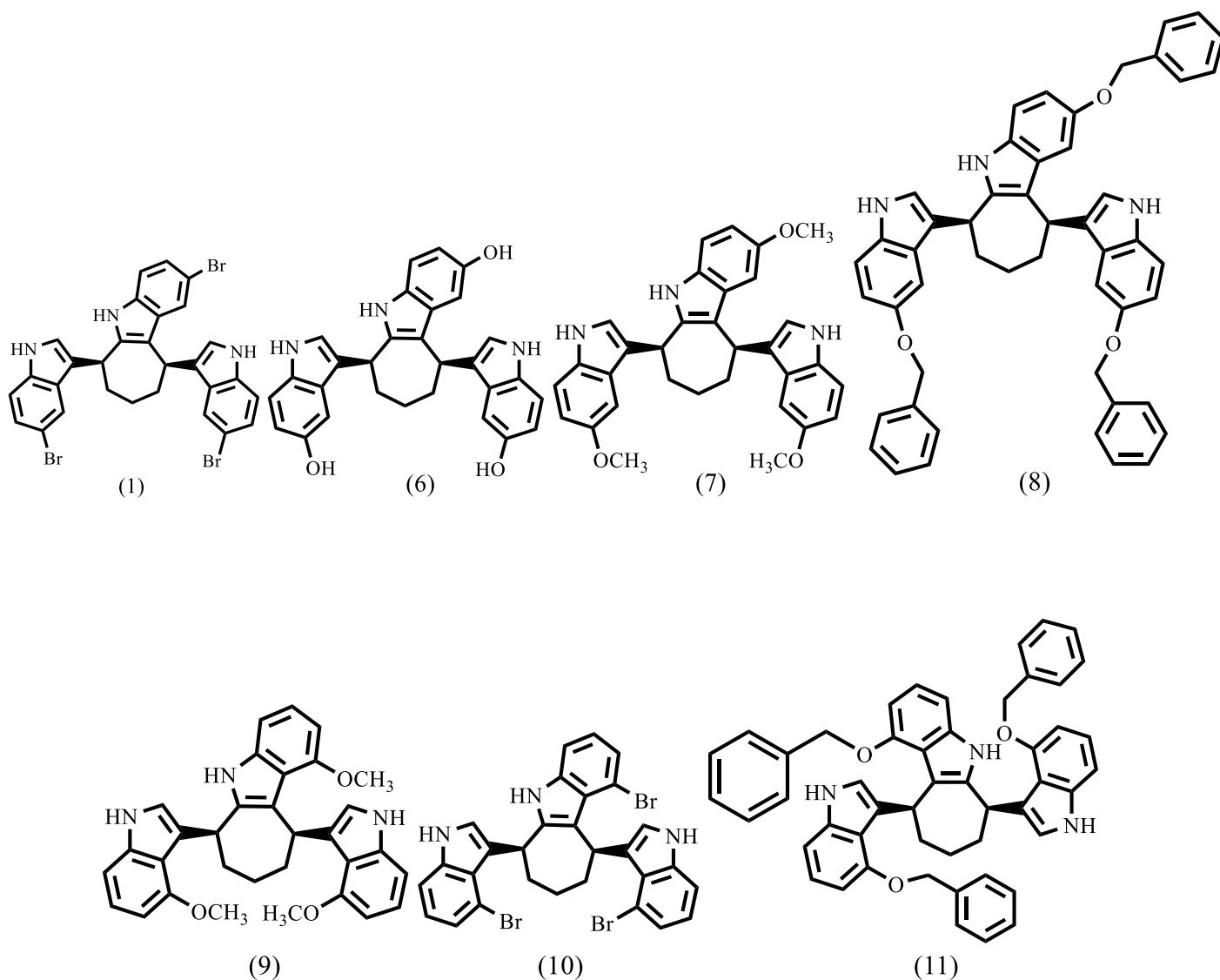


Fig. 46 The position of H,  $\text{H}_1$ , and  $\text{H}_2$  on unsubstituted indolylcarbazole, mono, and diacetylated derivatives

## 2.2 Bioassay part

In the next step of our work, we assessed the biological activities of our synthesized compounds. The primary objective of our project was to introduce new potent biologically active substances with respect to the anti-bacterial activity. In order to do this, our synthesized compounds were tested against Gram-positive and Gram-negative strains, and fungi species. Gram-positive bacterial strains were *S. aureus*, *S. aureus* MRSA standard, *S. epidermidis*, *E. faecalis*, *E. faecium*, and *B. subtilis*. Gram-negative bacterial strains were *E. coli*, *Pseudomonas aeruginosa*, and *Klebsiella pneumoniae*. Fungal species were also *C. albicans* and *C. krusei*. MICs (minimal inhibition concentrations) of our compounds were evaluated against these microorganisms. The MIC values of the following compounds were evaluated:





Among compounds 1, 6, 7, 8, 9, 10, and 11 against *S. aureus* strains, all compounds were active against MRSA standard. However, 9, 10, and 11 were more effective than 1, 6, 7, and 8 (MIC values of 50 versus 200 µg/ml). This confirms the importance of 5'-H in indole moiety against this bacterial strain. Against *S. aureus* every compound was also active. 5-Substituted compounds showed better activities than those of 4-Substituted ones with the exception of 11. Against *S. epidermidis* again all the compounds showed a residual activity; however, compounds with electron-donating groups such as OH, OMe, and benzyloxy at 4 and 5-positions showed better activities than those with Br (MICs of 32 against 64 and 128 µg/ml). Against *E. faecium*, the compounds did not show as well activity as compared to the *S. aureus* strains. Against *E. faecalis*, compounds with electron-donating groups showed better activities than those with halogen. Generally, against Gram-positive bacterial strains, the compounds with electron-donating groups were more active.

Table. 1 MIC values (µg/ml) of compounds 1, 6, 7, 8, 9, 10, 11 against Gram-positive bacteria

Compound	<i>S. aureus</i> ATCC 25923	<i>S. aureus</i> ATCC 29213	<i>S. aureus</i> ATCC 43300 MRSA Standard	<i>S. aureus</i>	<i>S. epidermidis</i> ATCC 35984	<i>S. epidermidis</i> ATCC 12228	<i>S. epidermidis</i>	<i>E. faecalis</i> ATCC 29212	<i>E. faecium</i>	<i>E. faecalis</i> ATCC 25212	<i>E. faecalis</i>	<i>Bacillus Subtilis</i> ATCC 6633
1	200	n.t	200	32	200	200	64	n.t	128	200	128	200
6	200	n.t	200	32	200	200	32	n.t	>128	200	64	200
7	200	n.t	200	32	200	200	32	n.t	>128	200	16	200
8	200	n.t	200	64	200	200	32	n.t	128	200	32	200
9	n.t	n.t	50	64	n.t	n.t	64	25	>128	n.t	64	n.t
10	n.t	50	50	>128	n.t	n.t	128	n.a	>128	n.t	128	n.t
11	n.t	n.t	50	32	n.t	n.t	32	50	128	n.t	16	n.t

n.a: not active, n.t: not tested

Against Gram-negative bacterial strains *E. coli* ATCC 35213, and *Klebsiella Pneumoniae*, the compounds showed residual activities with values of 200 µg/ml. Against *E. coli* ATCC 25922, the compounds were all active but only the compounds with OMe and benzyloxy at 4-position showed better activities (50 to 200 µg/ml). For *P. aeruginosa*, the same situation was

observed; however, compound 10 also showed good activity beside compounds 9 and 11. Generally, electron-donating groups at the 4-position enhanced the activity.

Table. 2 MIC values ( $\mu\text{g/ml}$ ) of compounds 1, 6, 7, 8, 9, 10, 11 against Gram-negative bacteria

Compound	<i>E. coli</i> ATCC 35213	<i>E. coli</i> ATCC 25922	<i>P. aeruginosa</i> ATCC 27853	<i>K. pneumoniae</i> RSKK 574
1	200	200	200	200
6	200	200	200	200
7	200	200	200	200
8	200	200	200	200
9	n.t	50	50	n.t
10	n.t	n.a	50	n.t
11	n.t	50	50	n.t

n.t: not tested, n.a: not active

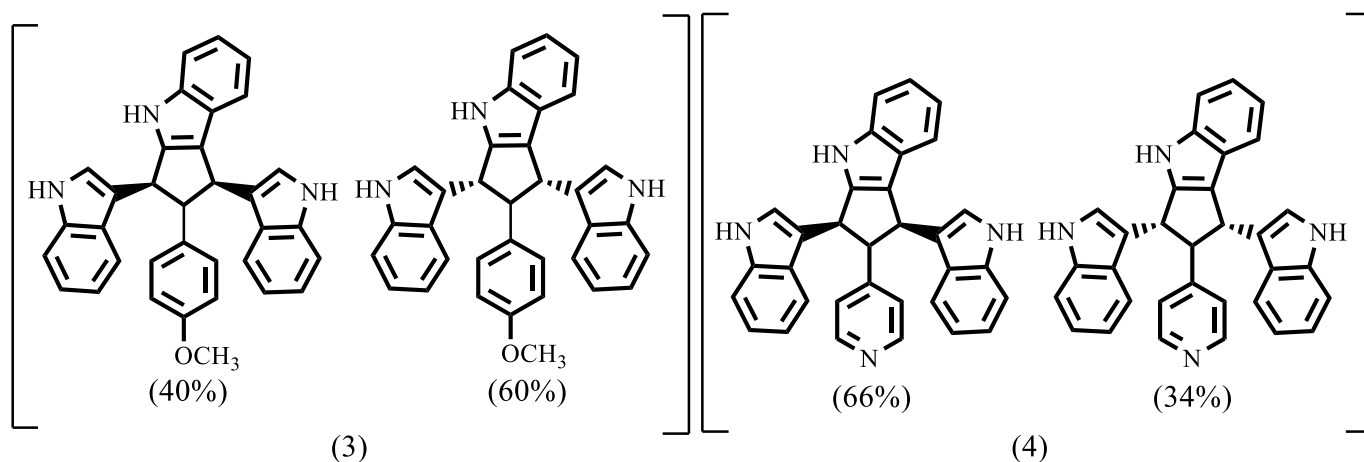
The compounds were more active towards Gram-positive bacteria than towards Gram-negative ones.

In terms of anti-fungal activities, against *C. albicans*, 4-substituted compounds showed better activities than other compounds (50 to 200  $\mu\text{g/ml}$ ). Against *C. krusei*, the compounds showed residual activities with the MICs of 100-200  $\mu\text{g/ml}$ .

Table. 3 MIC values ( $\mu\text{g/ml}$ ) of the compounds 1, 6, 7, 8, 9, 10, 11 against fungal species

Compound	<i>C. albicans</i> ATCC 10231	<i>C. krusei</i>
1	200	100
6	200	100
7	200	200
8	200	200
9	50	n.t
10	50	n.t
11	50	n.t

n.t: not tested



Among compounds 3 and 4, against *S. aureus* species, compound 4 showed much higher activities. This observation confirms an effect of electron-withdrawing pyridine ring on biological activities than that of 4-OMe phenyl ring. Against *S. epidermidis* ATC 35984, both compounds showed an equal activity. Against *S. epidermidis* again compound 4 was more active. However, compound 3 was more active than compound 4 against *S. epidermidis* ATCC 12228. Against *E. faecalis* ATCC 25212 and *E. faecalis* again compound 4 showed better activities (100 and 16 to 200 and 128). As a result, against Gram-positive bacteria, compound 4 was more active than compound 3.

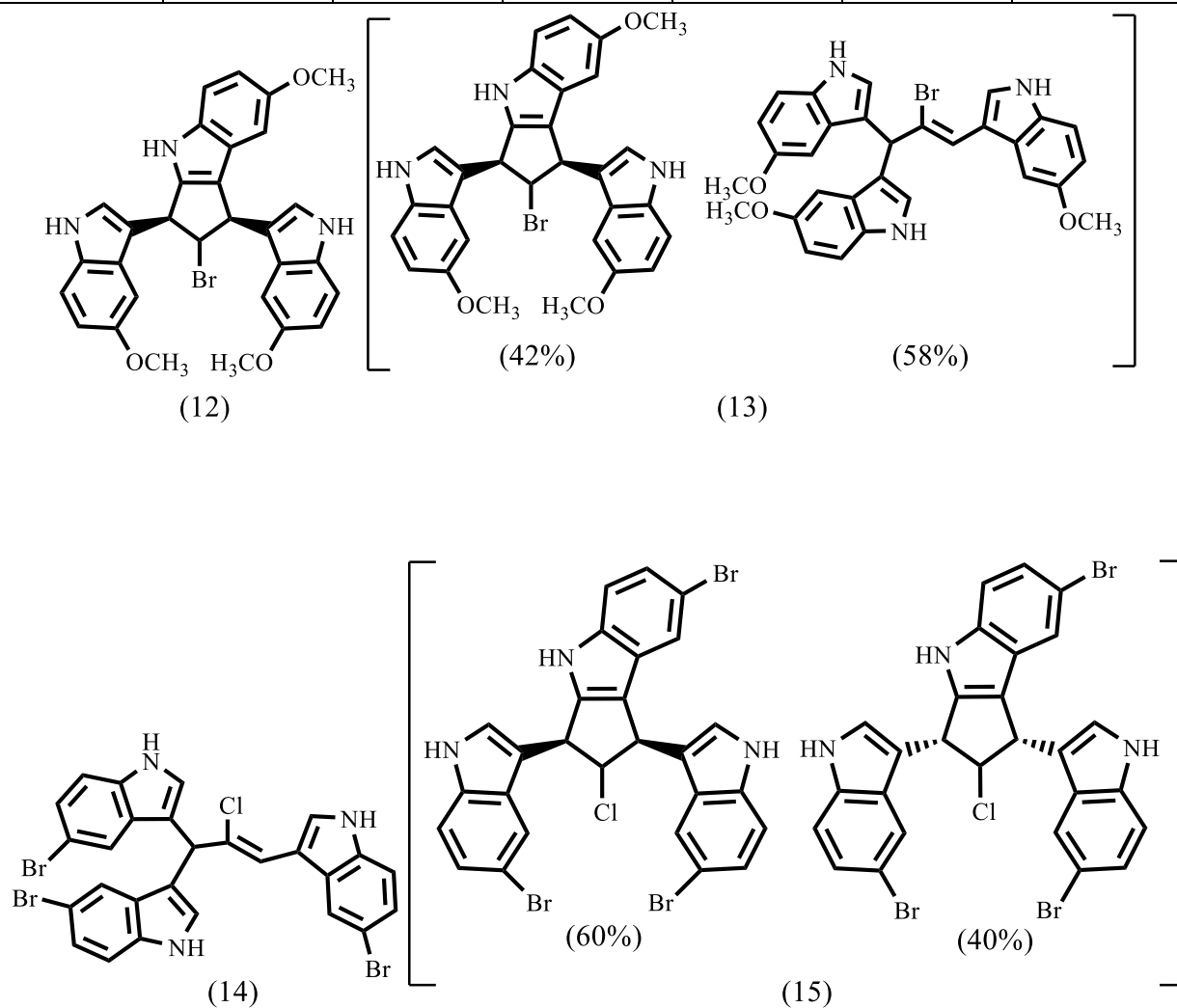
Table. 4 MIC values ( $\mu\text{g/ml}$ ) of the compounds 3 and 4 against Gram-positive bacteria

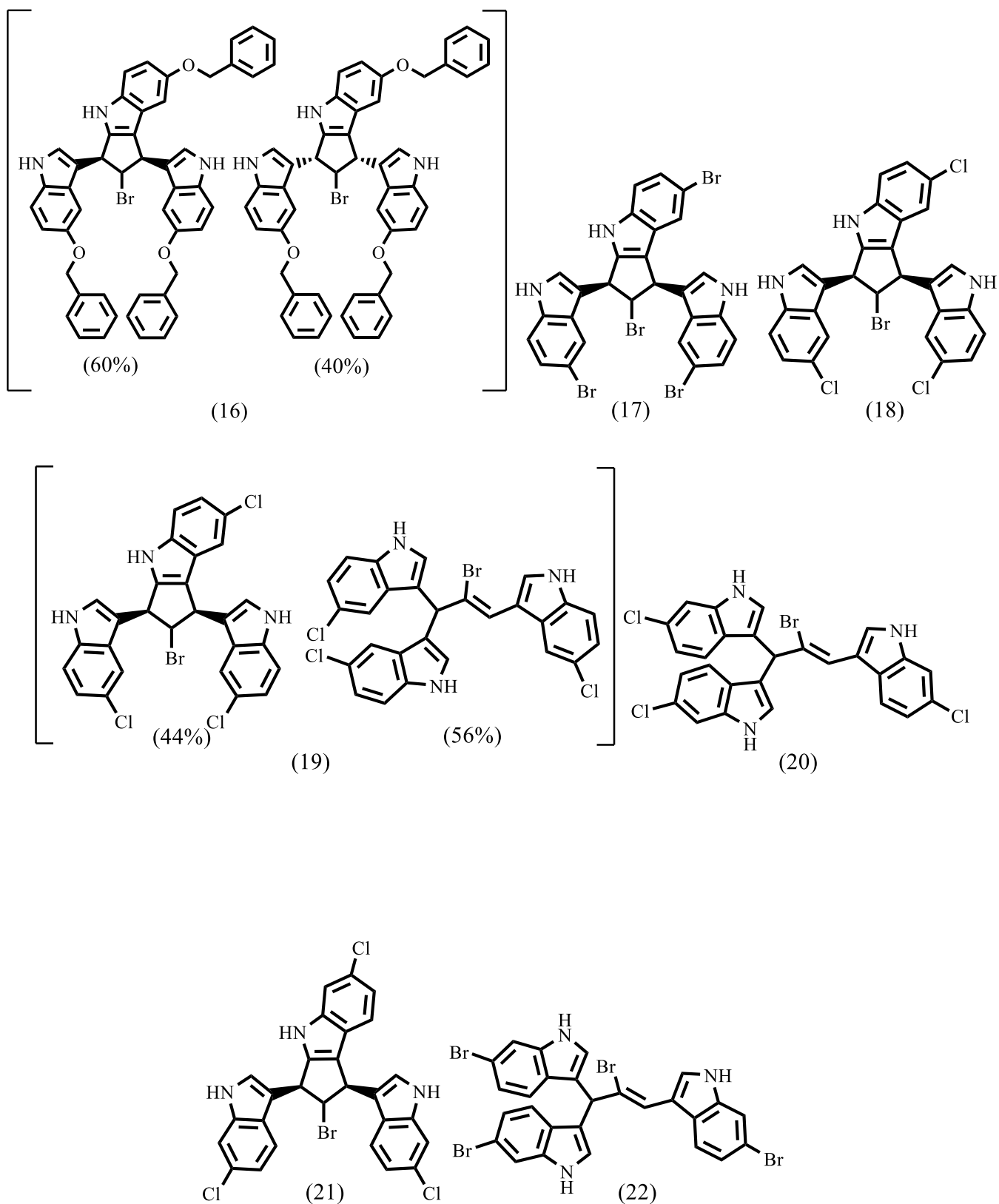
Compound	<i>S. aureus</i> ATCC 25923	<i>S. aureus</i> ATCC 43300 MRSA Standard	<i>S. aureus</i>	<i>S. epidermidis</i> ATCC 35984	<i>S. epidermidis</i> ATCC 12228	<i>S. epidermidis</i>	<i>E. faecium</i>	<i>E. faecalis</i> ATCC 25212	<i>E. faecalis</i>	<i>Bacillus subtilis</i> ATCC 6633
3	200	50	32	6.25	6.25	64	128	200	128	100
4	12.5	12.5	8	6.25	12.5	4	128	100	16	25

Against *B. subtilis*, compound 4 showed higher activity (MIC of 25 to 100  $\mu\text{g/ml}$ ). For other Gram-negative bacteria, the activities were similar. Anti-fungal activity of compound 4 (MICs  $\sim$  6.25 and 50  $\mu\text{g/ml}$ ) was also better than that of compound 3 (MIC  $\sim$  100  $\mu\text{g/ml}$ ).

Table. 5 MIC values ( $\mu\text{g/ml}$ ) of the compounds 3 and 4 against Gram-negative bacteria and fungal species

Compound	<i>E. coli</i> ATCC 35213	<i>E. coli</i> ATCC 25922	<i>P. aeruginosa</i> ATCC 27853	<i>K. pneumoniae</i> RSKK 574	<i>C. albicans</i> ATCC 10231	<i>C. krusei</i>
3	200	200	200	200	100	100
4	200	200	200	200	6.25	50





For the compounds 12-22, they showed enhanced activities against *S. aureus* compared to 1, 6, 7, 8, 9, 10, and 11 (1.56, 3.125, 6.25, and 8  $\mu\text{g/ml}$ ). This enhanced activity is most likely to be caused by the cyclopentane moiety (smaller size ring than cycloheptane) containing the

halogen like bromine. These compounds showed enhanced activities against MRSA than compounds 3 and 4 (3.125 µg/ml for compounds 18 and 20 and 6.25 µg/ml for compounds 19 and 21). This observation confirms the importance of halogen in cyclopentane and on indolyl moieties of the compounds. Against *S. epidermidis*, the same order was observed since the MIC of compound 18 was 8 µg/ml. Against *E. faecium* compounds 17, 18, and 19 showed significant activities than other compounds of this category that showed the importance of halogens such as bromine and chlorine at the 5'-position of indole moiety. A comparison between compounds 13 and 19 showed that compound 19 showed remarkable biological activities compared to compound 13. This observation is most likely because of the electronegative chlorine at the 5-position of indole in both products.

Table. 6 MIC values (µg/ml) of the compounds 12-22 against Gram-positive bacteria

Compound	<i>S. aureus</i> ATCC 29213	<i>S. aureus</i> ATCC 43300 MRSA Standard	<i>S. aureus</i> <i>Newman</i>	<i>S. epidermidis</i>	<i>E. faecium</i>	<i>E. faecium</i> ATCC 29212	<i>E. faecalis</i>
12	12.5	25	n.t	n.t	n.t	25	n.t
13	n.a	50	n.t	n.t	n.t	25	n.t
14	25	12.5	64	16	16	12.5	32
15	25	25	64	64	128	25	64
16	n.a	50	32	32	128	25	64
17	12.5	12.5	32	32	8	12.5	32
18	3.125	3.125	8	8	2	6.25	8
19	12.5	6.25	16	16	8	6.25	32
20	6.25	3.125	32	16	16	25	16
21	1.56	6.25	16	16	16	n.a	16
22	n.a	12.5	128	64	64	12.5	64

n.a: not active, n.t: not tested

Against Gram-negative bacteria, *E. coli* ATCC 25922 and *P. aeruginosa* enhanced activities were observed compared to 1, 6, 7, 8, 9, 10, and 11 and compounds 3 and 4 (MICs of 50 against 200 µg/ml). Compounds 13 and 19 both showed fair and similar biological activity.

Table. 7 MIC values (µg/ml) of the compounds 12-22 against Gram-negative bacteria

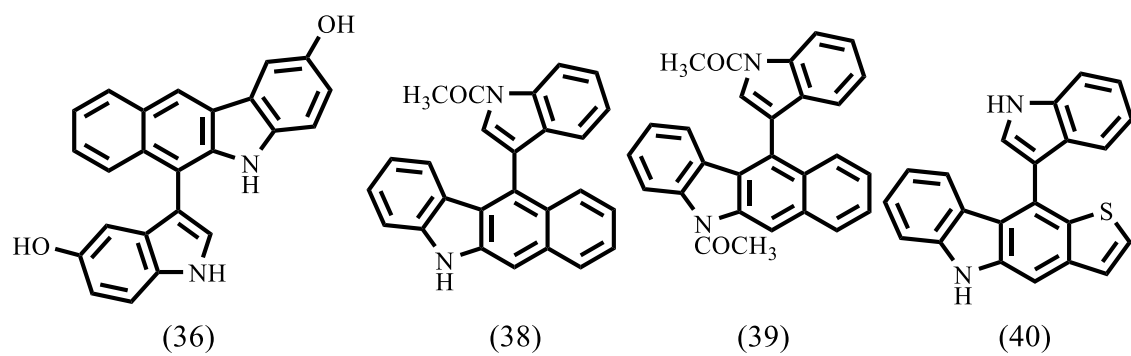
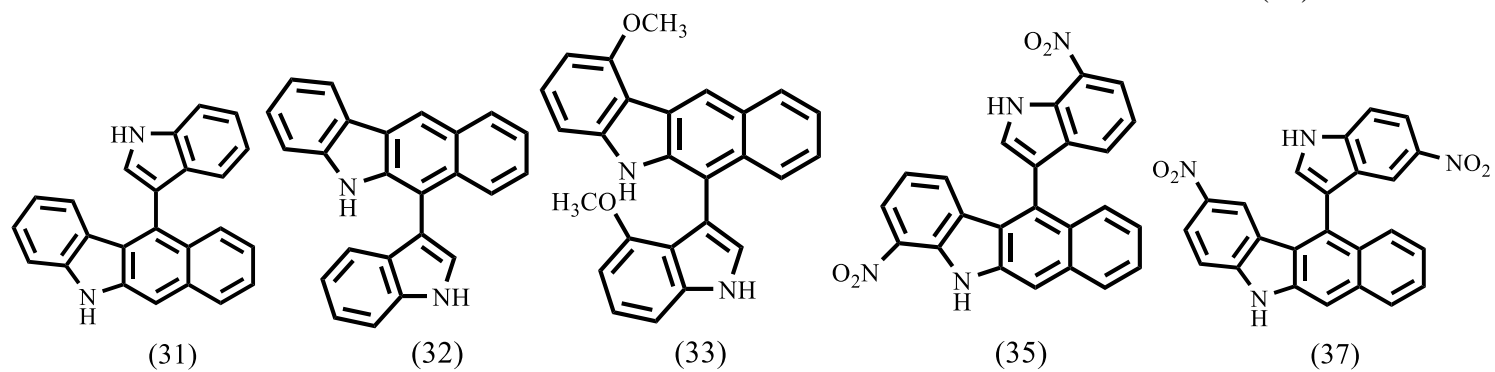
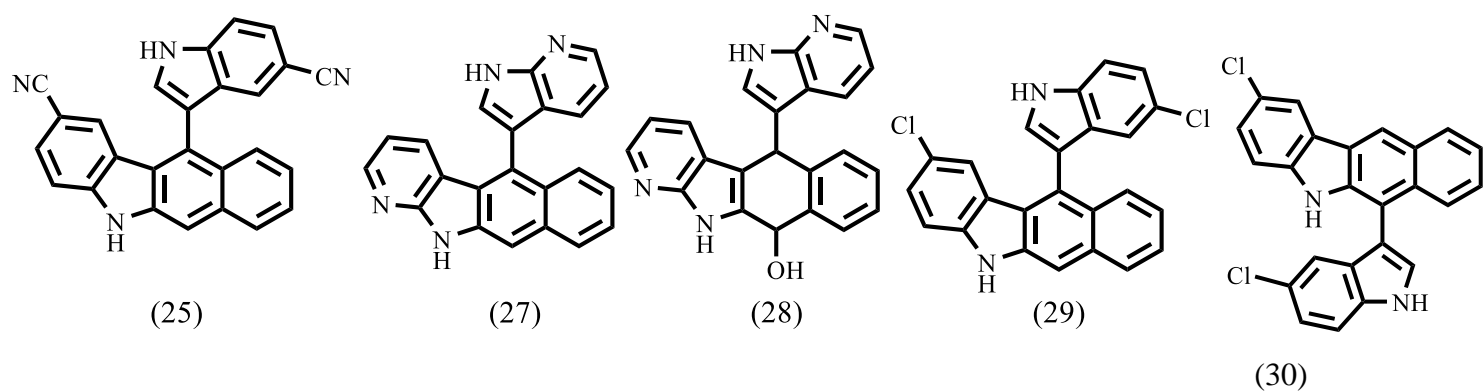
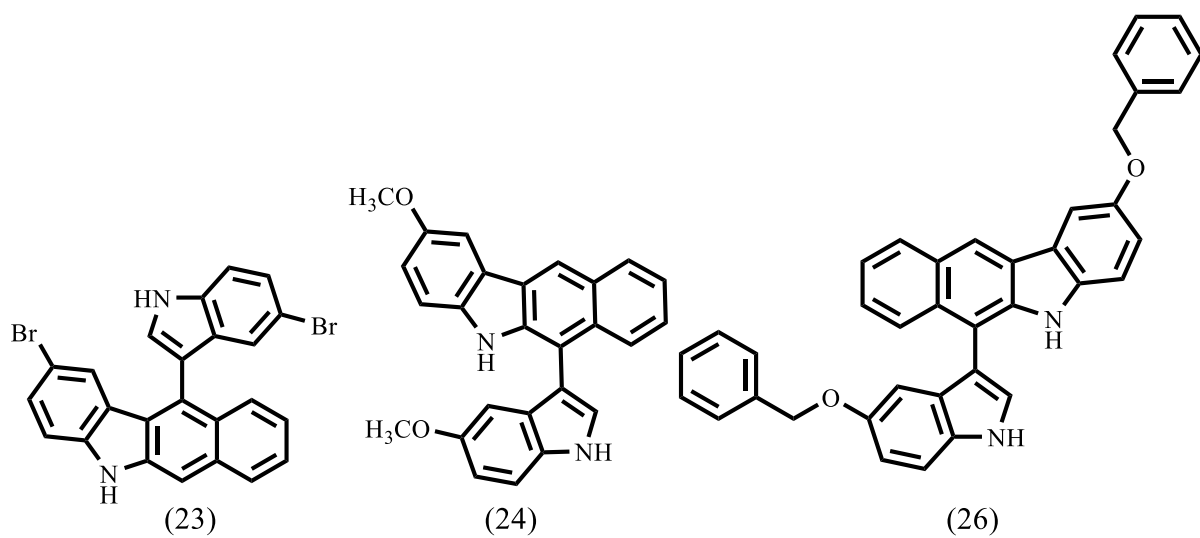
Compound	<i>E. coli</i> ATCC 25922	<i>P. aeruginosa</i> ATCC 27853
12	50	50
13	50	50
14	50	50
15	50	50
16	50	50
17	50	50
18	50	50
19	50	50
20	50	50
21	n.a	50
22	50	50

n.a: not active

Against *C. albicans*, compound 21 showed very good activity similar to compound 4 (MIC of 6.25 µg/ml) which was greater than that of compounds 17 and 18. This confirms the importance of halogen at the 6'-position on the indole moiety. Compounds 13 and 19 again showed similar activities.

Table. 8 MIC values (µg/ml) of the compounds 12-22 against *C. albicans*

Compound	<i>C. albicans</i> ATCC 10231
12	25
13	50
14	50
15	25
16	50
17	25
18	25
19	50
20	6.25
21	6.25
22	25





For indolylbenzo[b]carbazoles, against *S. aureus* Newman, The compound 40 showed the highest activity (MIC value of 1 µg/ml). This confirmed the difference between benzocarbazole and thiophenecarbazole moieties. After that, compound 25 with the electron-withdrawing group of CN showed very good activity (MIC value of 4 µg/ml).

Against *S.aureus* LAC MRSA, the importance of EWG at 5-position of indole moiety was again shown as compound 25 showed better activity than compound 29 with chlorine at 5-position of indole. Furthermore, the 5-substituted compounds showed enhanced activity than the 4-substituted ones.

Against *E. faecium* AW2VR, compound 32 (unsubstituted compound) showed the highest activity (MIC value of 4 µg/ml). After that, the compound with OH at 5-position (compound 36) showed remarkable activity (MIC of 8 µg/ml). Compound 25 showed lower activities than the first two compounds. Compounds 23 and then 29 showed the highest activities against *E. faecium* 2121198. After these two compounds, compound 36 showed good activity and compounds such as 35 and 37 with EDGs at 7 and 5-position, respectively, showed the least activities. Compounds 31 and 36 again showed highest activities against *E. faecalis* OG1X. This observation proved the importance of electron-donating groups such as OH in the biological activity of these compounds.

Against *E. faecalis* JH2-2, EWGs such as CN and NO<sub>2</sub> at 5-position on the indolyl moiety played a significant role in bioactivity.

Table. 9 MIC values ( $\mu\text{g/ml}$ ) of the compounds 23-40 against Gram-positive bacteria

Compound	<i>S. aureus</i> Newman	<i>S. aureus</i> USA LAC MRSA	<i>E. faecium</i> AW2VR	<i>E. faecium</i> 2121198	<i>E. faecalis</i> OG1X	<i>E. faecalis</i> JH2-2
23	>128	>128	64	0.5	64	8
24	32	32	n.t	n.t	n.t	n.t
25	2	2	64	4	16	4
26	32	64	n.t	n.t	n.t	n.t
27	64	64	n.t	n.t	n.t	n.t
28	n.t	n.t	64	8	16	128
29	4	4	64	1	64	8
30	8	32	n.t	n.t	n.t	n.t
31	8	32	16	2	64	128
32	4	64	4	2	4	8
33	64	128	n.t	n.t	n.t	n.t
35	32	32	64	128	64	128
36	4	4	8	2	4	8
37	32	64	64	128	8	8
38	128	128	n.t	n.t	n.t	n.t
39	64	128	n.t	n.t	n.t	n.t
40	1	16	n.t	n.t	n.t	n.t

n.t: not tested

Totally, the main factors affecting the anti-bacterial activities of compounds 23-40 against Gram-positive bacteria was the replacement of the benzene ring by electron-withdrawing thiophene ring. The presence of EWGs at 5-position of indolyl moiety also played an important role. The bioactivity of mono- and di-acetylated products was lower than that of the corresponding indolylbenzo[b]carbazole. This observation proved the importance of NH in the bioactivity of our compounds. Against *S. aureus*, the di-acetylated compound showed better activity than mono-acetylated compound. This could be as a result of the replacement of two NH functions by two hydrophilic acetyl groups that could possibly enhance the solubility of the compound because the presence of hydrophilic group may or may not result in the better activity against Gram-positive bacteria.

Table. 10 MIC values (µg/ml) of our standards against Gram-positive bacteria

Standard	<i>S. aureus</i> ATCC 25923	<i>S. aureus</i> ATCC 29213	<i>S. aureus</i> Newman	<i>S. aureus</i> ATCC 43300 MRSA Standard	<i>S. aureus</i> USA LAC MRSA	<i>S. epidermidis</i> ATCC 35984	<i>S. epidermidis</i> ATCC 12228	<i>E. faecalis</i> ATCC 29212	<i>E. faecalis</i> ATCC 29212	<i>B. subtilis</i> ATCC 6633
Ampicillin	1.56	n.t	n.t	50	n.t	n.t	n.t	0.19	n.t	50
Ciprofloxacin	0.19	0.625	n.t	0.625		12.5	12.5	n.t	3.125	0.09
Oxacillin	n.t	n.t	0.5	n.t	0.5	n.t	n.t	n.t	n.t	n.t
Sultamicillin	0.78	n.t	n.t	25	n.t	n.t	n.t	n.t	3.125	0.78
Vancomycin	n.t	n.t	n.t	n.t	n.t	n.t	n.t	n.t	n.t	n.t
Miconazole	n.t	n.t	n.t	n.t	n.t	n.t	n.t	n.t	n.t	n.t

n.t: not tested

Table. 11 MIC values (µg/ml) of our standards against Gram-negative bacteria and fungal species

Standard	<i>B. subtilis</i> ATCC 6633	<i>E. coli</i> ATCC 35213	<i>E. coli</i> ATCC 25922	<i>P. aeruginosa</i> ATCC 27853	<i>K. pneumoniae</i> RSKK 574	<i>C. albicans</i> ATCC 10231	<i>C. krusei</i>
Ampicillin	50	n.t	n.t	n.t	n.t	n.t	n.t
Ciprofloxacin	0.09	0.09	0.09	0.78	0.09	n.t	n.t
Vancomycin	n.t	n.t	n.t	n.t	n.t	n.t	n.t
Oxacillin	n.t	n.t	n.t	n.t	n.t	n.t	n.t
Sultamicillin	0.78	n.t	n.t	n.t	n.t	n.t	n.t
Miconazole	n.t	n.t	n.t	n.t	n.t	0.19	0.78

n.t: not tested

### 3. Summary of work and conclusion

#### 3.1 Summary of work

Our study was focused on the synthesis and biological evaluation of the novel-class of indolyl-derived compounds. We designed and proposed a novel one-pot synthetic approach for condensation reactions of substituted and unsubstituted indoles with various aromatic and aliphatic dialdehydes. We planned to employ glacial acetic acid as a mild protic acid and non-aqueous solvent to catalyse these reactions. In the first part of our study, we investigated the electrophilic substitution reaction of 5-Br, 5-OH, 5-OMe, 5-Benzyloxy (OBn), 5-CN, 4-OMe, 4-Br, 4-OBn, and 7-aza substituted indoles with glutaric dialdehyde in the presence of glacial acetic acid at room temperature to obtain hexahydrocyclohepta[b]indole (trisindolyl-cycloheptane products) derivatives (Compounds 1, 6, 7, 8, 9, 10, 11 of Experimental and Results and Discussion sections). The reactions between 7-aza and 5-CN substituted indoles with glutaric dialdehyde did not lead to the desired products. However, the 3,3'-(5-oxopentane-1,1-diyl)bis(1H-indole-5-carbonitrile) product as a result of the incomplete reaction of Indole-5-carbonitrile with glutaric dialdehyde led us to the possible mechanism of these reactions. During the above investigation, we also successfully isolated the 3,3',3'',3'''-(pentane-1,1,5,5-tetrayl)tetrakis(1H-indol-5-ol) and 1,1,5,5-tetrakis(5-(benzyloxy)-1H-indol-3-yl)pentane derivatives (tetraindolyl products) from the reactions of 5-OH and 5-OBn substituted indoles with glutaric dialdehyde (Experimental section). In the second part of our study, we investigated the electrophilic substitution reactions of 5-OMe, 5-Br, 5-OBn, 5-Cl, 6-Cl, 6-Br substituted indoles with 2-bromo and 2-chloromalondialdehyde and unsubstituted indole with 2-(4-methoxyphenyl)malondialdehyde and 2-(4-pyridyl)malondialdehyde. The aim of this investigation was to obtain tetrahydrocyclopenta[b]indole (trisindolyl-cyclopentane products) derivatives (compounds 3, 4, and 12-22). During this investigation, we also obtained (Z)-3,3',3'' tris derivatives as our new product beside trisindolyl-cyclopentane derivatives as well as second stereoisomers (diastereomers) of the some of the derivatives. In the third part of our study, we focused on the condensation reactions of substituted and unsubstituted indoles with *o*-phthaldialdehyde to obtain the indolylbenzo[b]carbazole (compounds 23-37) derivatives. In contrast to the first and second parts of our study, the reactants were heated up to 100 °C. In the investigation undertaken, the reactions between 5-Br, 5-OMe, 5-CN, 5-OBn, 5-Cl, 5-NO<sub>2</sub>, 5-OH, 4-OMe, 7-aza, 7-NO<sub>2</sub> substituted and unsubstituted indoles and *o*-phthaldialdehyde were examined. The 11-indolyl and 6-indolylbenzo[b]carbazole derivatives were the two stereoisomers (atropisomers) of the

above indolylbenzo[b]carbazole products which were isolated successfully. Based on our observations, we concluded that the electron-withdrawing groups (EWGs) such as Cl, Br, NO<sub>2</sub>, CN, and aza led to the formation of 11-indolylbenzo[b]carbazole derivatives as the major product and the electron-donating groups (EDGs) such as OMe, OBn, and OH led to the formation of 6-indolylbenzo[b]carbazole derivatives as the major product. Meanwhile, in the reactions between 5-Cl substituted and unsubstituted indoles with *o*-phthalaldialdehyde, two stereoisomers (11- and 6-indolylbenzo[b]carbazole derivatives) were isolated successfully and the 11-indolylbenzo[b]carbazole derivative was the major product in both reactions. In the reaction between 7-aza and *o*-phthalaldialdehyde, the intermediate 5-(1H-pyrrolo[2,3-b]pyridin-3-yl)-10,11-dihydro-5H-benzo[f]pyrido[2,3-b]indol-10-ol (compound 28) was also isolated. The structure of this compound was a firm proof to our proposed mechanism to the formation of indolylbenzo[b]carbazole derivatives. Among this investigation, we also examined the electrophilic substitution reaction of unsubstituted indole with thiophene-2,3-dicarbaldehyde instead of *o*-phthalaldialdehyde. 10-(1H-indol-3-yl)-5H-thieno[3,2-b]carbazole (compound 40) derivative was successfully isolated and the structure of the second stereoisomer 4-(1H-indol-3-yl)-9H-thieno[2,3-b]carbazole was also elucidated. In the last step of our third investigation, we acetylated the 11-(1H-indol-3-yl)-5H-benzo[b]carbazole (compound 31) derivative in the presence of dichloromethane (CH<sub>2</sub>Cl<sub>2</sub>), dimethylaminopyridine (DMAP), triethylamine (TEA), and acetic anhydride (Ac<sub>2</sub>O). In this experiment, we obtained both mono- and di-acetylated derivatives. The percentage yield of the mono-acetylated (compound 38) derivative was higher compared to that of di-acetylated (compound 39) one. The structure of every compound synthesized was elucidated by one-dimensional proton nuclear magnetic resonance (<sup>1</sup>H-NMR) and fourier-transform infrared (FT-IR, ATR (attenuated total reflection)). The (m/z) of every compound was obtained by electrospray ionization (ESI) and atmospheric pressure chemical ionization (APCI) mass spectrometry (MS) (Experimental section). The plausible mechanisms to the formation of our compounds were discussed in details in the results and discussion section. The important spectral data specifically <sup>1</sup>H-NMR data was also discussed in details in the results and discussion section and the interpretations are available in the experimental section.

In the part of biological evaluation, our synthesized compounds (1-40) were tested against Gram-positive and Gram-negative bacterial strains such as *S. aureus*, methicillin-resistant *S. aureus* standard (MRSA standard), *S. epidermidis*, *E. faecalis*, *E. faecium*, *B. subtilis*, *E. coli*, *Pseudomonas aeruginosa*, and *Klebsiella Pneumoniae* and fungal species such as *C. albicans*

and *C. krusei* . The MIC values (minimal inhibitory concentration) in µg/ml of our compounds were obtained and the structure-activity relationships (SARs) of these compounds were analysed accordingly. The SARs of compounds 1, 6, 7, 8, 9, 10, 11 in one category and of compounds 3, 4, 12-22 in another category, and of 23-40 in the last category were analysed and discussed separately in the bioassay part of the Results and Discussion section.

### 3.2 Conclusion

In this study, we focused on the synthetic approach to novel-indolyl derived compounds by utilizing glacial acetic acid. The advantages of our method are low cost and one-pot reactions. However, during our investigations, we were able to obtain interesting chemical and biological results. We successfully synthesized and isolated, for example, two stereoisomers of one compound which had not been obtained via a simple one-step reaction before. Furthermore, most of our compounds were biologically active against pathogenic bacterial strains and mostly showed fair activities compared with the standards as routine antibiotics and even more remarkable activity specifically towards resistant strains which have been of great interest to medicinal scientists because of the subsequent infections and struggles in clinical therapies nowadays. In terms of medicinal chemistry, this study provided a situation in structure-activity relationship analysis by introducing new compounds and new factors. Secondary, further investigations can also be made on drug delivery because of the positive results obtained. The next step regarding the most bioactive compounds will be the evaluation of cytotoxicity, coupling reactions with other biologically active functional groups, and/or drug delivery investigations to develop novel more biologically active compounds and to investigate their mechanisms. Hopefully, in the near future by focusing more on inexpensive methods, ground-breaking results can be gained and new biological agents would be introduced.

### 3. Zusammenfassung und Schlussfolgerung

#### 3.1 Zusammenfassung

Unsere Studie konzentrierte sich auf die Synthese und biologische Bewertung der neuartigen Klasse von Indolylverbindungen. Wir entwickelten und schlugen einen neuen Eintopf-Syntheseansatz für Kondensationsreaktionen von substituierten und unsubstituierten Indolen mit verschiedenen aromatischen und aliphatischen Dialdehyden vor. Wir wollten Eisessig als milde Protonensäure und nichtwässriges Lösungsmittel einsetzen, um diese Reaktionen zu katalysieren. Im ersten Teil unserer Studie untersuchten wir die elektrophile Substitutionsreaktion von 5-Br, 5-OH, 5-OMe, 5-Benzoyloxy (OBn), 5-CN, 4-OMe, 4-Br, 4-OBn, und 7-Aza-substituierten Indole mit Glutardialdehyd in Gegenwart von Eisessig bei Raumtemperatur und erhielten Hexahydrocyclohepta[b]indolderivate (trisindolylcycloheptanprodukte) (Verbindungen 1, 6, 7, 8, 9, 10, 11 von Experimenteller und Ergebnisse und Diskussionsabschnitte). Die Reaktionen zwischen 7-Aza- und 5-CN-substituierten Indolen mit Glutardialdehyd führten nicht zu den gewünschten Produkten. Das 3,3'-(5-Oxopentan-1,1-diyl)bis(1H-indol-5-carbonitril) -Produkt als Ergebnis der unvollständigen Reaktion von Indol-5-carbonitril mit Glutardialdehyd führte uns jedoch zum möglichen Mechanismus dieser Reaktionen. Während der obigen Untersuchung haben wir 3,3',3'',3'''-(Pentan-1,1,5,5-tetrayl)tetrakis(1H-indol-5-ol) erfolgreich isoliert, ebenso 1,5,5-Tetrakis(5-(benzyloxy)-1H-indol-3-yl)pentanderivate (Tetraindolylprodukte) aus den Reaktionen von 5-OH und 5-OBn-substituierten Indolen mit Glutardialdehyd (Experimenteller Teil). Im zweiten Teil unserer Studie untersuchten wir die elektrophilen Substitutionsreaktionen von 5-OMe-, 5-Br-, 5-OBn-, 5-Cl-, 6-Cl-, 6-Br-substituierten Indolen mit 2-Brom und 2-Chlormalondialdehyd und von unsubstituierten Indol mit 2-(4-Methoxyphenyl) malondialdehyd und 2-(4-Pyridyl)malondialdehyd. Ziel dieser Untersuchung war es, tetrahydrocyclopenta[b]indolderivate (trisindolylcyclopentanprodukte) (Verbindungen 3, 4 und 12-22) zu erhalten. Während dieser Untersuchung erhielten wir auch (Z)-3,3',3'''-Tris-Derivate als unser neues Produkt neben Trisindolylcyclopentan-Derivaten sowie zwei Stereoisomere (Diastereomere) einiger der Derivate. Im dritten Teil unserer Studie konzentrierten wir uns auf die Kondensationsreaktionen von substituierten und unsubstituierten Indolen mit *o*-Phthaldialdehyd, um die Indolylbenzo[b]carbazol-Derivate (Verbindungen 23-37) zu erhalten. Im Gegensatz zum ersten und zweiten Teil unserer Studie wurden die Reaktanten auf 100 °C erhitzt. Bei der durchgeführten Untersuchung wurden die Reaktionen zwischen 5-Br, 5-OMe, 5-CN, 5-OBn, 5-Cl, 5-NO<sub>2</sub>, 5-OH, 4-OMe, 7-Aza, 7-NO<sub>2</sub>

substituiert, und unsubstituierten Indolen und *o*-Phthaldialdehyd untersucht. Die 11-Indolyl- und 6-Indolylbenzo[b]carbazolderivate waren die beiden Stereoisomere (Atropisomere) der obigen Indolylbenzo[b]carbazolprodukte, die erfolgreich isoliert wurden. Aufgrund unserer Beobachtungen gelangten wir zu dem Schluss, dass die elektronenziehenden Gruppen (EWGs) wie Cl, Br, NO<sub>2</sub>, CN und Aza zur Bildung von 11-Indolylbenzo[b]carbazolderivaten als Hauptprodukt und Elektronendonator Gruppen (EDGs) wie OMe, OBn und OH führten zur Bildung von 6-Indolylbenzo[b]carbazolderivaten als Hauptprodukt. In den Reaktionen zwischen 5-Cl-substituierten und unsubstituierten Indolen mit *o*-Phthaldialdehyd wurden zwei Stereoisomere (11- und 6-Indolylbenzo[b]carbazolderivate) erfolgreich isoliert, und das 11-Indolylbenzo[b]carbazolderivat war das Hauptprodukt in beiden Reaktionen. Bei der Reaktion zwischen 7-Aza und *o*-Phthaldialdehyd wurde das Zwischenprodukt 5-(1H-Pyrrolo[2,3-b]pyridin-3-yl)-10,11-dihydro-5H-benzo[f]pyrido[2,3-b]Indol-10-ol (Verbindung 28) isoliert. Die Struktur dieser Verbindung war ein Beweis für unseren vorgeschlagenen Mechanismus zur Bildung von Indolylbenzo[b]carbazolderivaten. In diesen Untersuchungen untersuchten wir auch die elektrophile Substitutionsreaktion von unsubstituiertem Indol mit 2,3-Thiophenedicarboxaldehyd anstelle von *o*-Phthaldialdehyd. 10-(1H-Indol-3-yl)-5H-thieno[3,2-b]carbazolderivat (Verbindung 40) wurde erfolgreich isoliert und die Struktur des zweiten Stereoisomers 4-(1H-Indol-3-yl)-9H-Thieno[2,3-b]carbazol wurde ebenfalls aufgeklärt. Im letzten Schritt unserer dritten Untersuchung haben wir das 11-(1H-Indol-3-yl)-5H-benzo[b]carbazolderivat (Verbindung 31) in Gegenwart von Dichlormethan (CH<sub>2</sub>Cl<sub>2</sub>), Dimethylaminopyridin (DMAP), Triethylamin (TEA) und Essigsäureanhydrid (Ac<sub>2</sub>O) acetyliert. In diesem Experiment wurden sowohl mono- als auch di-acetylierte Derivate erhalten. Die prozentuale Ausbeute des monoacetylierten (Verbindung 38) Derivats war höher als diejenige des diacetylierten (Verbindung 39) Derivats. Die Struktur jeder synthetisierten Verbindung wurde durch eindimensionale Protonenkernelnresonanz (<sup>1</sup>H-NMR) und Fourier-Transform-Infrarot (FT-IR, ATR (attenuated total reflection)) aufgeklärt. Die (m/z) jeder Verbindung wurden durch Elektrospray-Ionisation (ESI) und mit chemischer Ionisation bei Atmosphärendruck (APCI) Massenspektrometrie (MS) erhalten (experimenteller Abschnitt). Die plausiblen Mechanismen zur Bildung unserer Verbindungen wurden im Abschnitt Ergebnisse und Diskussion ausführlich erörtert. Die wichtigen spektralen Daten, insbesondere die <sup>1</sup>H-NMR-Daten, wurden ebenfalls im Abschnitt Ergebnisse und Diskussion ausführlich erörtert, und die Interpretationen sind im Abschnitt Experimente verfügbar.



Im Rahmen der biologischen Bewertung wurden unsere synthetisierten Verbindungen (1-40) gegen grampositive und gramnegative Bakterienstämme wie *S. aureus*, Methicillin-resistenten *S. aureus*-Standard (MRSA-Standard), *S. epidermidis*, *E. faecalis*, *E. faecium*, *B. subtilis*, *E. coli*, *Pseudomonas aeruginosa* und *Klebsiella Pneumoniae* sowie Pilzarten wie *C. albicans* und *C. krusei*. Die MHK-Werte (minimale Hemm-konzentration) in µg/ml unserer Verbindungen wurden erhalten und die Struktur-Aktivitäts-Beziehungen (Struktur-Wirkungsbeziehung) (SARs) dieser Verbindungen wurden entsprechend analysiert. Die SARs der Verbindungen 1, 6, 7, 8, 9, 10, 11 in einer Kategorie und der Verbindungen 3,4, 12-22 in einer anderen Kategorie und der Verbindungen 23-40 in der letzten Kategorie wurden analysiert und separat diskutiert im Bioassy-Teil des Abschnitts Ergebnisse und Diskussion.

### 3.2 Schlussfolgerung

In dieser Studie konzentrierten wir uns auf den Syntheseansatz für neuartige Indolylverbindungen unter Verwendung von Eisessig. Die Vorteile unserer Methode sind niedrige Kosten und Eintopfreaktionen. Bei unseren Untersuchungen konnten wir jedoch interessante chemische und biologische Ergebnisse erzielen. Wir haben beispielsweise zwei Stereoisomere einer Verbindung erfolgreich synthetisiert und isoliert, die zuvor nicht über eine einfache einstufige Reaktion erhalten worden waren. Darüber hinaus waren die meisten unserer Verbindungen gegen pathogene Bakterienstämme biologisch aktiv und zeigten im Vergleich zu den Standards als Routineantibiotika zumeist eine faire Aktivität und eine noch bemerkenswertere Aktivität, insbesondere gegenüber resistenten Stämmen, die aufgrund der nachfolgenden Infektionen und Kämpfe von großem Interesse für klinischen Therapien sind. In Bezug auf die medizinische Chemie lieferte diese Studie durch die Struktur-Aktivitäts-Diskussion mit der Einführung neuer Verbindungen und neuer Faktoren. Zweitens können aufgrund der positiven Ergebnisse auch weitere Untersuchungen zur Arzneistoffforschung durchgeführt werden. Der nächste Schritt in Bezug auf die bioaktivsten Verbindungen wird die Bewertung der Zytotoxizität, Kupplungsreaktionen mit anderen biologisch aktiven funktionellen Gruppen und/oder Untersuchungen zur Wirkstoffabgabe sein, um neue, biologisch aktivere Verbindungen zu entwickeln und deren Mechanismen zu untersuchen. Hoffentlich können in naher Zukunft bahnbrechende Ergebnisse erzielt und neue biologische Wirkstoffe eingeführt werden, indem man sich stärker auf kostengünstige Methoden konzentriert.

#### 4. References

1. Warren, S; Wyatt, P; *Organic Synthesis: The Disconnection approach*. John Wiley & Sons. 2008: p. 301-311.
2. Larock, R.C. and E.K. Yum, *Synthesis of indoles via palladium-catalyzed heteroannulation of internal alkynes*. Journal of the American Chemical Society, 1991. **113**(17): p. 6689-6690.
3. Humphrey, G.R. and J.T. Kuethe, *Practical methodologies for the synthesis of indoles*. Chemical Reviews, 2006. **106**(7): p. 2875-2911.
4. Hickey, D.M.B., C.J. Moody, and C.W. Rees, *Synthesis of isoquinolines from azidocinnamates; the effect of iodine*. Journal of the Chemical Society, Chemical Communications, 1982(1): p. 3-4.
5. Robinson, B., *The Fischer Indole Synthesis*. Chemical Reviews, 1963. **63**(4): p. 373-401.
6. Hemetsberger, H., D. Knittel, and H. Weidmann, *Synthese von  $\alpha$ -Azidozimtsäureestern*. Monatshefte für Chemie / Chemical Monthly, 1969. **100**(5): p. 1599-1603.
7. Fukui, K., T. Yonezawa, and H. Shingu, *A molecular orbital theory of reactivity in aromatic hydrocarbons*. The Journal of Chemical Physics, 1952. **20**(4): p. 722-725.
8. Khan, M.T.H; *Bioactive Heterocycles V*. Springer. 2007(11): p. 2-24.
9. Harrington, P.E. and M.A. Kerr, *Reaction of Indoles with Electron Deficient Olefins Catalyzed by  $\text{Yb}(\text{OTf})_3 \cdot 3\text{H}_2\text{O}$* . Synlett, 1996(11): p. 1047-1048.
10. Frost, C. and J. Hartley, *New applications of indium catalysts in organic synthesis*. Mini-Reviews in Organic Chemistry, 2004. **1**(1): p. 1-7.
11. Yadav, J., et al.,  *$\text{InCl}_3$ -catalysed conjugate addition of indoles with electron-deficient olefins*. Synthesis, 2001(14): p. 2165-2169.
12. Bandini, M., et al., *A practical indium tribromide catalysed addition of indoles to nitroalkenes in aqueous media*. Synthesis, 2002(08): p. 1110-1114.
13. Bandini, M., et al., *Sequential one-pot  $\text{InBr}_3$ -catalyzed 1,4- then 1,2-nucleophilic addition to enones*. The Journal of Organic Chemistry, 2002. **67**(11): p. 3700-3704.

14. Yadav, J., B. Reddy, and T. Swamy, *InBr<sub>3</sub>-catalyzed conjugate addition of indoles to p-quinones: An efficient synthesis of 3-indolylquinones*. *Synthesis*, 2004(01): p. 106-110.
15. Alam, M.M., R. Varala, and S.R. Adapa, *Conjugate addition of indoles and thiols with electron-deficient olefins catalyzed by Bi(OTf)<sub>3</sub>*. *Tetrahedron Letters*, 2003. **44**(27): p. 5115-5119.
16. Zhan, Z.-P., R.-F. Yang, and K. Lang, *Samarium triiodide-catalyzed conjugate addition of indoles with electron-deficient olefins*. *Tetrahedron Letters*, 2005. **46**(22): p. 3859-3862.
17. Firouzabadi, H., N. Iranpoor, and A.A. Jafari, *Aluminumdodecatungstophosphate (AlPW<sub>12</sub>O<sub>40</sub>), a versatile and a highly water tolerant green Lewis acid catalyzes efficient preparation of indole derivatives*. *Journal of Molecular Catalysis A: Chemical*, 2006. **244**(1-2): p. 168-172.
18. Kumar, V., S. Kaur, and S. Kumar, *ZrCl<sub>4</sub> catalyzed highly selective and efficient Michael addition of heterocyclic enamines with  $\alpha$ ,  $\beta$ -unsaturated olefins*. *Tetrahedron Letters*, 2006. **47**(39): p. 7001-7005.
19. López-Alvarado, P., et al., *One-pot assembly of large heterocyclic quinones through three-component reactions*. *Tetrahedron Letters*, 2001. **42**(45): p. 7971-7974.
20. Banik, B.K., M. Fernandez, and C. Alvarez, *Iodine-catalyzed highly efficient Michael reaction of indoles under solvent-free condition*. *Tetrahedron Letters*, 2005. **46**(14): p. 2479-2482.
21. Wang, S.-Y., S.-J. Ji, and T.-P. Loh, *The Michael addition of indole to  $\alpha$ , $\beta$ -unsaturated ketones catalyzed by iodine at room temperature*. *Synlett*, 2003(15): p. 2377-2379.
22. Lin, C., et al., *I<sub>2</sub>-catalyzed Michael addition of indole and pyrrole to nitroolefins*. *Tetrahedron*, 2005. **61**(49): p. 11751-11757.
23. Ji, S.-J. and S.-Y. Wang, *Ultrasound-accelerated Michael addition of indole to  $\alpha$ , $\beta$ -unsaturated ketones catalyzed by ceric ammonium nitrate (CAN)*. *Synlett*, 2003(13): p. 2074-2076.
24. Ji, S.-J. and S.-Y. Wang, *An expeditious synthesis of  $\beta$ -indolylketones catalyzed by p-toluenesulfonic acid (PTSA) using ultrasonic irradiation*. *Ultrasonics Sonochemistry*, 2005. **12**(5): p. 339-343.
25. Zeng, X.F., S.J. Ji, and S.S. Shen, *Conjugate Addition of Indoles to  $\alpha$ , $\beta$ -Unsaturated Ketones (Chalcones) Catalyzed by KHSO<sub>4</sub> under Ultrasonic Conditions*. *Chinese Journal of Chemistry*, 2007. **25**(12): p. 1777-1780.

26. Zhuang, W., T. Hansen, and K.A. Jørgensen, *Catalytic enantioselective alkylation of heteroaromatic compounds using alkylidene malonates*. Chemical Communications, 2001(4): p. 347-348.
27. Palomo, C., et al., *Highly Enantioselective Friedel–Crafts Alkylations of Pyrroles and Indoles with  $\alpha'$ -Hydroxy Enones under Cu(II)-Simple Bis(oxazoline) Catalysis*. Journal of the American Chemical Society, 2005. **127**(12): p. 4154-4155.
28. Yamazaki, S. and Y. Iwata, *Catalytic Enantioselective Friedel–Crafts/Michael Addition Reactions of Indoles to Ethenetricarboxylates*. The Journal of Organic Chemistry, 2006. **71**(2): p. 739-743.
29. Zhou, J. and Y. Tang, *Enantioselective Friedel–Crafts reaction of indoles with arylidene malonates catalyzed by ipr-bisoxazoline–Cu(OTf)<sub>2</sub>*. Chemical Communications, 2004(4): p. 432-433.
30. Jia, Y.-X., et al., *Asymmetric Friedel–Crafts Alkylations of Indoles with Nitroalkenes Catalyzed by Zn(II)–Bisoxazoline Complexes*. The Journal of Organic Chemistry, 2006. **71**(1): p. 75-80.
31. Lu, S.-F., D.-M. Du, and J. Xu, *Enantioselective Friedel–Crafts Alkylation of Indoles with Nitroalkenes Catalyzed by Bifunctional Tridentate Bis(oxazoline)–Zn(II) Complex*. Organic Letters, 2006. **8**(10): p. 2115-2118.
32. Evans, D.A. and K.R. Fandrick, *Catalytic enantioselective pyrrole alkylations of  $\alpha,\beta$ -unsaturated 2-acyl imidazoles*. Organic Letters, 2006. **8**(11): p. 2249-2252.
33. Austin, J.F. and D.W. MacMillan, *Enantioselective organocatalytic indole alkylations. Design of a new and highly effective chiral amine for iminium catalysis*. Journal of the American Chemical Society, 2002. **124**(7): p. 1172-1173.
34. Bandini, M., et al., *Catalytic enantioselective conjugate addition of indoles to simple  $\alpha,\beta$ -unsaturated ketones*. Tetrahedron Letters, 2003. **44**(31): p. 5843-5846.
35. Bandini, M., et al., *Can simple enones be useful partners for the catalytic stereoselective alkylation of indoles?* The Journal of Organic Chemistry, 2004. **69**(22): p. 7511-7518.
36. Bandini, M., et al., *Catalytic enantioselective addition of indoles to aryl nitroalkenes: An effective route to enantiomerically enriched tryptamine precursors*. Chirality, 2005. **17**(9): p. 522-529.
37. Srivastava, N. and B.K. Banik, *Bismuth nitrate-catalyzed versatile Michael reactions*. The Journal of Organic Chemistry, 2003. **68**(6): p. 2109-2114.
38. Çavdar, H. and N. Saraçoğlu, *A new approach for the synthesis of 2-substituted indole derivatives via Michael type adducts*. Tetrahedron, 2005. **61**(9): p. 2401-2405.

39. Couthon-Gourvès, H., et al., *Synthesis of novel diethyl indolylphosphonates and tetraethyl indolyl-1,1-bisphosphonates by Michael addition*. *Synthesis*, 2006(01): p. 81-88.
40. Suda, K., et al., *Metalloporphyrin-catalyzed regioselective rearrangement of monoalkyl-substituted epoxides into aldehydes*. *Tetrahedron Letters*, 1999. **40**(40): p. 7243-7246.
41. Ranu, B.C. and U. Jana, *Indium(III) chloride-promoted rearrangement of epoxides: a selective synthesis of substituted benzylic aldehydes and ketones*. *The Journal of Organic Chemistry*, 1998. **63**(23): p. 8212-8216.
42. Kotsuki, H., et al., *High-pressure organic chemistry. 10. Novel neutral alkylations of indoles and pyrroles with vinyl epoxides at high pressure*. *The Journal of Organic Chemistry*, 1990. **55**(9): p. 2969-2972.
43. Kotsuki, H., et al., *High-Pressure Organic Chemistry. 19. High-Pressure-Promoted, Silica Gel-Catalyzed Reaction of Epoxides with Nitrogen Heterocycles1*. *The Journal of Organic Chemistry*, 1996. **61**(3): p. 984-990.
44. Bandini, M., et al., *InBr<sub>3</sub>-Catalyzed Friedel–Crafts Addition of Indoles to Chiral Aromatic Epoxides: A Facile Route to Enantiopure Indolyl Derivatives*. *The Journal of Organic Chemistry*, 2002. **67**(15): p. 5386-5389.
45. Bandini, M., A. Melloni, and A. Umani-Ronchi, *New catalytic approaches in the stereoselective Friedel–Crafts alkylation reaction*. *Angewandte Chemie International Edition*, 2004. **43**(5): p. 550-556.
46. Carey, F, A; Sundberg, R. J; *Advanced Organic Chemistry*. Kluwer Academic/Plenum Publishers. 2000(4): p. 91-398.
47. Noland, W.E., M.R. Venkiteswaran, and C. Richards, *Cyclizative Condensations. I. 2-Methylindole with Acetone and Methyl Ethyl Ketone1*. *The Journal of Organic Chemistry*, 1961. **26**(11): p. 4241-4248.
48. Chen, D., L. Yu, and P.G. Wang, *Lewis acid-catalyzed reactions in protic media. Lanthanide-catalyzed reactions of indoles with aldehydes or ketones*. *Tetrahedron Letters*, 1996. **37**(26): p. 4467-4470.
49. Nagarajan, R. and P.T. Perumal, *InCl<sub>3</sub> and In(OTf)<sub>3</sub> catalyzed reactions: synthesis of 3-acetyl indoles, bis-indolylmethane and indolylquinoline derivatives*. *Tetrahedron*, 2002. **58**(6): p. 1229-1232.
50. Mi, X., et al., *Dy(OTf)<sub>3</sub> in ionic liquid: an efficient catalytic system for reactions of indole with aldehydes/ketones or imines*. *Tetrahedron Letters*, 2004. **45**(23): p. 4567-4570.

51. Yadav, J.S., et al., *Lithium perchlorate catalyzed reactions of indoles: An expeditious synthesis of bis(indolyl)methanes*. Synthesis, 2001(05): p. 0783-0787.
52. Ji, S.-J., et al., *Facile synthesis of bis(indolyl)methanes using catalytic amount of iodine at room temperature under solvent-free conditions*. Tetrahedron, 2004. **60**(9): p. 2051-2055.
53. Deb, M.L. and P.J. Bhuyan, *An efficient and clean synthesis of bis(indolyl)methanes in a protic solvent at room temperature*. Tetrahedron Letters, 2006. **47**(9): p. 1441-1443.
54. Kobayashi, S., M. Araki, and M. Yasuda, *One-pot synthesis of  $\beta$ -amino esters from aldehydes using lanthanide triflate as a catalyst*. Tetrahedron Letters, 1995. **36**(32): p. 5773-5776.
55. Kamal, A., et al., *An efficient synthesis of bis(indolyl)methanes and evaluation of their antimicrobial activities*. Journal of Enzyme Inhibition and Medicinal Chemistry, 2009. **24**(2): p. 559-565.
56. Heydari, A., et al., *Lithium perchlorate/diethylether-catalyzed three-component coupling reactions of aldehydes, hydroxylamines and trimethylsilyl cyanide leading to  $\alpha$ -cyanohydroxylamines*. Tetrahedron Letters, 2000. **41**(14): p. 2471-2473.
57. Sankararaman, S. and J.E. Nesakumar, *Highly selective synthetic transformations catalyzed by lithium perchlorate in organic media*. European Journal of Organic Chemistry, 2000(11): p. 2003-2011.
58. Praveen, C., et al., *Synthesis, antimicrobial and antioxidant evaluation of quinolines and bis(indolyl)methanes*. Bioorganic & Medicinal Chemistry Letters, 2010. **20**(24): p. 7292-7296.
59. Damodiran, M., D. Muralidharan, and P.T. Perumal, *Regioselective synthesis and biological evaluation of bis (indolyl) methane derivatized 1,4-disubstituted 1,2,3-bis-triazoles as anti-infective agents*. Bioorganic & Medicinal Chemistry Letters, 2009. **19**(13): p. 3611-3614.
60. Giannini, G., et al., *Exploring bis(indolyl)methane moiety as an alternative and innovative CAP group in the design of histone deacetylase (HDAC) inhibitors*. Bioorganic & Medicinal Chemistry Letters, 2009. **19**(10): p. 2840-2843.
61. Grosso, C., et al., *Novel approach to bis(indolyl)methanes: De novo synthesis of 1-hydroxyiminomethyl derivatives with anti-cancer properties*. European Journal of Medicinal Chemistry, 2015. **93**: p. 9-15.
62. Reddy, B.S., et al., *Indium(III) chloride catalyzed three-component coupling reaction: A novel synthesis of 2-substituted aryl(indolyl)kojic acid derivatives as potent*

- antifungal and antibacterial agents*. Bioorganic & Medicinal Chemistry Letters, 2010. **20**(24): p. 7507-7511.
63. Reddy, B.S., et al., *Iodine-catalyzed condensation of isatin with indoles: A facile synthesis of di(indolyl)indolin-2-ones and evaluation of their cytotoxicity*. Bioorganic & Medicinal Chemistry Letters, 2012. **22**(7): p. 2460-2463.
  64. Praveen, C., A. Ayyanar, and P.T. Perumal, *Practical synthesis, anticonvulsant, and antimicrobial activity of N-allyl and N-propargyl di(indolyl)indolin-2-ones*. Bioorganic & Medicinal Chemistry Letters, 2011. **21**(13): p. 4072-4077.
  65. Edayadulla, N., N. Basavegowda, and Y.R. Lee, *Green synthesis and characterization of palladium nanoparticles and their catalytic performance for the efficient synthesis of biologically interesting di(indolyl)indolin-2-ones*. Journal of Industrial and Engineering Chemistry, 2015. **21**: p. 1365-1372.
  66. Kamal, A., et al., *Synthesis of 3,3-diindolyl oxyindoles efficiently catalysed by FeCl<sub>3</sub> and their in vitro evaluation for anticancer activity*. Bioorganic & Medicinal Chemistry Letters, 2010. **20**(17): p. 5229-5231.
  67. Rad-Moghadam, K., M. Sharifi-Kiasaraie, and H. Taheri-Amlashi, *Synthesis of symmetrical and unsymmetrical 3,3-di(indolyl)indolin-2-ones under controlled catalysis of ionic liquids*. Tetrahedron, 2010. **66**(13): p. 2316-2321.
  68. Wang, S.-Y. and S.-J. Ji, *Facile synthesis of 3,3-di(heteroaryl)indolin-2-one derivatives catalyzed by ceric ammonium nitrate (CAN) under ultrasound irradiation*. Tetrahedron, 2006. **62**(7): p. 1527-1535.
  69. Azizian, J., et al., *Silica sulfuric acid a novel and heterogeneous catalyst for the synthesis of some new oxindole derivatives*. Catalysis Communications, 2006. **7**(10): p. 752-755.
  70. Paira, P., et al., *Efficient synthesis of 3,3-diheteroaromatic oxindole analogues and their in vitro evaluation for spermicidal potential*. Bioorganic & Medicinal Chemistry Letters, 2009. **19**(16): p. 4786-4789.
  71. Azizian, J., et al., *KAl(SO<sub>4</sub>)<sub>2</sub>.12H<sub>2</sub>O as a recyclable Lewis acid catalyst for synthesis of some new oxindoles in aqueous media*. Journal of Chemical Research, 2004(6): p. 424-426.
  72. Svoboda, G.H., N. Neuss, and M. Gorman, *Alkaloids of Vinca rosea Linn.(Catharanthus roseus G. Don.) V. Preparation and characterization of alkaloids*. Journal of the American Pharmaceutical Association, 1959. **48**(11): p. 659-666.

73. Gunasekera, S.P., P.J. McCarthy, and M. Kelly-Borges, *Hamacanthins A and B, new antifungal bis indole alkaloids from the deep-water marine sponge, Hamacantha sp.* Journal of Natural Products, 1994. **57**(10): p. 1437-1441.
74. Bartik, K., et al., *Topsentins, new toxic bis-indole alkaloids from the marine sponge Topsentia genitrix.* Canadian Journal of Chemistry, 1987. **65**(9): p. 2118-2121.
75. Tsujii, S., et al., *Topsentin, bromotopsentin, and dihydrodeoxybromotopsentin: Antiviral and antitumor bis(indolyl)imidazoles from Caribbean deep-sea sponges of the family Halichondriidae. Structural and synthetic studies.* The Journal of Organic Chemistry, 1988. **53**(23): p. 5446-5453.
76. Roll, D.M., et al., *Fascaplysin, an unusual antimicrobial pigment from the marine sponge Fascaplysinopsis sp.* The Journal of Organic Chemistry, 1988. **53**(14): p. 3276-3278.
77. Fahy, E., et al., *6-Bromotryptamine derivatives from the Gulf of California tunicate Didemnum candidum.* Journal of Natural Products, 1991. **54**(2): p. 564-569.
78. Nishida, A., et al., *Solid-phase synthesis of 5-(3-indolyl)oxazoles that inhibit lipid peroxidation.* Tetrahedron Letters, 2000. **41**(24): p. 4791-4794.
79. Narkowicz, C.K., et al., *Convolutindole A and convolutamine H, new nematocidal brominated alkaloids from the marine bryozoan Amathia convoluta.* Journal of Natural Products, 2002. **65**(6): p. 938-941.
80. Moquin-Patthey, C. and M. Guyot, *Grossularine-1 and grossularine-2, cytotoxic  $\alpha$ -carboline derivatives from the tunicate: Dendrodia grossularia.* Tetrahedron, 1989. **45**(11): p. 3445-3450.
81. Higa, T. and M. Kuniyoshi, *Toxins associated with medicinal and edible seaweeds.* Journal of Toxicology: Toxin Reviews, 2000. **19**(2): p. 119-137.
82. Raub, M.F., J.H. Cardellina II, and J.G. Schwede, *The green algal pigment caulerpin as a plant growth regulator.* Phytochemistry, 1987. **26**(3): p. 619-620.
83. Bobzin, S.C. and D.J. Faulkner, *Aromatic alkaloids from the marine sponge Chelonaplysilla sp.* The Journal of Organic Chemistry, 1991. **56**(14): p. 4403-4407.
84. Fusetani, N., et al., *Orbiculamide A: A novel cytotoxic cyclic peptide from a marine sponge Theonella sp.* Journal of the American Chemical Society, 1991. **113**(20): p. 7811-7812.
85. Bewley, C.A., C. Debitus, and D.J. Faulkner, *Microsclerodermins A and B. Antifungal cyclic peptides from the Lithistid sponge Microscleroderma sp.* Journal of the American Chemical Society, 1994. **116**(17): p. 7631-7636.



86. Kobayashi, J.i., et al., *Keramamide A, a novel peptide from the Okinawan marine sponge Theonella sp.* Journal of the Chemical Society, Perkin Transactions 1, 1991(10): p. 2609-2611.
87. Uemoto, H., et al., *Keramamides K and L, new cyclic peptides containing unusual tryptophan residue from Theonella sponge.* Tetrahedron, 1998. **54**(24): p. 6719-6724.
88. Berlinck, R.G., et al., *Granulatimide and isogranulatimide, aromatic alkaloids with G2 checkpoint inhibition activity isolated from the Brazilian ascidian Didemnum granulatum: structure elucidation and synthesis.* The Journal of Organic Chemistry, 1998. **63**(26): p. 9850-9856.
89. Vervoort, H.C., et al., *Didemnimides A–D: novel, predator-deterrent alkaloids from the Caribbean mangrove ascidian didemnum conchyliatum.* The Journal of Organic Chemistry, 1997. **62**(5): p. 1486-1490.
90. Sakai, R., et al., *Manzamine B and C, two novel alkaloids from the sponge Haliclona sp.* Tetrahedron Letters, 1987. **28**(45): p. 5493-5496.
91. Roy, S., S. Haque, and G.W. Gribble, *Synthesis of novel oxazolyliindoles.* Synthesis, 2006(23): p. 3948-3954.
92. Pettit, G.R., et al., *Isolation of labradorins 1 and 2 from Pseudomonas syringae pv. coronafaciens.* Journal of Natural Products, 2002. **65**(12): p. 1793-1797.
93. Kaji, A., et al., *Four new metabolites of Aspergillus terreus.* Chemical and Pharmaceutical Bulletin, 1994. **42**(8): p. 1682-1684.
94. ARAI, K. and Y. YAMAMOTO, *Metabolic Products of Aspergillus terreus. X.: Biosynthesis of Asterriquinones.* Chemical and Pharmaceutical Bulletin, 1990. **38**(11): p. 2929-2932.
95. Zhang, B., et al., *Discovery of a small molecule insulin mimetic with antidiabetic activity in mice.* Science, 1999. **284**(5416): p. 974-977.
96. Toske, S.G., et al., *Aspergillamides A and B: modified cytotoxic tripeptides produced by a marine fungus of the genus Aspergillus.* Tetrahedron, 1998. **54**(44): p. 13459-13466.
97. Kaji, A., et al., *Relationship between the structure and cytotoxic activity of asterriquinone, an antitumor metabolite of Aspergillus terreus, and its alkyl ether derivatives.* Biological and Pharmaceutical Bulletin, 1998. **21**(9): p. 945-949.
98. Kaji, A., et al., *Mechanism of the cytotoxicity of asterriquinone, a metabolite of Aspergillus terreus.* Anticancer Research, 1997. **17**(5A): p. 3675-3679.

99. Patrick, G.L., *An introduction to medicinal chemistry*. Oxford University Press. 2013: p. 413-467.
100. Bergler, H., et al., *The enoyl-[acyl-carrier-protein] reductase (FabI) of Escherichia coli, which catalyzes a key regulatory step in fatty acid biosynthesis, accepts NADH and NADPH as cofactors and is inhibited by palmitoyl-CoA*. European Journal of Biochemistry, 1996. **242**(3): p. 689-694.
101. Heath, R.J., et al., *Broad spectrum antimicrobial biocides target the FabI component of fatty acid synthesis*. Journal of Biological Chemistry, 1998. **273**(46): p. 30316-30320.
102. Zhu, L., et al., *The two functional enoyl-acyl carrier protein reductases of Enterococcus faecalis do not mediate triclosan resistance*. MBio, 2013. **4**(5): p. e00613-13.
103. Seefeld, M.A., et al., *Inhibitors of bacterial enoyl acyl carrier protein reductase (FabI): 2,9-disubstituted 1,2,3,4-tetrahydropyrido[3,4-b]indoles as potential antibacterial agents*. Bioorganic & Medicinal Chemistry Letters, 2001. **11**(17): p. 2241-2244.
104. Kliegman, R. M; Stanton, B. F; St Geme, J. W; Schor, B. F; *Nelson Textbook of Pediatrics*. Elsevier. 2016(20): p. 1328-3562.
105. Thomas, G., *Fundamentals of medicinal chemistry*. John Wiley & Sons. 2004: p. 71-94.
106. Gürkök, G., T. Coban, and S. Suzen, *Melatonin analogue new indole hydrazide/hydrazone derivatives with antioxidant behavior: synthesis and structure–activity relationships*. Journal of Enzyme Inhibition and Medicinal Chemistry, 2009. **24**(2): p. 506-515.
107. Pordel, M., A. Abdollahi, and B. Razavi, *Synthesis and biological evaluation of novel isoxazolo[4,3-e]indoles as antibacterial agents*. Russian Journal of Bioorganic Chemistry, 2013. **39**(2): p. 211-214.
108. Speirs, R., J. Welch, and M. Cynamon, *Activity of n-propyl pyrazinoate against pyrazinamide-resistant Mycobacterium tuberculosis: investigations into mechanism of action of and mechanism of resistance to pyrazinamide*. Antimicrobial Agents and Chemotherapy, 1995. **39**(6): p. 1269-1271.
109. Tiwari, R.K., et al., *Synthesis and antibacterial activity of substituted 1,2,3,4-tetrahydropyrazino[1,2-a]indoles*. Bioorganic & Medicinal Chemistry Letters, 2006. **16**(2): p. 413-416.

110. Kinsman, O.S., D.G. Livermore, and C. Smith, *Antifungal properties in a novel series of triazino[5,6-b]indoles*. *Antimicrobial Agents and Chemotherapy*, 1993. **37**(6): p. 1243-1246.
111. PEREIRA, E.R., et al., *Syntheses and antimicrobial activities of five-membered ring heterocycles coupled to indole moieties*. *The Journal of Antibiotics*, 1996. **49**(4): p. 380-385.
112. PEREIRA, E.R., et al., *Synthesis and antimicrobial activities of 3-N-substituted-4,5-bis (3-indolyl)oxazol-2-ones*. *Bioorganic & Medicinal Chemistry Letters*, 1997. **7**(19): p. 2503-2506.
113. Prudhomme, M., et al., *Synthesis and antimicrobial activities of monoindolyl-and bisindolyloximes*. *European Journal of Medicinal Chemistry*, 1999. **34**(2): p. 161-165.
114. Kumar, D., et al., *Synthesis of Novel Indolyl-1,2,4-triazoles as Potent and Selective Anticancer Agents*. *Chemical Biology & Drug Design*, 2011. **77**(3): p. 182-188.
115. Jablonowski, J.A., et al., *The first potent and selective non-imidazole human histamine H4 receptor antagonists*. *Journal of Medicinal Chemistry*, 2003. **46**(19): p. 3957-3960.
116. Romero, D.L., et al., *Bis(heteroaryl)piperazine (BHAP) reverse transcriptase inhibitors: structure-activity relationships of novel substituted indole analogs and the identification of 1-[(5-methanesulfonamido-1H-indol-2-yl)carbonyl]-4-[3-[(1-methylethyl)amino]pyridinyl]piperazinemonomethanesulfonate (U-90152S), a second-generation clinical candidate*. *Journal of Medicinal Chemistry*, 1993. **36**(10): p. 1505-1508.
117. Xia, Y., et al., *Synthesis of adenosine analogues with indole moiety as human adenosine A3 receptor ligands*. *Royal Society Open Science*, 2018. **5**(2): p. 171596.
118. Yamamoto, Y. and M. Kurazono, *A new class of anti-MRSA and anti-VRE agents: preparation and antibacterial activities of indole-containing compounds*. *Bioorganic & Medicinal Chemistry Letters*, 2007. **17**(6): p. 1626-1628.
119. Korn, A., S. Fearheller, and E. Filachoine, *Glutaraldehyde: nature of the reagent*. *Journal of Molecular Biology*, 1972. **65**(3): p. 525-529.
120. Migneault, I., et al., *Glutaraldehyde: behavior in aqueous solution, reaction with proteins, and application to enzyme crosslinking*. *Biotechniques*, 2004. **37**(5): p. 790-802.
121. *Malondialdehyde, Encyclopedia of Reagents for Organic Synthesis*.
122. Barrera, G., et al., *Lipid peroxidation-derived aldehydes, 4-hydroxynonenal and malondialdehyde in aging-related disorders*. *Antioxidants*, 2018. **7**(8): p. 102.

123. El-Sayed, M.T., et al., *Novel tetraindoles and unexpected cycloalkane indoles from the reaction of indoles and aliphatic dialdehydes*. Journal of Heterocyclic Chemistry, 2017. **54**(1): p. 714-719.
124. Silverstein, R.M; Webster, F. X; Kiemle D. J; *Spectrometric identification of organic compounds*. John Wiley & Sons. 2005: p. 127-203.
125. Saebø, S., F.R. Cordell, and J.E. Boggs, *Structures and conformations of cyclopentane, cyclopentene, and cyclopentadiene*. Journal of Molecular Structure: THEOCHEM, 1983. **104**(1-2): p. 221-232.
126. BOTHNER-BY, A.A., *Geminal and vicinal proton-proton coupling constants in organic compounds*, in *Advances in Magnetic and Optical Resonance*. Elsevier. 1965: p. 195-316.
127. Cronin, J. and P. Hare, *Chromatographic analysis of amino acids and primary amines with o-phthalaldehyde detection*. Analytical Biochemistry, 1977. **81**(1): p. 151-156.
128. Zuman, P., *Reactions of orthophthalaldehyde with nucleophiles*. Chemical Reviews, 2004. **104**(7): p. 3217-3238.
129. Black, D.S., D.C. Craig, and M. Santoso, *Mechanism-controlled regioselective synthesis of indolylbenzo[b]carbazoles*. Tetrahedron Letters, 1999. **40**(36): p. 6653-6656.
130. Dräger, M., et al., *New potential DNA intercalators of the carbazole series from indole-2,3-quinodimethanes: Synthesis, crystal structure, and molecular modeling with a watson-crick mini-helix*. Monatshefte für Chemie/Chemical Monthly, 1993. **124**(5): p. 559-576.
131. Kansal, V.K. and P. Potier, *The biogenetic, synthetic and biochemical aspects of ellipticine, an antitumor alkaloid*. Tetrahedron, 1986. **42**(9): p. 2389-2408.
132. Woodward, R., G. Iacobucci, and I. Hochstein, *The synthesis of ellipticine*. Journal of the American Chemical Society, 1959. **81**(16): p. 4434-4435.
133. Bergman, J. and B. Pelcman, *Synthesis of carbazole alkaloids*. Pure and Applied Chemistry, 1990. **62**(10): p. 1967-1976.
134. Rao, M.V.B., et al., *Anionic [4+2] cycloaddition reactions of indole-2,3-dienolate with dienophiles: a facile regiospecific route to substituted carbazoles*. Tetrahedron Letters, 1995. **36**(19): p. 3385-3388.
135. Boogaard, A.T., U.K. Pandit, and G.-J. Koomen, *Ring D modifications of ellipticine. Part 2. Chlorination of ellipticine via its N-oxide and synthesis and selective acetylation of 5, 6, 11-trimethyl-5H-benzo[b]carbazole*. Tetrahedron, 1994. **50**(16): p. 4811-4828.

136. Paul, K., et al., *Fe-catalyzed novel domino isomerization/cyclodehydration of substituted 2-[(Indoline-3-ylidene)(methyl)]benzaldehyde derivatives: an efficient approach toward benzo[b]carbazole derivatives*. Organic Letters, 2014. **16**(8): p. 2166-2169.
137. Zhao, Z., et al., *Anionic indole N-Carbamoyl N→C translocation. A directed remote metalation route to 2-aryl- and 2-heteroarylindoles. Synthesis of benz[a]carbazoles and indeno [1, 2-b] indoles*. Organic Letters, 2008. **10**(13): p. 2617-2620.
138. Martínez-Esperón, M.F., et al., *Synthesis of carbazoles from ynamides by intramolecular dehydro Diels–Alder reactions*. Organic Letters, 2005. **7**(11): p. 2213-2216.
139. Tsuchimoto, T., et al., *Indium-catalyzed annulation of 2-aryl- and 2-heteroarylindoles with propargyl ethers: Concise synthesis and photophysical properties of diverse aryl- and heteroaryl-annulated[a]carbazoles*. Journal of the American Chemical Society, 2008. **130**(47): p. 15823-15835.
140. Rajeshwaran, G.G. and A.K. Mohanakrishnan, *Synthetic studies on indolocarbazoles: Total synthesis of staurosporine aglycon*. Organic Letters, 2011. **13**(6): p. 1418-1421.
141. Crich, D. and S. Rumthao, *Synthesis of carbazomycin B by radical arylation of benzene*. Tetrahedron, 2004. **60**(7): p. 1513-1516.
142. Hieda, Y., et al., *A novel total synthesis of the bioactive poly-substituted carbazole alkaloid carbazomadurin A*. Tetrahedron Letters, 2010. **51**(27): p. 3593-3596.
143. Senthilkumar, N., et al., *Synthesis of active metabolites of Carvedilol, an antihypertensive drug*. Synthetic Communications, 2010. **41**(2): p. 268-276.
144. Dubois, E.A., et al., *Synthesis and in Vitro and in Vivo Characteristics of an Iodinated Analogue of the  $\beta$ -Adrenoceptor Antagonist Carazolol*. Journal of Medicinal Chemistry, 1996. **39**(17): p. 3256-3262.
145. Zhang, A. and G. Lin, *The first synthesis of clausenamine-A and cytotoxic activities of three biscarbazole analogues against cancer cells*. Bioorganic & Medicinal Chemistry Letters, 2000. **10**(10): p. 1021-1023.
146. Zou, J.-F., et al., *Fe-catalyzed cycloaddition of indoles and o-phthalaldehyde for the synthesis of benzo[b]carbazoles with TMSCl- or acid-responsive properties*. RSC Advances, 2014. **4**(88): p. 47272-47277.

## **5. Experimental**

### **5.1 Materials**

#### **5.1.1 Thin Layer Chromatography (TLC)**

Aluminium foil fluorescent active TLC plates (silica gel 60 F254, thickness 0.2 mm) purchased from Merck KGaA was used. Retention factors ( $R_f$  Values) of each compound were calculated by dividing the run level of the compound in cm by that of the eluent after developing the samples.

#### **5.1.2 Column Chromatography**

Normal-phase liquid chromatography (NPLC) [Column Chromatography] was carried out at atmospheric pressure on silica gel 60, thickness 0.2 mm purchased from Merck KGaA.

#### **5.1.3 Ultra-Violet Lamp (UV Lamp)**

To be able to detect the TLC plates, UV lamp at 254 and 366 nm was used.

#### **5.1.4 Melting Points**

The melting points were measured on a Boetis-Mikroheiztisch the company "VEB weighing. Rapido Radebeul / VEB NAGEMA) and are uncorrected.

#### **5.1.5 Reagents and solvents**

Acetone (Roth)

Acetic anhydride (Roth)

5-Aminoindole (Acros organics)

Ammoniumhydroxide (Roth)

7-Azaindole (Acros organics)

4-Benzyloxyindole (Sigma-Aldrich)

5-Benzyloxyindole (Sigma-Aldrich)

4-Bromoindole (Acros organics)

5-Bromoindole (Acros organics)

6-Bromoindole (Acros organics)

2-Bromomalondiladehyde (Acros organics)

5-Carbonitrileindole (Acros organics)  
Chloroform (Roth)  
5-Chloroindole (Sigma-Aldrich and Acros organics)  
6-Chloroindole (Acros organics)  
2-Chloromalondialdehyde (Acros organics)  
Cyclohexane (Roth)  
Dichloromethane (Roth)  
Diethyl ether (Kraemer and Martin)  
4-(Dimethylamino) pyridine (Sigma-Aldrich)  
Ethylacetate (Roth)  
Glacial Acetic Acid (Roth)  
Glutaric dialdehyde (Acros organics)  
Hydrochloric acid (Roth)  
5-hydroxyindole (Acros organics)  
Indole (Merck)  
4-Methoxyindole (Acros organics)  
5-Methoxyindole (Acros organics)  
2-(4-Methoxyphenyl)Malondialdehyde (Acros organics)  
n-Hexane (Roth)  
5-Nitroindole (Acros organics)  
7-Nitroindole (Acros organics)  
*O*-phthalaldehyde (Acros Organics)  
2-(4-Pyridyl)malondialdehyde (Acros organics)  
Sodiumchloride (Roth)  
Sodiumhydroxide (Roth)  
Sodiumsulfate (Roth)  
2,3-Thiophenedicarboxaldehyde (Acros organics)  
1,1,3,3-Tetramethoxy propane (Acros organics)  
Triethylamine (Fluka)

## **5.2 Instruments**

### **5.2.1 Electrospray Ionization Mass Spectrometry (ESI-MS)**

The positive and negative ESI mass spectra were obtained by LCQ-Classic, the Thermo Finnigan Company Mass Spectrometer. The samples were injected directly with the injection rate of 20  $\mu\text{l}/\text{min}$  at the capillary temperature, voltage, and Sheath Flow rate of 220  $^{\circ}\text{C}$ , 5.0 KV, and 70 respectively. The samples were dissolved in either Chloroform or Methanol (ca. 1-5 mg/ml).

### **5.2.2 Atmospheric Pressure Chemical Ionization Mass Spectrometry (APCI-MS)**

The instrument is an expression CMS (compact mass spectrometer, Advion, USA) with an APCI (atmospheric pressure chemical ionization) source. Samples are introduced using a direct analysis probe (ASAP, atmospheric solids analysis probe), nitrogen is used for chemical ionization. Capillary temperature: 250 $^{\circ}\text{C}$ , capillary voltage 180V, source gas temperature: 350 $^{\circ}\text{C}$ , corona discharge current: 5  $\mu\text{A}$ , mass range: based on the users' settings. Samples are measured in positive and negative ionization mode.

### **5.2.3 Fourier Transform Infrared (FT-IR)**

The attenuated total reflection (ATR) technique was used on a FT-IR spectrometer "IFS 28" by "Bruker", the samples were prepared in a form of KBr discs on a FT-IR spectrometer "Spectrum BX" the Company "Perkin-Elmer". For each sample the Absorbance intensity (A) was plotted against Wavenumber ( $\bar{\nu}$ ) in the range of 680-4000  $\text{cm}^{-1}$ . S, m, w, and br stand for strong, moderate, weak, and broad peaks.

### **5.2.4 One Dimensional Proton Nuclear Magnetic Resonance (1D $^1\text{H}$ -NMR)**

400 or 500 MHz is the transmitter frequency which is directly proportional to the strength of the applied magnetic field (T), acetone- $\text{d}_6$ , DMSO- $\text{d}_6$  (dimethylsulfoxide), and methanol- $\text{d}_6$  are the deuterated solvents, and  $\delta$  is the chemical shift in parts per million (ppm) after the correction ( $\delta=0$ -12 ppm). Tetramethylsilane (TMS) was used as internal standard ( $\delta=0$ ). For  $\text{H}_a$ ,  $\delta$  (M, N, J); M is the multiplicity of the proton which could be s (singlet), d (doublet), t (triplet), q (quartet), and m (multiplet). The combinations of multiplicities as well as dd (doublet of doublet) or dt (doublet of triplet) were also observed. N is the number of the protons obtained by peak integration and J is the coupling constant in Hertz (Hz) whose magnitude enables us to understand the distance between coupling protons.



### 5.2.5 One Dimensional Carbon Nuclear Magnetic Resonance (1D $^{13}\text{C}$ -NMR)

100 MHz is the transmitter frequency, acetone- $\text{d}_6$  or DMSO- $\text{d}_6$  are the deuterated solvents, and  $\delta$  is the Chemical Shift in parts per million (ppm) after the correction ( $\delta = 0\text{--}210$  ppm).

#### 5.2.5.1 Proton Coupled Carbon NMR

Likewise proton NMR, the coupling of carbon by adjacent protons mainly single-bond protons is observed.

#### 5.2.5.2 APT (Proton Decoupled Carbon NMR)

Unlike the proton-NMR and proton coupled  $^{13}\text{C}$ -NMR, in APT the coupling of carbon by adjacent protons is erased; hence, only singlet peaks are observed. APT obtains signals for CH (tertiary),  $\text{CH}_2$  (secondary), and  $\text{CH}_3$  (primary) but no signal for C (quaternary). The signals of CH and  $\text{CH}_3$  are negative and those of  $\text{CH}_2$  are positive.

The NMR spectra were recorded on a "Gemini 2000" (400/100 MHz) or on an "INOVA 500" (500 MHz) of the firm "Varian measured" served as the internal standard residual resonance signal of the respective deuterated solvent. The interpretation of the NMR Spectra was carried out using the spectral simulation tools, ChemBioDraw (Level:Ultra, Version 13.0.0.3015) and MestReNova (Version 8.0.0-10524 ) were used to interpret the NMR Spectra. The assignment of the signals has been done by the inclusion of appropriate 2D-NMR Spectra.

### 5.2.6 Two Dimensional Nuclear Magnetic Resonance (2D-NMR)

COSY: Correlation spectroscopy

NOESY: Nuclear overhauser effect spectroscopy

HMBC: Heteronuclear multiple bond correlation

HSQC: Heteronuclear single quantum correlation

\*Correction;  $\delta$  (ppm) =  $[\nu_{\text{sample}} - \nu_{\text{ref}} (\text{Hz}) / \nu_{\text{instrument}} (\text{MHz}) \times 10^6] \times 10^6$

### 5.2.7 Reversed-phase high performance liquid chromatography (RP-HPLC)

The purity of the compounds was determined by analytical RP-HPLC (Shimadzu, Kyoto, Japan; LC-10AD, SIL-HAT auto sampler) with an XTerra RP-18 column (3.5  $\mu\text{M}$ , 3.9 x 100

mm) from Waters Company (Milford, MA, USA. The UV-Vis detector SPD-M10A VP PDA was set to 254 nm. The flow rate was 0.8 ml/min. The eluent was gradient mixture of MeOH and water. The MeOH content increased between 5% and 95%. For better performance, 0.1% trifluoroacetic acid ( $\text{CF}_3\text{COOH}$ ) (TFA) was also used.

### 5.3 General Experimental Protocol to synthesize the compounds 1-22

In a 50 or 100 ml round-bottomed flask containing a magnet stirrer, 15 ml glacial acetic acid was firstly poured. In the next step, 2 mmol aliphatic dialdehyde (either 2-substituted malondialdehyde or glutaric dialdehyde) was added and the mixture was left for a few minutes until the dialdehyde was fairly dissolved in acetic acid. 5 mmol Indole or its derivatives was lastly added to the solution leading to a change in the colour of the reaction mixture. The resulted solution was left stirring for a while (mostly one overnight). The reaction was monitored by TLC since one or two hour(s) after the reaction had started. The TLCs usually showed a few components with various  $R_f$  values. Unreacted Indole-excess reactant mostly placed at the top of the components followed by other products with lower  $R_f$ s. The reactions were qualitatively analysed by Mass spectrometry to prove the desired product. As soon as there was no change in terms of the quantity and quality of the components, the reactions would have been worked-up. This procedure involved in neutralizing reactions with diluted solution of NaOH (10% NaOH) resulting in a dark-coloured precipitate which contains our desired compound and the others, extracting with dichloromethane ( $\text{CH}_2\text{Cl}_2$ ) for three times, washing with saturated solution of NaCl (brine), adding drying agent such as sodium sulfate ( $\text{Na}_2\text{SO}_4$ ), filtering the solution after roughly quarter of an hour, and vapourizing the filtered solution under reduced pressures to get rid of the volatile solvent. The resulted mixture was purified via column chromatography by using different eluents as well as ethyleacetate and cyclohexane or diethylether and cyclohexane. The components containing the desired products were separately qualitatively analysed by electrospray ionization mass spectrometry (ESI-MS) or atmospheric pressure chemical ionization (APCI), were unified, and the structures of desired products were elucidated by 1D  $^1\text{H}$ -NMR, 1D  $^{13}\text{C}$ -NMR (APT (Proton Decoupled Carbon NMR) and Proton Coupled Carbon NMR), 2D NMR (DQCOSY, NOESY, gHMBC, gHSQCAD), and FT-IR. The purity of the products was determined by RP-HPLC.

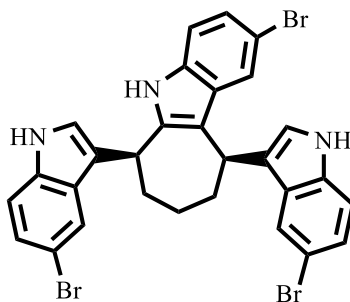
#### 5.4 General Experimental Protocol to synthesize the compounds 23-37 and 40

Likewise the previous protocol, in a 50 or 100 ml round-bottomed flask containing the magnet stirrer, 15 ml glacial acetic acid was firstly poured. Unlikely, 1 mmol aromatic dialdehyde (*o*-phthaldialdehyde or 2-3 thiophenedicarboxaldehyde) was added to the acetic acid and the mixture was left at room temperature for a few minutes until the dialdehyde was fairly dissolved. 2 mmol Indole or its derivatives was then added to this mixture and the reaction was heated at 100 °C for a while (from one overnight to four days). Likewise the first experimental protocol, the reaction was monitored and qualitatively analysed by TLC and ESI-MS or APCI respectively. The reaction was also similarly worked-up. The isolated components obtained via Column Chromatography were qualitatively analysed by ESI-MS and APCI. The structures of the desired products were elucidated by 1D <sup>1</sup>H-NMR and FT-IR and the purity was determined by RP-HPLC.

#### 5.5 Experimental Protocol to Acetylation of the compound 31 (compounds 38 and 39)

1 mmol compound 31 was added to a 50 ml round-bottomed flask containing 5 ml CH<sub>2</sub>Cl<sub>2</sub>, 0.1 mmol 4-(dimethylaminopyridine) (DMAP), 1.2 mmol acetic anhydride and triethylamine (TEA), and a magnet stirrer. The reaction mixture was left stirring at room temperature for some weeks; while, it was qualitatively and quantitatively monitored by TLC and was qualitatively analysed by ESI-MS. After about four weeks, the reaction was worked-up by neutralizing the solution with NH<sub>4</sub>OH, extracting with CH<sub>2</sub>Cl<sub>2</sub> for three times, washing with brine for twice, adding drying agent sodium sulfate, filtering the solution, and drying under reduced pressure. The mono- and di-acetylated indolylbenzo[b]carbazole components were isolated by column chromatography on silica gel and ethylacetate:Cyclohexane (0.7:1.3) and were identified by ESI-MS accordingly. The structures of these two components were elucidated by 1D <sup>1</sup>H-NMR.

**(6S,10R)-2-bromo-6,10-bis(5-bromo-1H-indol-3-yl)-5,6,7,8,9,10-hexahydrocyclohepta[b]indole**



**(1)**

**5-Bromoindole (5 mmol, 0.9802 gr) + glutaric dialdehyde (2 mmol, 0.2002 gr)**

**Chemical Formula:** C<sub>29</sub>H<sub>22</sub>N<sub>3</sub>Br<sub>3</sub>

**Molecular Weight:** 652.23 g/mol

**Appearance:** Light brown powder

**Melting point:** 108-115 °C

**Percentage Yield:** 190 mg (14.60%)

**R<sub>f</sub> Value:** 0.22 (Ethylacetate:n-Hexane, 1:1)

**RP-HPLC (R<sub>t</sub>):** 28.268 min (97.663%)

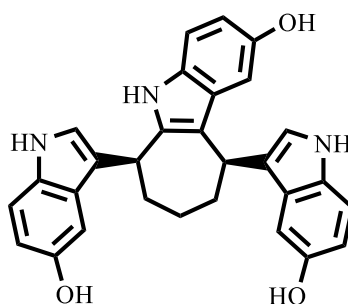
**ESI-MS (m/z):** 654.02 [M<sup>+</sup>] 24%, 652.54 [M<sup>+</sup>] 85%, 457.75 [M<sup>+</sup>-.Indole]<sup>+</sup> 4%

**FT-IR (ATR; 680-4000 1/cm):** 750 (CH<sub>2</sub> Rocking, w), 812 (C-H aromatic asymmetrical bending, w), 812 (NH asymmetrical (wagging) bending, w), 1125 (CH<sub>2</sub> aliphatic asymmetrical bending), ca. 1200 (C-H aromatic symmetrical bending, w), 1344 (CH<sub>2</sub> aliphatic alicyclic symmetrical bending, w), 1410 (C-N stretching, s), 1500- 1455 (C=C aromatic stretching, s), 1688-1625 (NH symmetrical (scissoring) bending, m to w), 2936-2859 (C-H cycloheptane stretching, s), ca. 3000 (C-H aromatic stretching, s), 3375 (NH stretching, s).

**<sup>1</sup>H-NMR (400 MHz, Acetone-d<sub>6</sub>) δ (ppm)** 2.40- 2.27 (m, 2H) [2.33 (dddddt, 2H, J= 16.00, 7.60, 7.50, 7.40, 7.00, 6.70 Hz)], 2.62- 2.53 (m, 4H) [2.57 (dddd, 4H, J= 12.60, 12.40, 7.60, 7.50, 7.40 Hz)], 4.03 (t, 1H, J= 6.67 Hz), 4.44 (dd, 1H, J= 9.2, 7.48 Hz), 7.10 (dd, 1H, J=

0.80, 0.58 Hz), 7.12 (dd, 1H, J= 0.80, 0.58 Hz), 7.29 (dddd, 4H, J= 8.70, 2.49, 0.80, 0.58 Hz), 7.33 (dd, 1H, J= 8.62, 0.60 Hz), 7.35 (dd, 1H, J= 8.64, 1.84 Hz), 7.64 (ddd, 1H, J= 1.75, 0.85, 0.80 Hz), 7.66 (ddd, 1H, J= 1.73, 0.85, 0.80 Hz), 7.68 (dd, 1H, J= 1.84, 0.44 Hz), 10.15 (s, br, 2NH), 10.45 (s, br, 1NH)

**3,3'-(((6S,10R)-2-hydroxy-5,6,7,8,9,10-hexahydrocyclohepta[b]indole-6,10-diyl)bis(1H-indol-5-ol)**



(6)

**5-hydroxyindole (5 mmol, 0.6657 gr) + glutaric dialdehyde (2 mmol, 0.2002 gr)**

**Chemical Formula:** C<sub>29</sub>H<sub>25</sub>N<sub>3</sub>O<sub>3</sub>

**Molecular Weight:** 463.54 g/mol

**Appearance:** Green solid

**Melting point:** 122-128 °C

**Percentage Yield:** 98 mg (10.54%)

**R<sub>f</sub> Value:** 0.34 (Isopropanol:n-Hexane, 0.6:1.4)

**RP-HPLC (R<sub>t</sub>):** 11.265 min (95.271%)

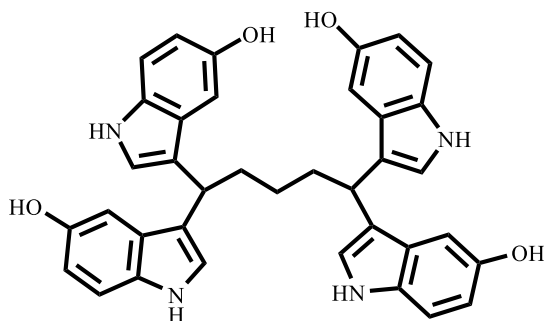
**ESI-MS (m/z):** 502.55 [M+K<sup>+</sup>]<sup>+</sup> 85%, 486.57 [M+Na]<sup>+</sup> 96%, 464.58 [M+H]<sup>+</sup> 36%, 463.21 [M<sup>+</sup>] 35%, 462.57 [M<sup>+</sup>-.H]<sup>+</sup> 99%

**FT-IR (ATR; 680-4000 1/cm):** ca. 750 (C-H Rocking CH<sub>2</sub>, w), 769 (OH bending out-of-plane, w), 837 (NH asymmetrical (wagging) bending, w), ca. 900 (CH aromatic asymmetrical bending, w), 1163 (C-H asymmetrical (wagging) CH<sub>2</sub>, w), ca. 1200 (C-H aromatic

symmetrical bending, m), 1260 (C-O stretching, m), 1330 (C-H in-plane bending (scissoring) CH<sub>2</sub>, m), 1400 (C-N aromatic stretching, s), 1413 (OH bending in-plane, m), 1584 (C=C aromatic stretching, m), 1624 (NH symmetrical bending, m), 3000-2850 (CH stretching symmetrical and asymmetrical CH<sub>2</sub> and CH cycloheptane, s), 3100-3000 (C-H aromatic stretching overlapped by OH stretching), ca. 3400 (NH stretching overlapped by OH stretching), 3700-3000 (OH stretching, br)

**<sup>1</sup>H-NMR (400 MHz, Acetone-d<sub>6</sub>) δ (ppm):** 1.93-1.80 (m, 2H) [1.86 (dtt, 2H, J= 13.00, 7.60 Hz)], 2.66-2.53 (m, 4H) [2.59 (ddtt, 4H, J= 12.50, 7.60, 7.14, 7.00 Hz) ], 4.03 (t, 1H, J= 7.00 Hz), 4.05 (t, 1H, J= 7.14 Hz), 6.72 (dd, 1H, J= 7.82, 2.0 Hz) , 6.73 (dd, 1H, J= 8.60, 2.20 Hz), 6.81 (dd, 1H, J= 2.40, 0.80 Hz), 7.15 (dd, 1H, J= 2.40, 1.20 Hz ), 7.17 (dd, 1H, J= 2.36, 1.20 Hz) , 7.21 (dd, 1H, J= 8.60, 2.80 Hz), 7.26-7.22 (m, 3H) [7.24 (ddd, 3H, J= 8.60, 3.60, 2.40 Hz)] , 7.28 (s, 1H), 7.30 (s, 1H), 7.53 (s, 1OH), 7.58 (s, 2OH), 8.61 (s, br, 1NH), 9.57 (s, br, 1NH), 9.90 (s, br, 1NH)

**3,3',3'',3'''-(pentane-1,1,5,5-tetrayl)tetrakis(1H-indol-5-ol)**



**Chemical Formula:** C<sub>37</sub>H<sub>32</sub>N<sub>4</sub>O<sub>4</sub>

**Molecular Weight:** 596.69 g/mol

**Appearance:** Black powder

**Melting point:** 125-130 °C

**Percentage Yield:** 170 mg (10.49%)

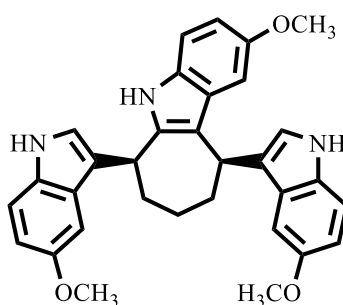
**R<sub>f</sub> Value:** 0.23 (Isopropanol:n-Hexane, 0.6:1.4)

**RP-HPLC (R<sub>t</sub>):** n.d (not determined)

**ESI-MS (m/z):** 619.55  $[M+Na^+]^+$  56%, 596.55  $[M^+]^+$  18%, 595.55  $[M^+-H]^+$  44%

**$^1H$ -NMR (400 MHz, Acetone- $d_6$ )  $\delta$  (ppm):** 1.22-1.19 (m, 2H), 2.39-2.35 (m, 4H), 4.27 (t, 2H,  $J = 7.43$  Hz), 6.62 (dd, 4H,  $J = 8.63, 2.36$  Hz), 6.96 (d, 2H,  $J = 2.40$  Hz), 6.97 (d, 4H,  $J = 8.4$  Hz), 6.99 (d, 2H,  $J = 2.40$  Hz) 7.13 (s, 2H), 7.15 (s, 2H), , 7.48 (s, br, 4OH), 9.56 (s, br, 4NH)

**(6S,10R)-2-methoxy-6,10-bis(5-methoxy-1H-indol-3-yl)-5,6,7,8,9,10  
hexahydrocyclohepta[b]indole**



**(7)**

**5-Methoxyindole (5 mmol, 0.7358 gr) + glutaric dialdehyde (2 mmol, 0.2002 gr)**

**Chemical Formula:**  $C_{32}H_{31}N_3O_3$

**Molecular Weight:** 505.62 g/mol

**Appearance:** Brown Powder

**Melting point:** 104-116  $^{\circ}C$

**Percentage Yield:** 104 mg (25.70%)

**$R_f$  Value:** 0.47 (Chloroform:Ethylacetate, 1.9: 0.1)

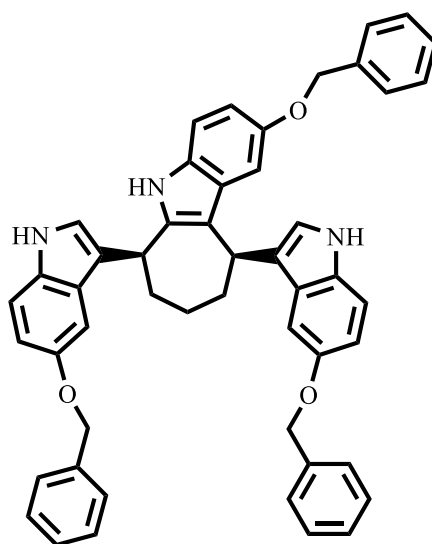
**RP-HPLC ( $R_t$ ):** 13.825 min (96.237%)

**ESI-MS (m/z):** 544.16  $[M+K^+]^+$  29%, 528.23  $[M+Na^+]^+$  100%, 506.25  $[M+H^+]^+$  7%, 505.41  $[M]^+$  21%, 504.27  $[M^+-H]^+$  59%, 490.20  $[M^+-CH_3]^+$  7%, 358.32  $[M^+-Indole]^+$  18%, 344.43  $[M^+-Indole-CH_2]^+$  11%

**FT-IR (ATR; 680-4000 1/cm):** ca. 745 (C-H aliphatic Rocking CH<sub>2</sub> cycloheptane, w), 800 (NH asymmetrical bending, w), 850-830 (C-H aromatic asymmetrical, w), 1030 (C-O-C aromatic symmetrical stretching, w), 1060-1050 (C-H out-of-plane (wagging) CH<sub>2</sub> bending, w), 1225 (C-H aromatic symmetrical bending, w), 1245 (C-O-C aromatic asymmetrical stretching, w), 1255 (C-H aliphatic symmetrical (scissoring) CH<sub>2</sub>, m), 1300 (C-N aromatic stretching, s), 1563, 1583 (C=C aromatic stretching, m), 1700-1650 (NH symmetrical bending, m) 3000-2850 (C-H aliphatic cycloheptane symmetrical and asymmetrical stretching, s), 3050-3000 (C-H aromatic stretching, s), 3450 (NH stretching, s)

**<sup>1</sup>H-NMR (400 MHz, Acetone-d<sub>6</sub>) δ (ppm):** 1.89 (t, 2H, J= 5.0 Hz), 2.75-2.64 (m, 4H), 3.64 (s, OCH<sub>3</sub>), 3.67 (s, OCH<sub>3</sub>), 3.76 (s, OCH<sub>3</sub>), 4.64 (t, 1H, J= 4.00 Hz), 4.94 (t, 1H, J= 4.30 Hz), 6.75 (ddd, 1H, J= 2.44, 0.52, 0.45 Hz), 6.77 (dd, 1H, J= 2.40, 0.52 Hz), 6.80 (ddd, 1H, J= 2.28, 0.57, 0.44 Hz), 6.86 (dd, 3H, J= 7.20, 2.58 Hz), 7.04 (dd, 1H, J= 8.62, 0.55 Hz), 7.27 (dd, 1H, J= 0.50, 0.46 Hz), 7.28 (ddd, 1H, J= 8.72, 0.54, 0.46 Hz), 7.29 (dd, 1H, J= 0.54, 0.44 Hz), 7.34 (ddd, 1H, J= 8.80, 0.57, 0.54 Hz), 8.83 (s, br, 1NH), 9.78 (s, br, 1NH), 10.04 (s, br, 1NH)

**(6S,10R)-2-(benzyloxy)-6,10-bis(5-(benzyloxy)-1H-indol-3-yl)-5,6,7,8,9,10-hexahydrocyclohepta[b]indole**



(8)

**5-Benzyloxyindole (5 mmol, 1.1163 gr) + glutaric dialdehyde (2 mmol, 0.2002 gr)**



**Chemical Formula:** C<sub>50</sub>H<sub>43</sub>N<sub>3</sub>O<sub>3</sub>

**Molecular Weight:** 733.91 g/mol

**Appearance:** Dark Brown Powder

**Melting point:** 90-95 °C

**Percentage Yield:** 225 mg (15.30%)

**R<sub>f</sub> Value:** 0.20 (Ethylacetate:Cyclohexane, 0.8:1.2)

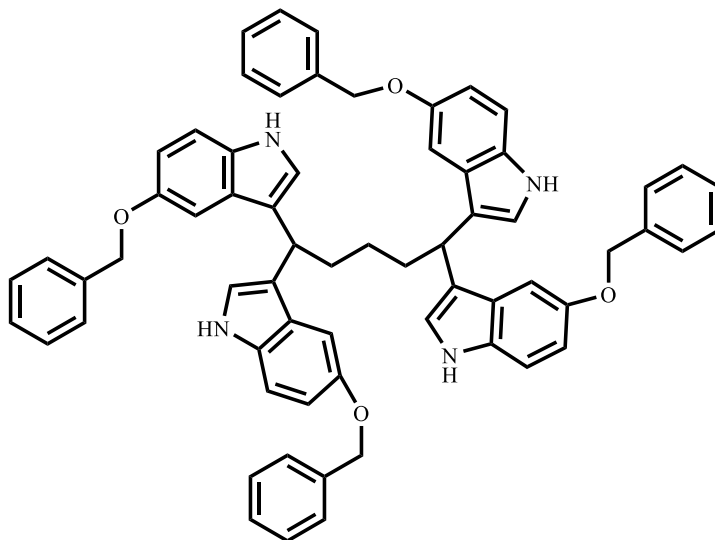
**RP-HPLC (R<sub>t</sub>):** n.d

**ESI-MS (m/z):** 772.14 [M+K<sup>+</sup>]<sup>+</sup> 3%, 756.14 [M+Na<sup>+</sup>]<sup>+</sup> 100%, 734.26 [M+H<sup>+</sup>]<sup>+</sup> 12%, 733.30 [M<sup>+</sup>] 52%, 732.27 [M<sup>+</sup>-H]<sup>+</sup> 100%, 642.34 [M<sup>+</sup>-phenyl-CH<sub>2</sub>(benzyl)]<sup>+</sup> 9%, 500.14 [M<sup>+</sup>-Indole]<sup>+</sup> 7%, 486.48 [M<sup>+</sup>-2.Indole-CH<sub>2</sub>]<sup>+</sup> 4%.

**FT-IR (ATR; 680-4000 1/cm):** 750 (C-H aliphatic Rocking CH<sub>2</sub> cycloheptane and benzyl, w), 800 (NH asymmetrical bending, w), 850 (C-H aromatic asymmetrical, w), 1050 (C-O-C aromatic symmetrical stretching, w), 1100 (C-H out-of-plane (wagging) CH<sub>2</sub> bending, w), 1200 (C-H aromatic symmetrical bending, w), 1225 (C-O-C aromatic asymmetrical stretching, w), 1300 (C-H aliphatic symmetrical (scissoring) CH<sub>2</sub>, m), 1400 (C-N aromatic stretching, s), 1650, 1600 (C=C aromatic stretching, m), 1700-1650 (NH symmetrical bending, m), 3000-2800 (C-H aliphatic cycloheptane and CH<sub>2</sub> benzyl symmetrical and asymmetrical stretching, s), 3100-3050 (C-H aromatic stretching, s), 3450 (NH stretching, s)

**<sup>1</sup>H-NMR (400 MHz, Acetone-d<sub>6</sub>) δ (ppm):** 1.91-1.88 (m, 2H) [1.88 (tt, 2H, J= 5.00, 4.34 Hz)], 2.72 - 2.63 (m, 4H), 4.61 (t, 1H, J= 7.00 Hz), 4.94 (t, 1H, J= 5.54 Hz), 4.95 (s, 6H (CH<sub>2</sub>)), 6.67 (dd, 1H, J= 8.62, 2.42 Hz), 6.84 (dd, 2H, J= 9.00, 2.28 Hz), 6.86 (dd, 2H, J= 9.00, 2.4 Hz), 6.93 (dd, 1H, J= 2.42, 1.06 Hz), 6.97 (dd, 1H, J= 2.41, 0.96 Hz), 7.07 (dd, 1H, J= 8.65, 7.65 Hz), 7.17 (dd, 1H, J= 2.42, 1.00 Hz), 7.23 (ddd, 2H, J= 7.65, 7.34, 0.96 Hz), 7.27 (dddd, 2H, J= 8.20, 7.65, 3.65, 2.27 Hz), 7.31 (dd, 3H, J= 7.65, 2.13 Hz), 7.35 (dd, 2H, J= 8.20, 3.65 Hz), 7.42-7.37 (m, 5H) [7.40 (5H, dddd, J= 7.60, 7.24, 3.1, 2.40 Hz), 7.47 (dd, 3H, J= 7.77, 1.06 Hz), 8.90 (s, br, 1NH), 9.81 (s, br, 1NH), 10.05 (s, br, 1NH)]

**1,1,5,5-tetrakis(5-(benzyloxy)-1H-indol-3-yl)pentane**



**Chemical Formula:** C<sub>65</sub>H<sub>56</sub>N<sub>4</sub>O<sub>4</sub>

**Molecular Weight:** 957.19 g/mol

**Appearance:** Light Brown Powder

**Melting point:** 90-100 °C

**Percentage Yield:** 200 mg (13.60%)

**R<sub>f</sub> Value:** 0.12 (Ethylacetate:Cyclohexane, 0.8:1.2)

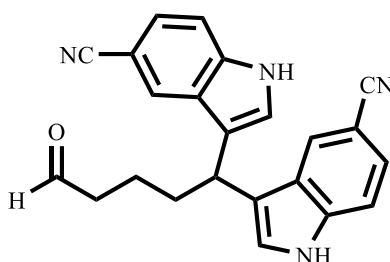
**RP-HPLC (R<sub>t</sub>):** n.d

**ESI-MS (m/z):** 996.09 [M+K<sup>+</sup>]<sup>+</sup> 11%, 980.21[M+Na<sup>+</sup>]<sup>+</sup> 67%, 957.24 [M<sup>+</sup>] 14%, 956.24 [M<sup>+</sup>-.H]<sup>+</sup> 14%, 866.52 [M<sup>+</sup>-.phenyl-.CH<sub>2</sub>(.benzyl)]<sup>+</sup> 3%, 485.48[M<sup>+</sup>-.CH<sub>2</sub>CH(Indole)<sub>2</sub>]<sup>+</sup> 8%.

**FT-IR (ATR; 680-4000 1/cm):** 745 (C-H aliphatic Rocking CH<sub>2</sub> cycloheptane and benzyl, w), 750 (NH asymmetrical bending, w), 800 (C-H aromatic asymmetrical, w), 1050 (C-O-C aromatic symmetrical stretching, w), 1100 (C-H out-of-plane (wagging) CH<sub>2</sub> bending, w), 1150 (C-H aromatic symmetrical bending, w), 1200 (C-O-C aromatic asymmetrical stretching, w), 1300 (C-H aliphatic symmetrical (scissoring) CH<sub>2</sub>, m), 1400 (C-N aromatic stretching, s), 1650, 1600 (C=C aromatic stretching, m), 1700-1650 (NH symmetrical bending, m), 2950-2850 (C-H aliphatic cycloheptane and CH<sub>2</sub> benzyl symmetrical and asymmetrical stretching, s), 3050-3025 (C-H aromatic stretching, s), 3450 (NH stretching, s)

**<sup>1</sup>H-NMR (400 MHz, Acetone-d<sub>6</sub>) δ (ppm):** 1.56 (quintet, 2H, J= 8.00 Hz), 2.33 (quartet, 4H, J= 7.52 Hz), 4.39 (t, 2H, J= 7.53 Hz), 4.95 (s, 8H, 4(CH<sub>2</sub>)), 6.75 (dd, 4H, J= 8.80, 2.42 Hz), 7.17 (d, 4H, J= 2.4 Hz), 7.22 (t, 4H, J= 0.49 Hz), 7.23 (dd, 4H, J= 7.46, 1.02 Hz), 7.28-7.25 (m, 4H) [7.27 (tt, 4H, J= 7.78, 1.48 Hz)], 7.32-7.29 (m, 8H) [7.31 (dd, 8H, J= 7.36, 7.40 Hz), 7.38-7.35 (m, 8H) [7.37 (dd, 4H, J= 7.49, 2.06 Hz), 7.37 (dd, 4H, J= 7.06, 2.03 Hz)], 9.70 (s, br, 4NH)

**3,3'-(5-oxopentane-1,1-diyl)bis(1H-indole-5-carbonitrile)**



**Indole-5-carbonitrile (5 mmol, 0.7108 gr) + glutaric dialdehyde (2 mmol, 0.2002 gr)**

**Chemical Formula:** C<sub>23</sub>H<sub>18</sub>N<sub>4</sub>O

**Molecular Weight:** 366.42 g/mol

**Appearance:** Light Brown Powder

**Melting point:** n.d

**Percentage Yield:** n.d

**R<sub>f</sub> Value:** n.d

**RP-HPLC (R<sub>t</sub>):** n.d

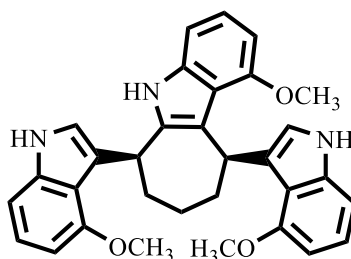
**ESI-MS (m/z):** 389.71 [M+Na<sup>+</sup>]<sup>+</sup> 42%, 367.53 [M+H<sup>+</sup>]<sup>+</sup> 4%, 366.53 [M<sup>+</sup>] 26%, 365.53 [M<sup>+</sup>-.H] 100%, 323.20 [M<sup>+</sup>-.CH<sub>2</sub>COH] 5%, 141.32 [M<sup>+</sup>]<sub>Indole</sub> 14%

**FT-IR (ATR; 680-4000 1/cm):** n.d

**<sup>1</sup>H-NMR (400 MHz, Acetone-d<sub>6</sub>) δ (ppm):** 1.73 (quintet, 2H, J= 7.52 Hz), 2.36 (quartet, 2H, J= 7.71 Hz), 2.55 (td, 2H, J= 7.28, 1.59 Hz), 4.67 (t, 1H, J= 7.68 Hz), 7.32 (dd, 2H, J=

8.43, 1.57 Hz), 7.53 (dd, 2H, J= 8.51, 0.71 Hz), 7.63 (dd, 2H, J= 2.45, 0.84 Hz), 7.99 (dt, 2H, J= 1.56, 0.80 Hz), 9.72 (t, 1H, J= 1.60 Hz), 10.62 (s, br, 2NH)

**(6S,10R)-1-methoxy-6,10-bis(4-methoxy-1H-indol-3-yl)-5,6,7,8,9,10-hexahydrocyclohepta[b]indole**



**(9)**

**4-Methoxyindole (5 mmol, 0.7358 gr) + glutaric dialdehyde (2 mmol, 0.2002 gr)**

**Chemical Formula:** C<sub>32</sub>H<sub>31</sub>N<sub>3</sub>O<sub>3</sub>

**Molecular Weight:** 505.62 g/mol

**Appearance:** Black solid

**Melting point:** 132-143 °C

**Percentage Yield:** 168 mg (16.60%)

**R<sub>f</sub> Value:** 0.32 (Acetone:Cyclohexane, 0.6:1.4)

**RP-HPLC (R<sub>t</sub>):** 14.471 min (96.025%)

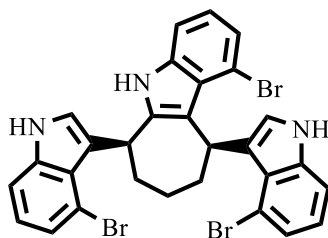
**ESI-MS (m/z):** 528.60 [M<sup>+</sup>+ Na<sup>+</sup>] 56%, 506.49[M<sup>+</sup>+ H<sup>+</sup>] 40%, 505. 72 [M<sup>+</sup>] 35%, 504. 67 [M<sup>+</sup>- .H]<sup>+</sup> 100%

**FT-IR (ATR; 680-4000 1/cm):** 750 (CH bending out of plane, w), 1150 (C-O stretching, m), 1700 (C=C aromatic stretching, m), 2850 (CH methyl stretching, m), 3000 (CH aromatic stretching, m), 3300 (NH stretching, s)

**<sup>1</sup>H-NMR (500 MHZ, Acetone-d<sub>6</sub>) δ (ppm):** 1.93-1.87 (m, 2H), 2.12-2.05 (m, 4H), 4.32 (s, 9H, 3OCH<sub>3</sub>), 5.64 (t, 1H, J= 4.2 Hz), 6.08 (t, 1H, J= 6.18 Hz), 6.37 (dd, 3H, J= 7.64, 1.5 Hz),

6.93 (dd, 3H, J= 8.03, 7.64 Hz), 7.03 (ddd, 3H, J= 8.03, 1.50, 0.45 Hz), 7.14 (dd, 2H, J= 1.5, 0.45 Hz), 8.88 (s, br, 2NH), 9.86 (s, br, 1NH)

**(6S,10R)-1-bromo-6,10-bis(4-bromo-1H-indol-3-yl)-5,6,7,8,9,10-hexahydrocyclohepta[b]indole**



**(10)**

**4-Bromoindole (5 mmol, 0.9802 gr) + glutaric dialdehyde (2 mmol, 0.2002 gr)**

**Chemical Formula:** C<sub>29</sub>H<sub>22</sub>Br<sub>3</sub>N<sub>3</sub>

**Molecular Weight:** 652.23 g/mol

**Appearance:** Light Brown solid

**Melting point:** 95-100 °C

**Percentage Yield:** 160 mg (12.2%)

**R<sub>f</sub> Value:** 0.23 (Chloroform:Cyclohexane, 1.4:0.6)

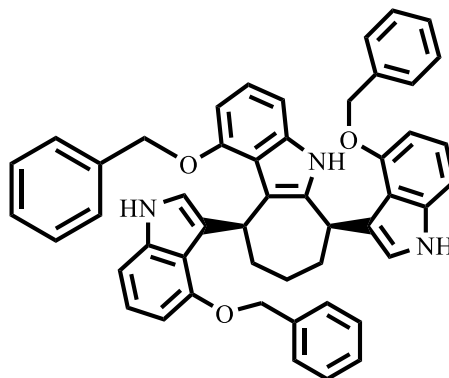
**RP-HPLC (R<sub>t</sub>):** 16.151 min (94.632%)

**ESI-MS (m/z):** 652.08 [M<sup>+</sup>] 99%, 654.06 [M<sup>+</sup>] 32%

**FT-IR (ATR; 680-4000 1/cm):** ca. 700-600 (C-Br bending, m), 1688-1625 (NH symmetrical (scissoring) bending, s), 3300 (NH stretching, s)

**<sup>1</sup>H-NMR (500 MHZ, Acetone-d<sub>6</sub>) δ (ppm):** 1.40-1.27 (m, 2H), 1.63-1.55 (m, 4H), 3.98 (td, 2H, J= 5.7, 0.9 Hz), 6.88- 6.81 (dd, 2H, J= 1.65, 0.60 Hz), 7.17 (dd, 3H, J= 8.1, 7.58 Hz), 7.43 (dd, 5H, J= 8.10, 2.64 Hz), 7.54 (dd, 1H, J= 7.63, 2.78 Hz), 9.69 (s, br, 2NH), 10.23 (s, br, 1NH)

**(6S,10R)-1-(benzyloxy)-6,10-bis(4-(benzyloxy)-1H-indol-3-yl)-5,6,7,8,9,10-hexahydrocyclohepta[b]indole**



**(11)**

**4-Benzoyloxyindole (5 mmol, 1.1163 gr) + glutaric dialdehyde (2 mmol, 0.2002 gr)**

**Chemical Formula:** C<sub>50</sub>H<sub>43</sub>N<sub>3</sub>O<sub>3</sub>

**Molecular weight:** 733.91 g/mol

**Appearance:** Grey Powder

**Melting point:** 120-127 °C

**Percentage Yield:** 230 mg (15.64%)

**R<sub>f</sub> Value:** 0.17 (Diethylether:Cyclohexane, 0.9:1.1)

**RP-HPLC (R<sub>t</sub>):** 16.199 min (96.969%)

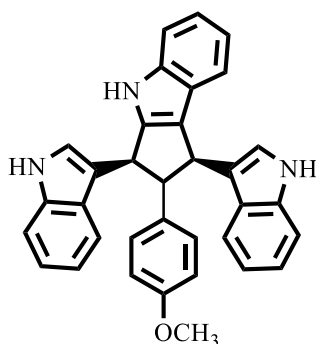
**ESI-MS (m/z):** 756.38 [M<sup>+</sup> + Na<sup>+</sup>] 100%, 722.36 [M<sup>+</sup> + K<sup>+</sup>] 35%, 732.48 [M<sup>+</sup> - .H]<sup>+</sup> 15%, 483.29 [M<sup>+</sup> - 2 .benzyl + Na<sup>+</sup>] 24%, 574.41[M<sup>+</sup> - .benzyl + Na<sup>+</sup>] 26%

**FT-IR (ATR; 680-4000 1/cm):** 1050 (C-O-C aromatic symmetrical stretching, w), 1225 (C-O-C aromatic asymmetrical stretching, w), 1300 (C-H aliphatic symmetrical (scissoring) CH<sub>2</sub>, m), 1400 (C-N aromatic stretching, s), 1700-1650 (NH symmetrical bending, m), 3450 (NH stretching, s)

**<sup>1</sup>H-NMR (500 MHZ, Acetone-d<sub>6</sub>) δ (ppm):** 2.18-2.12 (m, 2H), 2.81-2.75 (m, 4H), 5.13-4.96 (m, 2H), 5.19 (s, 2H, 1CH<sub>2</sub>), 5.25 (s, 4H, 2CH<sub>2</sub>), 6.56 (dd, 1H, J= 7.64, 1.99 Hz), 6.60 (dd, 2H, J= 7.64, 1.48 Hz), 6.78 (dd, 2H, J= 8.03, 7.64 Hz), 6.92 (dd, 1H, J= 7.78, 1.48 Hz), 6.96 (dd, 3H, J= 7.95, 1.65 Hz), 7.01 (d, 1H, J=0.45 Hz), 7.02 (d, 1H, J= 0.45 Hz), 7.06 (tt,

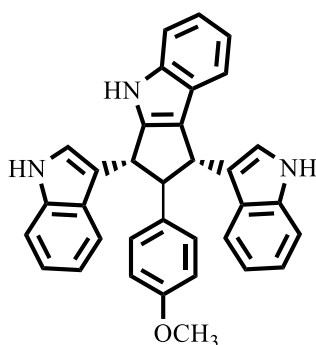
3H, J= 7.69, 1.25 Hz), 7.18 (dddd, 6H, J= 7.92, 7.69, 1.65, 0.5 Hz), 7.40 (dddd, 6H, J= 7.92, 1.25, 0.95, 0.5 Hz), 8.83 (s, br, 1NH), 9.70 (s, br, 1NH), 10.19 (s, br, 1NH)

**(1R,3S)-1,3-di(1H-indol-3-yl)-2-(4-methoxyphenyl)-1,2,3,4-tetrahydrocyclopenta[b]indole**



**First Stereoisomer (1) [40%] (3)**

**(1S,3R)-1,3-di(1H-indol-3-yl)-2-(4-methoxyphenyl)-1,2,3,4-tetrahydrocyclopenta[b]indole**



**Second Stereoisomer (2) [60%] (3)**

**Indole (5 mmol, 0.5857 gr) + 2-(4-Methoxyphenyl)malondiladehyde (2 mmol, 0.3564 gr)**

**Chemical Formula:** C<sub>34</sub>H<sub>27</sub>N<sub>3</sub>O

**Molecular weight:** 493.61 g/mol

**Appearance:** Brown powder

**Melting point:** 150-160 °C

**Percentage Yield:** 240 mg (15.45%)

**R<sub>f</sub> Value:** 0.17 (Dichloromethane:Cyclohexane, 1.5:0.5)

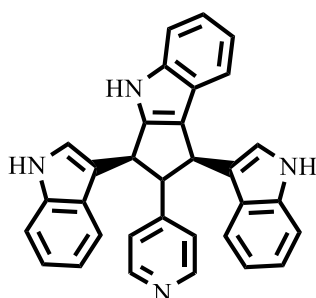
**RP-HPLC ( $R_t$ ):** 13.356 min (40%), 14.310 min (60%)

**ESI-MS ( $m/z$ ):** 492.71 [ $M^+ - .H$ ] $^+$  100%, 493.76 [ $M^+$ ] 47%

**FT-IR (ATR; 680-4000  $1/cm$ ):** 1075 (C-O-C aromatic symmetrical stretching, w), 1275 (C-O-C aromatic asymmetrical stretching, m), 1455 (C-H bending alicyclic, m to s), 1700 (C=C stretching alicyclic, s), 2900 (C-H stretching alicyclic, s), 3400 (NH stretching, s)

**$^1H$ -NMR (500 MHz, Acetone- $d_6$ )  $\delta$  (ppm) [1] [2]** 3.76 (s, 3H, OCH<sub>3</sub>), 4.12 (t, 1H,  $J$ = 8.00 Hz), 4.92 (dd, 1H,  $J$ = 7.55, 1.13 Hz), 4.94 (d, 1H,  $J$ = 7.55 Hz), 6.79 (td, 1H,  $J$ = 8.11, 1.43 Hz), 6.81 (td, 2H,  $J$ = 8.13, 1.25 Hz), 6.82 (dd, 2H,  $J$ = 8.05, 1.59 Hz), 6.84 (td, 1H,  $J$ = 8.65, 1.34 Hz), 6.87 (td, 2H,  $J$ = 7.85, 1.43 Hz), 6.98 (dd, 2H,  $J$ = 8.05, 1.48 Hz), 7.01 (ddd, 1H,  $J$ = 7.75, 1.27, 0.80 Hz), 7.05 (ddt, 2H,  $J$ = 8.00, 1.13, 0.63 Hz), 7.10 (d, 1H,  $J$ = 1.00 Hz), 7.12 (s, 1H), 7.25 (ddd, 1H,  $J$ = 7.95, 1.43, 0.55 Hz), 7.40 (ddd, 2H,  $J$ = 8.15, 1.23, 0.77 Hz), 9.97 (s, br, 2NH), 10.03 (s, br, 1NH)

**(1R,3S)-1,3-di(1H-indol-3-yl)-2-(pyridin-4-yl)-1,2,3,4-tetrahydrocyclopenta[b]indole**



**First Stereoisomer (66%) (4)**

**Indole (5 mmol, 0.5857 gr) + 2-(4-pyridyl)malondiladehyde (2 mmol, 0.2983 gr)**

**Chemical Formula:** C<sub>32</sub>H<sub>24</sub>N<sub>4</sub>

**Molecular weight:** 464.57 g/mol

**Appearance:** Red powder

**Melting point:** 94-101 °C

**Percentage Yield:** 200 mg (13.45%)

**$R_f$  Value:** 0.25 (Methanol:Chloroform, 0.1:1.9)



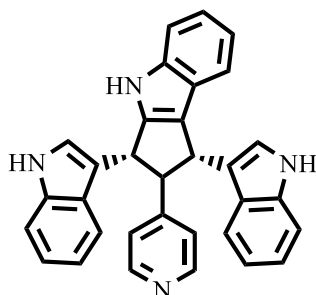
**RP-HPLC ( $R_t$ ):** 12.320 min (66%), 12.570 min (34%)

**ESI-MS ( $m/z$ ):** 465.59 [ $M^+ + H^+$ ] 79%, 463.56 [ $M^+ - .H$ ] $^+$  15%, 348.78 [ $M^+ - .Indole$ ] $^+$  14%

**FT-IR (ATR; 680-4000  $1/cm$ ):** 1470 (C-H bending alicyclic, m), 1600-1430 (C=C and C=N aromatic stretching, pyridine ring, m), 1700 (C=C stretching cyclopentene, s), 2860 (C-H stretching alicyclic, s), 3410 (NH stretching, s)

**$^1H$ -NMR (400MHz, Acetone- $d_6$ )  $\delta$  (ppm) [1]** 3.60 (d, 2H,  $J = 7.60$  Hz), 4.90 (t, 1H,  $J = 7.50$  Hz), 6.91 (ddd, 1H,  $J = 8.07, 7.79, 1.32$  Hz), 6.98 (d, 1H,  $J = 1.30$  Hz), 6.98 (ddd, 2H,  $J = 8.10, 7.60, 1.36$  Hz), 7.03 (dd, 1H,  $J = 8.30, 1.35$ ), 7.03 (s, 1H), 7.10 (dd, 2H,  $J = 8.04, 1.23$  Hz), 7.28 (dd, 2H,  $J = 5.19, 1.03$  Hz), 7.30 (dd, 1H,  $J = 8.00, 1.34$  Hz), 7.42 (dd, 2H,  $J = 8.17, 1.00$  Hz), 7.71 (d, 2H,  $J = 7.96$  Hz), 7.78 (d, 1H,  $J = 8.00$  Hz), 8.42 (ddd, 2H,  $J = 6.00, 1.64, 0.75$  Hz), 10.04 (s, br, 1NH), 10.06 (s, br, 2NH)

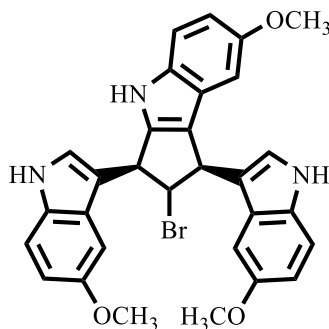
**(1S,3R)-1,3-di(1H-indol-3-yl)-2-(pyridin-4-yl)-1,2,3,4-tetrahydrocyclopenta[b]indole**



**Second stereoisomer (34%) (4)**

**$^1H$ -NMR (400MHz, Acetone- $d_6$ )  $\delta$  (ppm) [2]** 3.60 (d, 2H,  $J = 7.60$  Hz), 4.90 (t, 1H,  $J = 7.53$  Hz), 6.87 (ddd, 2H,  $J = 8.07, 7.79, 1.32$  Hz), 7.03 (d, 1H,  $J = 1.33$  Hz), 7.10 (dd, 2H,  $J = 8.04, 1.23$  Hz), 7.16 (dd, 2H,  $J = 8.08, 1.66$  Hz), 7.16 (s, 1H), 7.23 (dd, 2H,  $J = 5.13, 1.03$  Hz), 7.24 (d, 1H,  $J = 7.95$  Hz), 7.33 (dd, 2H,  $J = 8.22, 1.00$  Hz), 7.54 (d, 1H,  $J = 8.00$  Hz), 7.59 (d, 2H,  $J = 7.97$  Hz), 8.31 (ddd, 2H,  $J = 6.00, 1.64, 0.75$  Hz), 9.92 (s, br, 1NH), 9.95 (s, br, 2NH)

**(1R,3S)-2-bromo-7-methoxy-1,3-bis(5-methoxy-1H-indol-3-yl)-1,2,3,4-tetrahydrocyclopenta[b]indole**



**(12)**

**5-Methoxyindole (5 mmol, 0.7358 gr) + 2-Bromomalondiladehyde (2 mmol, 0.3019 gr)**

**Chemical Formula:** C<sub>30</sub>H<sub>26</sub>N<sub>3</sub>O<sub>3</sub>Br

**Molecular weight:** 556.46 g/mol

**Appearance:** Red Powder

**Melting point:** 110-116 °C

**Percentage Yield:** 183 mg (16.20%)

**R<sub>f</sub> Value:** 0.24 (Ethylacetate:Cyclohexane, 0.7:1.3)

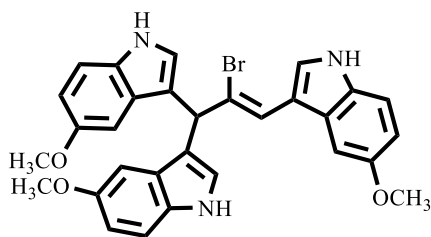
**RP-HPLC (R<sub>t</sub>):** 14.464 min (96.931%)

**ESI-MS (m/z):** 477.73 [M<sup>+</sup>-.Br]<sup>+</sup> 39%, 476.74 [M<sup>+</sup>-.Br-.H]<sup>+</sup> 100%, 579.51 [M<sup>+</sup>+ Na<sup>+</sup>] 58%,

**FT-IR (ATR; 680-4000 1/cm):** n.d

**<sup>1</sup>H-NMR (500 MHz, Acetone-d<sub>6</sub>) δ (ppm):** 3.60 (s, 3H, 1OCH<sub>3</sub>), 3.61 (s, 3H, 1OCH<sub>3</sub>), 3.70 (s, 3H, 1OCH<sub>3</sub>), 4.78 (t, 1H, J= 6.96 Hz), 5.08 (ddd, 1H, J= 7.04, 1.83, 0.68 Hz), 5.09 (dd, 1H, J= 7.04, 1.48 Hz), 6.64 (d, 1H, J= 2.44 Hz), 6.73 (dd, 1H, J= 8.64, 2.44 Hz), 6.75 (dd, 1H, J= 8.56, 2.17 Hz), 6.77 (dd, 1H, J= 8.72, 2.25 Hz), 6.87 (d, 1H, J= 2.53 Hz), 7.26 (d, 1H, J= 2.52 Hz), 7.27 (d, 1H, J= 2.50 Hz), 7.30 (dt, 2H, J= 8.79, 0.63 Hz), 7.31 (d, 1H, J= 1.37 Hz), 7.31 (dd, 1H, J= 8.73, 0.59 Hz), 10.01 (s, br, 2NH), 10.09 (s, br, 1NH)

**(Z)-3,3',3''-(2-bromoprop-2-ene-1,1,3-triyl)tris(5-methoxy-1H-indole)**



**58% (13), 42% (12)**

**Chemical Formula:** C<sub>30</sub>H<sub>26</sub>N<sub>3</sub>O<sub>3</sub>Br

**Molecular weight:** 556.46 g/mol

**Appearance:** Dark Red Solid

**Melting point:** 112-120 °C

**Percentage Yield:** 210 mg (18.20%)

**R<sub>f</sub> Value:** 0.17 (Ethylacetate:Cyclohexane, 0.7:1.3)

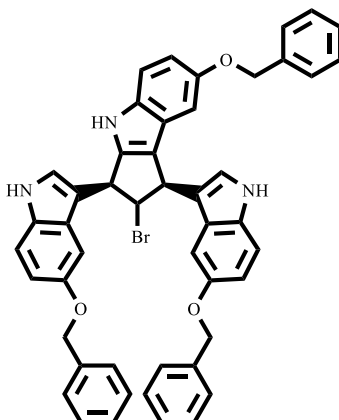
**RP-HPLC (R<sub>t</sub>):** 13.752 min (58%)

**ESI-MS (m/z):** 556.36 [M<sup>+</sup>] 10%

**FT-IR (ATR; 680-4000 1/cm):** n.d

**<sup>1</sup>H-NMR (500 MHz, Acetone-d<sub>6</sub>) δ (ppm):** 3.62 (s, 6H, 2OCH<sub>3</sub>), 3.67 (s, 3H, 1OCH<sub>3</sub>), 6.05 (t, 1H, J= 1.1 Hz), 6.96 (d, 1H, J= 1.20 Hz), 6.96 (dd, 3H, J= 8.52, 2.60 Hz), 7.16 (d, 1H, J= 2.48 Hz), 7.20 (d, 2H, J= 2.05 Hz), 7.26 (dd, 2H, J= 8.78, 0.59 Hz), 7.33 (dd, 1H, J= 8.81, 0.59 Hz), 7.69 (d, 1H, J= 2.48 Hz), 8.11 (d, 2H, J= 2.41 Hz), 9.76 (s, br, 2NH), 9.98 (s, br, 1NH)

**(1R,3S)-7-(benzyloxy)-1,3-bis(5-(benzyloxy)-1H-indol-3-yl)-2-bromo-1,2,3,4-tetrahydrocyclopenta[b]indole**



**First Stereoisomer [1] (60%) (16)**

**5-Benzyloxyindole (5 mmol, 1.1164 gr) + 2-Bromomalonaldialdehyde (2mmol, 0.3019 gr)**

**Chemical Formula:** C<sub>48</sub>H<sub>38</sub>Br N<sub>3</sub>O<sub>3</sub>

**Molecular Weight:** 784.75 g/mol

**Appearance:** Dark Red Powder

**Melting point:** 97-110 °C

**Percentage Yield:** 180 mg (16.60%)

**R<sub>f</sub> Value:** 0.25 (Ethylacetate:Cyclohexane, 0.7:1.3)

**RP-HPLC (R<sub>t</sub>):** 15.782 min (59.476%), 16.394 min (40.524%)

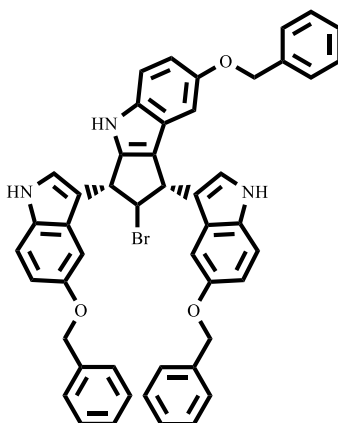
**ESI-MS (m/z):** 784.50 [M<sup>+</sup>] 28%

**FT-IR (ATR; 680-4000 1/cm):** ca. 700-600 (C-Br stretching alicyclic, w), 1080 (C-O-C aromatic symmetrical stretching, m), 1235 (C-O-C aromatic asymmetrical stretching, m to s), 1460 (C-H bending alicyclic, m to s), 1650 (C=C stretching alicyclic, s), 2900 (C-H stretching alicyclic, s), 3465 (NH stretching, s)

**<sup>1</sup>H-NMR (500 MHz, Acetone-d<sub>6</sub>) δ (ppm):** 4.73 (t, 1H, J= 7.80 Hz), 4.91 (s, 2H, 1OCH<sub>2</sub>), 4.93 (s, 4H, 2OCH<sub>2</sub>), 4.96 (d, 2H, J= 7.68 Hz), 6.86 (dd, 1H, J= 7.80, 1.40 Hz), 6.97 (dd, 2H, J= 8.00, 0.65 Hz), 7.20 (dd, 2H, J= 7.80, 1.55 Hz), 7.23 (dd, 1H, J= 1.25, 0.65 Hz), 7.25 (dd,

1H, J= 8.00, 0.60 Hz), 7.26 (dd, 2H, J= 1.37, 0.55 Hz), 7.28 (d, 1H, J= 1.00 Hz), 7.30 (s, 1H), 7.31 (tt, 3H, J= 8.10, 1.33 Hz), 7.33 (tdd, 2H, J= 7.69, 1.25, 0.60 Hz), 7.35 (tdd, 4H, J= 8.12, 1.23, 0.70 Hz), 7.38 (ddd, 2H, J= 7.77, 1.25, 0.55 Hz), 7.39 (ddd, 4H, J= 8.00, 1.35, 0.65 Hz), 10.01 (s, br, 2NH), 10.37 (s, br, 1NH)

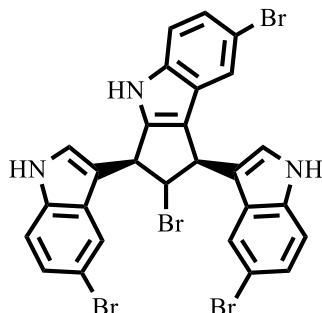
**(1S,3R)-7-(benzyloxy)-1,3-bis(5-(benzyloxy)-1H-indol-3-yl)-2-bromo-1,2,3,4-tetrahydrocyclopenta[b]indole**



**Second Stereoisomer [2] (40%) (16)**

**<sup>1</sup>H-NMR (500 MHz, Acetone-d<sub>6</sub>) δ (ppm):** 4.83 (t, 1H, J= 7.90 Hz), 4.91 (s, 2H, 1OCH<sub>2</sub>), 4.93 (s, 4H, 2OCH<sub>2</sub>), 5.01 (d, 2H, J= 7.83 Hz), 6.80 (dd, 1H, J= 7.70, 1.50 Hz), 6.85 (dd, 2H, J= 7.75, 1.45 Hz), 7.19 (dd, 2H, J= 8.00, 1.35 Hz), 7.21 (dd, 1H, J= 1.35, 0.70 Hz), 7.22 (dd, 1H, J= 8.07, 0.70 Hz), 7.24 (dd, 2H, J= 1.40, 0.66 Hz), 7.27 (d, 1H, J= 0.95 Hz), 7.28 (d, 1H, J= 1.00 Hz), 7.33 (tt, 3H, J= 8.08, 1.20 Hz), 7.36 (tdd, 2H, J= 7.79, 1.10, 0.60 Hz), 7.37 (tdd, 4H, J= 8.06, 1.12, 0.85 Hz), 7.40 (ddd, 2H, J= 7.87, 1.34, 0.60 Hz), 7.54 (ddd, 4H, J= 8.00, 1.25, 0.70 Hz), 9.76 (s, br, 2NH), 10.03 (s, br, 1NH)

**(1R,3S)-2,7-dibromo-1,3-bis(5-bromo-1H-indol-3-yl)-1,2,3,4-tetrahydrocyclopenta[b]indole**



**(17)**

**5-Bromoindole (5 mmol, 0.9802 gr) + 2-Bromomalondialdehyde (2 mmol, 0.3019 gr)**

**Chemical Formula:** C<sub>27</sub>H<sub>17</sub>N<sub>3</sub>Br<sub>4</sub>

**Molecular weight:** 703.07 g/mol

**Appearance:** Black Powder

**Melting point:** 110-120 °C

**Percentage Yield:** 145 mg (12.57%)

**R<sub>f</sub> Value:** 0.24 (Ethylacetate:Cyclohexane, 0.7:1.4)

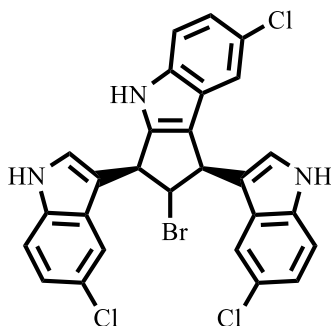
**RP-HPLC (R<sub>t</sub>):** 15.835 min (96.17%)

**ESI-MS (m/z):** 701.99 [M<sup>+</sup>-.H]<sup>+</sup> 59%, 622.18 [M<sup>+</sup>-.Br]<sup>+</sup> 38%, 507.47 [M<sup>+</sup>-.Br Indole-.H]<sup>+</sup> 26%, 158.16 [M<sup>+</sup>- 2 .Br Indole-.Br]<sup>+</sup> 7%

**FT-IR (ATR; 680-4000 1/cm):** ca. 700-600 (C-Br stretching alicyclic and aromatic, w), 1460 (C-H bending alicyclic, m to s), 1740 (C=C stretching alicyclic, s), 2900 (C-H stretching alicyclic, m), 3465 (NH stretching, s)

**<sup>1</sup>H-NMR (500 MHz, Acetone-d<sub>6</sub>) δ (ppm):** 4.73 (dd, 1H, J= 7.34, 7.22 Hz), 5.09 (ddd, 1H, J= 7.16, 1.57, 0.64 Hz), 5.16 (dd, 1H, J= 7.37, 1.55 Hz), 7.20 (dd, 1H, J= 8.58, 2.00 Hz), 7.25-7.22 (m, 4H) [7.23 (dd, 2H, J= 8.73, 1.90 Hz), 7.23 (d, 1H, J= 1.75 Hz), 7.22 (d, 1H, J= 2.08 Hz)], 7.39 (dd, 1H, J= 8.64, 0.60 Hz), 7.42 (dd, 1H, J= 8.73, 0.64 Hz), 7.43 (dd, 1H, J= 8.52, 0.58 Hz), 7.48 (d, 1H, J= 2.26 Hz), 7.61 (dd, 1H, J= 1.80, 0.70 Hz), 7.86 (dd, 1H, J= 1.92, 0.68 Hz), 10.50 (s, br, 2NH), 10.53 (s, br, 1NH)

**(1R,3S)-2-bromo-7-chloro-1,3-bis(5-chloro-1H-indol-3-yl)-1,2,3,4-tetrahydrocyclopenta[b]indole**



**(18)**

**5-Chloroindole (5 mmol, 0.7579 gr) + 2-Bromomalondialdehyde (2 mmol, 0.3019 gr)**

**Chemical Formula:** C<sub>27</sub>H<sub>17</sub>N<sub>3</sub>BrCl<sub>3</sub>

**Molecular weight:** 569.71 g/mol

**Appearance:** Black Powder

**Melting point:** 200-210 °C

**Percentage Yield:** 130 mg (11.27%)

**R<sub>f</sub> Value:** 0.25 (Diethylether:Cyclohexane, 1.3:0.7)

**RP-HPLC (R<sub>t</sub>):** 15.586 min (96.748%)

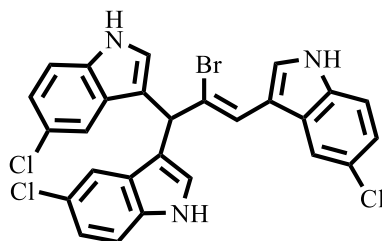
**ESI-MS (m/z):** 592.18 [M<sup>+</sup>+Na<sup>+</sup>] 66 %, 569.34 [M<sup>+</sup>] 46 %, 568.58 [M<sup>+</sup>-.H]<sup>+</sup> 100 %, 490.34 [M<sup>+</sup>-.Br]<sup>+</sup> 56 %, 419.47 [M<sup>+</sup>-.Indole]<sup>+</sup> 43%

**FT-IR (ATR; 680-4000 1/cm):** ca. 700-600 (C-Br stretching alicyclic, w), ca. 800-700 (C-Cl stretching aromatic, m), 1460 (C-H bending alicyclic, m to s), 1745 (C=C stretching alicyclic, m), 3400 (NH stretching, s)

**<sup>1</sup>H-NMR (500 MHz, Acetone-d<sub>6</sub>) δ (ppm):** 4.73 (t, 1H, J= 7.47 Hz), 5.08 (ddd, 1H, J= 7.30, 1.64, 0.67 Hz), 5.16 (dd, 1H, J= 7.48, 1.44 Hz), 7.08-7.05 (m, 2H), 7.10 (d, 1H, J= 1.79 Hz), 7.11 (dd, 1H, J= 2.01 Hz), 7.42 (dd, 1H, J= 8.49, 0.66 Hz), 7.44 (dd, 1H, J= 2.10, 0.63 Hz), 7.45 (d, 1H, J= 2.00 Hz), 7.46 (dd, 1H, J= 8.00, 2.30 Hz), 7.48 (dd, 1H, J= 2.00, 0.59 Hz),

7.51 (d, 1H, J= 2.16 Hz), 7.68 (dd, 1H, J= 1.89, 0.63 Hz), 10.48 (s, br, 2NH), 10.51 (s, br, 1NH)

**(Z)-3,3',3''-(2-bromoprop-2-ene-1,1,3-triyl)tris(5-chloro-1H-indole)**



**(19)**

**(19) 56% + (18) 44%**

**Chemical Formula:** C<sub>27</sub>H<sub>17</sub>N<sub>3</sub>BrCl<sub>3</sub>

**Molecular weight:** 569.71 g/mol

**Appearance:** Black powder

**Melting point:** 96-106 °C

**Percentage Yield:** 144 mg (12.48%)

**R<sub>f</sub> Value:** 0.19 (Diethylether:Cyclohexane, 1.3: 0.7)

**RP-HPLC (R<sub>t</sub>):** 15.166 min (97.61%)

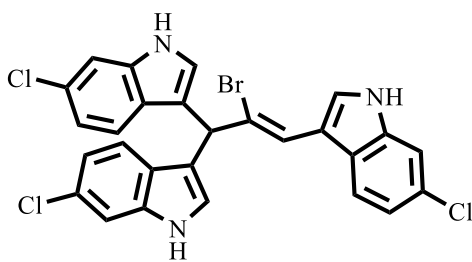
**ESI-MS (m/z):** 570.43 [M<sup>+</sup>+H<sup>+</sup>] 24%, 569.34 [M<sup>+</sup>] 15%, 568.43 [M<sup>+</sup>-.H]<sup>+</sup> 32%

**FT-IR (ATR; 680-4000 1/cm):** 1700-1600 (C=C conjugated asymmetrical stretching aliphatic, w), 3400 (NH stretching, s)

**<sup>1</sup>H-NMR (500 MHz, Acetone-d<sub>6</sub>) δ (ppm):** 5.92 (s, 1H), 7.10 (dd, 2H, J= 8.75, 2.03 Hz), 7.29 (d, 1H, J= 2.15 Hz), 7.32 (dd, 1H, J= 8.48, 2.13 Hz), 7.41 (d, 1H, J= 8.70 Hz), 7.46 (d, 2H, J= 8.55 Hz), 7.52 (s, 2H), 7.65 (d, 1H, J= 2.03 Hz), 7.85 (d, 1H, J= 2.40 Hz), 8.25 (d, 1H, J= 2.15 Hz), 8.27 (d, 1H, J= 2.45 Hz), 10.48 (s, br, 2NH), 10.71 (s, br, 1NH)



**(Z)-3,3',3''-(2-bromoprop-2-ene-1,1,3-triyl)tris(6-chloro-1H-indole)**



**(20)**

**6-Chloroindole (5 mmol, 0.7579 gr) + 2-Bromomalondialdehyde (2 mmol, 0.3019 gr)**

**Chemical Formula:** C<sub>27</sub>H<sub>17</sub>N<sub>3</sub>BrCl<sub>3</sub>

**Molecular weight:** 569.71 g/mol

**Appearance:** Light brown powder

**Melting point:** 149-153 °C

**Percentage Yield:** 180 mg (15.60%)

**R<sub>f</sub> Value:** 0.25 (Diethylether:Cyclohexane, 1:1)

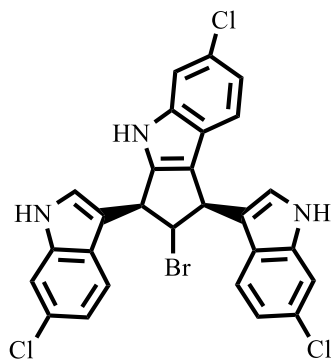
**RP-HPLC (R<sub>t</sub>):** 15.697 min (95.844%)

**ESI-MS (m/z):** 571.72 [M<sup>+</sup>] 32%, 570.43 [M<sup>+</sup>-.H]<sup>+</sup> 86%, 568.43 [M<sup>+</sup>-.H]<sup>+</sup> 100%, 499.71 [M<sup>+</sup>-2.Cl]<sup>+</sup> 13%, 419.13 [M<sup>+</sup>-.Indole]<sup>+</sup> 57%, 384.13 [M<sup>+</sup>-Cl-.Indole]<sup>+</sup> 7%, 163.55 [M<sup>+</sup>-3Cl-.Indole]<sup>+</sup> 10%

**FT-IR (ATR; 680-4000 1/cm):** ca. 800-700 (C-Cl aromatic stretching, w), 1700-1600 (C=C conjugated asymmetrical stretching aliphatic, w), 3400 (NH stretching, s)

**<sup>1</sup>H-NMR (500 MHZ, Acetone-d<sub>6</sub>) δ (ppm):** 5.86 (quartet, 1H, J= 0.82 Hz), 6.99 (dd, 2H, J= 8.51, 1.90 Hz), 7.02 (dd, 1H, J= 8.50, 1.88 Hz), 7.26 (d, 2H, J= 2.48, 0.89 Hz), 7.37 (dt, 1H, J= 8.52, 0.68 Hz), 7.45 (d, 1H, J= 0.93 Hz), 7.48 (dd, 1H, J= 1.91, 0.57 Hz), 7.49 (dd, 2H, J= 1.86, 0.55 Hz), 7.58 (dt, 2H, J= 8.48, 0.65 Hz), 8.24 (dd, 1H, J= 2.66, 0.75 Hz), 10.32 (s, br, 2NH), 10.65 (s, br, 1NH)

**(1R,3S)-2-bromo-6-chloro-1,3-bis(6-chloro-1H-indol-3-yl)-1,2,3,4-tetrahydrocyclopenta[b]indole**



**(21)**

**Chemical Formula:** C<sub>27</sub>H<sub>17</sub>N<sub>3</sub>BrCl<sub>3</sub>

**Molecular weight:** 569.71 g/mol

**Appearance:** Black powder

**Melting point:** 130-140 °C

**Percentage Yield:** 164 mg (14.22%)

**R<sub>f</sub> Value:** 0.21 (Diethylether:Cyclohexane, 1:1)

**RP-HPLC (R<sub>t</sub>):** 15.665 min (96.844%)

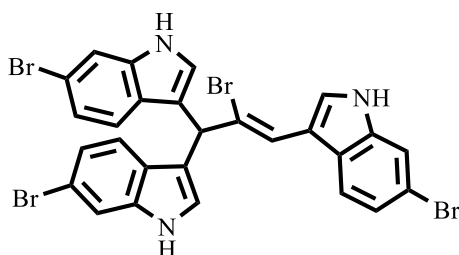
**ESI-MS (m/z):** 571.42 [M<sup>+</sup>] 32%, 570.43 [M<sup>+</sup>-.H]<sup>+</sup> 86%, 568.43 [M<sup>+</sup>-.H]<sup>+</sup> 100%, 499.71 [M<sup>+</sup>-2.Cl]<sup>+</sup> 13%, 490.53 [M<sup>+</sup>-.Br]<sup>+</sup> 47%, 420.71 [M<sup>+</sup>-.Br-.Cl]<sup>+</sup> 59%, 419.13 [M<sup>+</sup>-.Indole]<sup>+</sup> 57%, 385.71 [M<sup>+</sup>-.Br-3.Cl]<sup>+</sup> 7%, 384.13 [M<sup>+</sup>-.Cl-.Indole]<sup>+</sup> 7%, 340.13 [M<sup>+</sup>-.Indole-.Br]<sup>+</sup> 5%, 340.13 [M<sup>+</sup>-.Br-2.Cl]<sup>+</sup> 10%, 305.13 [M<sup>+</sup>-.Indole-.Br-.Cl]<sup>+</sup> 17%, 163.55 [M<sup>+</sup>-3.Cl-.Indole]<sup>+</sup> 10%

**FT-IR (ATR; 680-4000 1/cm):** ca. 700-600 (C-Br stretching alicyclic, w), ca. 800-700 (C-Cl stretching aromatic, m), 1430 (C-H bending alicyclic, m to s), 1746 (C=C stretching alicyclic, m), 2900 (C-H stretching alicyclic, m to s), 3300 (NH stretching, s)

**<sup>1</sup>H-NMR (500 MHz, Acetone-d<sub>6</sub>) δ (ppm):** 4.71 (dd, 1H, J= 7.6, 7.5 Hz), 5.06 (ddd, 1H, J= 7.6, 1.52, 0.57 Hz), 5.12 (dd, 1H, J= 7.5, 1.1 Hz), 6.92 (dd, 1H, J= 7.6, 1.9 Hz), 6.99 (dd, 1H, J= 7.6, 1.9 Hz), 7.25 (dd, 1H, J= 2.3, 0.76 Hz), 7.27 (dd, 1H, J= 7.6, 1.9 Hz), 7.40 (dt, 1H, J=

1.9, 0.4 Hz), 7.41 (dt, 1H, J= 2.3, 0.57 Hz), 7.43 (dt, 1H, J= 1.9, 0.5 Hz), 7.44 (dt, 1H, J= 1.9, 0.5 Hz), 7.47 (dt, 1H, J= 7.6, 0.5 Hz), 7.49 (dt, 1H, J= 7.6, 0.4 Hz), 7.58 (dt, 1H, J= 7.6, 0.38 Hz), 10.38 (s, br, 1NH), 10.40 (s, br, 1NH), 10.45 (s, br, 1NH)

**(Z)-3,3',3''-(2-bromoprop-2-ene-1,1,3-triyl)tris(6-bromo-1H-indole)**



**(22)**

**6-Bromoindole (5 mmol, 0.9802 gr) + 2-Bromomalondiladehyde (2 mmol, 0.30192 gr)**

**Chemical Formula:** C<sub>27</sub>H<sub>17</sub>N<sub>3</sub>Br<sub>4</sub>

**Molecular weight:** 703.07 g/mol

**Appearance:** Red powder

**Melting point:** 164-172 °C

**Percentage Yield:** 216 mg (16.34%)

**R<sub>f</sub> Value:** 0.29 (Diethylether:Cyclohexane, 1.1: 0.9)

**RP-HPLC (R<sub>t</sub>):** 15.959 min (96.603%)

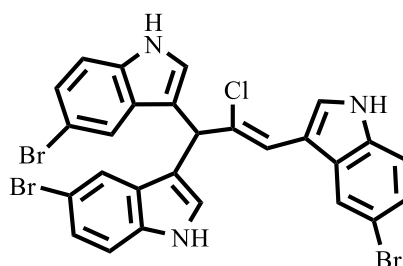
**ESI-MS (m/z):** 705.40 [M<sup>+</sup>] 24%, 704.29 [M<sup>+</sup>-.H]<sup>+</sup> 70%, 702.31 [M<sup>+</sup>-.H]<sup>+</sup> 100%, 624.07 [M<sup>+</sup>-.Br]<sup>+</sup> 32%, 508.02 [M<sup>+</sup>-.Indole]<sup>+</sup> 15%, 429.02 02 [M<sup>+</sup>-.Indole-.Br]<sup>+</sup> 3%, 350.02 [M<sup>+</sup>-.Indole-2.Br]<sup>+</sup> 12%, 312.97 [M<sup>+</sup>-2.Indole]<sup>+</sup> 30%, 271.02 [M<sup>+</sup>-.Indole-3.Br]<sup>+</sup> 7%

**FT-IR (ATR; 680-4000 1/cm):** ca. 700-600 (C-Br stretching aromatic and alicyclic, w to m), 1700-1625 (C=C conjugated asymmetrical stretching aliphatic, w), 3300 (NH stretching, s)

**<sup>1</sup>H-NMR (500 MHz, Acetone-d<sub>6</sub>) δ (ppm):** 5.88 (quartet, 1H, J= 0.84 Hz), 7.13 (dd, 2H, J= 8.49, 1.78 Hz), 7.16 (dd, 1H, J= 8.49, 1.76 Hz), 7.26 (dd, 2H, J= 2.48, 0.95 Hz), 7.34 (d, 1H,

J= 8.57 Hz), 7.46 (d, 1H, J= 1.00 Hz), 7.55 (dt, 2H, J= 8.44, 0.59 Hz), 7.65 (dd, 1H, J= 2.07, 0.55 Hz), 7.66 (dd, 2H, J= 1.75, 0.59 Hz), 8.24 (dd, 1H, J= 2.63, 0.82 Hz), 10.35 (s, br, 2NH), 10.68 (s, br, 1NH)

**(Z)-3,3',3''-(2-chloroprop-2-ene-1,1,3-triyl)tris(5-bromo-1H-indole)**



**(14)**

**5-Bromoindole (5 mmol, 0.9802 gr) + 2-Chloromalondialdehyde (2 mmol, 0.213 gr)**

**Chemical Formula:** C<sub>27</sub>H<sub>17</sub>N<sub>3</sub>Br<sub>3</sub> Cl

**Molecular weight:** 658.62 g/mol

**Appearance:** Black powder

**Melting point:** 125-130 °C

**Percentage Yield:** 200 mg (17.34%)

**R<sub>f</sub> Value:** 0.25 (Diethylether:Cyclohexane, 1.5:0.5)

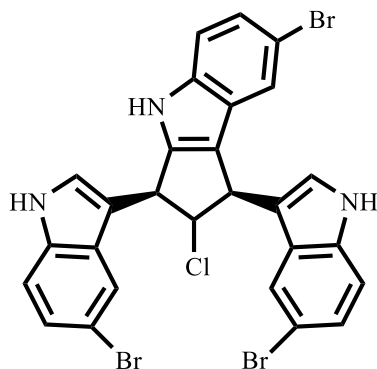
**RP-HPLC:** 15.716 min (97.231%)

**ESI-MS (m/z):** 660.43 [M<sup>+</sup>] 50 %, 658.50 [M<sup>+</sup>] 97 %, 657.40 [M<sup>+</sup>-.H]<sup>+</sup> 94 %

**FT-IR (ATR; 680-4000 1/cm):** ca. 700-600 (C-Br stretching aromatic, w), 1700-1600 (C=C conjugated asymmetrical stretching aliphatic, w), 3450 (NH stretching, s)

**<sup>1</sup>H-NMR (500 MHz, DMSO-d<sub>6</sub>) δ (ppm):** 5.87 (s, 1H), 7.17 (dd, 2H, J= 8.62, 1.97 Hz), 7.23 (dd, 1H, J= 8.57, 1.93 Hz), 7.30 (d, 2H, J= 2.05 Hz), 7.35 (dd, 2H, J= 8.59, 0.55 Hz), 7.36 (dd, 1H, J= 8.59, 0.56 Hz), 7.40 (s, 1H), 7.78 (d, 2H, J= 1.92 Hz), 7.80 (d, 1H, J= 1.96 Hz), 7.93 (d, 1H, J= 2.65 Hz), 11.18 (s, br, 2NH), 11.55 (s, br, 1NH)

**(1R,3S)-7-bromo-1,3-bis(5-bromo-1H-indol-3-yl)-2-chloro-1,2,3,4-tetrahydrocyclopenta[b]indole**



**First Stereoisomer (1) [60 %] (15)**

**Chemical Formula:** C<sub>27</sub>H<sub>17</sub>N<sub>3</sub>Br<sub>3</sub> Cl

**Molecular weight:** 658.62 g/mol

**Appearance:** Dark brown powder

**Melting point:** 140-155 °C

**Percentage Yield:** 215 mg (18.64%)

**R<sub>f</sub> Value:** 0.20 (Diethylether:Cyclohexane, 1.5:0.5)

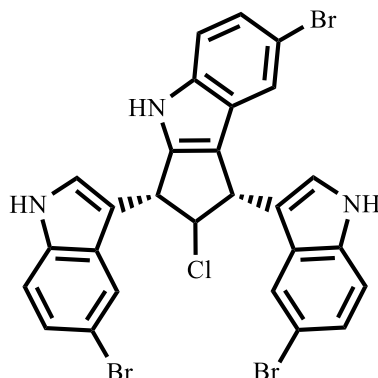
**RP-HPLC:** 15.925 min (60%)

**ESI-MS (m/z):** 658.49 [M<sup>+</sup>] 63%

**FT-IR (ATR; 680-4000 1/cm):** ca. 800-700 (C-Cl stretching alicyclic, m), ca. 700-600 (C-Br aromatic stretching, m), 1430 (C-H bending alicyclic, m to s), 1746 (C=C stretching alicyclic, m), 2910 (C-H stretching alicyclic, m), 3430 (NH stretching, s)

**<sup>1</sup>H-NMR (500 MHZ, DMSO-d<sub>6</sub>) δ (ppm):** 4.56 (dd, 1H, J= 7.6, 2.0 Hz), 4.82 (dd, 1H, J= 7.6, 1.9 Hz), 5.47 (t, 1H, J= 7.6 Hz), 7.09 (d, 2H, J= 5.6 Hz), 7.11 (d, 1H, J= 5.6 Hz), 7.18 (d, 1H, J= 1.54 Hz), 7.22 (d, 1H, J= 1.92 Hz), 7.29 (dd, 1H, J= 7.68, 2.3 Hz), 7.35 (dd, 2H, J= 5.76, 1.92 Hz), 7.57 (d, 1H, J= 1.54 Hz), 7.65 (d, 1H, J= 1.92 Hz), 7.89 (d, 1H, J= 1.92 Hz), 11.15 (s, br, 2NH), 11.29 (s, br, 1NH)

**(1S,3R)-7-bromo-1,3-bis(5-bromo-1H-indol-3-yl)-2-chloro-1,2,3,4-tetrahydrocyclopenta[b]indole**



**Second Stereoisomer (2) [40 %] (15)**

**Chemical Formula:** C<sub>27</sub>H<sub>17</sub>N<sub>3</sub>Br<sub>3</sub>Cl

**Molecular weight:** 658.62 g/mol

**Appearance:** Dark brown powder

**Melting point:** 140-155 °C

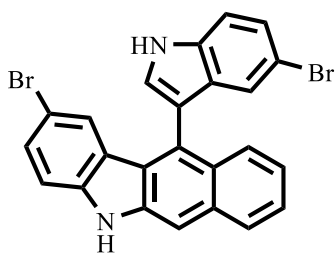
**R<sub>f</sub> Value:** 0.19 (Diethylether:Cyclohexane, 1.5:0.5)

**RP-HPLC (R<sub>t</sub>):** 16.300 min (40%)

**ESI-MS (m/z):** 658.49 [M<sup>+</sup>] 63%

**<sup>1</sup>H-NMR (500 MHz, DMSO-d<sub>6</sub>) δ (ppm):** 4.50 (dd, 2H, J= 7.6, 2.0 Hz), 5.43 (t, 1H, J= 7.6 Hz), 7.08 (d, 2H, J= 5.4 Hz), 7.10 (d, 1H, J= 5.0 Hz), 7.17 (d, 1H, J= 1.54 Hz), 7.19 (d, 1H, J= 1.92 Hz), 7.27 (dd, 1H, J= 5.0, 1.54 Hz), 7.32 (dd, 2H, J= 6.9, 2.0 Hz), 7.53 (d, 1H, J= 1.54 Hz), 7.61 (d, 1H, J= 1.92 Hz), 7.86 (d, 1H, J= 1.54 Hz), 11.12 (s, br, 2NH), 11.26 (s, br, 1NH)

**2-bromo-11-(5-bromo-1H-indol-3-yl)-5H-benzo[b]carbazole**



**(23)**

**5-Bromoindole (2 mmol, 0.39208 gr) + *o*-phthaldialdehyde (1 mmol, 0.13413 gr)**

**Chemical Formula:** C<sub>24</sub>H<sub>14</sub>Br<sub>2</sub>N<sub>2</sub>

**Molecular weight:** 490.20 g/mol

**Appearance:** Brown powder

**Melting point:** 245-250 °C

**Percentage Yield:** 150 mg (49.6%)

**R<sub>f</sub> Value:** 0.45 (Ethylacetate:Cyclohexane, 0.6:1.4)

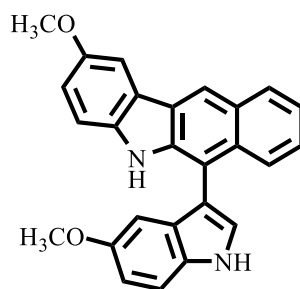
**RP-HPLC (R<sub>t</sub>):** 15.328 min (96.682%)

**ESI (m/z):** 491.16 [M<sup>+</sup>+H<sup>+</sup>] 100%, 489.53 [M<sup>+</sup>-.H]<sup>+</sup> 100%

**FT-IR (ATR; 680-4000 1/cm):** 800-600 (C-Br aromatic stretching, m), 3408 (NH stretching, s)

**<sup>1</sup>H-NMR (500 MHz, Acetone-d<sub>6</sub>) δ (ppm):** 7.11 (dt, 1H, J= 1.72, 0.73 Hz), 7.13 (dt, 1H, J= 1.91, 0.65 Hz), 7.27 (dd, 1H, J= 8.67, 1.28 Hz), 7.29 (dd, 1H, J= 8.75, 1.29 Hz), 7.36 (dt, 1H, J= 8.75, 0.52, 0.45 Hz), 7.46-7.44 (m, 2H), 7.47 (td, 1H, J= 6.96, 1.44 Hz), 7.70 (dd, 1H, J= 1.80, 0.60 Hz), 7.82 (dtd, 1H, J= 8.70, 1.82, 0.92 Hz), 8.00 (t, 1H, J= 0.72 Hz), 8.05 (ddt, 1H, J= 8.50, 1.25, 0.61 Hz), 10.52 (s, br, 1NH), 11.03 (s, br, 1NH)

**2-methoxy-6-(5-methoxy-1H-indol-7-yl)-5H-benzo[b]carbazole**



**(24)**

**5-Methoxyindole (2 mmol, 0.29434 gr) + *o*-phthalaldialdehyde (1 mmol, 0.13413 gr)**

**Chemical Formula:** C<sub>26</sub>H<sub>20</sub>N<sub>2</sub>O<sub>2</sub>

**Molecular weight:** 392.46 g/mol

**Appearance:** Light brown powder

**Melting point:** 105-110 °C

**Percentage Yield:** 145 mg (40.41%)

**R<sub>f</sub> Value:** 0.29 (Diethylether:Cyclohexane, 1:1)

**RP-HPLC (R<sub>t</sub>):** 14.287 min (96.246%)

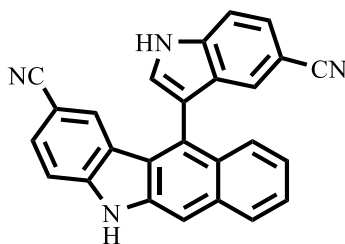
**ESI (m/z):** 391.53 [M<sup>+</sup>-.H]<sup>+</sup> 100%

**FT-IR (ATR; 680-4000 1/cm):** 1230 (C-O-C aromatic stretching, s), 3411 (NH stretching, s)

**<sup>1</sup>H-NMR (400 MHz, Acetone-d<sub>6</sub>) δ (ppm):** 3.56 (s, 3H, 1OCH<sub>3</sub>), 3.94 (s, 3H, 1OCH<sub>3</sub>), 6.60 (d, 1H, J= 2.42, 0.47 Hz), 6.87 (dd, 1H, J= 8.88, 2.48 Hz), 7.08 (dd, 1H, J= 8.77, 2.52 Hz), 7.36 (dt, 1H, J= 7.79, 1.32 Hz), 7.40-7.32 (m, 3H), 7.51 (t, 1H, J= 0.68 Hz), 7.61 (dd, 1H, J= 2.60, 0.56 Hz), 7.90 (d, 1H, J= 2.52 Hz), 7.93 (dtd, 1H, J= 7.32, 2.41, 0.71 Hz), 8.12 (ddt, 1H, J= 6.77, 2.04, 0.49 Hz), 9.55 (s, br, 1NH), 10.55 (s, br, 1NH)



**11-(5-cyano-1H-indol-3-yl)-5H-benzo[b]carbazole-2-carbonitrile**



**(25)**

**Indole-5-carbonitrile (2 mmol, 0.28432 gr) + *o*-phthalaldialdehyde (1 mmol, 0.13413 gr)**

**Chemical Formula:** C<sub>26</sub>H<sub>14</sub>N<sub>4</sub>

**Molecular weight:** 382.43 g/mol

**Appearance:** Green powder

**Melting point:** 210-215 °C

**Percentage Yield:** 134 mg (36.55%)

**R<sub>f</sub> Value:** 0.26 (Ethylacetate:Cyclohexane, 1:1)

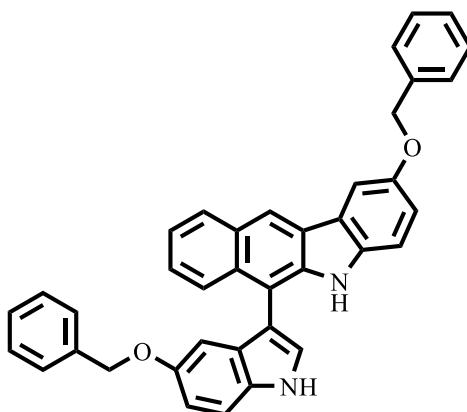
**RP-HPLC (R<sub>t</sub>):** 14.029 min (99.227%)

**ESI (m/z):** 381.64 [M<sup>+</sup>-.H]<sup>+</sup> 100%

**FT-IR (ATR; 680-4000 1/cm):** 2247 (CN stretching, s), 3311 (NH stretching, s)

**<sup>1</sup>H-NMR (400 MHz, Acetone-d<sub>6</sub>) δ (ppm):** 7.19 (ddd, 1H, J= 1.84, 1.01, 0.83 Hz). 7.34 (td, 1H, J= 7.62, 1.24 Hz), 7.43 (dt, 1H, J= 2.89, 0.69 Hz), 7.54 (td, 1H, J= 7.49, 1.27 Hz), 7.58 (dd, 1H, J= 8.50, 1.57 Hz), 7.65 (dt, 1H, J= 8.38, 0.75 Hz), 7.68 (dd, 1H, J= 8.45, 1.56 Hz), 7.84 (dd, 1H, J= 8.75, 1.13 Hz), 7.94-7.91 (m, 2H) [7.92(dd, 1H, J= 7.98, 0.73 Hz), 7.92 (d, 1H, J= 2.36 Hz)], 8.10 (dd, 1H, J= 7.07, 2.00 Hz), 8.11 (s, 1H), 10.97 (s, br, 1NH), 11.43 (s, br, 1NH)

**2-(benzyloxy)-6-(5-(benzyloxy)-1H-indol-3-yl)-5H-benzo[b]carbazole**



**(26)**

**5-Benzyloxyindole (2 mmol, 0.44654 gr) + *o*-phthaldialdehyde (1 mmol, 0.13413 gr)**

**Chemical Formula:** C<sub>38</sub>H<sub>28</sub>N<sub>2</sub>O<sub>2</sub>

**Molecular weight:** 544.65 g/mol

**Appearance:** Green powder

**Melting point:** 100-105 °C

**Percentage Yield:** 100 mg (22.10%)

**R<sub>f</sub> Value:** 0.19 (Diethylether:Cyclohexane, 0.4:1.6)

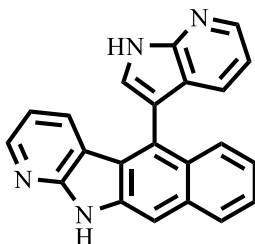
**RP-HPLC (R<sub>t</sub>):** 16.164 min (98.337%)

**ESI (m/z):** 543.26 [M<sup>+</sup>-.H]<sup>+</sup> 45%, 545.35 [M<sup>+</sup>+ H<sup>+</sup>] 27%

**FT-IR (ATR; 680-4000 1/cm):** 1267(C-O-C aromatic stretching, s), 3415 (NH stretching, s)

**<sup>1</sup>H-NMR (500 MHZ, Acetone-d<sub>6</sub>) δ (ppm):** 4.88 (s, 2H, 1OCH<sub>2</sub>Ph), 5.28 (s, 2H, 1OCH<sub>2</sub>Ph), 6.75 (d, 1H, J= 2.4 Hz), 6.97 (ddd, 1H, J= 8.8, 2.4, 0.5 Hz), 7.18 (dd, 1H, J= 8.7, 2.5 Hz), 7.22 (dddd, 1H, J= 8.3, 8.0, 1.4, 0.7 Hz), 7.26 (dt, 1H, J= 8.8, 1.8 Hz), 7.27 (dt, 1H, J= 8.6, 1.6 Hz), 7.33 (dtd, 2H, J= 8.6, 1.3, 0.6 Hz), 7.35 (dddd, 2H, J= 8.8, 8.6, 1.3, 0.6 Hz), 7.38 (ddd, 1H, J= 8.8, 8.3, 1.6 Hz), 7.41 (dd, 1H, J= 1.6, 0.6 Hz), 7.43 (dddd, 2H, J= 8.8, 8.6, 1.3, 0.6 Hz), 7.52 (dd, 1H, J= 8.8, 0.6 Hz), 7.58 (dddd, 2H, J= 8.4, 8.2, 1.5, 0.6 Hz), 7.62 (dt, 1H, J= 1.4, 0.7 Hz), 7.92 (dtd, 1H, J= 8.3, 1.6, 0.8 Hz), 8.01 (d, 1H, J= 2.5 Hz), 8.12 (ddt, 1H, J= 8.3, 1.3, 0.6 Hz), 8.68 (s, 1H), 9.57 (s, br, 1NH), 10.57 (s, br, 1NH)

**5-(1H-pyrrolo[2,3-b]pyridin-3-yl)-11H-benzo[f]pyrido[2,3-b]indole**



**(27)**

**7-azaindole (2 mmol, 0.23628 gr) + *o*-phthalaldialdehyde (1 mmol, 0.13413 gr)**

**Chemical Formula:** C<sub>22</sub>H<sub>14</sub>N<sub>4</sub>

**Molecular weight:** 334.38 g/mol

**Appearance:** Dark brown powder

**Melting point:** > 320 °C

**Percentage Yield:** 60 mg (11.63%)

**R<sub>f</sub> Value:** 0.12 (Diethylether:Cyclohexane:Ethylacetate, 0.1:0.7:1.2)

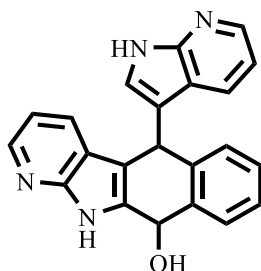
**RP-HPLC (R<sub>t</sub>):** 9.917 min (99.758%)

**APCI (m/z):** 335.70 [M<sup>+</sup> + H<sup>+</sup>] 100%

**FT-IR (ATR; 680-4000 1/cm):** 1600-1400 (C=N stretching, s), 3134 (NH stretching, s)

**<sup>1</sup>H-NMR (500 MHz, DMSO-d<sub>6</sub>) δ (ppm):** 6.84 (t, 1H, J = 4.86 Hz), 6.98 (t, 1H, J = 4.59 Hz), 7.05 (dt, 1H, J = 7.75, 1.62 Hz), 7.32-7.26 (m, 2H)[7.31 (td, 1H, J = 8.33, 1.55 Hz), 7.27 (d, 1H, J = 1.62 Hz)], 7.48 (td, 1H, J = 7.48, 1.22 Hz), 7.80-7.77 (m, 2H), 7.93 (s, 1H), 8.08 (dd, 1H, J = 8.31, 1.73 Hz), 8.30 (dd, 1H, J = 4.95, 1.66 Hz), 8.33 (dd, 1H, J = 4.66, 1.59 Hz), 11.83 (s, br, 1NH), 12.17 (s, br, 1NH)

**5-(1H-pyrrolo[2,3-b]pyridin-3-yl)-10,11-dihydro-5H-benzo[f]pyrido[2,3-b]indol-10-ol**



**(28)**

**Chemical Formula:** C<sub>22</sub>H<sub>16</sub>N<sub>4</sub>O

**Molecular weight:** 352.40 g/mol

**Appearance:** Brown powder

**Melting point:** 285-290 °C

**R<sub>f</sub> Value:** 0.06 (Diethylether:Cyclohexane:Ethylacetate, 0.1:0.7:1.2)

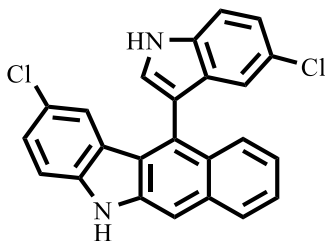
**RP-HPLC (R<sub>t</sub>):** 12.646 min (97.118%)

**APCI (m/z):** 351.1 [M<sup>+</sup>-.H]<sup>+</sup>

**FT-IR (ATR; 680-4000 1/cm):** 1687 (C=N stretching, s), 3130 (NH stretching, s), 3550-3200 (OH stretching, br, s)

**<sup>1</sup>H-NMR (500 MHz, DMSO-d<sub>6</sub>) δ (ppm):** 5.95 (s, br, 1OH), 6.42 (dd, 1H, J= 2.40, 1.13 Hz), 6.89 (m, 1H), 7.22 (t, 1H, J= 6.33 Hz), 7.32 (t, 1H, J= 7.32 Hz), 7.48-7.39 (m, 2H), 7.51 (t, 1H, J= 7.27 Hz), 7.63 (dd, 1H, J= 7.76, 1.6 Hz), 7.66 (dd, 1H, J= 7.65, 1.25 Hz), 7.84 (dd, 1H, J= 8.08, 1.42 Hz), 8.05 (dd, 1H, J= 4.65, 1.60 Hz), 8.14 (dd, 1H, J= 7.83, 1.60 Hz), 8.34 (dd, 1H, 4.69, 1.53 Hz), 11.14 (s, br, 1NH), 13.04 (s, br, 1NH)

**2-chloro-11-(5-chloro-1H-indol-3-yl)-5H-benzo[b]carbazole**



**(29)**

**5-Chloroindole (2 mmol, 0.30318 gr) + *o*-phthalaldialdehyde (1 mmol, 0.13413 gr)**

**Chemical Formula:** C<sub>24</sub>H<sub>14</sub>N<sub>2</sub>Cl<sub>2</sub>

**Molecular weight:** 401.29 g/mol

**Appearance:** Green powder

**Melting point:** 230-235 °C

**Percentage Yield:** 130 mg (37.12%)

**R<sub>f</sub> Value:** 0.32 (Diethylether:Cyclohexane, 1:1)

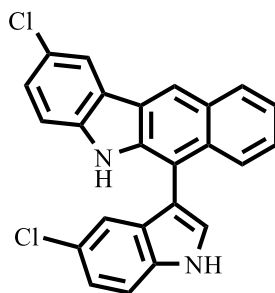
**RP-HPLC (R<sub>t</sub>):** 15.087 min (99.186%)

**APCI (m/z):** 402.10 [M<sup>+</sup> + H<sup>+</sup>] 42%

**FT-IR (ATR; 680-4000 1/cm):** 800-700 (C-Cl aromatic stretching, s), 3409 (NH stretching, s)

**<sup>1</sup>H-NMR (500 MHz, DMSO-d<sub>6</sub>) δ (ppm):** 6.72 (d, 1H, J= 2.12 Hz), 6.78 (d, 1H, J= 2.02 Hz), 7.19 (dd, 1H, J= 8.70, 2.09 Hz), 7.25 (tdd, 1H, J=7.50, 1.26, 0.77 Hz), 7.34 (dd, 1H, J= 8.60, 2.19 Hz), 7.44 (dd, 1H, J= 8.37, 0.53 Hz), 7.46 (td, 1H, J= 7.46, 1.24 Hz), 7.66 (dd, 1H, J= 8.65, 0.65 Hz), 7.70 (dtd, 1H, J= 8.46, 1.04, 0.60 Hz), 7.73 (d, 1H, J= 2.37 Hz), 7.95 (t, 1H, J= 0.86 Hz), 8.07 (ddt, 1H, J= 8.09, 1.61, 0.74 Hz), 11.45 (s, br, 1NH), 11.83 (s, br, 1NH)

**2-chloro-6-(6-chloro-1H-indol-3-yl)-5H-benzo[b]carbazole**



**(30)**

**Chemical Formula:** C<sub>24</sub>H<sub>14</sub>N<sub>2</sub>Cl<sub>2</sub>

**Molecular weight:** 401.29 g/mol

**Appearance:** Grey powder

**Melting point:** 255-260 °C

**Percentage Yield:** 64 mg (18.81%)

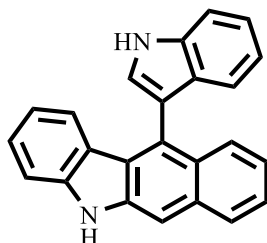
**R<sub>f</sub> Value:** 0.17 (Diethylether:Cyclohexane, 1:1)

**RP-HPLC (R<sub>t</sub>):** 16.681 min (97.748%)

**APCI (m/z):** 402.10 [M<sup>+</sup>+ H<sup>+</sup>] 32%

**<sup>1</sup>H-NMR (500 MHz, DMSO-d<sub>6</sub>) δ (ppm):** 6.91 (d, 1H, J= 2.05 Hz), 7.18 (dd, 1H, J= 8.66, 2.09 Hz), 7.41-7.35 (m, 3H), 7.42 (dd, 1H, J= 8.57, 1.95 Hz), 7.60 (dd, 1H, J= 8.65, 0.61 Hz), 7.71 (dd, 1H, J= 7.58, 2.42 Hz), 7.78 (d, 1H, J= 2.43 Hz), 8.11 (dd, 1H, J= 7.22, 1.97 Hz), 8.37 (d, 1H, J= 1.92 Hz), 8.79 (s, 1H), 10.66 (s, br, 1NH), 11.79 (s, br, 1NH)

**11-(1H-indol-3-yl)-5H-benzo[b]carbazole**



**(31)**

**Indole (2 mmol, 0.2343 gr) + *o*-phthaldialdehyde (1 mmol, 0.13413 gr)**

**Chemical Formula:** C<sub>24</sub>H<sub>16</sub>N<sub>2</sub>

**Molecular weight:** 332.41 g/mol

**Appearance:** Light green powder

**Melting point:** 255-260 °C

**Percentage Yield:** 170 mg (48.85%)

**R<sub>f</sub> Value:** 0.27 (Diethylether:Cyclohexane, 0.7:1.3)

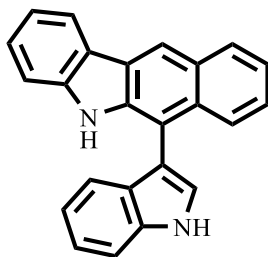
**RP-HPLC (R<sub>t</sub>):** 14.098 min (98.269%)

**APCI (m/z):** 333.2 [M<sup>+</sup> + H<sup>+</sup>] 100%

**FT-IR (ATR; 680-4000 1/cm):** 3408 (NH stretching, s)

**<sup>1</sup>H-NMR (400 MHz, Acetone-d<sub>6</sub>) δ (ppm):** 6.75 (td, 1H, J= 7.60, 0.98 Hz), 6.94 (td, 1H, J= 7.43, 1.02 Hz), 7.01 (td, 1H, J= 6.44, 1.27 Hz), 7.03 (td, 1H, J= 6.84, 1.56 Hz), 7.21 (dd, 1H, J= 6.92, 1.36 Hz), 7.23 (dd, 1H, J= 6.77, 1.43 Hz), 7.31 (td, 1H, J=7.65, 1.24 Hz), 7.44 (td, 1H, J= 8.04, 1.26 Hz), 7.45 (dd, 1H, J= 7.39, 2.40 Hz), 7.57 (d, 1H, J= 2.24 Hz), 7.68 (dt, 1H, J= 8.24, 0.90 Hz), 7.88 (ddt, 1H, J= 8.61, 1.31, 0.92 Hz), 7.94 (s, 1H), 8.01 (ddd, 1H, J= 8.28, 1.36, 0.70 Hz), 10.29 (s, br, 1NH), 10.74 (s, br, 1NH)

**6-(1H-indol-3-yl)-5H-benzo[b]carbazole**



**(32)**

**Chemical Formula:** C<sub>24</sub>H<sub>16</sub>N<sub>2</sub>

**Molecular weight:** 332.41 g/mol

**Appearance:** Light green powder

**Melting point:** 115-120 °C

**Percentage Yield:** 90 mg (31.35%)

**R<sub>f</sub> Value:** 0.22 (Diethylether:Cyclohexane, 0.7:1.3)

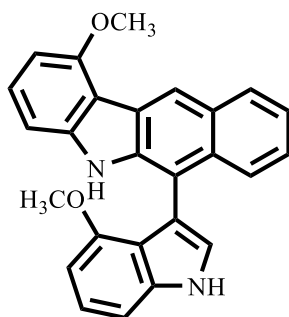
**RP-HPLC (R<sub>t</sub>):** 14.650 min (99.444%)

**APCI (m/z):** 333.1 [M<sup>+</sup> + H<sup>+</sup>] 100%

**<sup>1</sup>H-NMR (400 MHz, Acetone-d<sub>6</sub>) δ (ppm):** 7.00 (td, 1H, J= 7.46, 1.0 Hz), 7.13 (ddt, 1H, J= 7.80, 1.27, 0.72 Hz), 7.25-7.19 (m, 2H), 7.48-7.31 (m, 4H), 7.62 (dt, 1H, J= 8.25, 0.88 Hz), 7.67 (d, 1H, J= 2.50 Hz), 7.91 (ddt, 1H, J= 8.4, 1.47, 0.77 Hz), 8.15 (ddt, 1H, J= 8.10, 1.12, 0.53 Hz), 8.31 (dtd, 1H, J= 7.68, 1.28, 0.73 Hz), 8.72 (t, 1H, J= 0.63 Hz), 9.77 (s, br, 1NH), 10.69 (s, br, 1NH)



**1-methoxy-6-(4-methoxy-1H-indol-3-yl)-5H-benzo[b]carbazole**



**(33)**

**4-Methoxyindole (2 mmol, 0.29434 gr) + *o*-phthalaldialdehyde (1 mmol, 0.13413 gr)**

**Chemical Formula:** C<sub>26</sub>H<sub>20</sub>N<sub>2</sub>O<sub>2</sub>

**Molecular weight:** 392.46 g/mol

**Appearance:** Brown powder

**Melting point:** 165-170 °C

**Percentage Yield:** 36 mg (11.55%)

**R<sub>f</sub> Value:** 0.16 (Ethylacetate:Cyclohexane, 0.4:1.6)

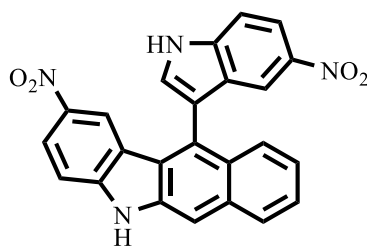
**RP-HPLC (R<sub>t</sub>):** n.d

**APCI (m/z):** 393.2 [M<sup>+</sup> + H<sup>+</sup>] 76%

**FT-IR (ATR; 680-4000 1/cm):** n.d

**<sup>1</sup>H-NMR (400 MHz, Acetone-d<sub>6</sub>) δ (ppm):** 4.15 (s, 6H, 2OCH<sub>3</sub>), 6.79 (d, 1H, J= 8.05 Hz), 6.94 (t, 1H, J= 8.23 Hz), 7.11 (dd, 1H, J= 8.03, 0.64 Hz), 7.36 (td, 1H, J= 7.45, 1.31 Hz), 7.41 (t, 1H, J= 8.04 Hz), 7.42 (td, 1H, J= 7.49, 1.37 Hz), 7.52 (t, 1H, J= 7.90 Hz), 7.83 (d, 1H, J= 0.9 Hz), 7.94 (dd, 1H, J= 8.35, 1.29 Hz), 8.01 (s, 1H), 8.05 (dd, 1H, J= 7.68, 1.43 Hz), 8.76 (s, 1H), 10.24 (s, br, 1NH), 11.26 (s, br, 1NH)

**2-nitro-11-(5-nitro-1H-indol-3-yl)-5H-benzo[b]carbazole**



(37)

**5-Nitroindole (2 mmol, 0.3243 gr) + *o*-phthalaldialdehyde (1 mmol, 0.13413 gr)**

**Chemical Formula:** C<sub>24</sub>H<sub>14</sub>N<sub>4</sub>O<sub>4</sub>

**Molecular weight:** 422.40 g/mol

**Appearance:** Red powder

**Melting point:** 140-150 °C

**Percentage Yield:** 74 mg (20%)

**R<sub>f</sub> Value:** 0.27 (Diethylether:Cyclohexane, 0.7:1.3)

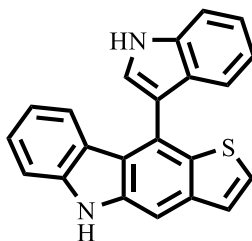
**RP-HPLC (R<sub>t</sub>):** 12.579 min (96.05%)

**ESI (m/z):** 423.10 [M<sup>+</sup>+H<sup>+</sup>] 90%, 421.32 [M<sup>+</sup>-.H]<sup>+</sup> 100%

**FT-IR (ATR; 680-4000 1/cm):** 870 (C-N aromatic stretching, m), 1324 (N=O symmetrical stretching, s), 1610 (N=O asymmetrical stretching, s), 3350 (NH stretching, s)

**<sup>1</sup>H-NMR (400 MHz, DMSO-d<sub>6</sub>) δ (ppm):** 7.62-7.54 (m, 2H), 7.75 (d, 1H, J= 1.84 Hz), 7.77 (dt, 1H, J= 6.87, 0.54 Hz), 7.89 (dd, 1H, J= 7.22, 0.46 Hz), 7.98 (dd, 1H, J= 7.21, 1.83 Hz), 8.06 (d, 1H, J= 1.89 Hz), 8.13 (dd, 1H, J= 7.29, 1.86 Hz), 8.16 (s, 1H), 8.18 (dd, 1H, J= 6.78, 0.95 Hz), 8.26 (dd, 1H, J= 7.16, 1.89 Hz), 8.56 (d, 1H, J= 1.81 Hz), 12.23 (s, br, 1NH), 12.50 (s, br, 1NH),

**10-(1H-indol-3-yl)-5H-thieno[3,2-b]carbazole**



**First Stereoisomer [1] (40)**

**Indole (2 mmol, 0.2343 gr) + 2,3-Thiophenedicarboxaldehyde (1 mmol, 0.14016 gr)**

**Chemical Formula:** C<sub>22</sub>H<sub>14</sub>N<sub>2</sub>S

**Molecular weight:** 338.43 g/mol

**Appearance:** Grey powder

**Melting point:** 255-258 °C

**Percentage Yield:** 110 mg (33%)

**R<sub>f</sub> Value:** 0.24 (Diethylether:Cyclohexane, 0.6:1.4)

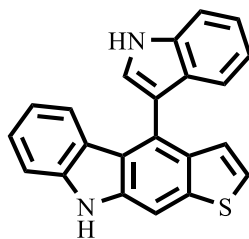
**RP-HPLC:** 12.579 min (96.05%)

**APCI (m/z):** 339.1 [M<sup>+</sup>+H<sup>+</sup>] 100%

**FT-IR (ATR; 680-4000 1/cm):** n.d

**<sup>1</sup>H-NMR (400 MHz, Acetone-d<sub>6</sub>) δ (ppm) [1]:** 6.77 (td, 1H, J= 7.61, 1.04 Hz), 6.97 (td, 1H, J= 7.50, 1.00 Hz), 7.13 (d, 1H, J= 7.92 Hz), 7.25-7.19 (m, 3H) [7.22 (td, 1H, J= 7.45, 1.20 Hz), 7.21 (dd, 1H, J= 7.61, 0.9 Hz), 7.21 (dd, 1H, J= 5.74, 1.03 Hz)], 7.28 (td, 1H, J= 7.60, 1.25 Hz), 7.33 (d, 1H, J= 5.63 Hz), 7.47 (dd, 1H, J= 8.16 Hz), 7.66-7.63 (m, 2H), 8.03 (s, 1H), 10.36 (s, br, 1NH), 10.70 (s, br, 1NH)

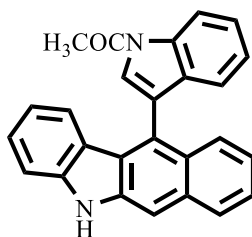
**4-(1H-indol-3-yl)-9H-thieno[2,3-b]carbazole**



**40 (60.48%), Second Stereoisomer [2] (39.52%)**

**<sup>1</sup>H-NMR (400 MHz, Acetone-d<sub>6</sub>) δ (ppm) [2]:** 6.76 (td, 1H, J= 7.65, 1.10 Hz), 6.96 (td, 1H, J= 7.50, 1.00 Hz), 7.13 (d, 1H, J= 7.50 Hz), 7.16 (d, 1H, J= 6.37 Hz), 7.25-7.19 (m, 2H) [7.21 (td, 1H, J= 7.00, 1.00 Hz), 7.21 (dd, 1H, J= 7.20, 0.90 Hz)], 7.27 (td, 1H, J= 8.00, 1.10 Hz), 7.51 (d, 1H, J= 4.46 Hz), 7.47 (d, 1H, J= 7.20 Hz), 7.57 (d, 1H, J= 4.43 Hz), 7.65 (dd, 1H, J= 8.0, 1.8 Hz), 7.96 (s, 1H), 10.35 (s, br, 1NH), 10.72 (s, br, 1NH)

**1-(3-(5H-benzo[b]carbazol-11-yl)-1H-indol-1-yl)ethan-1-one**



**(38)**

**Compound 31 (1 mmol, 0.33241 gr) + dichloromethane (CH<sub>2</sub>Cl<sub>2</sub>) (5 ml), 4-(dimethylaminopyridine) (DMAP) (0.1 mmol, 0.0122 gr) + aceticanhydride (1.2 mmol, 0.11 ml) and triethylamine (TEA) (1.2 mmol, 0.17 ml)**

**Chemical Formula:** C<sub>26</sub>H<sub>18</sub>N<sub>2</sub>O

**Molecular weight:** 374.44 g/mol

**Appearance:** White powder

**Melting point:** 100-105 °C

**Percentage Yield:** 50 mg (15%)

**R<sub>f</sub> Value:** 0.5 (Ethylacetate:Cyclohexane, 0.7:1.3)

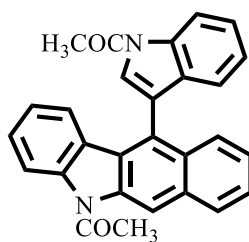
**RP-HPLC:** n.d

**ESI (m/z):** 375.41 [M<sup>+</sup>+H<sup>+</sup>] 38%, 373.79 [M<sup>+</sup>-.H]<sup>+</sup> 100%

**FT-IR (ATR; 680-4000 1/cm):** n.d

**<sup>1</sup>H-NMR (500 MHz, Acetone-d<sub>6</sub>) δ (ppm):** 2.83 (s, 3H, 1COCH<sub>3</sub>), 6.81 (td, 1H, J= 7.57, 0.96 Hz), 6.97 (ddd, 1H, J= 7.80, 1.0, 0.92 Hz), 7.14 (td, 1H, J= 7.52, 1.00 Hz), 7.27 (td, 1H, J= 7.60, 1.28 Hz), 7.35 (td, 1H, J= 7.50, 1.15 Hz), 7.50-7.42 (m, 4H), 7.86 (ddd, 1H, J= 8.65, 1.00, 0.5 Hz), 8.02 (s, 1H), 8.05 (s, 1H), 8.05 (dt, 1H, J= 8.48, 0.70 Hz), 8.66 (dt, 1H, J= 8.37, 0.62 Hz), 10.41 (s, br, 1NH)

**1-(11-(1-acetyl-1H-indol-3-yl)-5H-benzo[b]carbazol-5-yl)ethan-1-one**



**(39)**

**Chemical Formula:** C<sub>28</sub>H<sub>20</sub>N<sub>2</sub>O

**Molecular weight:** 416.48 g/mol

**Appearance:** White powder

**Melting point:** 225-230 °C

**Percentage Yield:** 30 mg (9%)

**R<sub>f</sub> Value:** 0.43 (Ethylacetate:Cyclohexane, 0.7:1.3)

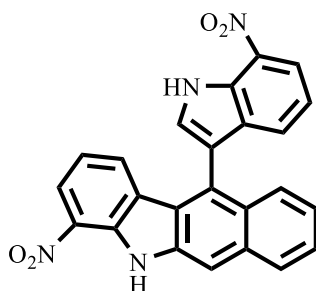
**RP-HPLC:** n.d

**ESI (m/z):** 417.66 [M<sup>+</sup>+H<sup>+</sup>] 13%

**FT-IR (ATR; 680-4000 1/cm):** n.d

**<sup>1</sup>H-NMR (500 MHz, Acetone-d<sub>6</sub>) δ (ppm):** 2.82 (s, 3H, 1COCH<sub>3</sub>), 3.05 (s, 3H, 1COCH<sub>3</sub>), 6.97 (ddd, 1H, J= 7.77, 0.97, 0.80 Hz), 7.02 (td, 1H, J= 7.59, 0.97 Hz), 7.12 (ddd, 1H, J= 7.87, 0.83, 0.73 Hz), 7.16 (td, 1H, J= 7.52, 1.00 Hz), 7.47-7.40 (m, 3H), 7.59 (td, 1H, J= 7.51, 1.20 Hz), 7.82 (ddd, 1H, J= 8.61, 0.93, 0.83 Hz), 8.07 (s, 1H), 8.20 (ddd, 1H, J= 8.30, 0.82, 0.73 Hz), 8.33 (ddd, 1H, J= 8.56, 0.98, 0.80 Hz), 8.66 (dt, 1H, J= 8.36, 0.89 Hz), 8.99 (s, 1H)

**4-nitro-11-(7-nitro-1H-indol-3-yl)-5H-benzo[b]carbazole**



**(35)**

**7-Nitroindole (2 mmol, 0.3243 gr) + o-phthaldialdehyde (1 mmol, 0.13413 gr)**

**Chemical Formula:** C<sub>24</sub>H<sub>14</sub>N<sub>4</sub>O<sub>4</sub>

**Molecular weight:** 422.40 g/mol

**Appearance:** Brown powder

**Melting point:** > 320 °C

**Percentage Yield:** 160 mg (55%)

**R<sub>f</sub> Value:** 0.3 (Ethylacetate:Cyclohexane, 0.4:1.6)

**RP-HPLC (R<sub>t</sub>):** 14.823 min (95.99%)

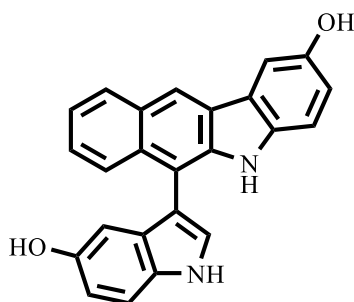
**ESI (m/z):** 421.37 [M<sup>+</sup>-.H]<sup>+</sup> 100%

**FT-IR (ATR; 680-4000 1/cm):** 870 (C-N stretching, m), 1530 (NO stretching, s), 3400 (NH stretching, s)

**<sup>1</sup>H-NMR (400 MHz, DMSO-d<sub>6</sub>) δ (ppm):** 6.95 (t, 1H, J= 7.70 Hz), 7.11 (t, 1H, J= 8.35 Hz), 7.35 (dt, 1H, J= 1.60, 0.52 Hz), 7.38 (tdd, 1H, J= 8.25, 1.70, 0.55 Hz), 7.54 (td, 1H, J= 8.30,

1.65 Hz), 7.72 (dd, 1H, J= 7.10, 1.50 Hz), 7.85 (ddd, 1H, J= 8.30, 1.40, 0.45 Hz), 7.87 (dtd, 1H, J= 8.20, 1.60, 0.40 Hz), 8.17 (d, 1H, J= 0.45 Hz), 8.21 (ddt, 1H, J= 8.50, 1.70, 0.50 Hz), 8.26 (dd, 1H, J= 8.40, 1.70 Hz), 8.28 (dd, 1H, J= 8.30, 1.50 Hz), 12.31 (s, br, 1NH), 12.47 (s, br, 1NH)

**11-(5-hydroxy-1H-indol-3-yl)-5H-benzo[b]carbazol-2-ol**



**(36)**

**5-Hydroxyindole (2 mmol, 0.2663 gr) + *o*-phthalaldialdehyde (1 mmol, 0.13413 gr)**

**Chemical Formula:** C<sub>24</sub>H<sub>16</sub>N<sub>2</sub>O<sub>2</sub>

**Molecular weight:** 364.40 g/mol

**Appearance:** Black powder

**Melting point:** 205-210 °C

**Percentage Yield:** 63 mg (17%)

**R<sub>f</sub> Value:** 0.2 (Ethylacetate:Cyclohexane, 1:1)

**RP-HPLC (R<sub>t</sub>):** 13.670 min (96.487%)

**ESI (m/z):** 365.19 [M<sup>+</sup>+H<sup>+</sup>] 100%, 363.38 [M<sup>+</sup>-.H]<sup>+</sup> 100%

**FT-IR (ATR; 680-4000 1/cm):** 3500-3150 (OH stretching) [overlapping NH stretching]

**<sup>1</sup>H-NMR (400 MHz, DMSO-d<sub>6</sub>) δ (ppm):** 6.34 (s, br, 1H, 1OH), 6.67 (dd, 1H, J= 7.40, 1.7 Hz), 6.91 (dt, 1H, J= 1.84, 0.56 Hz), 7.27 (dt, 1H, J= 7.34, 0.57 Hz), 7.29 (dd, 1H, J= 7.70, 1.70 Hz), 7.30 (dd, 1H, J= 7.81, 0.44 Hz), 7.32 (tdd, 1H, J= 7.23, 1.75, 0.67 Hz), 7.51 (dd, 1H, J= 1.7, 0.47 Hz), 7.58 (td, 1H, J= 7.00, 2.00 Hz), 7.77 (dt, 1H, J= 2.0, 0.65 Hz), 8.08 (dtd,

1H, J= 7.46, 2.00, 0.70 Hz), 8.49 (t, 1H, J= 0.55 Hz), 8.58 (ddt, 1H, J= 6.90, 1.70, 0.47 Hz),  
8.97 (s, br, 1H, 1OH), 10.07 (s, br, 1NH), 11.22 (s, br, 1NH)



## **5.6 The experimental protocols to the MIC values determination**

### **5.6.1 The protocol to the bioassay of the compounds 1-22**

The compounds and the standards were dissolved in 12.5% DMSO at concentrations of 200 µg/ml. Further dilutions of the compounds and standard drugs in the test medium were prepared at the required quantities of 400, 200, 100, 50, 25, 12.5, 6.25, 3.12, 1.56 and 0.78 µg/ml concentrations with Mueller-Hinton broth and Sabouraud dextrose broth. The minimum inhibitory concentrations (MIC) were determined using the 2-fold serial dilution technique. All the compounds were tested for their in vitro growth inhibitory activity. ATCC strains of the microorganisms used in this study were obtained from the culture collection of the Refik Saydam Health Institution of Health Ministry, Ankara, and maintained at the Microbiology Department of the Faculty of Pharmacy of the Ankara University. The cultures were obtained from Mueller-Hinton broth (Difco) for all the bacterial strains after 24 h of incubation at  $37 \pm 1$  °C. *C. albicans* was maintained in Sabouraud dextrose broth (Difco) after incubation for 24 h at  $25 \pm 1$  °C. Testing was carried out in Mueller-Hinton broth and Sabouraud dextrose broth (Difco) at pH 7.4 and the 2-fold serial dilution technique was applied. The final inoculum size was  $10^5$  CFU/ml for the antibacterial assay and  $10^4$  CFU/ml for the antifungal assay. A set of tubes containing only inoculated broth was used as controls. After incubation for 24 h at  $37 \pm 1$  °C for the antibacterial assay and for 48 h at  $25 \pm 1$  °C for the antifungal assay, the last tube with no growth of microorganism was recorded to represent the MIC (expressed in µg/ml). Every experiment in the antibacterial and antifungal assays was performed in duplicate.

### 5.6.2 The protocols to the bioassay of the compounds 23-40

1. The compounds and the standard were dissolved in 12.5% DMSO at concentrations of 512 µg/ml. Further dilutions of the compounds and standard drug in the test medium were prepared at the required quantities of 256, 128, 64, 32, 16, 8, 4, 2, 1, 0.5 and 0.25 µg/ml concentrations with Mueller-Hinton broth. The minimum inhibitory concentrations (MIC) were determined using the 2-fold serial dilution technique. All the compounds were tested for their in vitro growth inhibitory activity against *Enterococcus faecalis* strains OG1X and JH22, *Enterococcus faecium* strain 2121198, and the vancomycin-resistant strain AW2. All strains were cultivated from the strain collection of the Institute of Molecular Infection Biology, University of Würzburg. The cultures were obtained from Mueller-Hinton broth (Difco) for all the bacterial strains after 24 h of incubation at  $37 \pm 1$  °C. Testing was carried out in Mueller-Hinton broth at pH 7.4 and the 2-fold serial dilution technique with Mueller-Hinton broth was applied using microtiter plates. Each test well was inoculated with 100 µl of the respective compound and 100 µl bacterial suspension. The final inoculum size was  $5 \times 10^5$  CFU/ml for the antibacterial assay. A set of wells containing only inoculated broth was used as control. After incubation for 24 h at  $37 \pm 1$  °C, the last well with no growth of microorganism was recorded to represent the MIC (expressed in µg/ml). Two experimental and biological replicates were performed with consistent results.

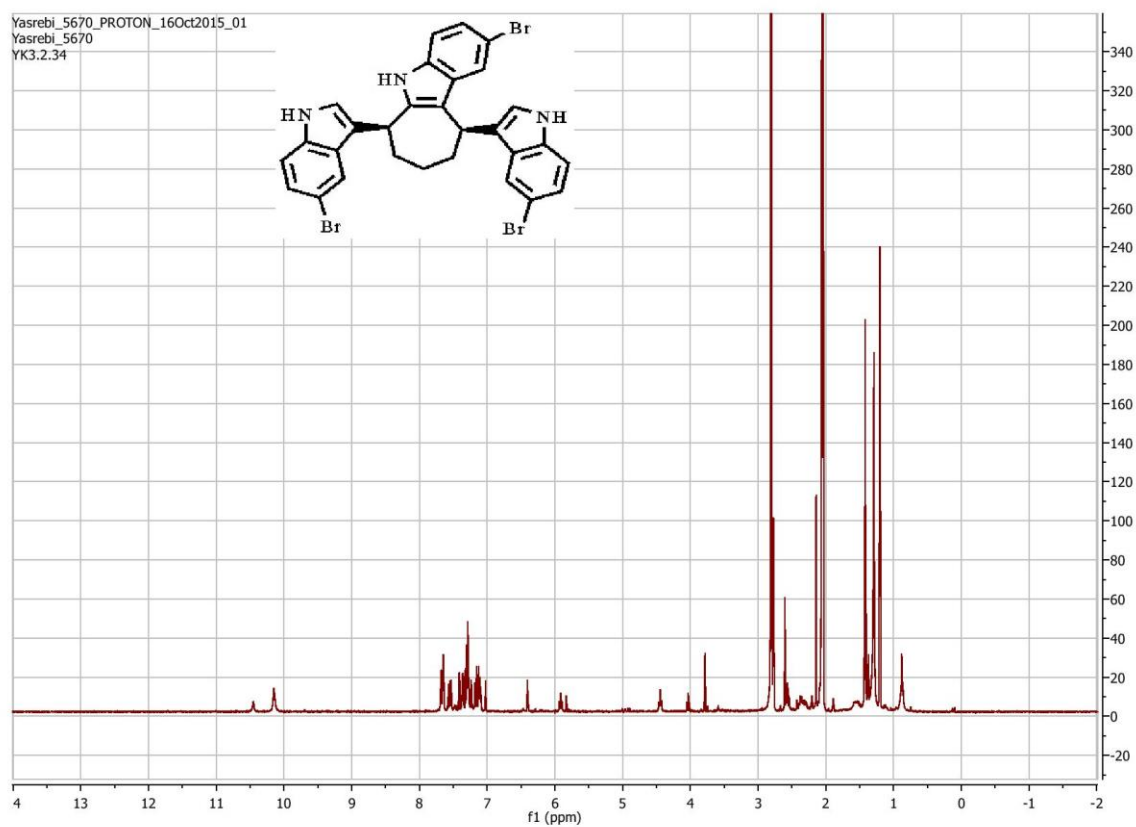
2. The minimal inhibitory concentrations (MIC) of all compounds and standard antibiotics were determined by microdilution according to the recommendations of the Clinical and Laboratory Standard Institute guidelines. Standard antibiotics oxacillin, vancomycin, and linezolid were purchased from Sigma-Aldrich (Taufkirchen, Germany). The MICs were determined in 96-well microtiter plates using a final volume of 100 µl Mueller-Hinton broth (MHB) containing beef infusion solids (20 g/l), casein hydrolysate (17.5 g/l), and starch (1.5 g/l). For MIC determination against oxacillin, 2% sodium chloride was added. The compounds and standard antibiotics linezolid and vancomycin were dissolved in dimethyl sulfoxide (DMSO) and diluted with MHB to a final concentration of 512 µg/ml containing 12.5% DMSO. The chosen DMSO percentage should avoid any precipitation during the following dilution procedures of the compounds which easily dissolved in the undiluted stock solution. The 12.5% DMSO has been used as a negative control. Further dilutions of the compounds and standard drugs in the test medium were prepared at the required quantities of 256, 128, 64, 32, 16, 8, 4, 2, 1, 0.5 and 0.25 µg/ml concentrations with MHB serially decreasing the final DMSO percentage. Oxacillin was dissolved in H<sub>2</sub>O at a concentration of

50 µg/ml and further diluted in MHB to the same concentrations as the compounds and other standard antibiotics. All the compounds were tested in duplicate for their in vitro growth inhibitory activity against *S. aureus Newman* and MRSA USA300 LAC. Both strains belong to the *S. aureus* clonal complex 8 and are highly pathogenic. *S. aureus* strain *Newman* was isolated in 1952 from a human infection and owns a general antibiotic susceptibility due to a lack of drug resistance genes. MRSA USA300 strain LAC as MRSA confers resistance toward β-lactam antibiotics by the acquired *mecA* gene that encodes alternative transpeptidase penicillin binding protein 2a with a low affinity to the β-lactam antibiotics. The final inoculum size was 5×10<sup>5</sup> CFU/ml for the antibacterial assay. A set of tubes containing only inoculated broth was used as controls. After incubation for 20 hours at 36°C±1°C, the last tube with no growth of microorganisms determined by visual examination under an inverse microscope was recorded to represent the MIC (expressed in µg/ml).

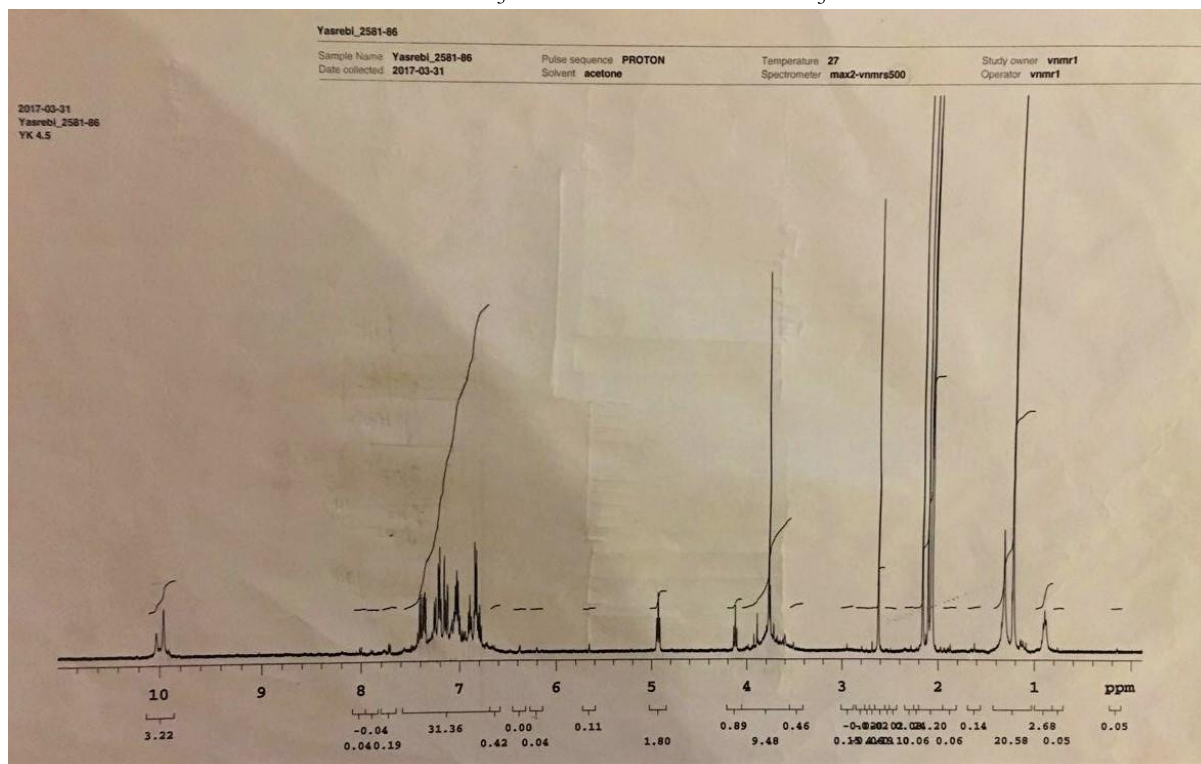
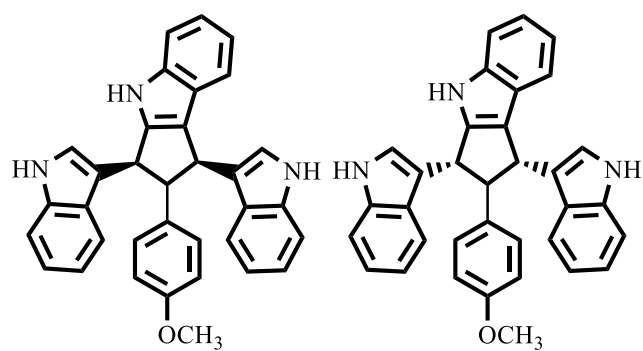
## 6. Appendix

### 6.1 NMR spectra

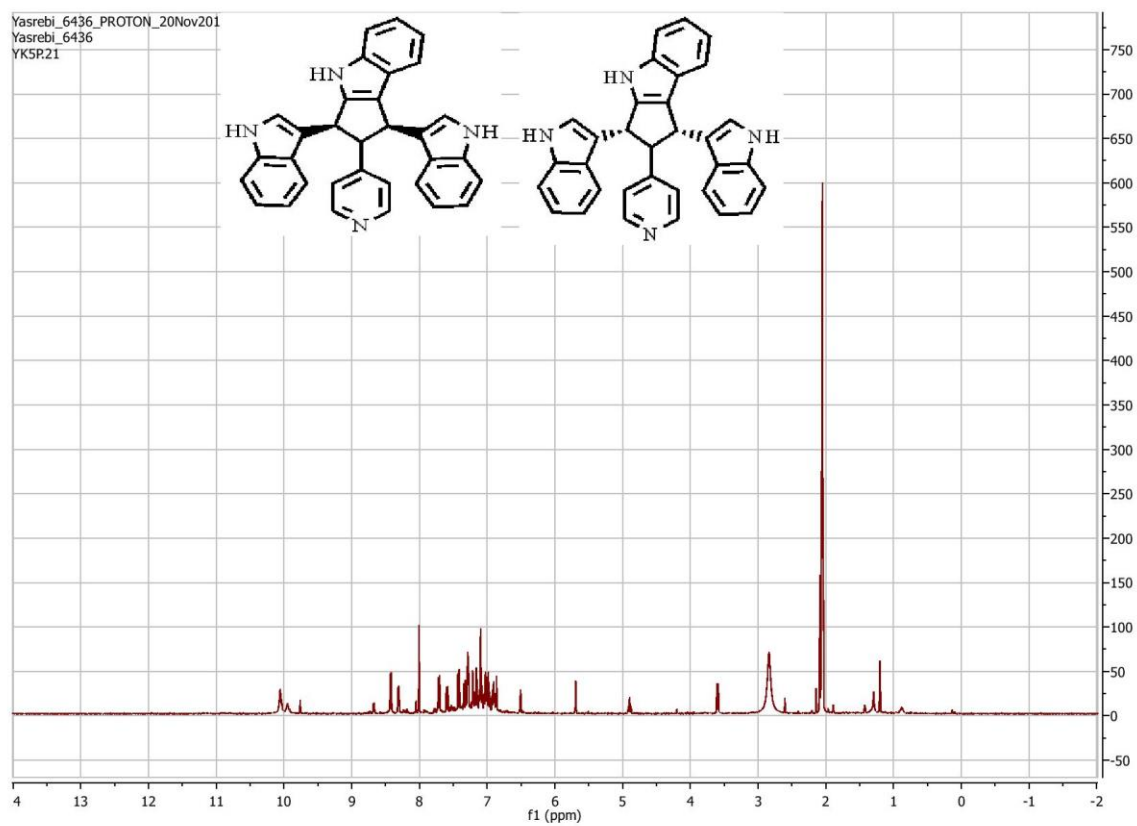
Compound [1]



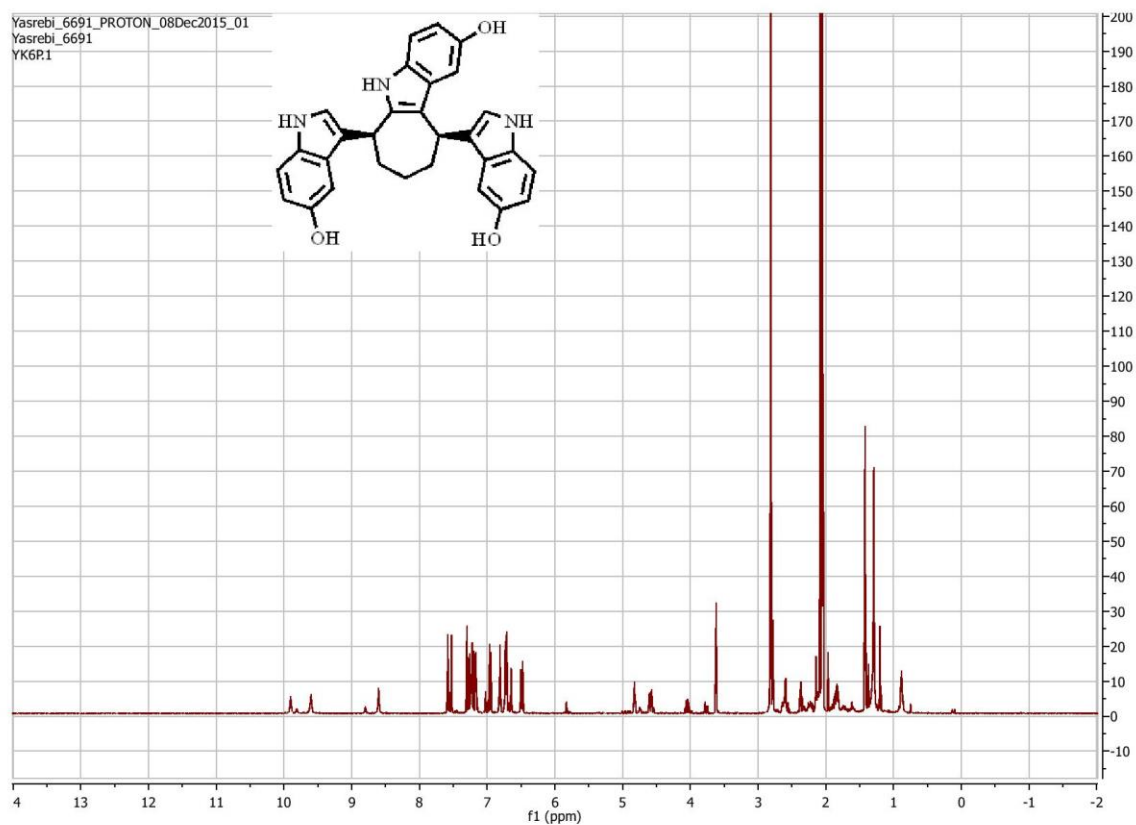
# Compound [3]

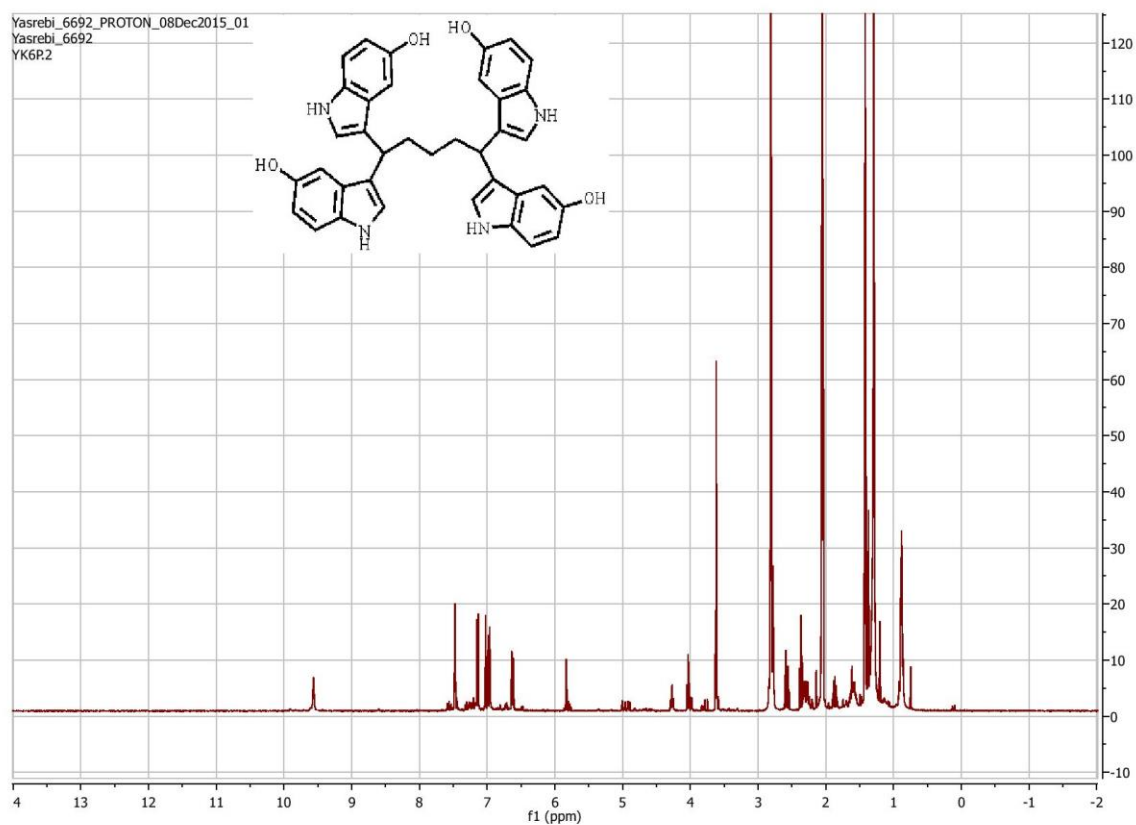


# Compound [4]



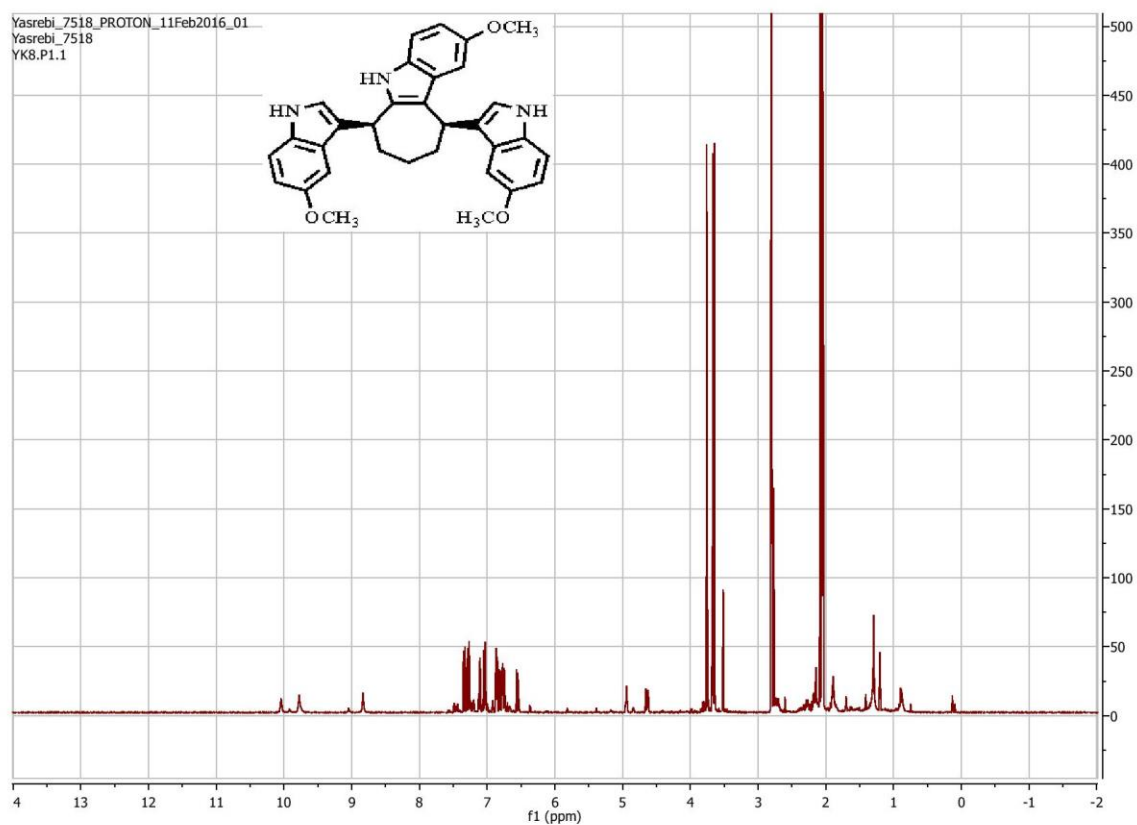
# Compound [6]





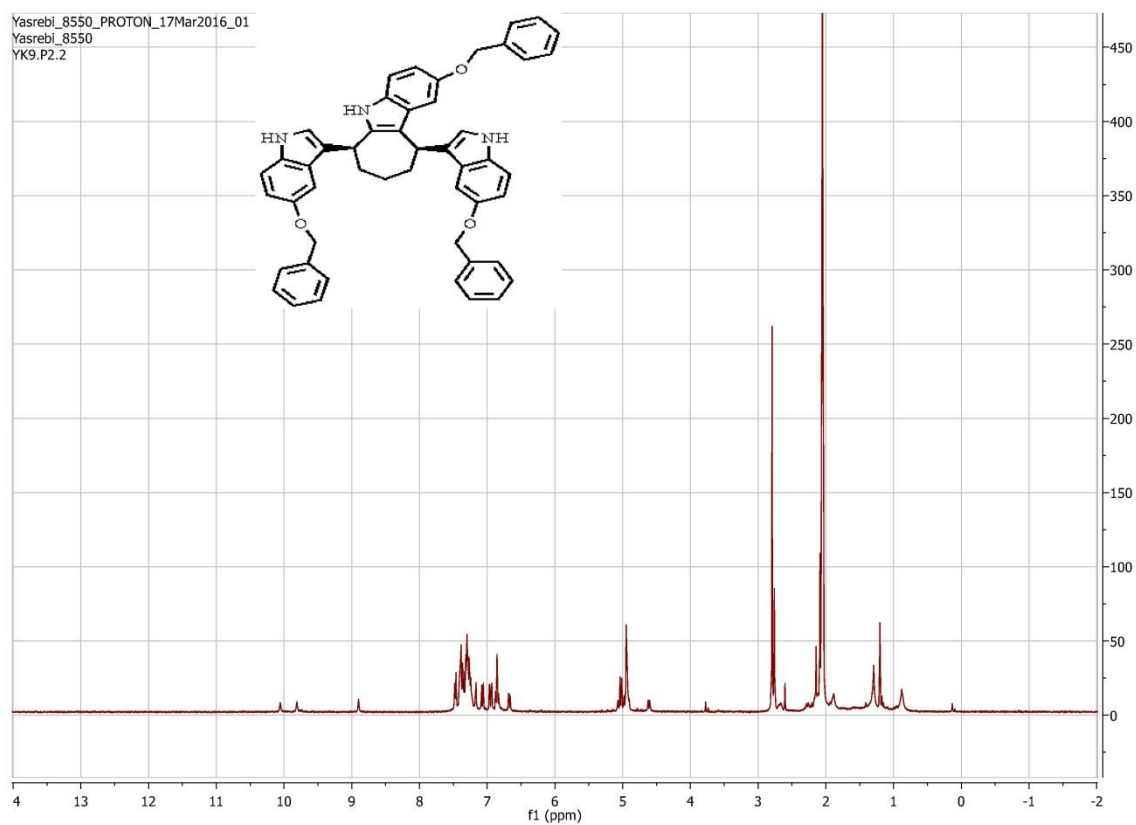


# Compound [7]

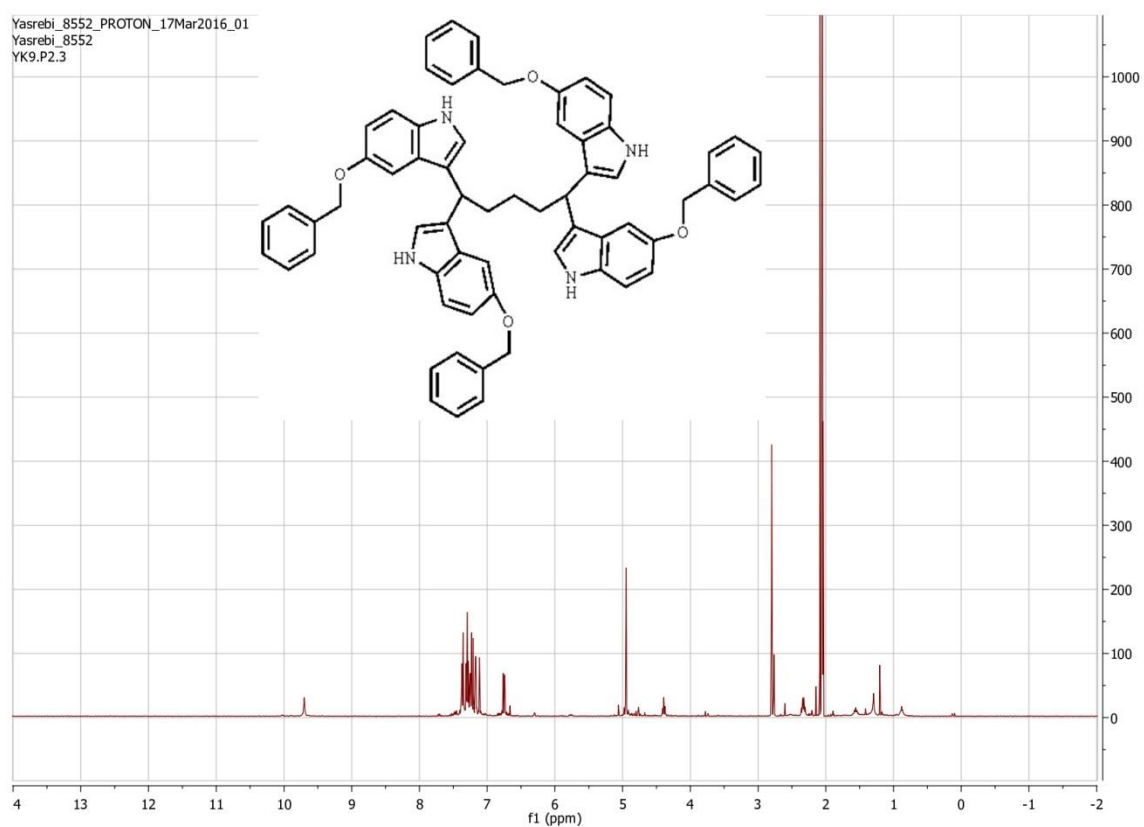


# Compound [8]

Yasrebl\_8550\_PROTON\_17Mar2016\_01  
Yasrebl\_8550  
YK9.P2.2

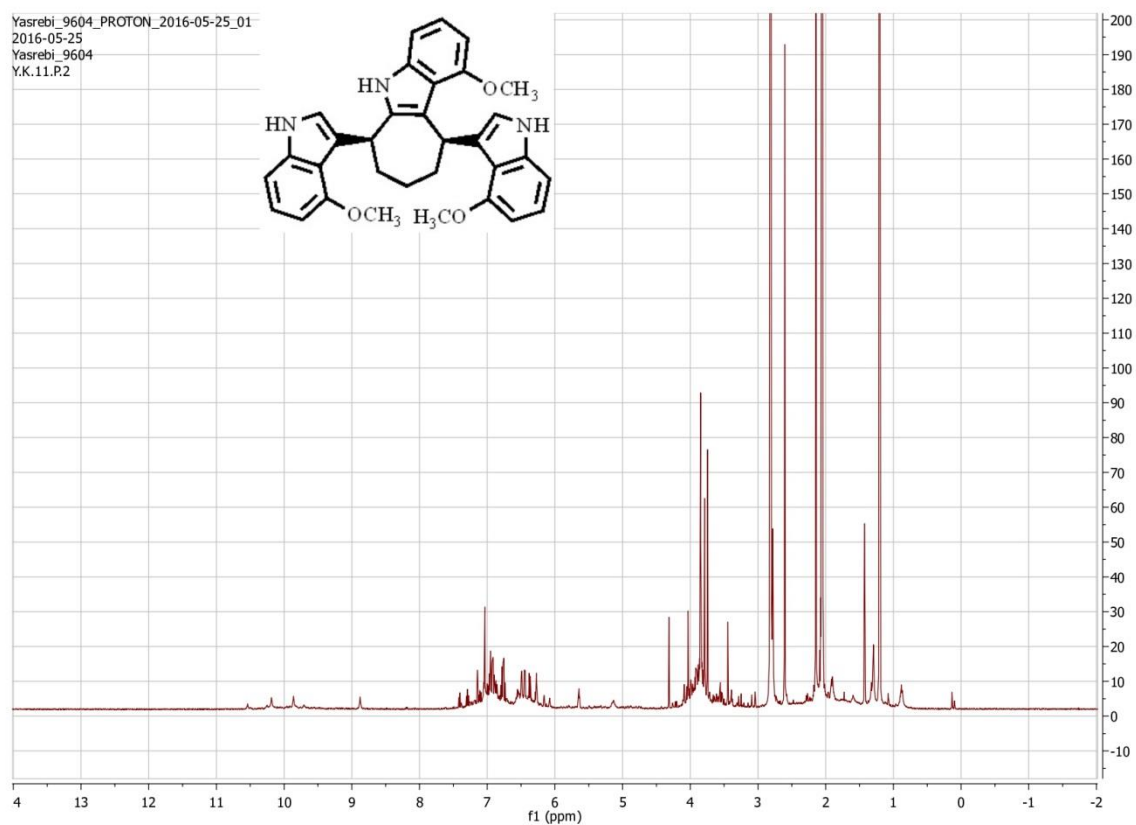


Yasrebi\_8552\_PROTON\_17Mar2016\_01  
Yasrebi\_8552  
YK9.P2.3

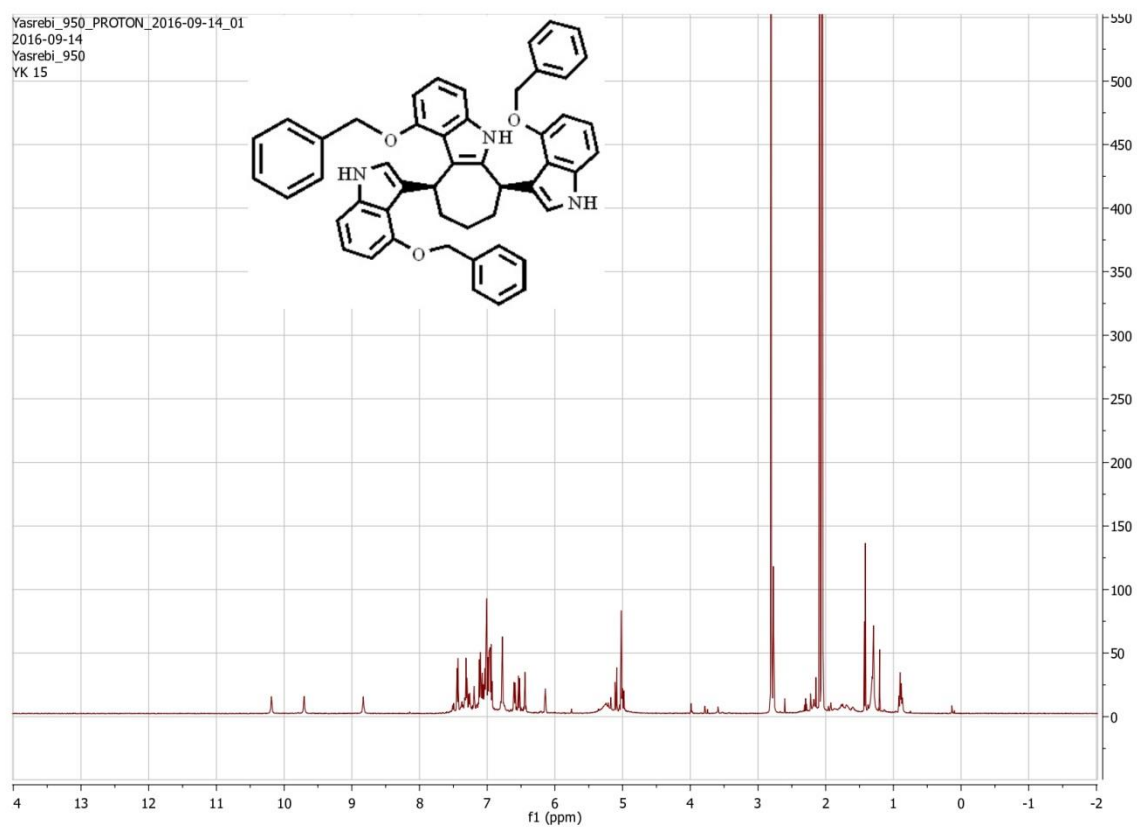


# Compound [9]

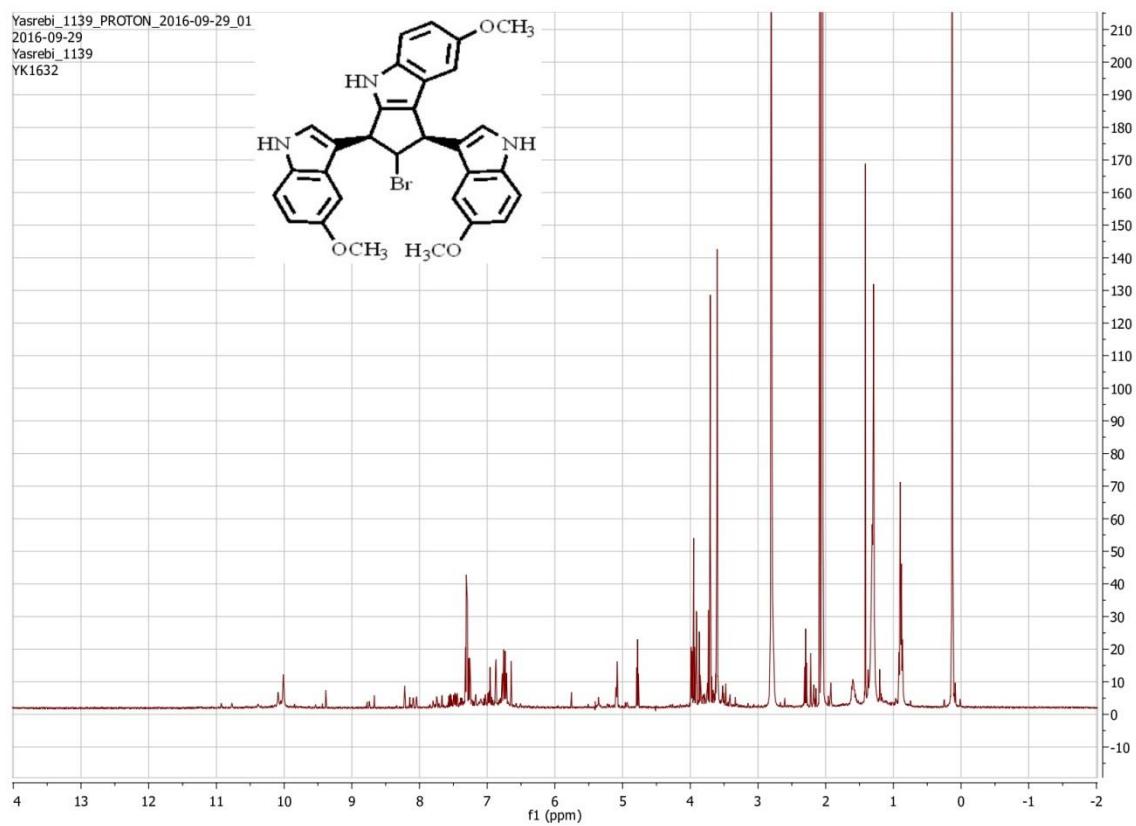
Yasrebi\_9604\_PROTON\_2016-05-25\_01  
2016-05-25  
Yasrebi\_9604  
Y.K.11.P.2



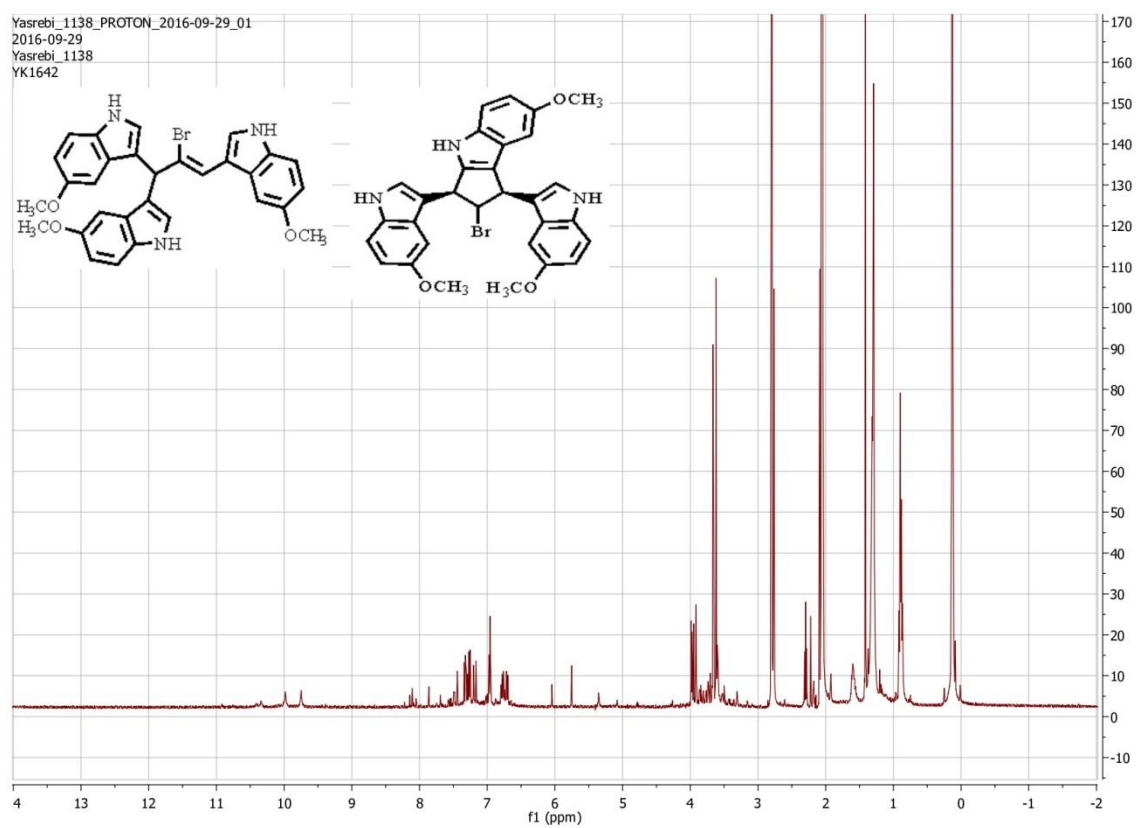
# Compound [11]



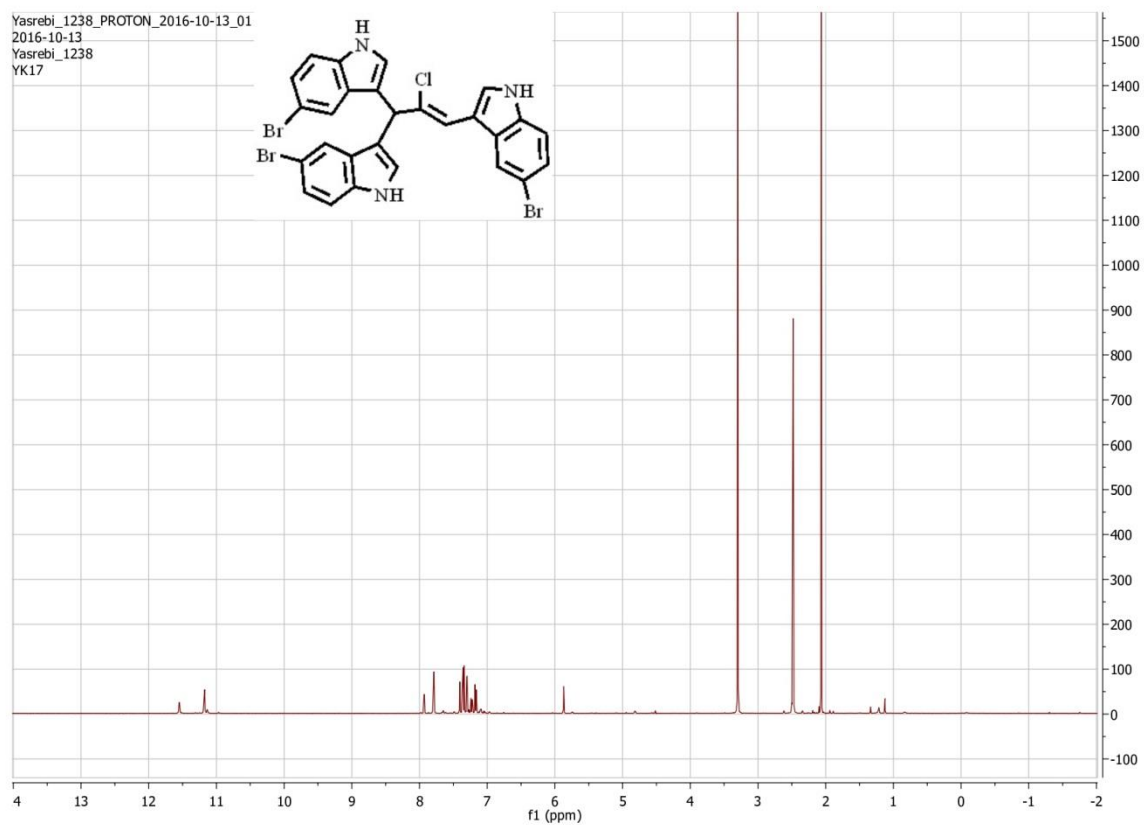
# Compound [12]



# Compound [13]

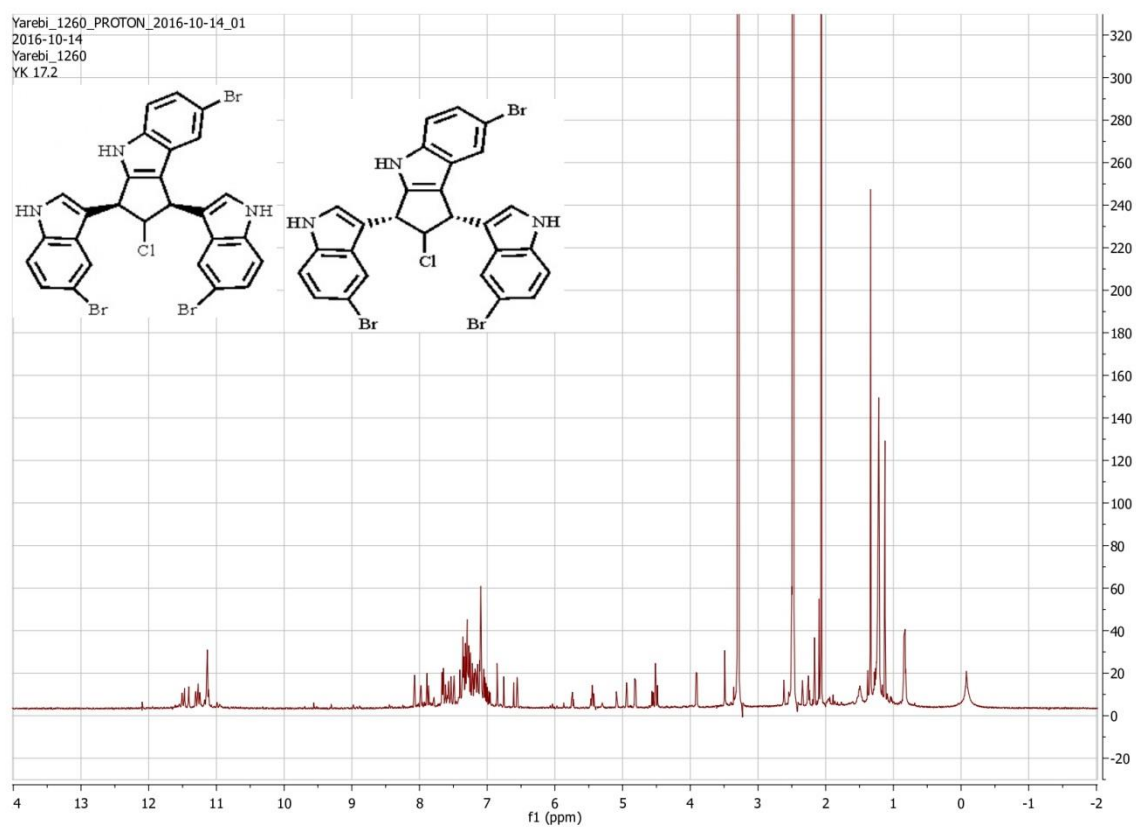


# Compound [14]

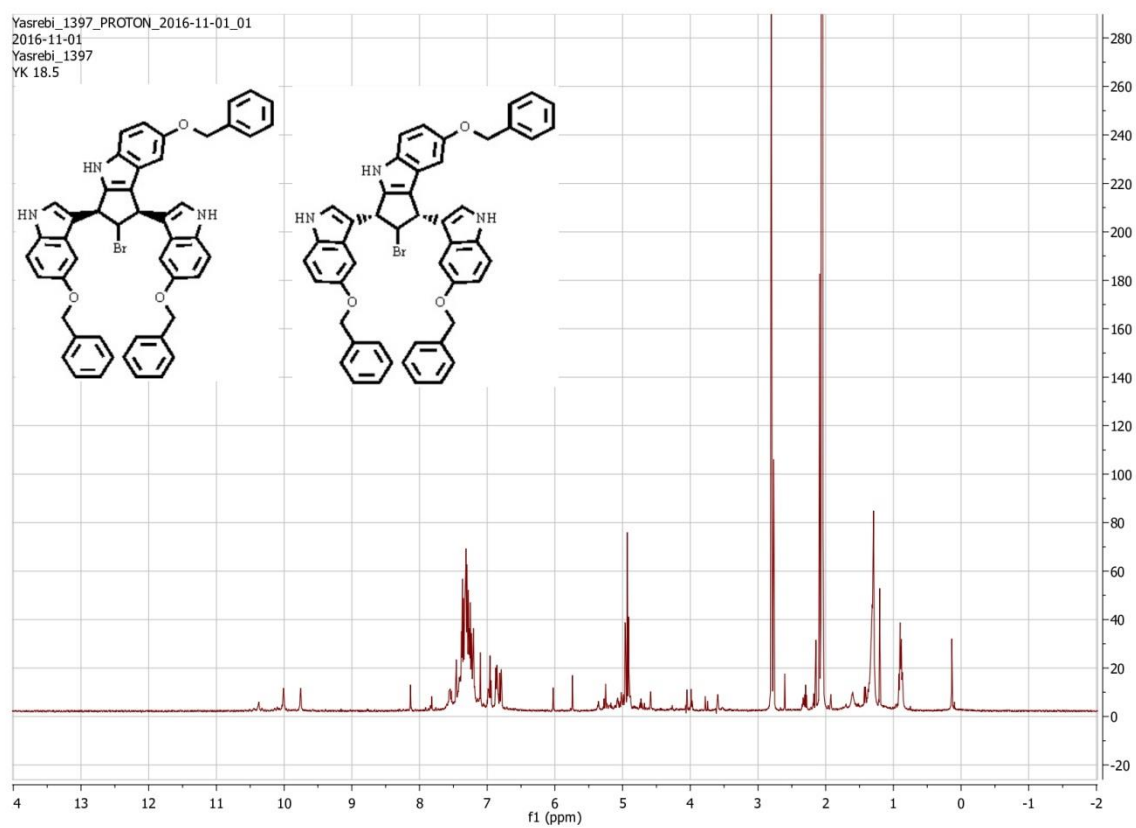




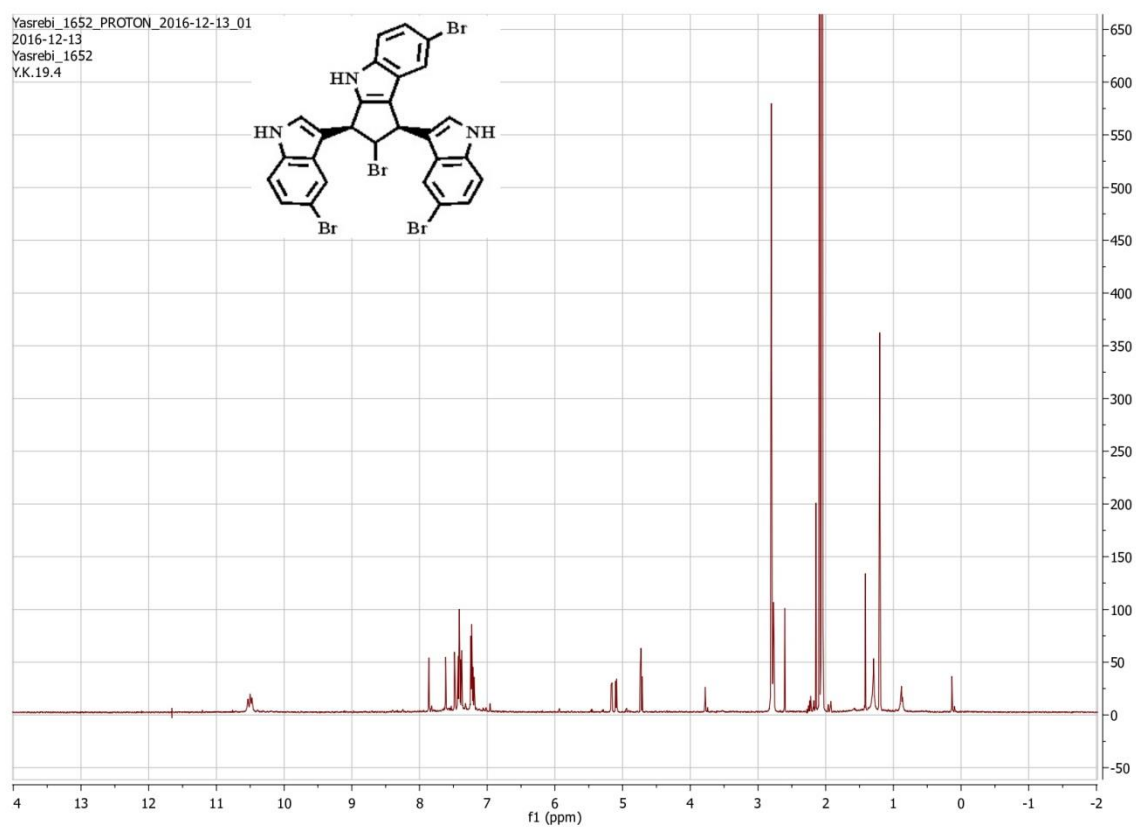
# Compound [15]



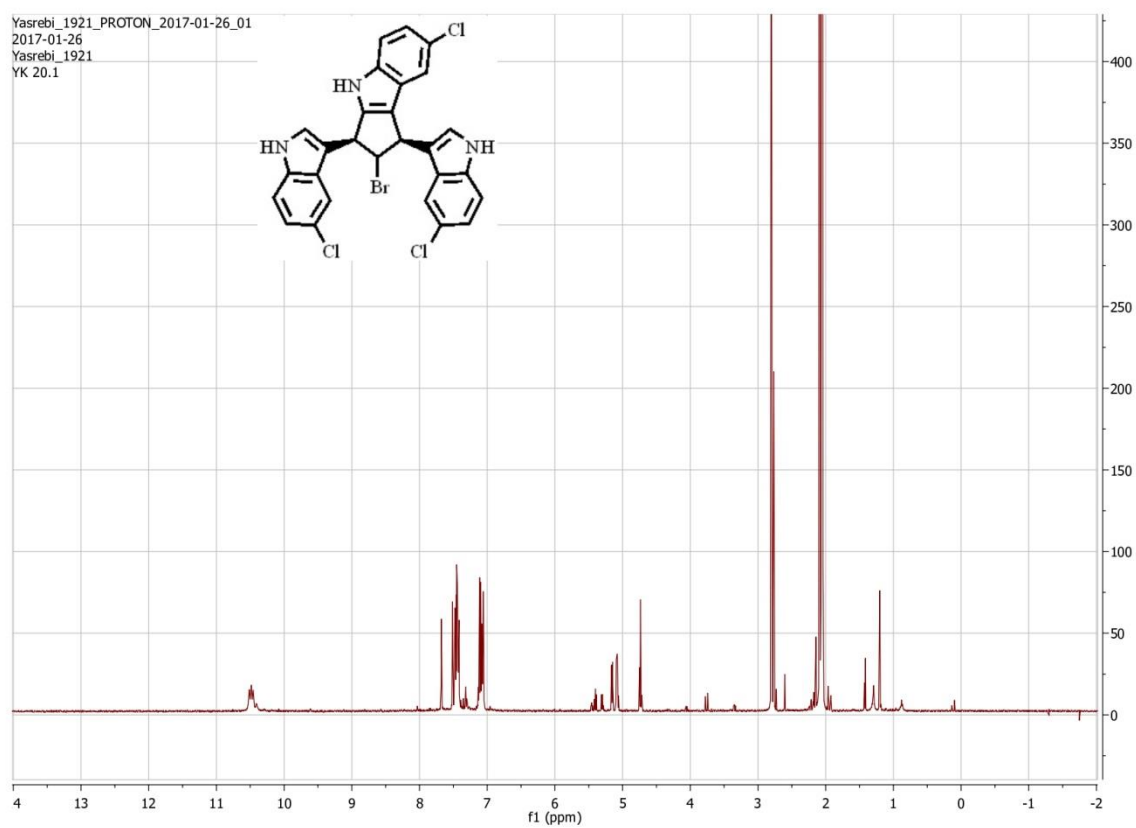
# Compound [16]



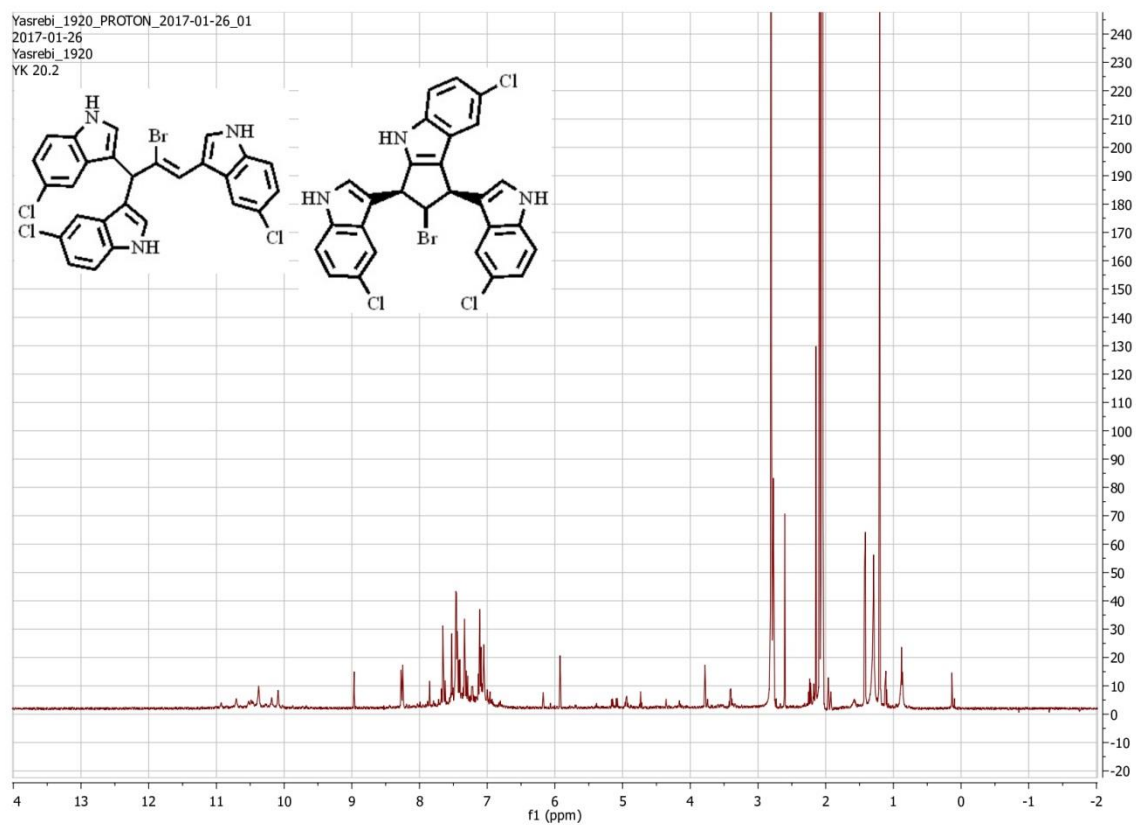
# Compound [17]



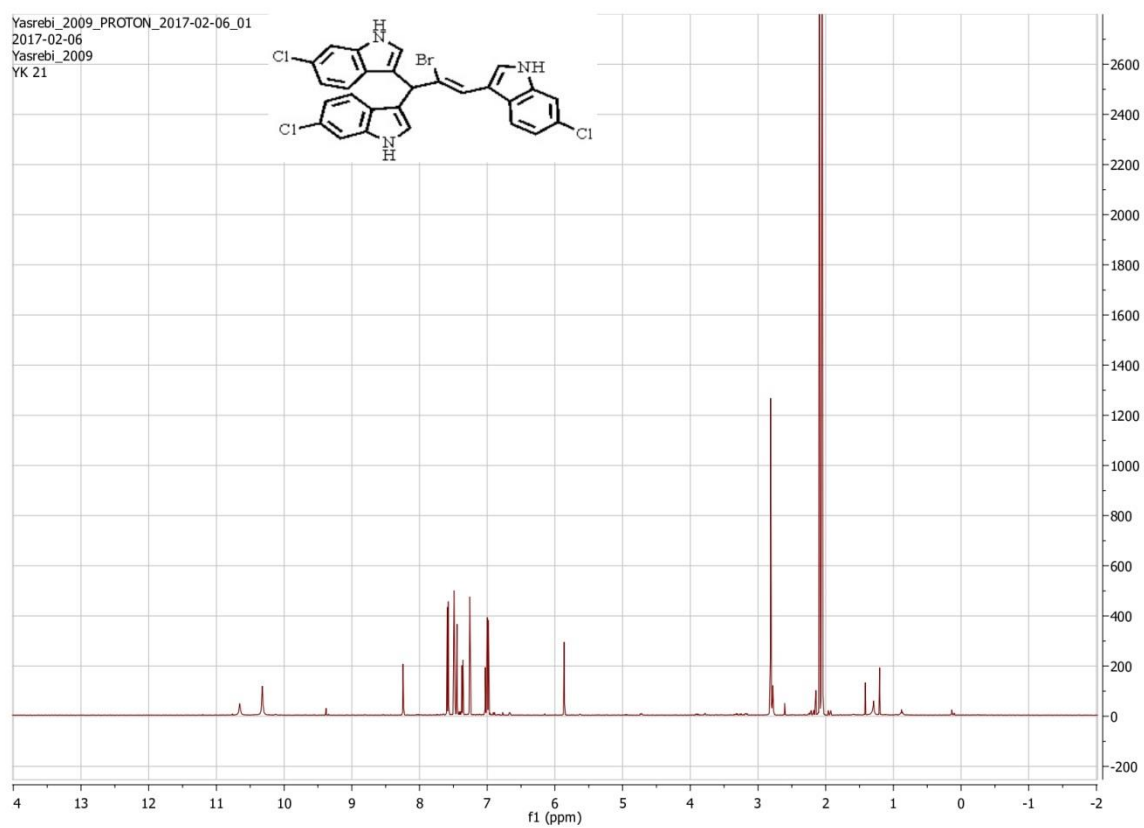
# Compound [18]



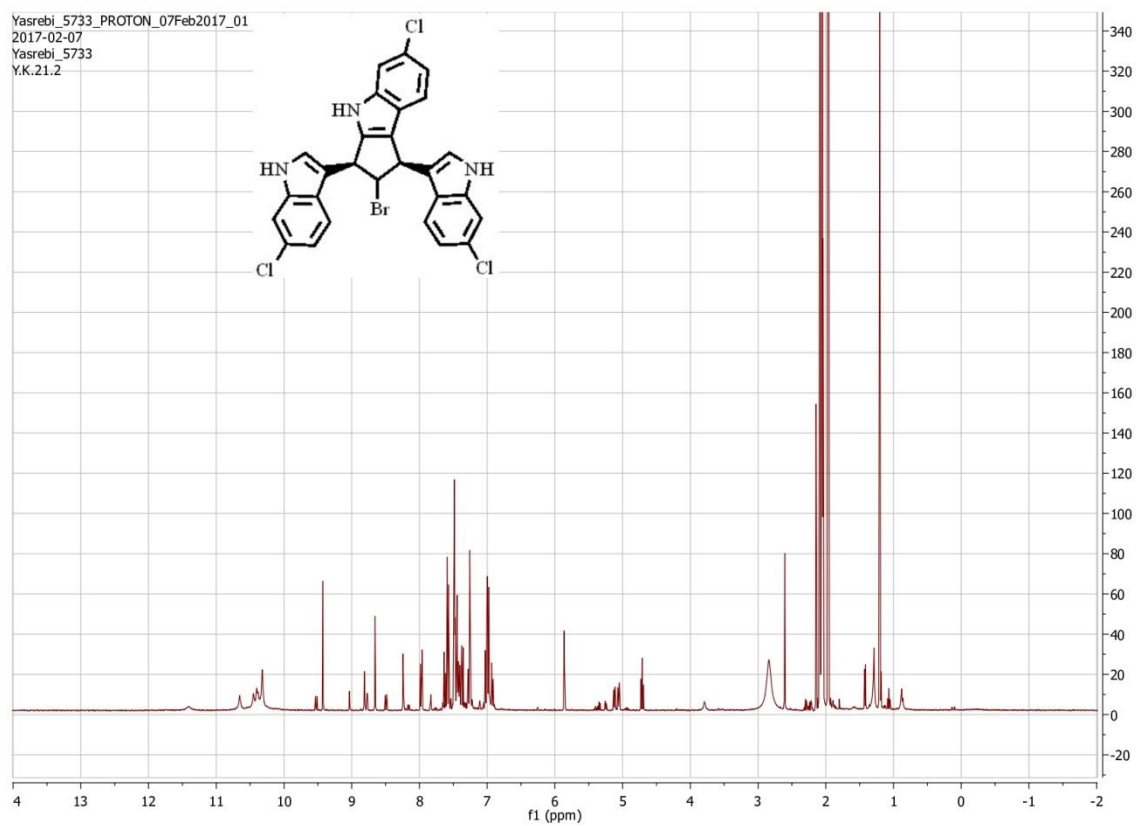
# Compound [19]



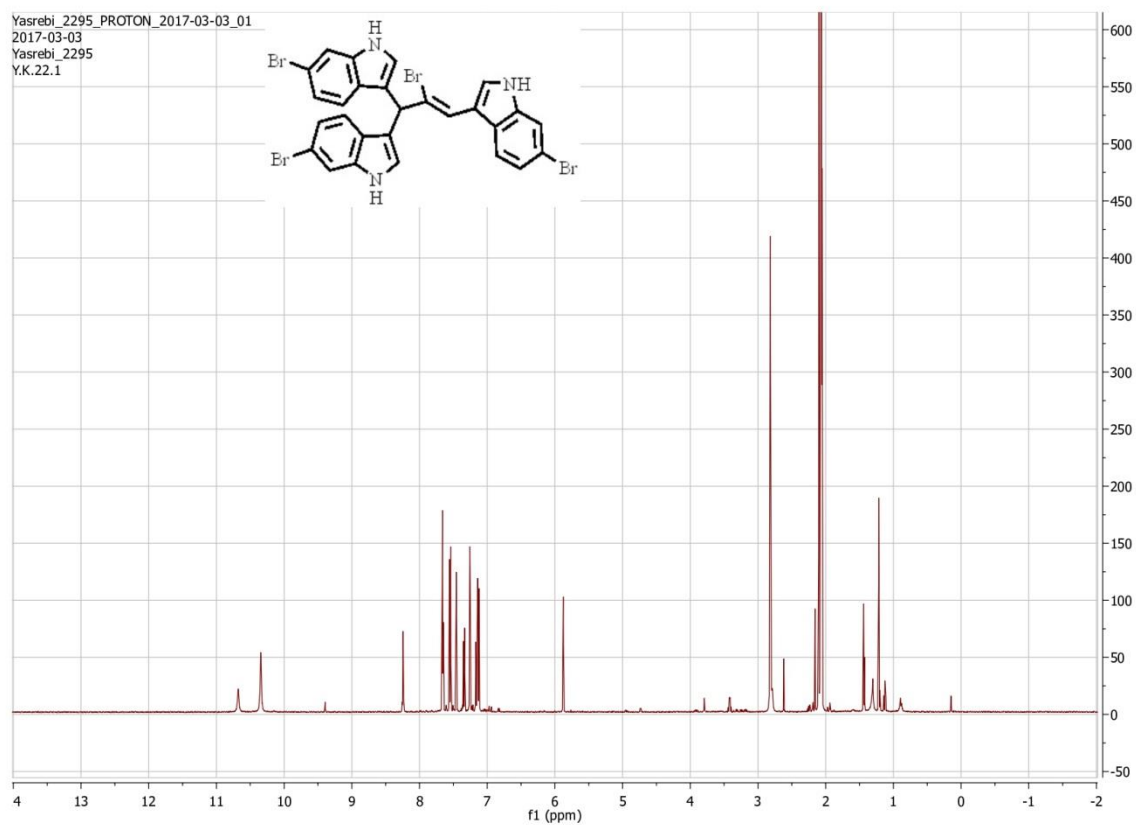
# Compound [20]



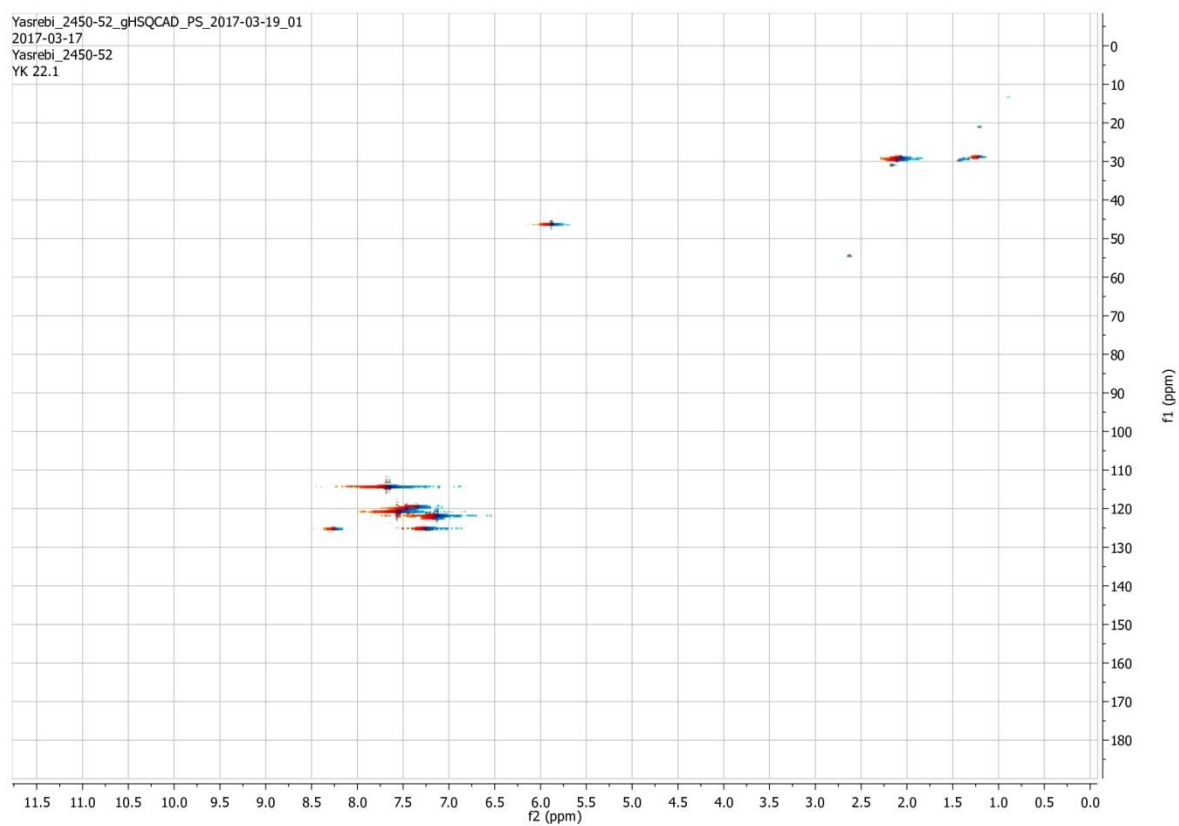
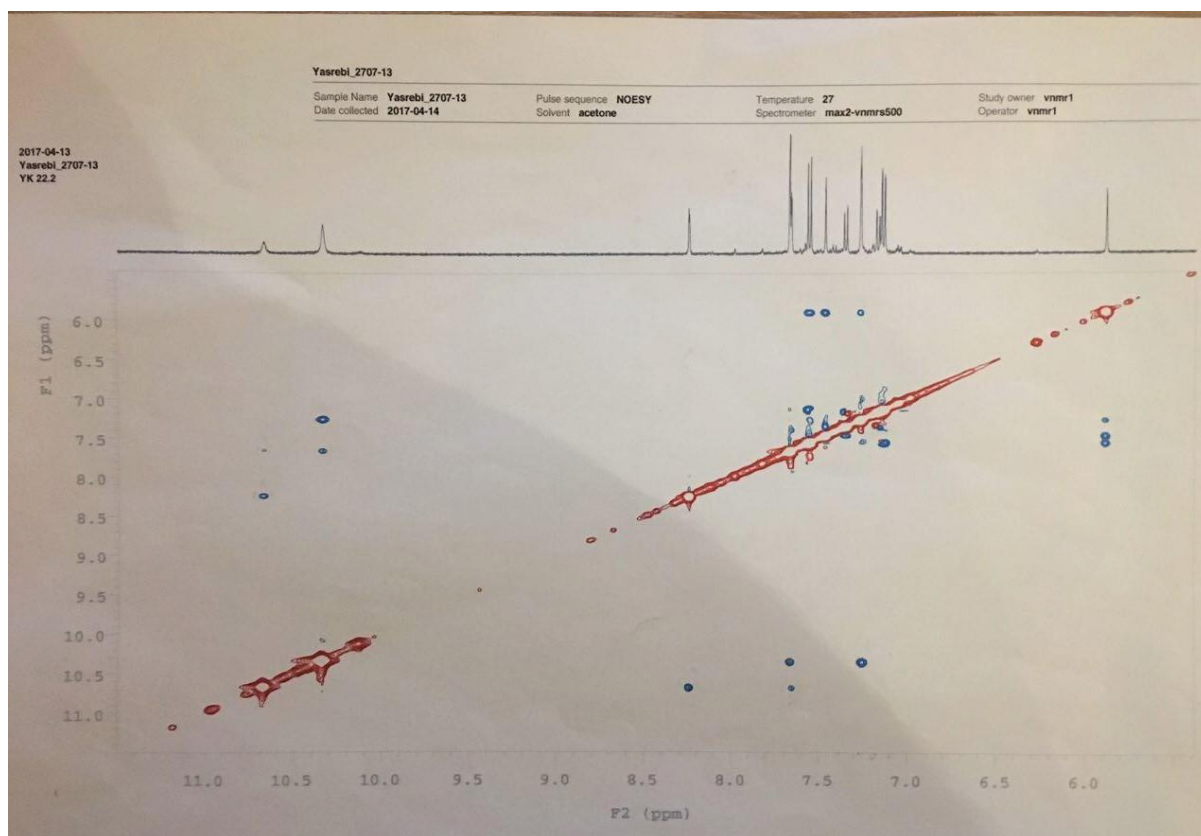
# Compound [21]

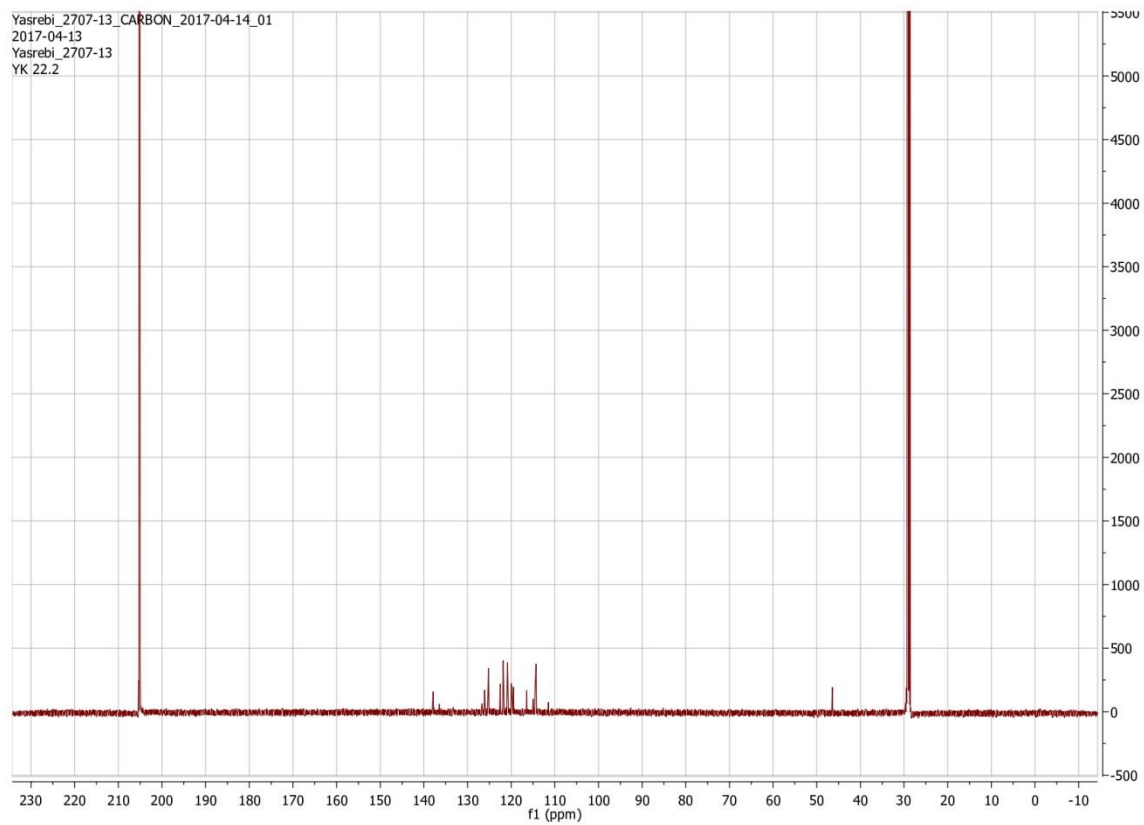
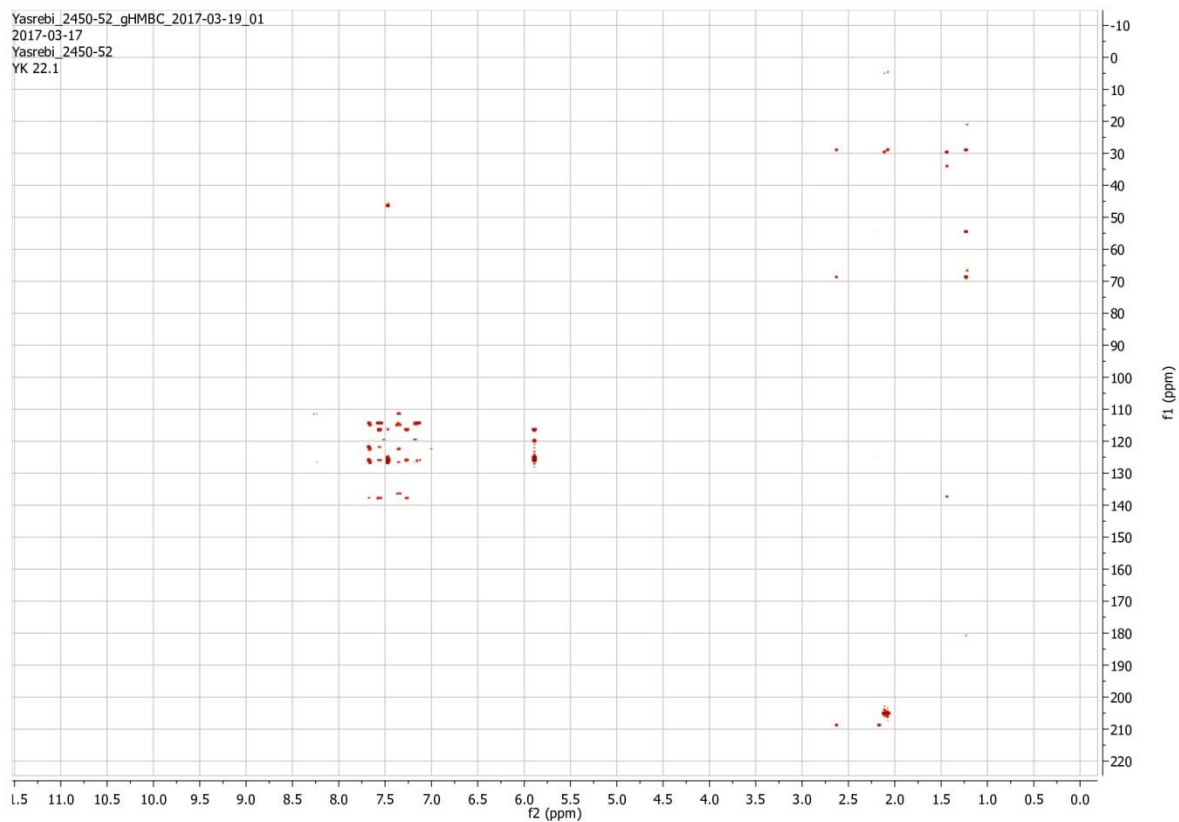


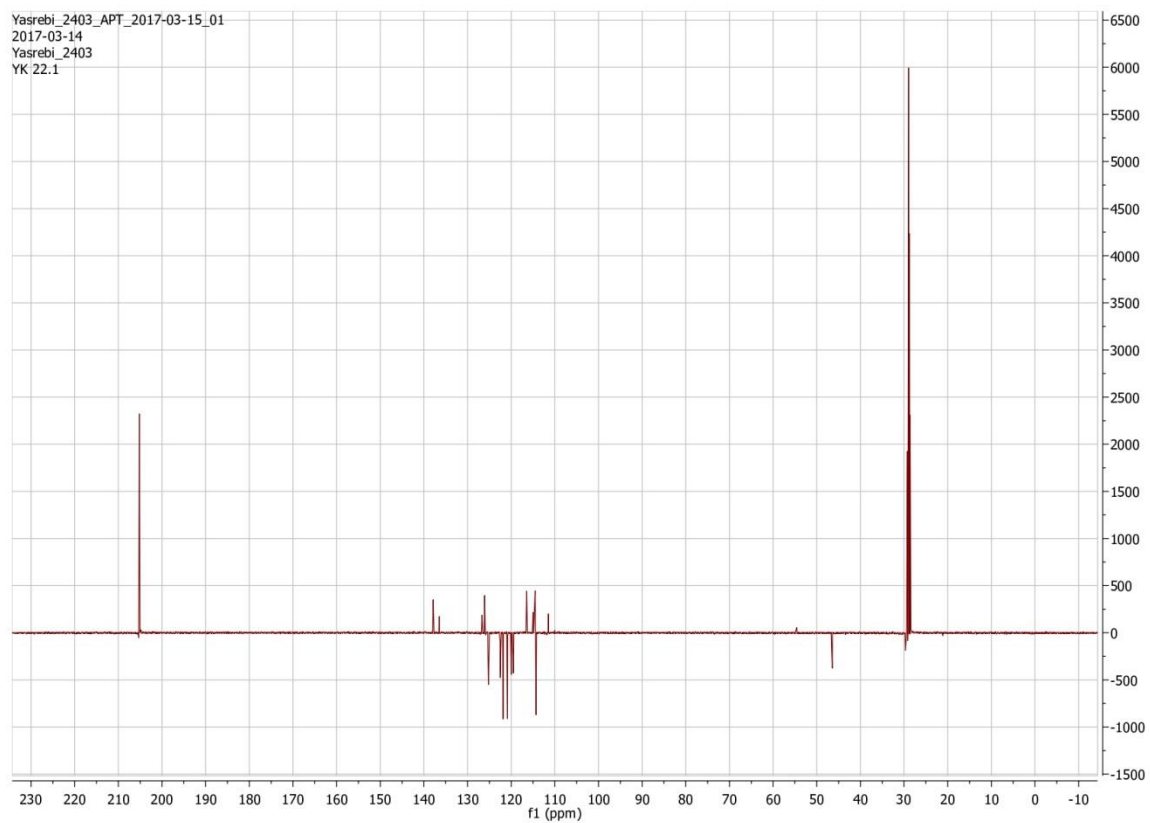
# Compound [22]



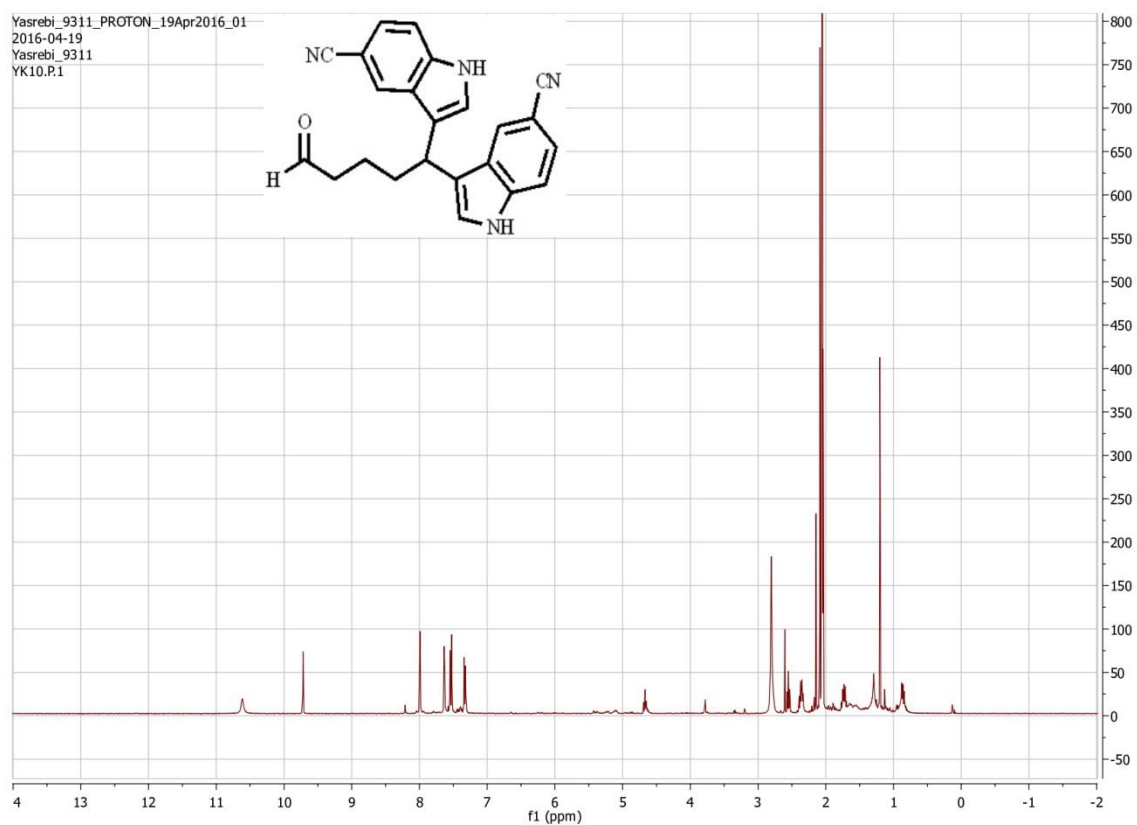






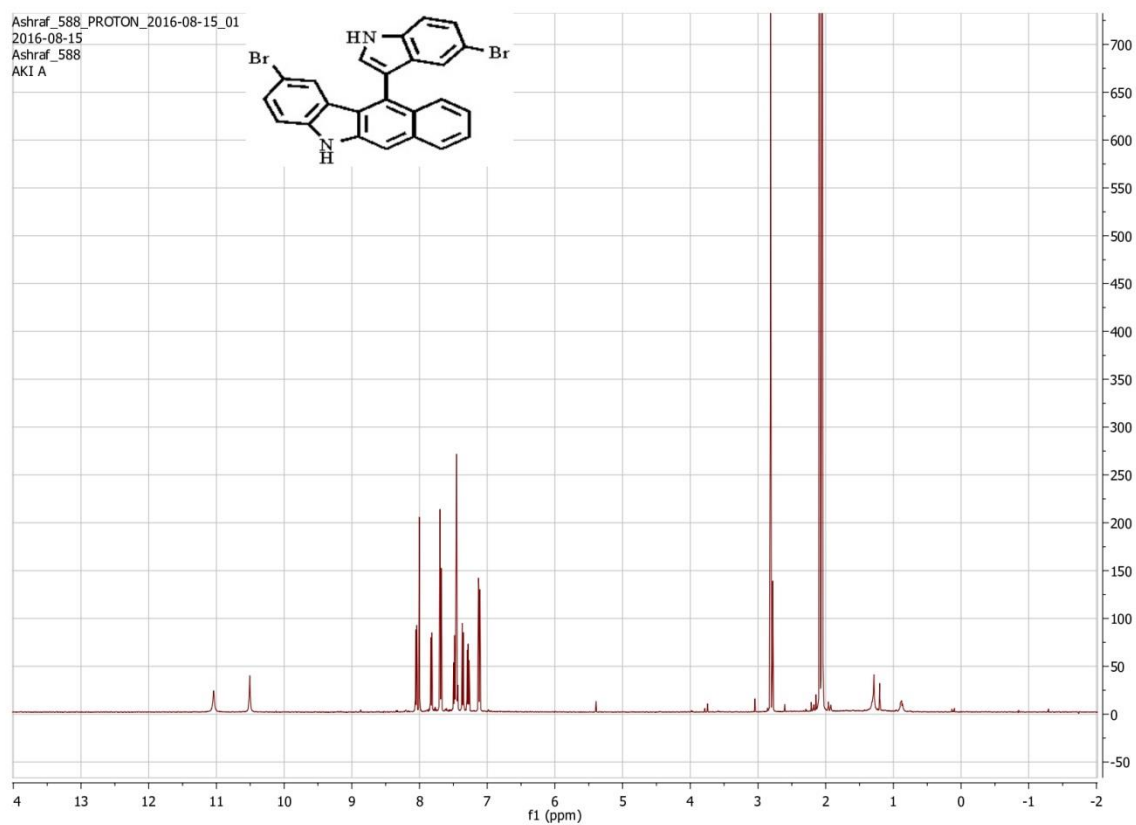


Yasrebi\_9311\_PROTON\_19Apr2016\_01  
2016-04-19  
Yasrebi\_9311  
YK10.P1

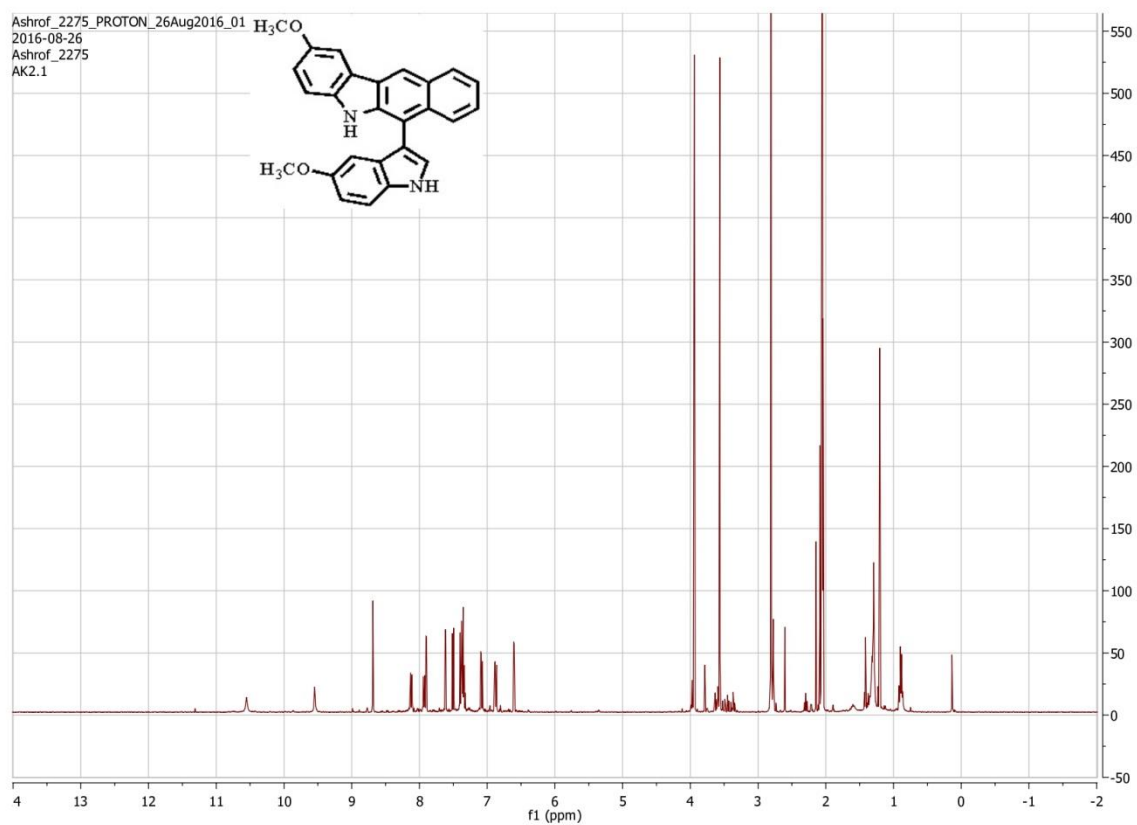


# Compound [23]

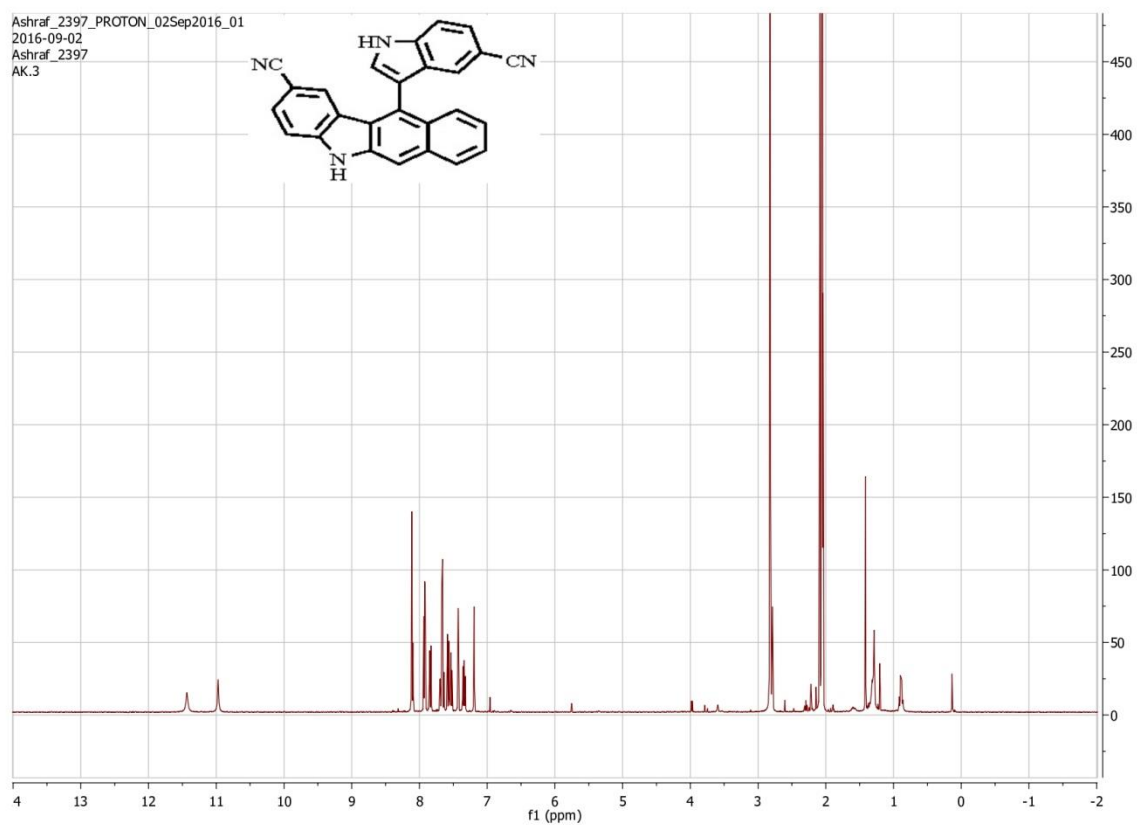
Ashraf\_588\_PROTON\_2016-08-15\_01  
2016-08-15  
Ashraf\_588  
AKI A



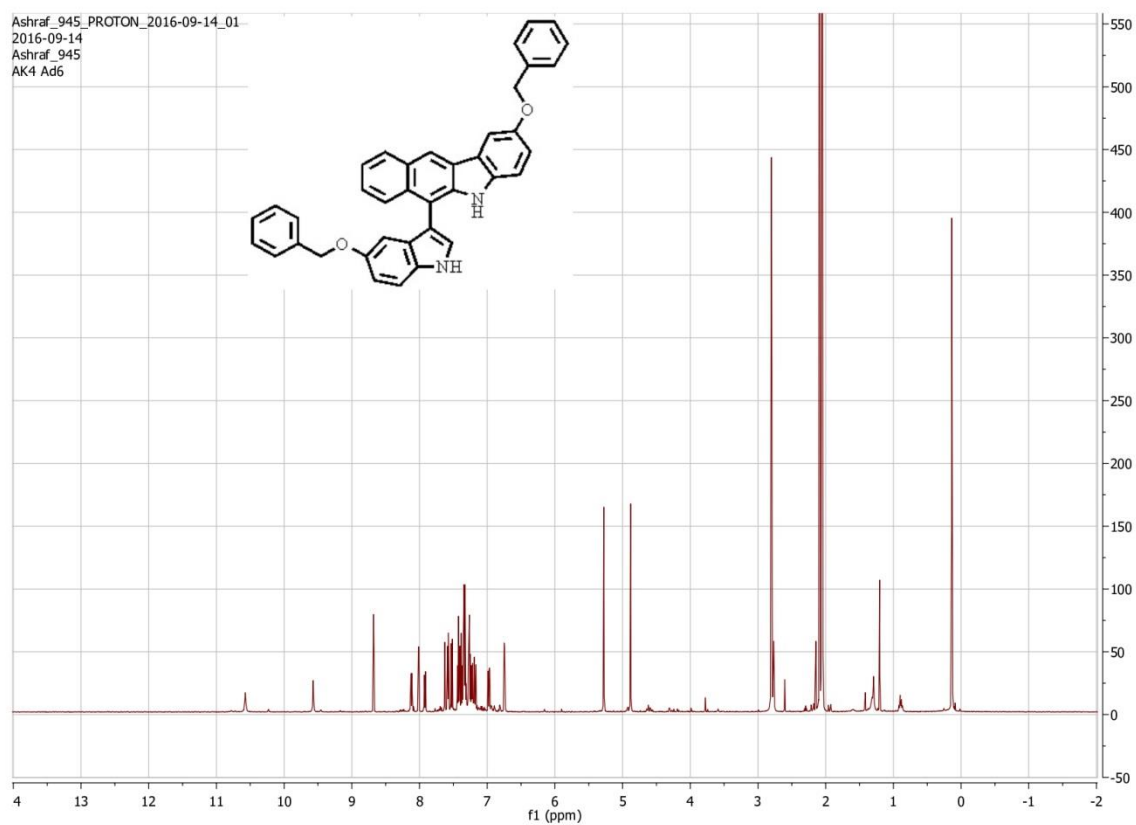
# Compound [24]



Compound [25]



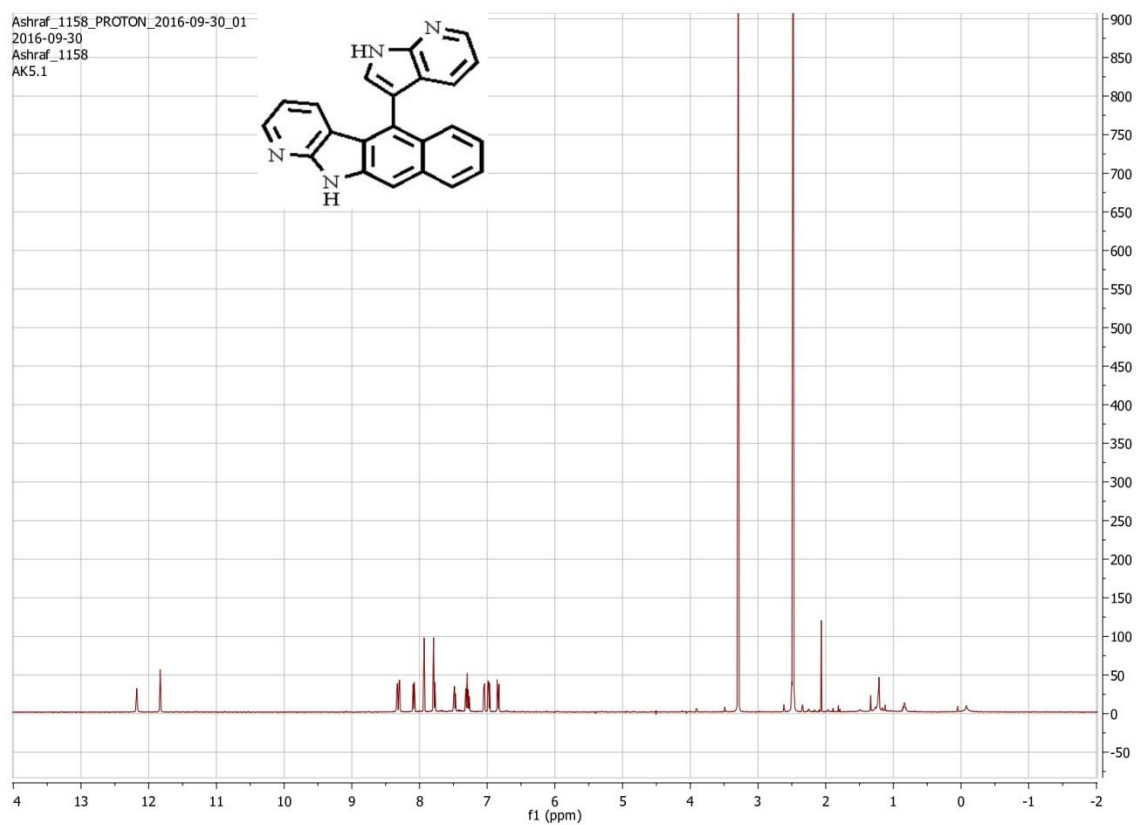
# Compound [26]



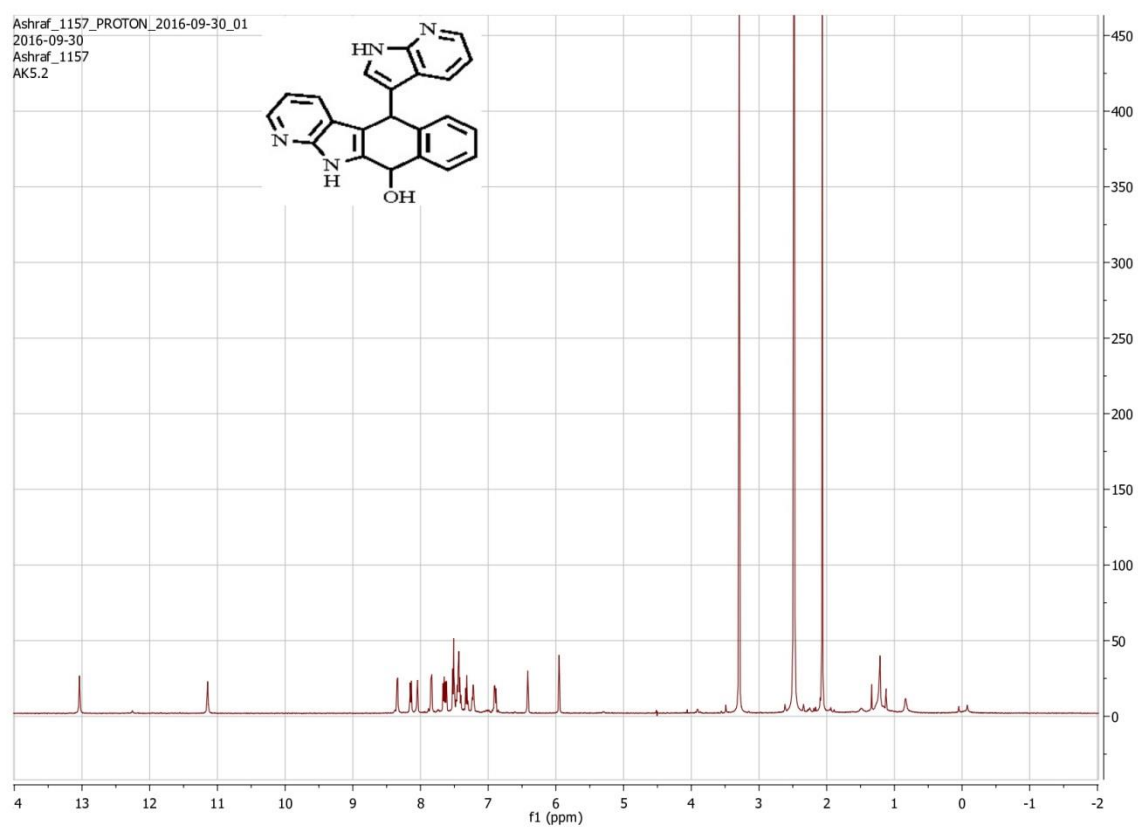


# Compound [27]

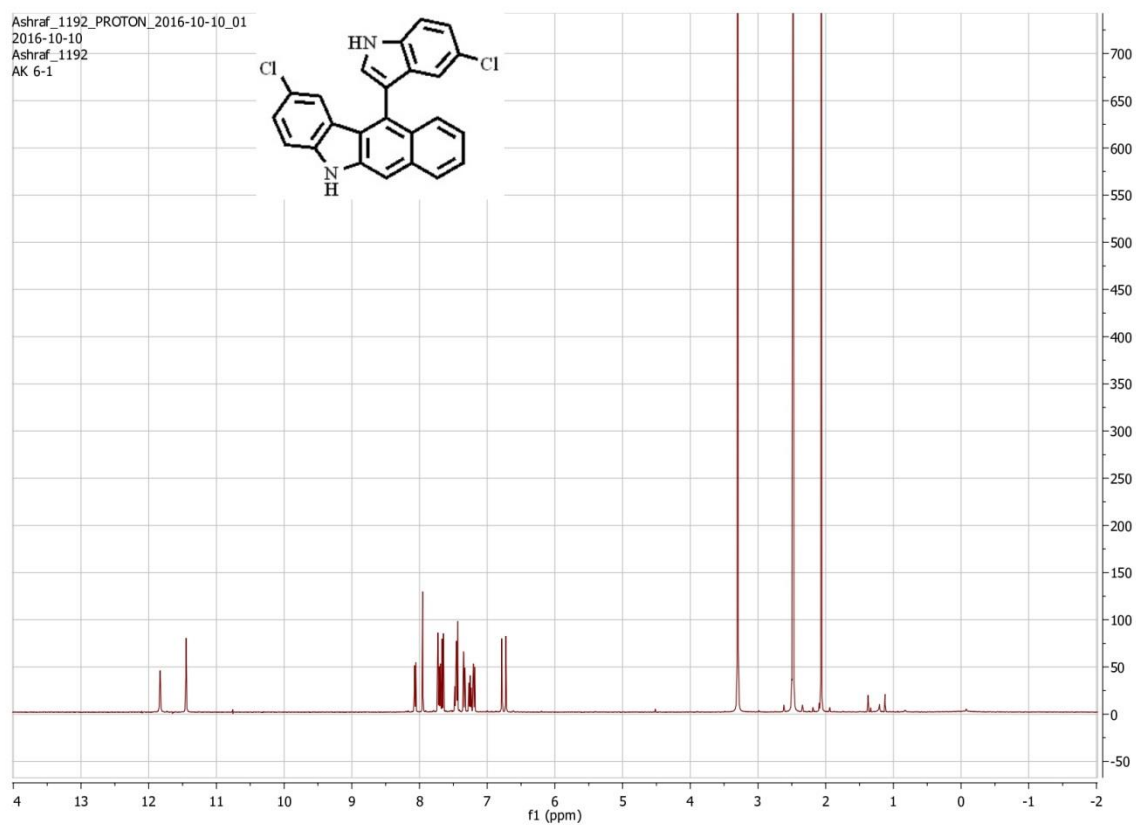
Ashraf\_1158\_PROTON\_2016-09-30\_01  
2016-09-30  
Ashraf\_1158  
AK5.1



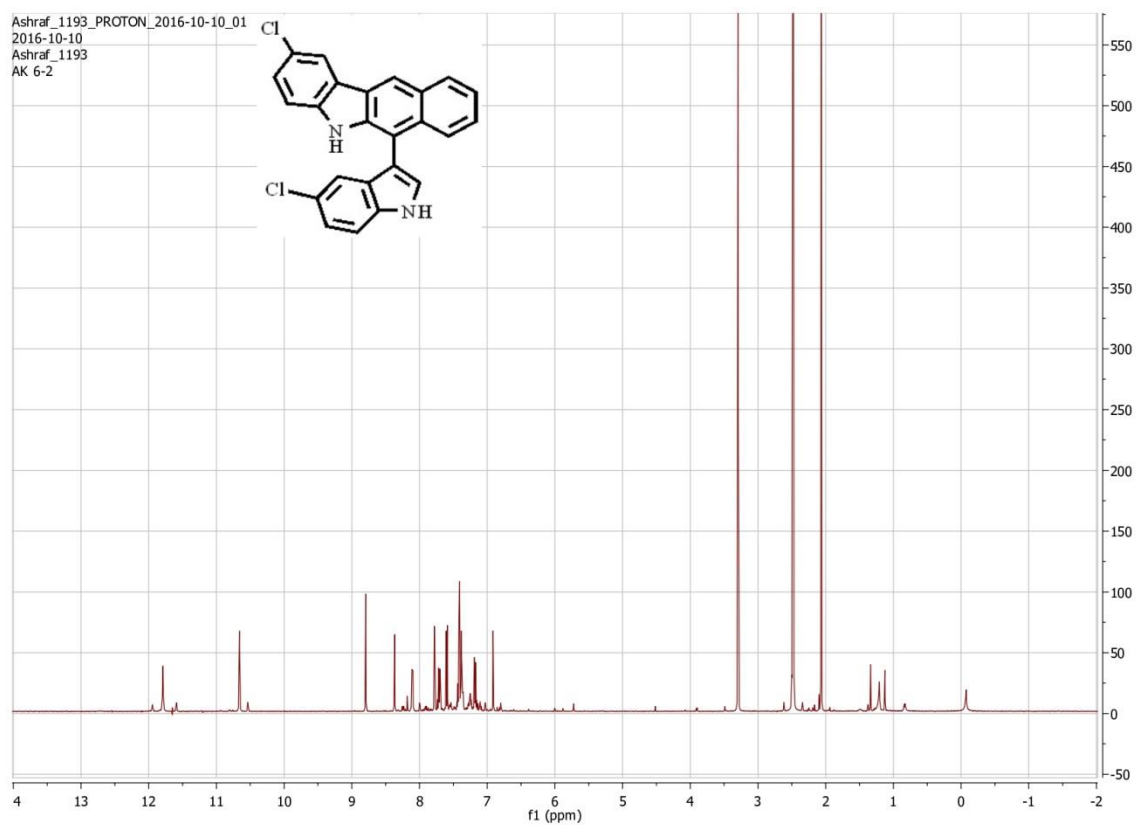
# Compound [28]



# Compound [29]

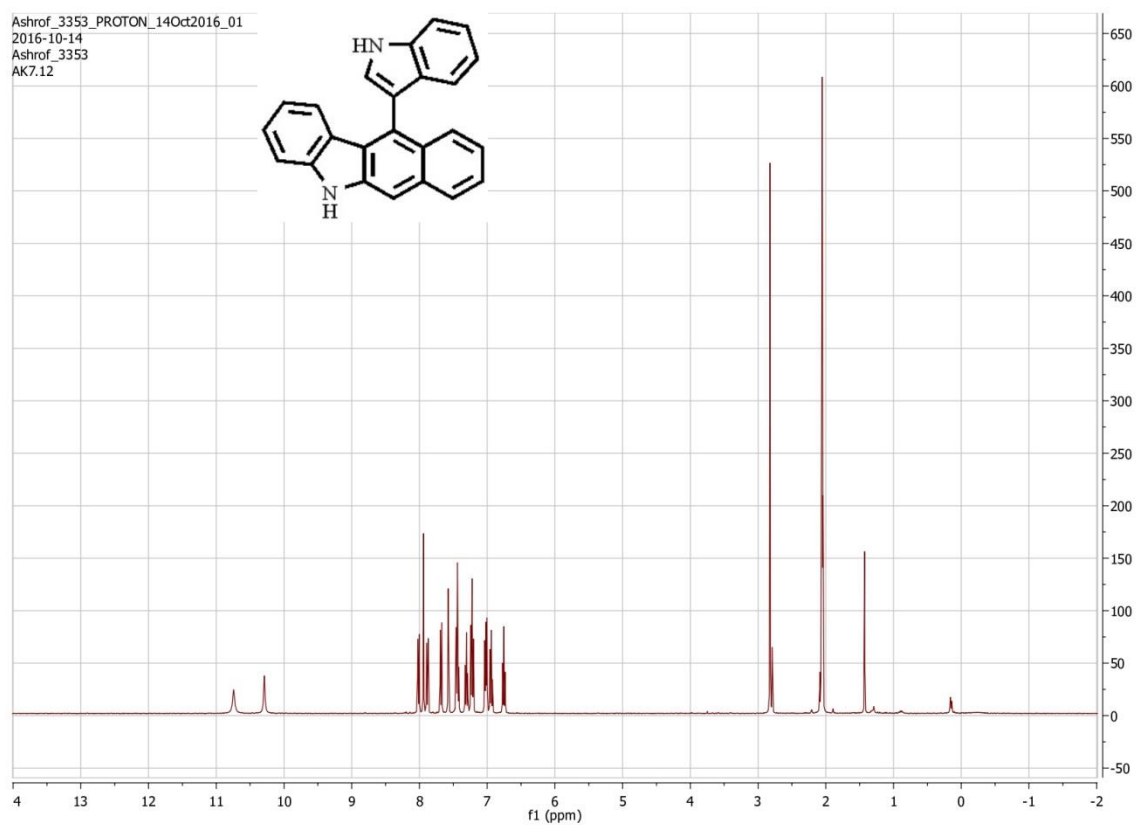


# Compound [30]

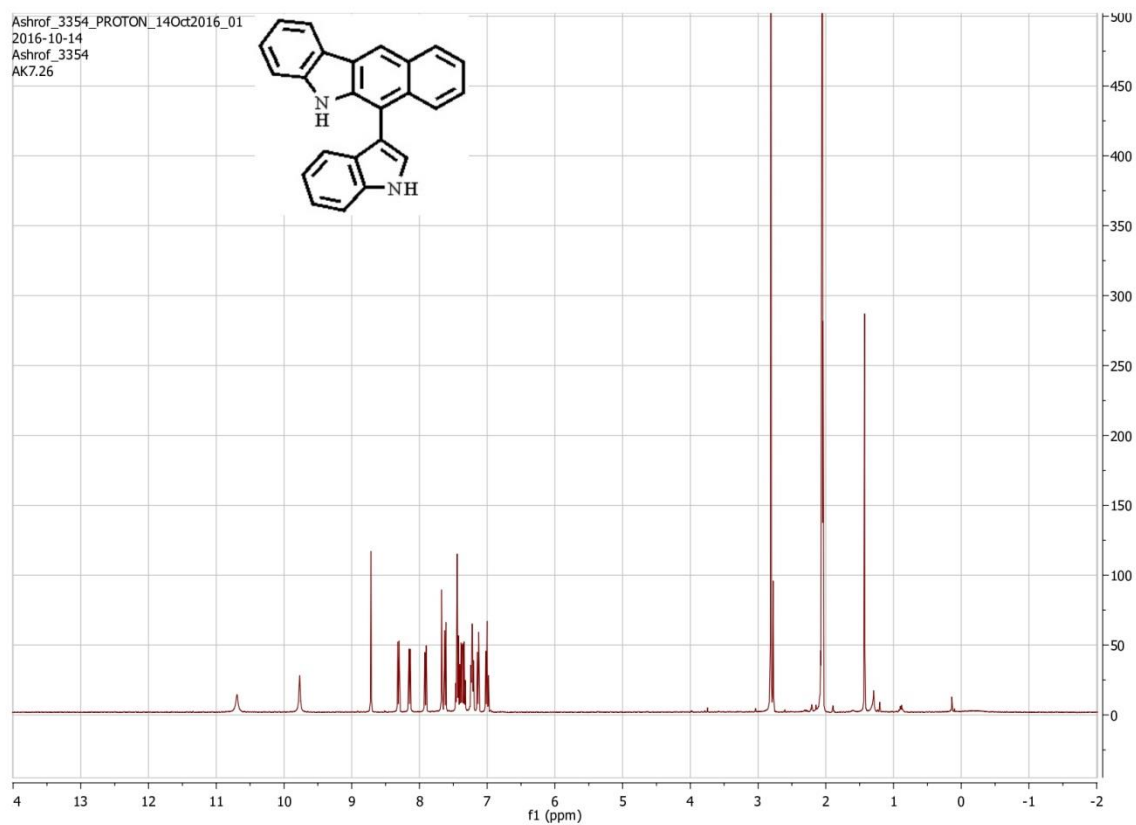


# Compound [31]

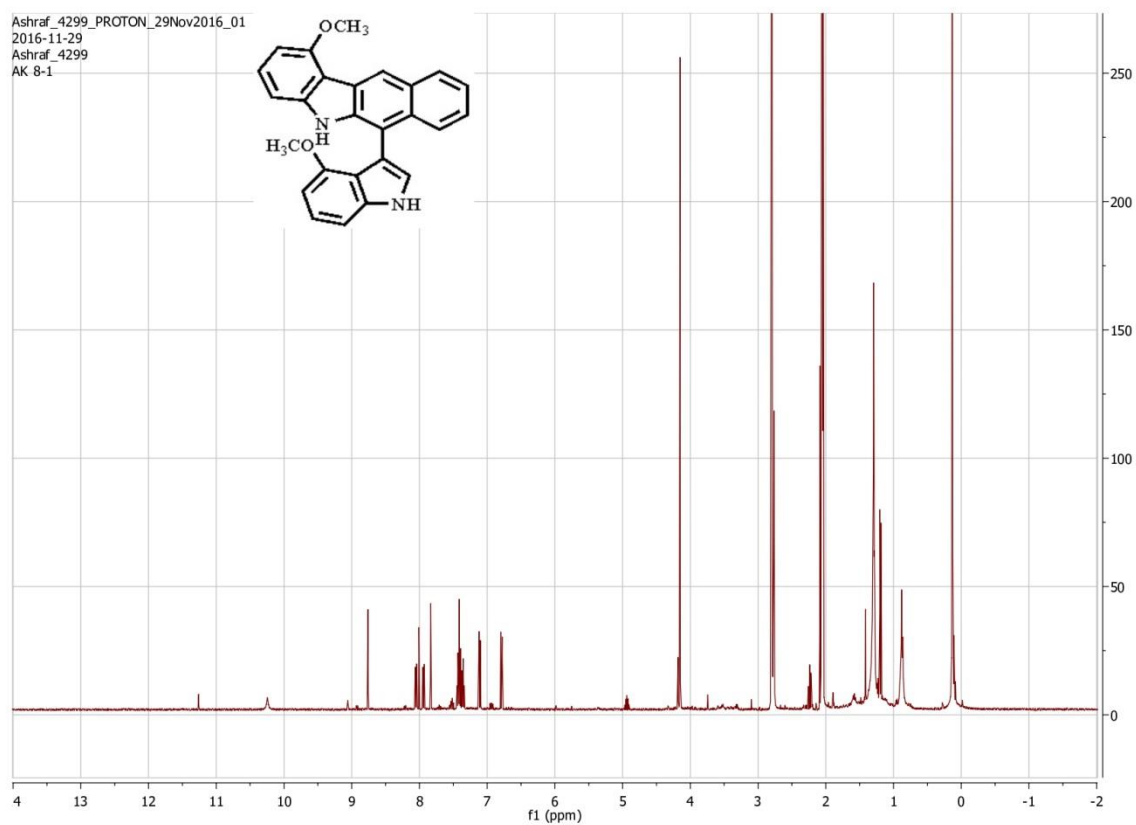
Ashrof\_3353\_PROTON\_14Oct2016\_01  
2016-10-14  
Ashrof\_3353  
AK7.12



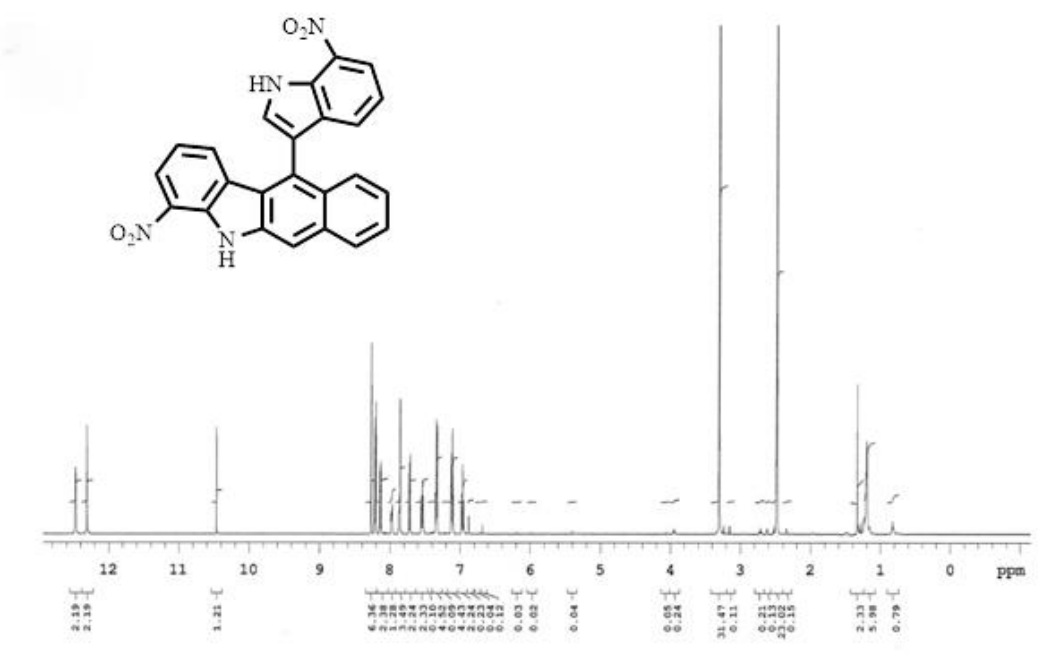
# Compound [32]



# Compound [33]

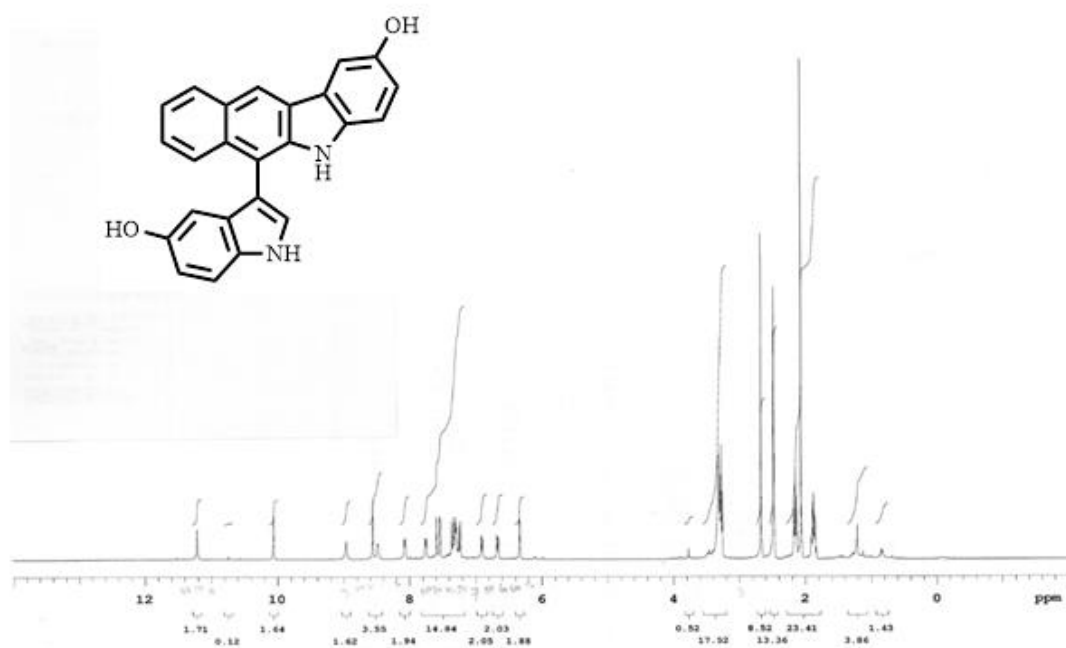


Compound [35]

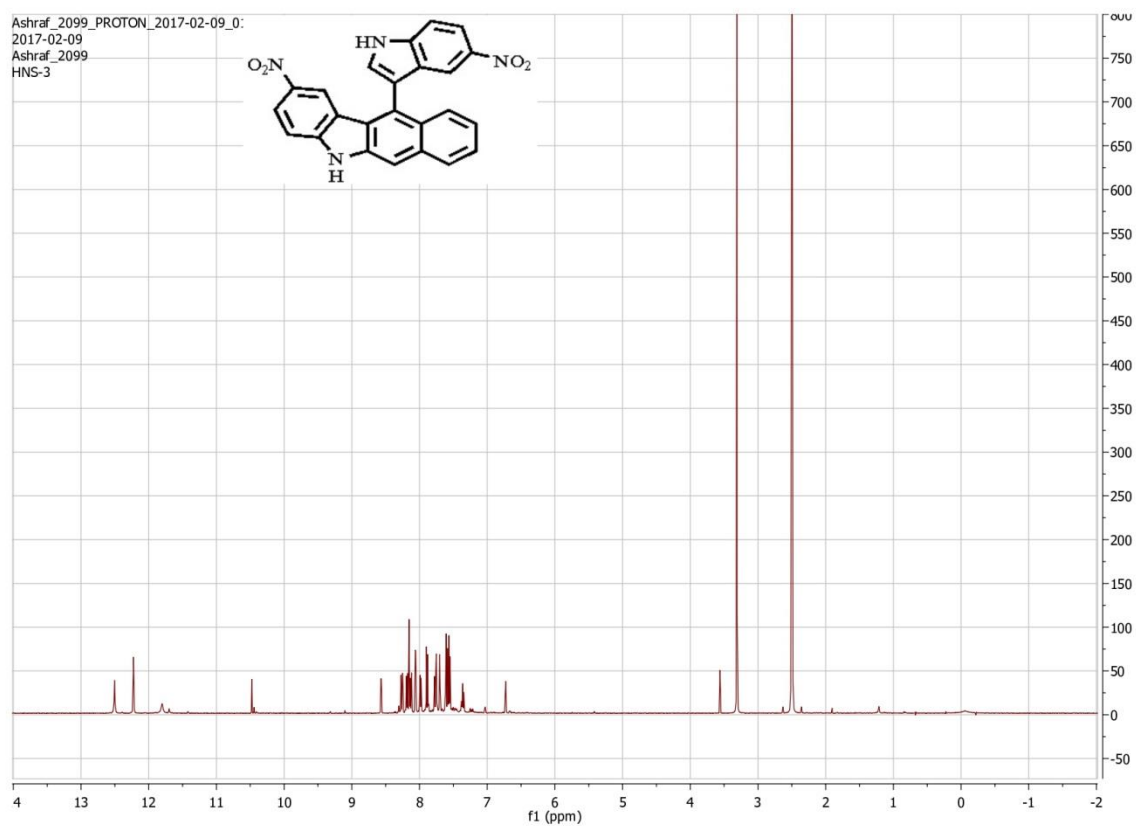




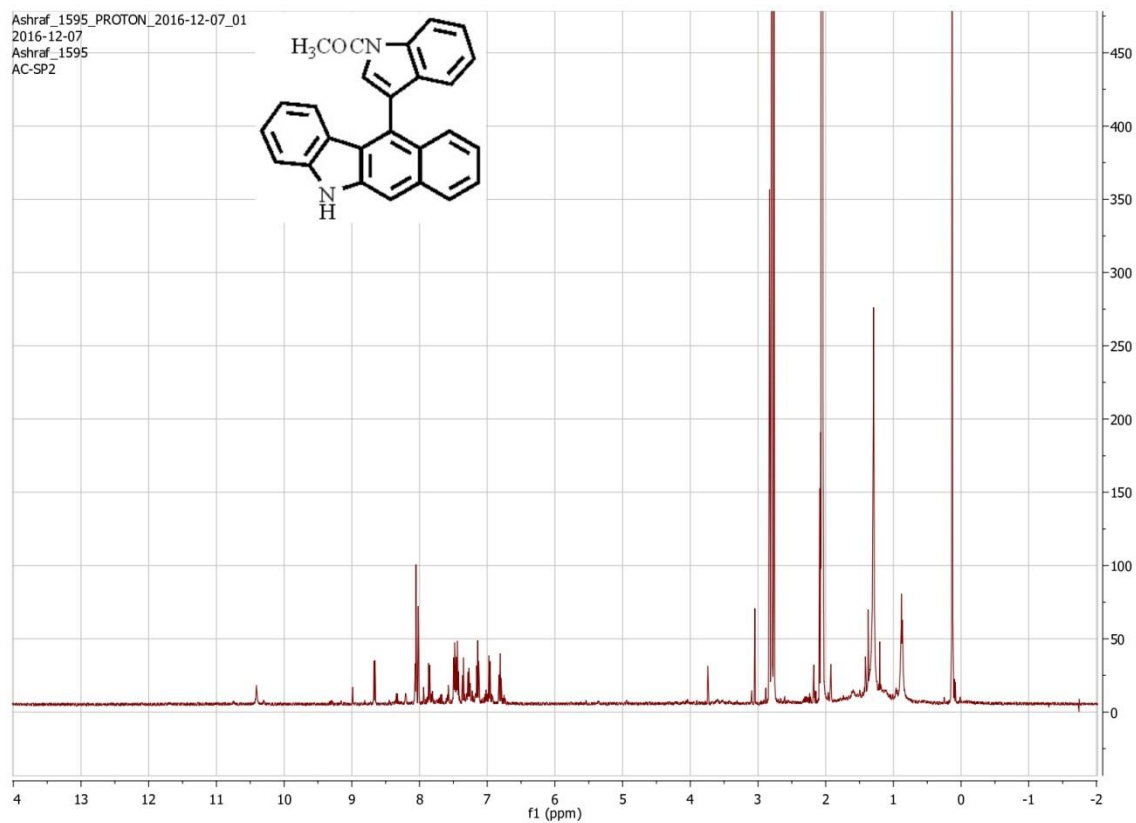
Compound [36]



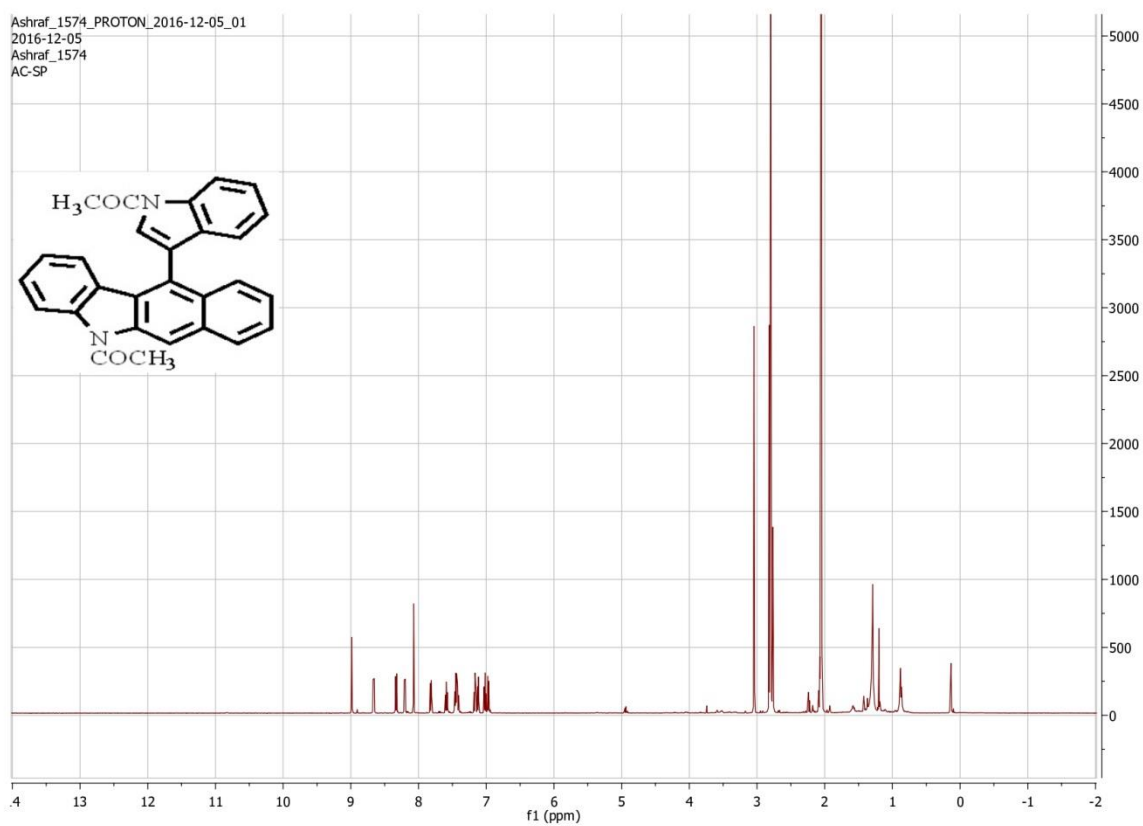
# Compound [37]



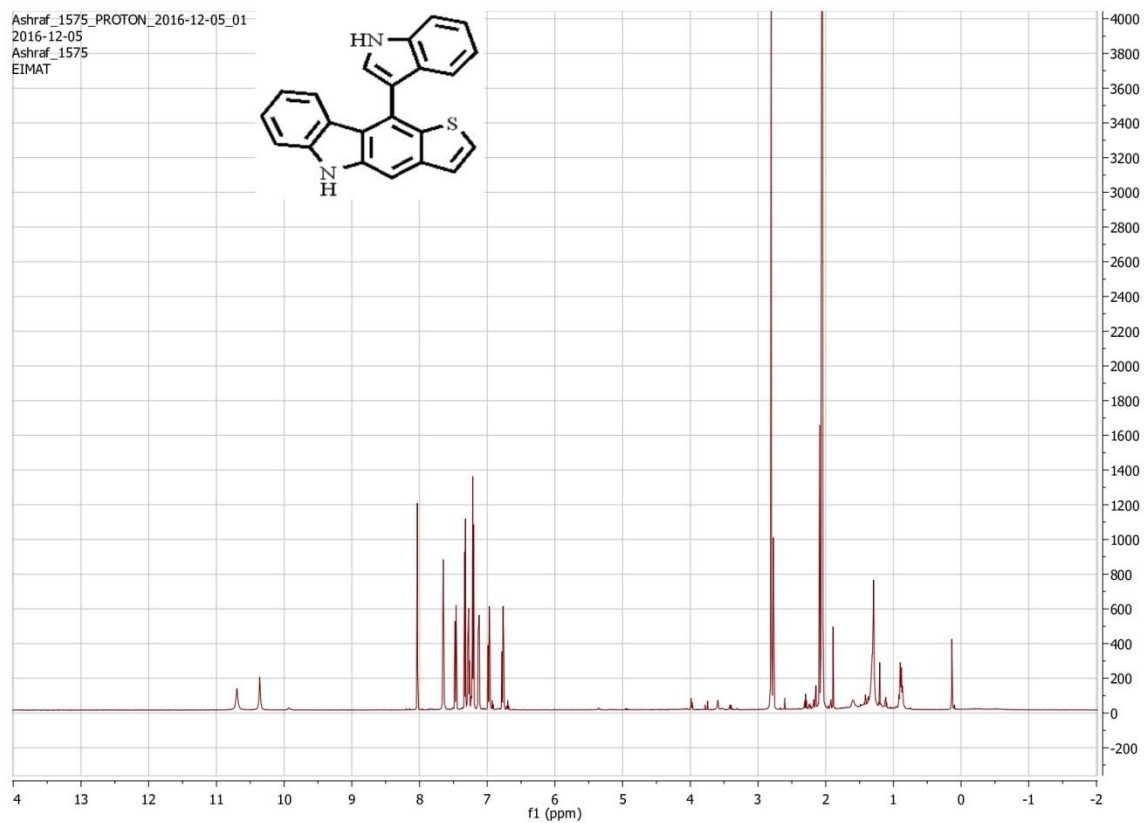
# Compound [38]



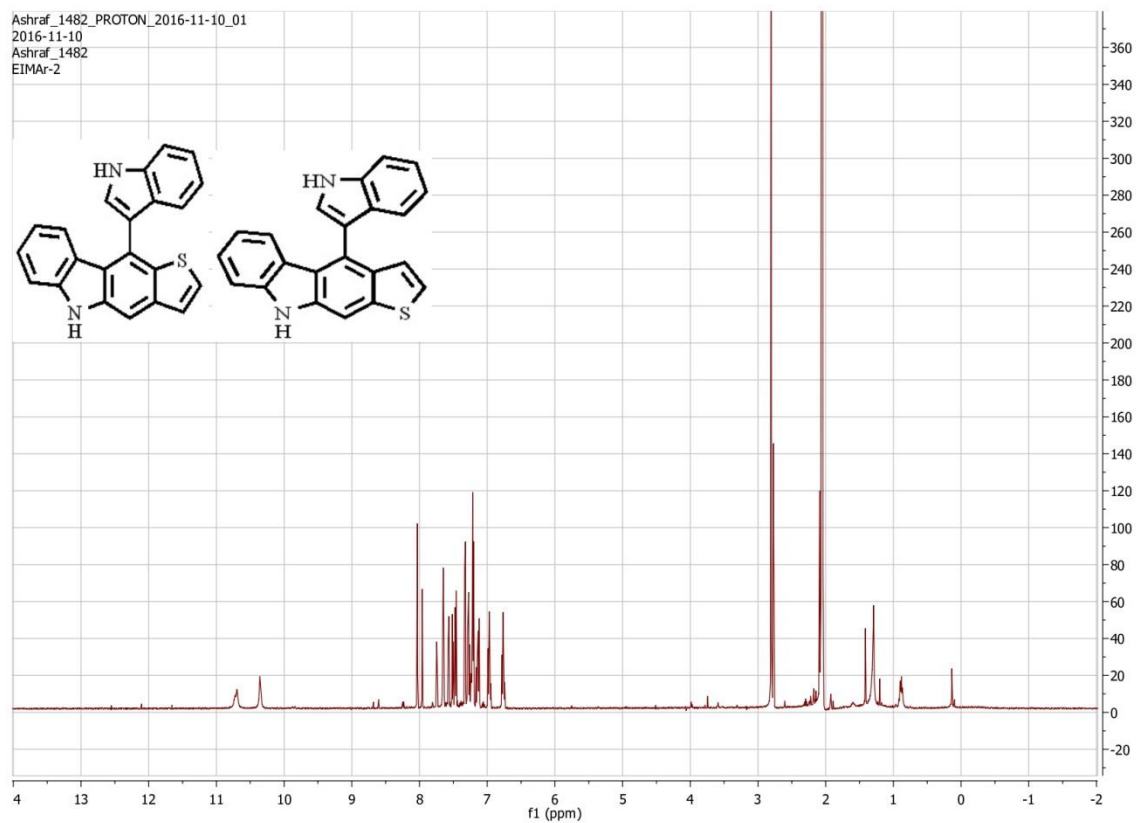
# Compound [39]



# Compound [40]



Ashraf\_1482\_PROTON\_2016-11-10\_01  
2016-11-10  
Ashraf\_1482  
EIMAr-2



## 6.2 Curriculum Vitae

First Name	Kaveh
Surname	Yasrebi
Date/Place of Birth	14.09.1987/Teheran, Iran (Islamic Republic)

### Education

June 2015-Present	Doctoral Research (Ph.D.), Martin- Luther-Universität Halle-Wittenberg, Germany
Sep 2012-Nov 2013	MSc Taught Chemistry, the University of Manchester, UK
Sep 2006-June 2011	BSc Pure Chemistry, the University of Mazandaran, Iran

### 6.3 Publications

[1] Hilgeroth, A., Yasrebi, K., Suzen S., Hertlein T., Ohlsen K., Lalk M. *Antibacterial Evaluation of Novel Substituted Cycloheptaindoles in Staphylococcus and Enterococcus strains*. Journal of Medicinal Chemistry (Sharjah (United Arab Emirates)). 2019/2  
DOI: [10.2174/1573406415666190208170126](https://doi.org/10.2174/1573406415666190208170126)

[2] Ashraf, K., Yasrebi, K., Adeniyi. T, E., Hertlein, T., Ohlsen, K., Lalk, M., Erdmann, F., Hilgeroth, A. *Antistaphylococcal evaluation of indole– naphthalene hybrid analogs*. Journal of Drug Design, Development, and Therapy. 2019: 13, 275-283  
DOI: [10.2147/DDDT.S184965](https://doi.org/10.2147/DDDT.S184965)

[3] Ashraf, K., Yasrebi, K., Hertlein, T., Ohlsen, K., Lalk, M., Hilgeroth A. *Novel Effective Small-Molecule Antibacterials against Enterococcus Strains*. Journal of Molecules. 2017, 22 (12), 2193  
DOI: [10.3390/molecules22122193](https://doi.org/10.3390/molecules22122193)